

International Space Station Increment-2 Microgravity Environment Summary Report

Kenol Jules
Glenn Research Center, Cleveland, Ohio

Kenneth Hrovat and Eric Kelly
Zin Technologies, Inc., Brook Park, Ohio

Kevin McPherson
Glenn Research Center, Cleveland, Ohio

Timothy Reckart
Zin Technologies, Inc., Brook Park, Ohio

The NASA STI Program Office . . . in Profile

Since its founding, NASA has been dedicated to the advancement of aeronautics and space science. The NASA Scientific and Technical Information (STI) Program Office plays a key part in helping NASA maintain this important role.

The NASA STI Program Office is operated by Langley Research Center, the Lead Center for NASA's scientific and technical information. The NASA STI Program Office provides access to the NASA STI Database, the largest collection of aeronautical and space science STI in the world. The Program Office is also NASA's institutional mechanism for disseminating the results of its research and development activities. These results are published by NASA in the NASA STI Report Series, which includes the following report types:

- **TECHNICAL PUBLICATION.** Reports of completed research or a major significant phase of research that present the results of NASA programs and include extensive data or theoretical analysis. Includes compilations of significant scientific and technical data and information deemed to be of continuing reference value. NASA's counterpart of peer-reviewed formal professional papers but has less stringent limitations on manuscript length and extent of graphic presentations.
- **TECHNICAL MEMORANDUM.** Scientific and technical findings that are preliminary or of specialized interest, e.g., quick release reports, working papers, and bibliographies that contain minimal annotation. Does not contain extensive analysis.
- **CONTRACTOR REPORT.** Scientific and technical findings by NASA-sponsored contractors and grantees.

- **CONFERENCE PUBLICATION.** Collected papers from scientific and technical conferences, symposia, seminars, or other meetings sponsored or cosponsored by NASA.
- **SPECIAL PUBLICATION.** Scientific, technical, or historical information from NASA programs, projects, and missions, often concerned with subjects having substantial public interest.
- **TECHNICAL TRANSLATION.** English-language translations of foreign scientific and technical material pertinent to NASA's mission.

Specialized services that complement the STI Program Office's diverse offerings include creating custom thesauri, building customized data bases, organizing and publishing research results . . . even providing videos.

For more information about the NASA STI Program Office, see the following:

- Access the NASA STI Program Home Page at <http://www.sti.nasa.gov>
- E-mail your question via the Internet to help@sti.nasa.gov
- Fax your question to the NASA Access Help Desk at 301-621-0134
- Telephone the NASA Access Help Desk at 301-621-0390
- Write to:
NASA Access Help Desk
NASA Center for Aerospace Information
7121 Standard Drive
Hanover, MD 21076



International Space Station Increment-2 Microgravity Environment Summary Report

Kenol Jules
Glenn Research Center, Cleveland, Ohio

Kenneth Hrovat and Eric Kelly
Zin Technologies, Inc., Brook Park, Ohio

Kevin McPherson
Glenn Research Center, Cleveland, Ohio

Timothy Reckart
Zin Technologies, Inc., Brook Park, Ohio

National Aeronautics and
Space Administration

Glenn Research Center

Acknowledgments

The authors would like to acknowledge a number of people who contributed significantly to this report. Without their contribution, this report would have not been possible. Significant contributions were made in the area of software development, which enabled both MAMS and SAMS to acquire acceleration data aboard the ISS, process, analyze, and display the data on the web as well as systems troubleshooting, by Nissim Lugasy, Ted Wright, and Gene Liberman. We would like to acknowledge the development efforts of the SAMS-II team and the MAMS project team/Canopus, Inc.

PIMS would like to acknowledge the tremendous help received from the ADVASC team, especially Don Isham (University of Wisconsin), in providing PIMS with timeline information and operating characteristics of their experiment. Also, we thank Ted Bartkiewicz, ISS Loads Dynamist, Boeing, for providing us with a TVIS timeline. Finally, we would like to thank Richard DeLombard, Carlos Grodsinsky, and Emily S. Nelson for their technical review, comments, and suggestions.

Dedication

The PIMS project dedicates this report to the memory of William O. Wagar, the MAMS accelerometer project manager, who passed away recently.

Available from

NASA Center for Aerospace Information
7121 Standard Drive
Hanover, MD 21076

National Technical Information Service
5285 Port Royal Road
Springfield, VA 22100

Available electronically at <http://gltrs.grc.nasa.gov/GLTRS>

Table of Contents

Table of Contents.....	iii
List of Tables.....	iv
List of Figures.....	v
1. Introduction	1
2. International Space Station.....	2
2.1 Configuration at Assembly Complete	2
2.2 ISS Analysis Coordinate System	3
2.3 ISS Flight Attitude at Assembly Complete	3
2.4 United States Laboratory Module (Destiny) Coordinate System	3
3. ISS Increment-2	4
3.1 Increment-2 Configuration	4
3.2 Increment-2 Coordinate Systems	4
3.3 Increment-2 Overall Attitude.....	4
3.4 Increment-2 Crew Members	4
4. Accelerometer Systems' Description and Locations.....	5
4.1 Microgravity Acceleration Measurement System (MAMS)	5
4.2 MAMS Coordinate Systems	5
4.3 Space Acceleration Measurement System (SAMS).....	6
4.4 SAMS Coordinate Systems	6
5. ISS Increment-2 Facilities Supported by PIMS.....	7
6. ISS Increment-2 Experiments Supported by PIMS	8
7. MAMS and SAMS Data Flow Descriptions	9
8. Data Analysis Techniques and Processing.....	10
8.1 Quasi-steady Regime.....	10
8.1.1 Trimmed mean Filter	11
8.1.2 OSS Bias Measurements.....	12
8.1.3 OSS Bias Calibration Anomaly.....	13
8.1.4 Quasi-steady Plot Types	13
8.1.4.1 OSS Trimmed Mean Acceleration versus Time.....	13
8.1.4.2 Quasi-steady Three-dimensional Histogram (QTH).....	13
8.2 Vibratory Regime.....	13
8.2.1 Demeaned Vibratory Acceleration Data.....	14
8.2.2 Interval Statistics	14
8.2.3 Interval Average	14
8.2.4 Interval Root-Mean-Square.....	15
8.2.5 Interval Minimum/Maximum.....	15
8.2.6 Power Spectral Density.....	15
8.2.7 Power Spectral Density Versus Time (Spectrogram).....	15
8.2.8 RMS Acceleration Versus One-Third Octave Frequency Bands.....	15
8.2.9 Cumulative RMS Acceleration Versus Frequency.....	16
8.2.10 Principal Component Spectral Analysis (PCSA)	16

PIMS ISS Increment-2 Microgravity Environment Summary Report: May to August 2001

9. ISS Increment-2 Reduced Gravity Environment Description	16
9.1 Quasi-steady Microgravity Environment	16
9.1.1 XVV Torque Equilibrium Attitude	17
9.1.2 XPOP Inertial Flight Attitude	17
9.2 Docking and Undocking Events	18
9.2.1 Soyuz TM-31 Undocking	18
9.2.2 Progress 4P docking	18
9.2.3 STS-104 and STS-105 Dockings	18
9.2.4 STS-105 Undocking	19
9.2.5 10.2 psi Cabin Depressurization.....	19
9.2.6 Station Reboost.....	19
9.3 Vibratory Microgravity Environment	20
9.3.1 Vehicle Operations	21
9.3.1.1 Dockings and Undockings	21
9.3.1.1.1 Progress, Flight 4P	21
9.3.1.1.2 Space Shuttle Atlantis (STS-104), Flight 7A	21
9.3.1.1.3 Space Shuttle Discovery (STS-105), Flight 7A.1	22
9.3.2 Vehicle Subsystems.....	23
9.3.2.1 SKV-1 FGB Air Conditioner/Dehumidifier.....	23
9.3.3 Structural Modes	24
9.3.4 Vehicle Vibratory Requirements.....	25
9.3.5 Experiment Operations	26
9.3.5.1 EXPPCS Sample Mix	26
9.3.5.2 EXPPCS Rheology	27
9.3.6 ADVASC	29
9.3.7 MAMS Thermal Cooling Fan Characterization.....	31
9.3.8 Crew Activity	32
9.3.8.1 Crew Wake.....	33
9.3.8.2 Exercise.....	33
9.3.8.2.1 Ergometer	33
10. PCSA.....	34
11. Summary of Findings	36
11.1 Quasi-steady Acceleration Regime Summary	36
11.2 Vibratory Acceleration Regime Summary	36
12. References	38
Appendix A. On-line Access to PIMS Acceleration Data Archive.....	41
Appendix B. Some Useful Acceleration Data and Microgravity Related URLs	43
Appendix C. Acronym List and Definition.....	45

List of Tables

Table 2.1-1 ISS Specifications at Assembly Complete	2
Table 4.2-1 MAMS Sensor Coordinate Systems.....	6
Table 4.4-1 SAMS SE Coordinate Systems.....	7
Table 6-1 Increment-2 Payloads.....	8

PIMS ISS Increment-2 Microgravity Environment Summary Report: May to August 2001

Table 7-1 SAMS Data Flow Rates	9
Table 8.1-1 MAMS OSS Power On/Off Cycles for Increment-2	11
Table 9.3-1 ISS Increment-2 Disturbance	20
Table 9.3.1.1.2-1 STS-104, Flight 7A Ku-Band Antenna Dither Transmission	22
Table 9.3.1.1.3-1 STS-105, Flight 7A.1 Ku-Band Antenna Dither Transmission	23
Table 9.3.2.1-1 SKV-1 RMS Acceleration ($23 < f < 24$ Hz)	24
Table 9.3.3-1 Target Modes For ISS Assembly Complete Configuration.....	25
Table 9.3.5.2-1 EXPPCS Operations Timeline	28
Table 9.3.6-1 ADVASC Experiment Operations Timeline	29
Table 9.3.6-2 Snapshot of ADVASC RMS Acceleration Contributions.....	30
Table 9.3.7-1 Snapshot of MAMS Fan RMS Acceleration Contribution.....	32
Table 10-1 MAMS HiRAP (100 Hz) PCSA Parameters	34
Table 10-2 SAMS 121f06 (200 Hz) PCSA Parameters.....	35
Table 10-3 SAMS 121f03 (200 Hz) PCSA Parameters.....	35
Table 11.1-1 Summary of Findings for Increment-2: Quasi-steady.....	36
Table 11.2-1 Summary of Findings for Increment-2: Vibratory Analysis.....	37

List of Figures

Figure 1 On-Line Data Access Flow Chart.....	41
Figure 2 Screenshot of Sample PAD File Listing	42
Figure 2.1-1 International Space Station at Assembly Complete.....	47
Figure 2.2-1 Space Station Analysis Coordinate System.....	48
Figure 2.3-1 ISS XVV Flight Attitude.....	48
Figure 2.4-1 United States Laboratory Module (Destiny) Coordinate System.....	49
Figure 3.1-1 ISS Increment-2 Configuration.....	50
Figure 3.2-1 Increment-2 Coordinate Systems.....	51
Figure 3.3-1 ISS in the XPOP Inertial Flight Attitude.....	52
Figure 5-1 EXPRESS Rack 1 6A On-Orbit Configuration.....	53
Figure 5-2 EXPRESS Rack 2 6A/7A On-Orbit Configuration.....	53
Figure 8.1.1-1 Trimmed Mean Filter Process	54
Figure 8.2-1 PAD Profile for May of 2001	55
Figure 8.2-2 PAD Profile for June of 2001	56
Figure 8.2-3 PAD Profile for July of 2001.....	57
Figure 8.2-4 PAD Profile for August of 2001	58
Figure 9.1.1-1 Time Series of Crew Sleep Period During Torque Equilibrium Attitude (OSS).....	59
Figure 9.1.1-2 Time Series of Crew Sleep During Torque Equilibrium Attitude (OSS)	60
Figure 9.1.1-3 QTH of Torque Equilibrium Attitude Compilation of GMT 123/21:00:10 for 187 hours and GMT 184/08:00:09 for 168 hours (OSS).....	61
Figure 9.1.1-4 QTH of Crew Sleep Periods Compilation During TEA of GMT 123/21:00:10 and GMT 184/08:00:09 for 82 hours (OSS)	62
Figure 9.1.2-1 Time Series of Crew Sleep Period During XPOP Attitude.....	63

PIMS ISS Increment-2 Microgravity Environment Summary Report: May to August 2001

Figure 9.1.2-2 QTH Summary of XPOP Attitude 101 hours beginning GMT 143/06:00:07, 167 hours beginning GMT 150/16:00:13 and 108 hours beginning GMT 157/18:00:09 (OSS).....	64
Figure 9.1.2-3 QTH Summary of Crew Sleep Periods During XPOP Attitude 101 hours beginning GMT 143/06:00:07, 167 hours beginning GMT 150/16:00:13 and 108 hours beginning GMT 157/18:00:09 (OSS).....	65
Figure 9.2.1-1 Time Series of Attitude Change for Undocking of Soyuz TM-31 (OSS).....	66
Figure 9.2.2-1 Time Series of Docking Attitude for Progress (4P) Docking (OSS).....	67
Figure 9.2.3-1 Time Series of Atlantis Docking During STS-104 (OSS)	68
Figure 9.2.3-2 Time Series of Discovery Docking During STS-105 (OSS).....	69
Figure 9.2.3-3 +ZLV +XVV Bias Attitude for STS-105	70
Figure 9.2.3-4 QTH of STS-105 Joint Operations (OSS).....	71
Figure 9.2.4-1 Time Series of STS-105 Undocking Events (OSS).....	72
Figure 9.2.5-1 Time Series of Cabin Depressurization in Preparation for EVA (OSS)	73
Figure 9.2.5-2 QTH of Orbiter Depressurization (OSS).....	74
Figure 9.2.6-1 Time Series of MAMS OSS Sensor Saturation During Station Reboost (OSS).....	75
Figure 9.2.6-2 Interval Magnitude of STS-105 Reboost #3 (121f02)	76
Figure 9.3.1.1.1-1 Acceleration Magnitude of Progress (4P) Docking (HiRAP)	77
Figure 9.3.1.1.1-2 Time Series of Progress (4P) Docking (HiRAP)	78
Figure 9.3.1.1.2-1 Spectrogram of Shuttle (7A) Docking (HiRAP).....	79
Figure 9.3.1.1.2-2 Acceleration Magnitude of Shuttle (7A) Docking Softmate (HiRAP).....	80
Figure 9.3.1.1.2-3 Acceleration Magnitude of Shuttle (7A) Docking Hardmate (HiRAP).....	81
Figure 9.3.1.1.2-4 Spectrogram of Shuttle (7A) Undocking (HiRAP).....	82
Figure 9.3.1.1.2-5 Time Series of Shuttle (7A) Undocking (HiRAP)	83
Figure 9.3.1.1.2-6 Time Series of Shuttle (7A) Undocking (HiRAP)	84
Figure 9.3.1.1.3-1 Spectrogram of Shuttle (7A.1) Docking (HiRAP).....	85
Figure 9.3.1.1.3-2 Acceleration Magnitude of Shuttle (7A.1) Docking Softmate (HiRAP).....	86
Figure 9.3.1.1.3-3 Acceleration Magnitude of Shuttle (7A.1) Docking Hardmate (HiRAP).....	87
Figure 9.3.1.1.3-4 Spectrogram of Shuttle (7A.1) Undocking (HiRAP).....	88
Figure 9.3.1.1.3-5 Spectrogram of Shuttle's Ku-band Dither Signature Off (HiRAP)	89
Figure 9.3.1.1.3-6 Time Series of Shuttle (7A.1) Undocking (HiRAP)	90
Figure 9.3.1.1.3-7 Time Series of Shuttle (7A.1) Undocking (HiRAP)	91
Figure 9.3.2.1-1 Spectrogram of SKV-1 Air Conditioner/Dehumidifier Turn Off (HiRAP)	92
Figure 9.3.2.1-2 PSD of SKV-1 Air Conditioner/Dehumidifier On (HiRAP).....	93
Figure 9.3.2.1-3 PSD of SKV-1 Air Conditioner/Dehumidifier Off (HiRAP)	94

PIMS ISS Increment-2 Microgravity Environment Summary Report: May to August 2001

Figure 9.3.2.1-4 Spectrogram of SKV-1 Spectral Signature On (121f02).....	95
Figure 9.3.2.1-5 Spectrogram of SKV-1 Spectral Signature Off (121f02).....	96
Figure 9.3.2.1-6 Spectrogram of SKV-1 Spectral Signature On (121f02).....	97
Figure 9.3.2.1-7 Interval RMS of SKV-1 Off (121f02).....	98
Figure 9.3.2.1-8 Interval RMS of SKV-1 Off (121f04).....	99
Figure 9.3.2.1-9 Interval RMS of SKV-1 On (121f02)	100
Figure 9.3.2.1-10 Interval RMS of SKV-1 On (121f04).....	101
Figure 9.3.3-1 Spectrogram of Below 2 Hz (HiRAP)	102
Figure 9.3.3-2 PSD of Spectral Averaged 8-Hour Period Below 2 Hz (HiRAP).....	103
Figure 9.3.4-1 OTO of ADVASC On and Crew Awake (HiRAP)	104
Figure 9.3.4-2 OTO of EXPPCS and ADVASC On and Crew Asleep (HiRAP)	105
Figure 9.3.4-3 OTO of EXPPCS and ADVASC On and Crew Asleep (121f06).....	106
Figure 9.3.5.1-1 Spectrogram of EXPPCS Sample Mix Operation (121f06)	107
Figure 9.3.5.1-2 Interval Min/Max of EXPPCS Sample Mix Operation On (121f06)	108
Figure 9.3.5.1-3 PSD of EXPPCS Sample Mix Operation On (121f06)	109
Figure 9.3.5.1-4 PSD of EXPPCS Sample Mix Operation Off (121f06)	110
Figure 9.3.5.1-5 Cumulative RMS of EXPPCS Sample Mix Operation On (121f06)	111
Figure 9.3.5.1-6 Cumulative RMS of EXPPCS Sample Mix Operation Off (121f06).....	112
Figure 9.3.5.1-7 Spectrogram of EXPPCS Sample Mix Operation On (121f03)	113
Figure 9.3.5.1-8 Spectrogram of EXPPCS Sample Mix Operation On (121f04)	114
Figure 9.3.5.1-9 Interval Min/Max of EXPPCS Sample Mix Operation On (121f03).....	115
Figure 9.3.5.1-10 Interval Min/Max of EXPPCS Sample Mix Operation On (121f04)	116
Figure 9.3.5.2-1 Spectrogram of EXPPCS Rheology On (121f06).....	117
Figure 9.3.6-1 Spectrogram of ADVASC Equipment On and Off (HiRAP).....	118
Figure 9.3.6-2 Spectrogram of ADVASC Deactivation (HiRAP)	119
Figure 9.3.6-3 PSD of ADVASC Equipment On and Off (HiRAP)	120
Figure 9.3.6-4 Cumulative RMS of ADVASC Equipment On and Off (HiRAP)	121
Figure 9.3.6-5 Interval RMS of ADVASC Equipment On and Off (HiRAP)	122
Figure 9.3.6-6 PSD of ADVASC Equipment Frequency Shift (HiRAP)	123
Figure 9.3.7-1 Spectrogram of MAMS Fan On and Off (121f02)	124
Figure 9.3.7-2 PSD of MAMS Fan On and Off (121f02).....	125
Figure 9.3.8.1-1 PSD of Crew Sleep and Wake (HiRAP)	126
Figure 9.3.8.2.2-1 Spectrogram of Ergometer Signature (HiRAP)	127
Figure 10-1 PCSA of Below 100 Hz (HiRAP).....	128
Figure 10-2 PCSA of Below 200 Hz (121f06).....	129
Figure 10-3 PCSA of Below 200 Hz (121f03).....	130

1 Introduction

The NASA Physical Science Division sponsors science experiments on various reduced-gravity carriers/platforms and facilities such as the Space Transportation System (STS), parabolic flight-path aircraft, sounding rockets, drop towers and the International Space Station (ISS). To provide support for the science experiments which require acceleration data measurement on the ISS, the Physical Science Division sponsors two microgravity accelerometer systems, the Space Acceleration Measurement System (SAMS) and the Microgravity Acceleration Measurement System (MAMS). SAMS measures vibratory acceleration data in the range of 0.01 to 300 Hz for payloads requiring such measurement. MAMS consists of two sensors, the Orbital Acceleration Research Experiment (OARE) Sensor Subsystem (OSS), a low frequency range sensor (up to 1 Hz), used to characterize the quasi-steady environment for payloads and the ISS vehicle, and the High Resolution Accelerometer Package (HiRAP) used to characterize the ISS vibratory environment from 0.01 Hz to 100 Hz. Both MAMS and SAMS were flown to the ISS on STS-100 launched on April 19, 2001 from the Kennedy Space Center (KSC).

The residual acceleration environment of an orbiting spacecraft in a low earth orbit is a complex phenomenon [1]. Many factors, such as experiment operation, life-support systems, crew activities, aerodynamic drag, gravity gradient, rotational effects and the vehicle structural resonance frequencies (structural modes) contribute to form the overall reduced gravity environment. Weightlessness is an ideal state, which cannot be achieved in practice because of the various sources of acceleration present in an orbiting spacecraft. As a result, the environment in which experiments are conducted is *not zero* gravity, and most experiments can be affected by the residual acceleration because of their dependency on acceleration magnitude, frequency, orientation and duration. Therefore, experimenters must know what the environment was when their experiments were performed in order to analyze and correctly interpret the result of their experimental data. In a terrestrial laboratory, researchers are expected to know and record certain parameters such as pressure, temperature, humidity level in their laboratory prior to and possibly throughout their experiment. The same holds true in space, except that acceleration effects emerge as an important consideration.

The NASA Glenn Research Center (GRC) Principal Investigator Microgravity Services (PIMS) project has the responsibility for processing and archiving acceleration measurements, analyzing these measurements, characterizing the reduced gravity environment in which the measurements were taken, and providing expertise in reduced gravity environment assessment for a variety of carriers/platforms and facilities, such as the Space Shuttle, parabolic flight-path aircraft, sounding rockets, drop towers and the ISS in support of NASA's PSD Principal Investigators (PIs). The PIMS project supports PIs from the microgravity science disciplines of biotechnology, combustion science, fluid physics, material science and fundamental physics. The PIMS project is funded by NASA Headquarters and is part of NASA GRC's Microgravity Measurement and Analysis Project (MMAP), which integrates the analysis and interpretation component of PIMS with various NASA sponsored acceleration measurement systems. The PIMS project is responsible for receiving, processing, displaying, distributing, and archiving the

acceleration data for SAMS and MAMS during ISS operations. This report presents to the microgravity scientific community the results of some of the analyses performed by the PIMS using the acceleration data collected by the two-accelerometer systems during the period from May to August, 2001 aboard the ISS.

2 International Space Station

2.1 Configuration at Assembly Complete

The ISS represents a global partnership of many nations. This project is an engineering, scientific and technological marvel ushering in a new era of human space exploration. Assembly of the ISS began in late 1998 [2] and will continue until completion sometime around the year 2004. During its assembly and over its nominal 10-year lifetime, the ISS will serve as an orbital platform for the United States and its International Partners to make advances in microgravity, space, life, and earth sciences, as well as in engineering research and technology development. The completed space station will have six fully equipped laboratories, nearly 40 payload racks [3] or experiment storage facilities, and more than 15 external payload locations for conducting experiments in the vacuum of space. The six main laboratories, which will house research facilities, are: Destiny (US), the Centrifuge Accommodations Module (CAM-US), Columbus (ESA), Kibo (NASDA) and two Russian Research Modules (yet to be named). The pressurized living and working space aboard the completed ISS will be approximately 43,000 ft³ [4] (Table 2.1-1). Its giant solar arrays will generate the electricity needed. An initial crew of three, increasing to seven when assembly is complete (Figure 2.1-1), is living aboard the ISS. The space station represents a quantum leap in our ability to conduct research on orbit and explore basic questions in a variety of disciplines [4] such as biomedical, fundamental biology, biotechnology, fluid physics, advanced human support technology, material science, combustion science, fundamental physics, earth science and space science.

TABLE 2.1-1 ISS SPECIFICATIONS AT ASSEMBLY COMPLETE

Wingspan Width	356 feet (108.5 m)
Length	290 feet (88.4 m)
Mass (weight)	About 1 million pounds (453,592 kg)
Operating Altitude	220 nautical miles average (407 km)
Inclination	51.6 degrees to the Equator
Atmosphere inside	14.7 psi (101.36 kilopascals)
Pressurized Volume	43,000 ft ³ (1,218 m ³) in 6 laboratories
Crew Size	3, increasing to 7

2.2 ISS Analysis Coordinate System

For ISS operations, PIMS reports acceleration data to the microgravity scientific community using the ISS analysis coordinate system or in a specific sensor's coordinate system. The ISS analysis system [5] is derived using the Local Vertical Local Horizontal (LVLH) flight orientation. When defining the relationship between this coordinate system and another, the Euler angle sequence to be used is a yaw, pitch, roll sequence around the Z_A , Y_A , and X_A axes, respectively (Figure 2.2-1). The ISS Analysis frame is aligned with the S0 Coordinate frame, and the origin is located at the geometric center of the Integrated Truss Segment (ITS) S0. The X_A -axis is parallel to the longitudinal axis of the module cluster. The positive X-axis is in the forward (flight) direction. The Y_A -axis is identical to the S0 axis. The nominal alpha solar array joint rotational axis is parallel with the Y_A -axis. The positive Y_A -axis is in the starboard direction. The positive Z_A -axis is in the direction of Nadir (toward earth) and completes the right-handed Cartesian system (RHCS). This analysis coordinate system will be used by PIMS in its analysis and reporting of the acceleration data measured on ISS unless sensor coordinate system is specified. A more detailed description of the ISS coordinate systems can be found in [5].

2.3 ISS Flight Attitude at Assembly Complete

The basic flight attitude [6] for ISS is called XVV Z Nadir TEA, or XVV TEA for short. XVV Z Nadir (XVV for short) stands for X body axis toward the velocity vector, Z body axis toward Nadir (earth), and TEA is for torque equilibrium attitude. The ISS vehicle design is optimized for the XVV attitude (Figure 2.3-1). That attitude places the most modules in the microgravity volume; supports altitude reboosts, services vehicle dockings, and minimizes aerodynamic drag. The ISS is designed to tolerate deviations from perfect XVV Z Nadir of +/- 15 degrees in each axis. This envelope was expanded to -20 degrees in pitch.

2.4 United States Laboratory Module (Destiny) Coordinate System

The US Laboratory module makes use of a RHCS [5], body-fixed to the pressurized module. The origin is located forward of the pressurized module such that the center of the bases of the aft trunnions have X_{LAB} components nominally equal to 1000 inches. The X_{LAB} -axis is perpendicular to the nominal aft Common Berthing Mechanism (CBM) interface plane and pierces the geometric center of the array of mating bolts at the aft end of the pressurized module. The positive X_{LAB} -axis is toward the pressurized module from the origin. The Y_{LAB} -axis completes the RHCS. The Z_{LAB} -axis is parallel to the perpendicular line from the X_{LAB} -axis to the center base of the keel pin base, and positive in the opposite direction as shown in Figure 2.4-1.

3 ISS Increment-2

3.1 Increment-2 Configuration

An increment should average about 4 months and is determined by crew rotations and flights to/from ISS. Each increment has a theme that focuses on the primary science or activities to be performed. This report focuses on Increment-2 or Expedition Two and its theme [7] is: Radiation. The 3-member crew for Increment-2 mission was launched to the ISS on March 2001 on STS-102 from KSC. Increment-2 has four modules on-orbit [8]: Unity (Node), Zarya (Functional Cargo Block), Zvezda (Service Module) and Destiny, Figure 3.1-1.

3.2 Increment-2 Coordinate Systems

The coordinate systems [9] shown in Figure 3.2-1 were used in performing the data analysis presented in this report. Figure 3.2-1 shows MAMS OSS and MAMS HiRAP positive acceleration axes alignment relative to the ISS analysis coordinate system (for SAMS, see section 4.4). However, the origin of the coordinate systems shown is not exactly at the location shown (except for the ISS analysis coordinate system). They are shown here for relative alignment only, not their origin. For their location relative to the ISS analysis coordinate system, the reader should refer to Table 4.2-1. In Figure 3.2-1, XYZ_A refers to the ISS analysis coordinate system, XYZ_H refers to the MAMS HiRAP coordinate system, XYZ_{OSS} refers to the MAMS OSS coordinate system. Figure 3.2-1 is applicable only to Increment-2.

3.3 Increment-2 Overall Attitude

During the assembly stages (stages 2A through 12A.1), the ISS will not be capable of generating enough power to sustain the required electrical loads in the XVV flight attitude at mid-to-high solar beta angles because these vehicle configurations have only a single solar array gimbal axis, which is aligned so that it only perfectly tracks the Sun when the solar beta angle is near zero. Therefore, the ISS is designed to accommodate a second basic flight orientation for these increments. This attitude is referred to as XPOP, Figure 3.3-1, which stands for X principal axis perpendicular to the orbit plane, Z Nadir at orbital noon. The XPOP flight attitude [6] sets up geometry between the ISS and the Sun so that the Sun aligns with the ISS/XZ body axis plane. This allows all the solar arrays to track the Sun regardless of the solar beta angle. XPOP also places the dominant inertia axis in the local horizontal to minimize gravity gradient torques and allow Control Moment Gyro (CMG) non-propulsive attitude control.

3.4 Increment-2 Crew Members

During Increment-2 (Expedition Two), the crew worked with 18 different experiments. The Increment-2 was designed to characterize the space station environment by measuring effects such as radiation exposure and vibration, which could impact humans and experiments on the station. Other research included studies of the human body in space, observations of the earth, crystal growth and plant growth in space [10].

Increment-2 had two astronauts and one cosmonaut. The commander was cosmonaut Yuri Usachev; Flight Engineer 1 was James Voss and Susan Helms was Flight Engineer 2. The crew was launched to the ISS on March 8, 2001 aboard the Space Shuttle Discovery STS-102 and returned to KSC on August 22, 2001 aboard STS-105.

4 Accelerometer Systems' Description and Locations

One of the major goals of ISS is to provide a quiescent reduced gravity environment to perform fundamental scientific research. However, small disturbances aboard the Space Station impact the overall environment in which experiments are being performed. Such small disturbances need to be measured in order to assess their potential impact on the experiments. Two accelerometer systems developed by NASA's GRC in Cleveland, Ohio, are being used aboard the station to acquire such measurements. These two systems were flown to the ISS on April 19, 2001 aboard the space shuttle flight STS-100.

4.1 Microgravity Acceleration Measurement System (MAMS)

MAMS measures acceleration caused by aerodynamic drag, vehicle rotations, and vents of air and water. MAMS consists of two sensors, the MAMS OSS, a low frequency sensor (up to 1 Hz) used to characterize the quasi-steady environment for payloads and the vehicle and MAMS HiRAP [11] used to characterize the ISS vibratory environment up to 100 Hz. For Increment-2, MAMS was located in a double middeck locker, in the US Laboratory Module (Destiny). Specifically in the EXpedite the PROcessing of Experiments to the Space Station (EXPRESS) Rack 1 (Figure 5-1).

4.2 MAMS Coordinate Systems

MAMS was located in middeck lockers 3 and 4 of EXPRESS Rack 1, in overhead bay 2 of the US Laboratory Module (LAB1O2). The origin of the OSS coordinate system is located at the center of gravity of the OSS proof mass. Table 4.2-1 gives the orientation and location of the OSS and HiRAP coordinate systems with respect to Space Station Analysis coordinate system.

TABLE 4.2-1 MAMS SENSOR COORDINATE SYSTEMS

Sensor	Location (inches)			Orientation (degrees)			Unit Vector in Analysis Coordinates			
	X _A	Y _A	Z _A	Roll	Pitch	Yaw	Axes	X _A	Y _A	Z _A
OSS	135.28	-10.68	132.12	90	0	0	X _{OSS}	1	0	0
							Y _{OSS}	0	0	1
							Z _{OSS}	0	-1	0
HiRAP	138.68	-16.18	142.35	180	0	0	X _H	1	0	0
							Y _H	0	-1	0
							Z _H	0	0	-1

4.3 Space Acceleration Measurement System (SAMS)

SAMS measures accelerations caused by vehicle, crew, and experiment disturbances. SAMS measures the vibratory/transient accelerations which occur in the frequency range of 0.01 to 300 Hz. For Increment-2, there were five SAMS sensor heads located in and around the EXPRESS Racks 1 and 2. The sensors measure the accelerations electronically and transmit the data to the Interim Control Unit (ICU) located in the EXPRESS Rack drawer. Data is collected from all the sensors and downlinked to the Telescience Support Center (TSC) at GRC. The PIMS project processes, and displays the data on the PIMS Web site for easy access by the microgravity scientific community at:

<http://tsccrusader.grc.nasa.gov/pims>.

4.4 SAMS Coordinate Systems

During Increment-2, there were five SAMS Sensor Enclosures (SE) heads activated, 121f02 through 121f06. Each sensor head has a defined coordinate system whose location and orientation is with respect to the Space Station Analysis Coordinate System. The origin is defined as the triaxial center point of the three accelerometers that comprise the head.

SAMS SE 121f02 was mounted in the SAMS ISIS drawer 1 in EXPRESS Rack 1. SAMS SE heads 121f03, 121f04 and 121f05 were installed in support of ARIS-ICE activities. Head 121f03 was mounted on the lower Z Panel assembly below EXPRESS Rack 2, head 121f04 was mounted on the lower Z Panel assembly below EXPRESS Rack 1, and head 121f05 was mounted on a bracket around the upper Z Panel light assembly of EXPRESS Rack 2. SAMS SE 121f06 was mounted on the front panel of the EXPPCS test section on EXPRESS Rack 2. Table 4.4-1 summarizes the SAMS SE coordinate systems.

TABLE 4.4-1 SAMS SE COORDINATE SYSTEMS

Sensor	Location (inches)			Orientation (degrees)			Unit Vector in Analysis Coordinates			
	X _A	Y _A	Z _A	Roll	Pitch	Yaw	Axes	X _A	Y _A	Z _A
121f02	128.73	-23.53	144.15	-90	0	-90	X _{F02}	0	-1	0
							Y _{F02}	0	0	-1
							Z _{F02}	1	0	0
121f03	191.54	-40.54	135.25	0	30	-90	X _{F03}	0	-.866	-.500
							Y _{F03}	1	0	0
							Z _{F03}	0	-.5	.866
121f04	149.54	-40.54	135.25	0	30	-90	X _{F04}	0	-.866	-.500
							Y _{F04}	1	0	0
							Z _{F04}	0	-.5	.866
121f05	185.17	38.55	149.93	90	0	90	X _{F05}	0	1	0
							Y _{F05}	0	0	1
							Z _{F05}	1	0	0
121f06	179.90	-6.44	145.55	180	90	0	X _{F06}	0	0	-1
							Y _{F06}	0	-1	0
							Z _{F06}	-1	0	0

5 ISS Increment-2 Facilities Supported by PIMS

During Increment-2, the following facilities were activated: the Human Research Facility, two EXPRESS Racks, one of which was equipped with the Active Rack Isolation System (ARIS) and the Payload Equipment Restraint System. Over the life of the Space Station, these facilities will support a wide range of experiments [10]. During Increment-2, the PIMS project supported EXPRESS Racks 1 and 2.

The EXPRESS Rack [12] is a standardized payload rack system that transports, stores and supports experiments aboard the International Space Station. The EXPRESS Rack system supports science payloads in several disciplines, including biology, chemistry, physics, ecology and medicine. The EXPRESS Rack with its standardized interfaces enables quick, simple integration of multiple payloads aboard the station. Each EXPRESS Rack is housed in an International Standard Payload Rack – a refrigerator-size container that acts as the EXPRESS Rack's exterior shell – and can be divided into segments. The first two EXPRESS Racks [13] have eight middeck locker locations and two drawer locations each (Figures 5-1, 5-2).

6 ISS Increment-2 Experiments Supported by PIMS

During this increment, the PIMS project supported the following experiments, which require acceleration data measurements to assess the impact of the ISS reduced gravity environment on the science: Active Rack Isolation System ISS Characterization Experiment (ARIS-ICE), Protein Crystal Growth-Biotechnology Ambient Generic (PCG-BAG) and Experiment of Physics of Colloids in Space (EXPPCS). Table 6-1 [14] shows the experiments that were performed by the Increment-2 crew.

TABLE 6-1 INCREMENT-2 PAYLOADS

Facility/Experiment	Mission information	Duration	Location on ISS	Research Area
Active Rack Isolation System	Mission 6A STS-100	15 years	Express Rack 2 Destiny module	
Express Racks 1 & 2	Mission 6A STS-100	15 years	Destiny module	Multidisciplinary
Human Research Facility	Mission 5A.1 STS-102	15 years	Destiny module	Human Life sciences
Payload Equipment Restraint System	Mission 5A.1 STS-102	15 years	Destiny module	
Advanced Astroculture (ADVASC)	Mission 6A STS-100	3 months (return on Mission STS-105, 7A.1)	Express Rack 1 Destiny module	Space Product Development Commercial biotechnology
Bonner Ball Neutron Detector Radiation	Mission 5A.1 STS-102	8 months	Destiny module	Human Life Sciences -- Radiation
Commercial Genetic Bioprocessing Apparatus (CGBA)	Mission 6A STS-100	3 months (return on Mission STS-105, 7A.1)	Express Rack 1 Destiny module	Space Product Development Biotechnology
Commercial Protein Crystal Growth—High Density (CPCG-H)	Mission 6A STS-100	3 months (return on mission STS-105, 7A.1)	Express Rack 1 Destiny module	Space Product Development--Protein crystallization
Crew Earth Observation	Mission 4A STS-97	15 years	Destiny and Zvezda modules	Space Flight Utilization Earth observation
Dosimetric Mapping (DOSMAP)	Mission 5A.1 STS-102	4 months	Destiny module	Human Life Sciences -- Radiation
Earth Knowledge Acquired by Middle Schools (EarthKAM)	Mission 5A STS-98	15 years	Destiny module window	Space Flight Utilization—Earth observation and outreach
H-Reflex	Mission 5A.1 STS-102	4 months (assigned for Exp. 2-4)	Human Research Facility Rack Destiny module	Human Life Sciences---Neurovestibular
Interactions	Mission 5A.1 STS-102	2 years, 4 months assigned to Exp. 2-6)	Human Research Facility Rack Destiny module	Human Life Sciences--Psychosocial
ARIS-ISS Characterization	Mission 6A STS-100	7 months (?)	Active Rack Isolation	Space Flight Utilization
Experiment (ARIS-ICE)		Mission UF1, STS-105)	System	Earth Observation and Outreach
Microgravity Acceleration Measurement System (MAMS)	Mission 6A STS-100	15 years	Express Rack 1 Destiny module	Physical Sciences--Environmental
Phantom Torso	Mission 6A STS-100	3 months (return on mission STS-105, 7A.1)	Destiny module	Human Life Sciences--Radiation
Physics of Colloids in Space (EXPPCS)	Mission 6A STS-100	1 year (return on mission UF2 STS-111)	Express Rack 2 Destiny module	Physical Sciences—Fluids science
Protein Crystal Growth—Biotechnology Ambient Generic (PCG-BAG)	Mission 7A STS-104	2 months (return on mission STS-105, 7A.1)	Destiny module stowage space	Physical Sciences—Protein crystallization
Protein Crystal Growth—Single Locker Thermal Enclosure System (PCG-STES)	Mission 6A STS-100 and 7A STS-104	2 months (return on mission STS-105, 7A.1)	Express Rack 1 Destiny module	Physical Sciences—Protein crystallization
Space Acceleration Measurement System II (SAMS-II)	Mission 6A STS-100	15 years	Destiny module	Physical Sciences--Environmental
Sub-regional Assessment of Bone Loss in Axial Skeleton (Sub-regional Bone	Mission 5A.1 STS-102	2 years, 4 months (assigned to Exp. 2-6)	N/A—Preflight and post-flight data collection only	Human Life Sciences—Bone and muscle

7 MAMS and SAMS Data Flow Descriptions

The MAMS hardware contains two acceleration measurement systems called MAMS-OSS and MAMS HiRAP, each with a distinct measurement objective. The purpose of the MAMS OSS data is to measure the quasi-steady accelerations on the ISS. MAMS-OSS data are obtained at a rate of 10 samples per second and are low-pass filtered with a cutoff frequency of 1 Hz. Each MAMS OSS data packet contains 16 seconds of MAMS-OSS acceleration data and is transmitted in real-time at a rate of one data packet every 16 seconds. MAMS has the capability to store 25.6 hours of MAMS OSS data on board. Activated at MAMS power up or via ground command, this on board storage capability allows capturing of critical quasi-steady acceleration events for later downlink. These stored acceleration data can be transmitted to ground at a ground commanded rate between 20 and 200 kbps.

The MAMS HiRAP data are obtained at a fixed rate of 1000 samples per second and low pass filtered with a cutoff frequency of 100 Hz. The purpose of the MAMS HiRAP data is to measure the vibratory and transient accelerations on the ISS. Each MAMS HiRAP data packet contains 192 acceleration readings and is transmitted at a rate of one data packet every 0.192 seconds. MAMS does not have any capability to store MAMS-HiRAP data on board.

Like MAMS HiRAP, the SAMS sensor heads are designed to measure the vibratory and transient accelerations on the ISS. Each SAMS sensor can be commanded to measure and downlink acceleration data at one of five sampling rates, with five corresponding cutoff frequencies. Since the SAMS sampling rate can be varied, the number of readings per packet and the number of packets per second varies as a function of the user selected sampling rate. Table 7-1 illustrates the relationship amongst sampling rate, cutoff frequency, acceleration readings per packet, and acceleration data packets per second for the SAMS sensors.

TABLE 7-1 - SAMS DATA FLOW RATES

Sampling Rate (samples/sec)	Cutoff Frequency (Hz)	Readings Per Packet	Packets Per Second
62.5	25	31 or 32	2
125	50	62 or 63	2
250	100	74 or 51	4
500	200	74 or 28	8
1000	400	74 or 56	14

Telemetry from the ISS is not continuous. A time interval where real time data downlink is available is referred to as an Acquisition of Signal (AOS) interval. Similarly, the lack of real time data downlink availability is referred to as a Loss of Signal (LOS) interval. Both SAMS and MAMS acceleration data must rely on ISS on board storage capabilities to eventually obtain acceleration data collected during LOS intervals. This ISS on board storage capability is provided by the Medium-rate Communication Outage Recorder

(MCOR). Consequently, real time acceleration data are available on the ground during AOS periods and acceleration data are stored on the MCOR during LOS periods for eventual downlink. Under normal circumstances, both SAMS and MAMS will measure and transmit acceleration data continuously throughout a given increment.

When acceleration data are transmitted to the ground, either real time data downlink or data transmitted from a dump of the MCOR memory, the resultant acceleration data packets are routed through the White Sands Facility, through Johnson Space Center (JSC), through the Marshall Space Flight Center (MSFC), Huntsville Operation Support Center (HOSC), and ultimately to PIMS Ground Support Equipment (GSE) located at the TSC. The PIMS GSE writes each received packet into a database table dedicated to each accelerometer supported by PIMS. Therefore, a separate database table exists for MAMS OSS, MAMS HiRAP, and for each of the five SAMS sensor heads.

The primary function of the database tables is to automatically merge AOS and LOS data packets for each accelerometer. As there exists overlap between the AOS and LOS acceleration data packets received, each sensor's dedicated database table discards any redundant data packets, resulting in a table containing a contiguous set of acceleration data packets.

Data are accessed from the database table to serve two separate purposes. The first purpose involves obtaining the most recent acceleration data from the table to generate real time plots of the acceleration data in a variety of plot formats supported by PIMS [15]. These real time plots are updated during AOS intervals and electronic snapshots of the data are routed to the PIMS ISS web page (<http://tscrcrusader.grc.nasa.gov/pims>).

The second purpose involves obtaining the oldest acceleration data from the “bottom” of the table. These acceleration data are used to generate the PIMS acceleration data archives used by the PIMS data analysts to generate the plots described in this report. Since the data are processed from the “bottom” of the table, MCOR dumps will have had time to be downlinked, received, and merged by the database table. PIMS currently waits 24 hours before generating any acceleration data archives. Like the electronic snapshots of the real time acceleration data plots, the acceleration data archives are available for download via the PIMS ISS web page.

8 Data Analysis Techniques and Processing

This section briefly describes some assumptions, considerations, and procedures used to acquire and analyze the acceleration data measurements made by the two accelerometer systems: MAMS and SAMS.

8.1 Quasi-steady Regime

MAMS OSS data is collected at 10 samples per second, lowpass filtered with a cutoff frequency of 1 Hz and sent to ground support equipment (GSE) for further processing and storage. PIMS is currently storing the OSS data as raw acceleration files and also

trimmed mean filtered data that are compensated for sensor bias. There are numerous gaps in the data collected during Increment-2, due to data transfer and other problems that result from being a payload during early ISS operations. Table 8.1-1 shows the power on/off times for the MAMS OSS sensor for Increment-2.

TABLE 8.1-1 MAMS OSS POWER ON/OFF CYCLES FOR INCREMENT-2

Power On (GMT)	Power Off (GMT)
May 03, 2001 123/15:58:24	May 11, 2001 131/16:08:26
May 21, 2001 141/07:35:22	May 27, 2001 147/11:05:40
May 28, 2001 148/13:53:08	June 09, 2001 160/13:54:11
June 26, 2001 177/19:13:18	July 12, 2001 193/14:43:07
July 12, 2001 193/22:21:51	July 18, 2001 199/17:08:53*
July 18, 2001 199/17:12:56	July 19, 2001 200/02:33:47*
July 22, 2001 203/02:47:41	July 24, 2001 205/17:42:10*
July 24, 2001 205/17:48:59	Aug 09, 2001 221/14:01:55*
Aug 09, 2001 221/14:05:48	Aug 20, 2001 232/15:00:00**

* MAMS Control Processor Subsystem (MCPS) Reset due to gimbal anomaly troubleshooting

** End of Increment-2

8.1.1 Trimmed mean Filter

The OSS data is processed with an adaptive trimmed mean filter (TMF) to provide an estimate of the quasi-steady acceleration signal by rejecting higher magnitude transients such as thruster firings, crew activity, etc. The trimmed mean filter algorithm used by the MAMS GSE operates on a sliding window of 480 samples, every 16 seconds. The filtering procedure, depicted in Figure 8.1.1-1, sorts the data by magnitude and calculates the deviation from a normal distribution using the Q parameter according to the equation:

$$Q = \frac{[Upper(20\%) - Lower(20\%)]}{[Upper(50\%) - Lower(50\%)]}$$

Where the upper and lower percentage is determined from the sorted data set. Q is used in the following equation to calculate α , an adaptively determined amount of data to trim from the tails.

$$\alpha(Q) = \begin{cases} 0.05 & Q \leq 1.75 \\ 0.05 + 0.35 * \frac{(Q - 1.75)}{0.25} & 1.75 < Q < 2.0 \\ 0.4 & Q \geq 2.0 \end{cases}$$

The quasi-steady acceleration level is computed to be the arithmetic mean of the trimmed set. Trimmed mean filtered data is stored in the PAD archive under “ossbtmf”. Further information concerning the trimmed mean filter can be found in [16-18].

8.1.2 OSS Bias Measurements

MAMS OSS triaxial sensor bias is measured by a sequence of Bias Calibration Table Assembly (BCTA) rotations. A complete bias measurement for a given axis consists of 50 seconds of data recorded in a normal orientation and 50 seconds of data recorded when the axis has been rotated 180 degrees to its opposite orientation. The 50 seconds of data are processed by the MAMS GSE with TMF algorithm applied to the resulting 500 points. Four measurements are made, corresponding with normal X_{oss} and Y_{oss} , opposite X_{oss} and Y_{oss} , opposite X_{oss} and normal Z_{oss} , and normal X_{oss} opposite Z_{oss} . The outputs for each axis and its opposite are summed and divided by two to obtain the bias value. The value is evaluated in relation to the collection of past bias measurements for a given power cycle and is included in the new mean bias calculation or ignored if determined to be out of range. A disturbance in the microgravity environment is sufficient to cause an up ranging in the OSS sensor, which, in turn, will automatically cause the bias to fail. Failed bias calibrations are not repeated. One of the initial goals during Increment-2 operations for MAMS was the characterization of the OSS sensor bias. To accomplish this, bias measurements were initially performed once per hour, but has since been set to one every six hours. A detailed look at the OSS bias calculations will be included in a later report.

In the past, MAMS predecessor, the Orbital Acceleration Research Experiment (OARE), showed a significant initial transient in the bias measurements that would take one to two days to settle out. This phenomenon was not observed in the MAMS OSS data suggesting that the transient was a launch effect. However, there is a bias temperature dependency, seen only during the first 6 hours following a MAMS power on event. At power up, the MAMS instrument takes roughly 4-6 hours to reach the nominal operating temperature of 40 °C, at which point, the bias values can be considered constant. Ground testing indicates a temperature bias coefficient of 0.05 $\mu g/^\circ C$ [19]. We have not yet verified this temperature dependency on orbit, due to an insufficient amount of valid bias points collected during the initial temperature turn on transient. For this reason, PIMS is recommending that users avoid using OSS data within the first 6 hours after a MAMS

power on event. When MAMS OSS support is requested, this 6-hour “settling” time must be taken into consideration.

8.1.3 OSS Bias Calibration Anomaly

At GMT 197/17:10, a failure of a MAMS limit sensor disabled bias calibration measurements for OSS data. The sensor slows the inner gimbal of the BCTA [20] as it nears the end of rotation to facilitate a mild stop. After consultation with the MAMS vendor, an adaptation parameter was modified on-orbit to go to the backup BCTA control mode. This mode uses software control to slow the gimbal and does not affect the bias calibration in any way. Bias calibration ability was restored at GMT 221/14:05:48.

Due to the uncertainty of the orientation of the inner gimbal between GMT 197/17:10 and GMT 203/02:47, the OSS data from this time period has been quarantined.

8.1.4 Quasi-steady Plot Types

The two types of plots used in the analysis of quasi-steady data are acceleration versus time and the quasi-steady three-dimensional histogram (QTH). Unless otherwise noted, these plot types use trimmed mean filtered OSS data.

8.1.4.1 OSS Trimmed Mean Acceleration versus Time

These are single (X, Y, Z, or vector magnitude) or three axes (X, Y, and Z) plots of acceleration in units of μg versus time. These plots give the best accounting of the quasi-steady acceleration vector as a function of time.

8.1.4.2 Quasi-steady Three-dimensional Histogram (QTH)

This type of analysis results in three orthogonal views of the quasi-steady vector. The time series is analyzed using a two-dimensional histogram method where the percentage of time the acceleration vector falls within a two-dimensional bin is plotted as a color. Areas showing colors toward the red end of the spectrum indicate a higher number of occurrences. Conversely, areas showing colors towards the blue end are indicative of a lower percentage, with no occurrences being shown as white. This plot provides a summary of the quasi-steady vector during the total time period considered. Exact timing of an acceleration event is lost in this type of plot.

8.2 Vibratory Regime

The frequency response of the accelerometer systems used to collect vibratory data may extend below 0.01 Hz down to DC, but those instruments are not optimized for making quasi-steady or DC measurements. The MAMS OSS instrument is specialized for this

purpose. Therefore, unless otherwise noted, it is assumed that the vibratory data have been demeaned for plots and analyses of vibratory data. Figures 8.2-1 to 8.2.4 show the available data for the five SAMS SEs and MAMS HiRAP for the Increment-2 time span analyzed in this report. These four figures show sensor designations on the y-axis and the time span (typically one month) on the x-axis. Cutoff frequencies for the sensor heads are listed at the top. Notice that the figures are color-coded. Each color is associated with a cutoff frequency. The white vertical lines in-between the color bars are the gaps in the acceleration data collected by that specific sensor. This means that data is not available for that time span. These figures should be used to determine whether certain sets of data are available before filling out and submitting a data request form at:

<http://tsccrusader.grc.nasa.gov/pims/html/RequestDataPlots.html>.

8.2.1 Demeaned Vibratory Acceleration Data

In the analysis of the vibratory regime, it is understood that a certain amount of bias intrinsic to the measurement process does exist. This bias is manifest as a DC shift of the acceleration measurements away from the true mean value. Similar bias considerations also exist for measurements collected with the intent of analyzing the quasi-steady regime. However, much effort is expended to account for and remove bias from quasi-steady acceleration measurements, whereas in the vibratory regime, the mean value is effectively ignored in the process of demeaning. That is, for vibratory acceleration data, the mean value of the acceleration (on a per-axis basis) is subtracted over the time frame under consideration leaving effectively zero mean acceleration.

8.2.2 Interval Statistics

A plot of acceleration interval statistics in units of g versus time gives some measure of acceleration fluctuations as a function of time. This display type allows relatively long periods to be displayed on a single plot. There are three such interval statistic plots that are employed for this and other reasons as described below: (1) interval average, (2) interval root-mean-square and (3) interval minimum/maximum.

8.2.3 Interval Average

Interval average plots show net accelerations, which last for a number of seconds equal to or greater than the interval parameter, used. Short duration, high amplitude accelerations can also be detected with this type of plot; however, the exact timing and magnitude of specific acceleration events cannot be extracted. This type of display is useful for identifying overall effects of extended thruster firings and other activities that tend to cause the mean acceleration levels to shift. This display type is rarely used for vibratory data.

8.2.4 Interval Root-Mean-Square

Interval root-mean-square (RMS) plots show oscillatory content in the acceleration data. For the period of time considered, this quantity gives a measure of the variance of the acceleration signal. This data representation is useful for identifying gross changes in acceleration levels usually caused by the initiation or cessation of activities such as crew exercise or equipment operations.

8.2.5 Interval Minimum/Maximum

An interval minimum/maximum plot shows the peak-to-peak variations of the acceleration data. For each interval, this plot type shows both the minimum and maximum values, and thereby shows the acceleration data envelope. This type of display is another way to track gross changes in acceleration.

8.2.6 Power Spectral Density

The power spectral density (PSD) is computed from the Fourier transform of an acceleration time series and gives an estimate of the distribution of power with respect to frequency in the acceleration signal. It is expressed in units of g^2/Hz . The method used for computation of the PSD is consistent with Parseval's theorem, which states that the RMS value of a time series signal is equal to the square root of the integral of the PSD across the frequency band represented by the original signal.

8.2.7 Power Spectral Density Versus Time (Spectrogram)

Spectrograms provide a road map of how acceleration signals vary with respect to both time and frequency. To produce a spectrogram, PSDs are computed for successive intervals of time. The PSDs are oriented vertically on a page such that frequency increases from bottom to top. PSDs from successive time slices are aligned horizontally across the page such that time increases from left to right. Each time-frequency bin is imaged as a color corresponding to the base 10 logarithm of the PSD magnitude at that time and frequency. Spectrograms are particularly useful for identifying structure and boundaries in time and frequency over relatively long periods of time.

8.2.8 RMS Acceleration Versus One-Third Octave Frequency Bands

This type of plot quantifies the spectral content in proportional bandwidth frequency bands for a given time interval of interest (nominally 100 seconds). The (nearly) one-third octave bands are those defined by the ISS microgravity requirements; see Table 4 [21]. The results of this analysis are typically plotted along with a bold stair step curve representing the ISS combined vibratory limits in order to compare the acceleration

environment to these prescribed limits. These plots are not particularly useful for identifying the source of a disturbance for a band that exceeds the desired limits.

8.2.9 Cumulative RMS Acceleration Versus Frequency

A plot of cumulative RMS acceleration versus frequency quantifies, in cumulative fashion, the contributions of spectral components to the overall measured RMS acceleration level for the time frame of interest. This plot is also derived from the PSD using Parseval's theorem. It quantitatively highlights key spectral regions; steep slopes indicate strong narrowband disturbances that contribute significantly to the acceleration environment, while shallow slopes indicate relatively quiet portions of the spectrum.

8.2.10 Principal Component Spectral Analysis (PCSA)

The PCSA histogram is computed from a large number of constituent PSDs. The resultant three-dimensional plot serves to summarize magnitude and frequency variations of significant or persistent spectral contributors and envelops all of the computed spectra over the time frame of interest. The two-dimensional histogram is comprised of frequency bins in units of Hz and PSD magnitude bins in units of $\log_{10}(g^2/Hz)$. The third dimension, represented by a color scale, is the percentage of time that a spectral peak was counted within a given frequency-magnitude bin.

9 ISS Increment-2 Reduced Gravity Environment Description

9.1 Quasi-steady Microgravity Environment

The quasi-steady regime is comprised of accelerations with frequency content below 0.01 Hz with magnitudes expected to be on the order of $2 \mu g$ or less. These low-frequency accelerations are associated with phenomena related to the orbital rate, such as aerodynamic drag. Gravity gradient (location of orbiting point not coincident with CM) and rotational effects also contribute to the quasi-steady regime. These effects may dominate dependent on various conditions such as location and vehicle attitude. A final source of acceleration to consider in this regime is venting of air or water from the spacecraft. This action results in a nearly constant, low-level propulsive force. The different quasi-steady environment characteristics seen on the ISS for Increment-2 are primarily related to altitude and attitude of the station. Variation in atmospheric density with time and altitude contribute to the differences in the aerodynamic drag component. Different attitudes will affect the drag component due to the variation of the frontal cross-sectional area of the station with respect to the velocity vector. This section summarizes the effects of different station attitudes, dockings and undockings of the Russian Progress vehicle, Soyuz, STS-104 and 105, cabin depressurization and station reboost, on the quasi-steady acceleration environment.

9.1.1 XVV Torque Equilibrium Attitude

Torque Equilibrium Attitude (TEA) is an attitude that balances the vehicle's gravity gradient and aerodynamic drag torques. This is the attitude that will be flown during microgravity mode to support research. However, TEA will vary with station configuration because of change in mass and aerodynamic properties. During Increment-2, the TEA attitude was nominally YPR = (350.0, 350.7, 0.0) relative to the LVLH coordinate system; where YPR stands for degrees of (yaw, pitch, roll). Figure 9.1.1-1 shows a plot of trimmed mean filtered data taken during a crew sleep period while the station was in TEA on GMT 127/22:30:04. From this figure, note that the Z-axis contribution dominated with a mean value of about $-1 \mu g$, while the Y-axis was about half that.

Figure 9.1.1-2 is also a plot of data measured during TEA and crew sleep starting at GMT 185/23:00:12 but note the different profile especially in the Y and Z-axes. The X-axis magnitude levels are nearly the same value as in the earlier plot (in both cases, an X-axis mean value of about $-0.2 \mu g$ over the span plotted), but the Y and Z axes are not, as seen from the mean values shown on the right margin of this figure. The reason for these differences has not yet been characterized, but one obvious candidate is the state of the solar arrays. A different quasi-steady profile would be expected if the arrays were rotating than if they were locked in position. Further study on the effect of array position will be included in subsequent increment reports.

The QTH plot is a useful tool in comparing the stability of the quasi-steady vector over a long period of time. Figure 9.1.1-3 shows a summary of nearly 355 hours of MAMS OSS data measured during TEA. This data is a compilation of 187 hours beginning GMT 123/21:00:10 and 168 hours beginning GMT 184/08:00:09. Periods were chosen to avoid vehicle dockings, although the Soyuz TM-31 undocking was included in the first period. Figure 9.1.1-4 is a compilation of 82 hours of sleep periods from the same time spans as in Figure 9.1.1-3. It can be clearly seen in comparing the two plots that the quasi-steady vector is much more stable during crew sleep due to some equipment being off and crew activity being minimal.

9.1.2 XPOP Inertial Flight Attitude

XPOP is a sun-tracking, quasi-inertial flight attitude used for power generation. In this attitude, the vehicle's X_A axis is maintained perpendicular to the direction of flight, while the Y_A and Z_A axes are alternately subjected to the drag vector as the vehicle completes an orbit. The time series plot for XPOP attitude in Figure 9.1.2-1 illustrates this nicely, showing a fairly constant X-axis acceleration component near $2 \mu g$, compared to the Y and Z axes, which show a more pronounced cyclical drag profile. The cyclical variation at 45 minutes intervals is due to the twice-per-orbit variation of frontal area in the XPOP attitude.

The summary plot seen in Figure 9.1.2-2 is a 376 hour compilation of MAMS OSS data comprised of 101 hours beginning GMT 143/06:00:07, 167 hours beginning GMT 150/16:00:13 and 108 hours beginning GMT 157/18:00:09. Figure 9.1.2-3 is a plot of the subset of data from the previous QTH plot consisting of only the periods in which the crew was asleep. This plot shows better the characteristic “ring” profile in the YZ plane that was masked by the effects of crew activity.

9.2 Docking and Undocking Events

9.2.1 Soyuz TM-31 Undocking

In terms of the quasi-steady environment, the actual undocking event is less of an impact than the attitude adjustments in preparation for the event. The first undocking event captured in MAMS OSS data, was the Soyuz TM-31 undocking at GMT 126/02:20:49. Referring to Figure 9.2.1-1, at GMT 126/00:19:58 (1.3 hours in the plot) the station began an attitude maneuver to change from +XVV/+ZLV to -XVV/+ZLV, which was a yaw of 180 degrees about the Z_A axis. This maneuver is seen as an offset between 10-15 μg in the X_A axis, and to a lesser extent for the Y and Z axes. The return to +XVV/+ZLV is also evident 2 hours later with greater acceleration seen on the X_A axis.

9.2.2 Progress 4P docking

In Figure 9.2.2-1, the Progress docking at GMT 143/00:24 was preceded by an attitude change from TEA to the docking attitude at approximately GMT 142/22:10. The docking attitude was a YPR = (231, 14.7, 54), relative to the J2000 coordinate system (inertial coordinate system). In this orientation, the X_A axis is close to alignment with the orbital plane.

9.2.3 STS-104 and STS-105 Dockings

MAMS recorded data for a portion of two joint operations with shuttles during Increment 2. The orbiter Atlantis docked to the ISS during mission STS-104 at GMT 195/03:08. Prior to the docking at GMT 194/23:50, the ISS performed a short maneuver from YPR = (350, 351, 0) to YPR = (0, 0, 0) and maintained this attitude until free drift at docking. The attitude maneuvers are the large disturbers with regard to the quasi-steady environment, with the docking event itself not evident in the data. Figure 9.2.3-1 shows the two attitude changes performed before and after docking and the large change in the quasi-steady vector. The quasi-steady profile of the docking of the orbiter Discovery at GMT 224/18:42 during STS-105 is nearly identical, as can be seen in Figure 9.2.3-2. In both cases, there are prominent shifts of about 1 μg and 4 μg in the X_A and Z_A components, respectively. There is a slight change in the Y_A component.

During docked operations the flight attitude was nominally $YPR = (0, 23, 0)$, referred to as +ZLV / +XVV Bias. In this configuration, the orbiter is attached to the Pressurized Mating Adaptor at the end of the USLAB module (PMA-2) and the belly of the orbiter is into the wind, tilted in the direction of nadir (see Figure 9.2.3-3). A summary of the quasi-steady profile during STS-105 can be seen in the QTH plot in Figure 9.2.3-4. Comparing these results with those in Figure 9.1.1-3 give an estimated difference in mean of the quasi-steady vector of $-1.08 \mu g$, $0.85 \mu g$ and $3.44 \mu g$ in the X_A , Y_A and Z_A axes respectively, and a difference in the magnitudes of the mean of $1.61 \mu g$.

9.2.4 STS-105 Undocking

At GMT 232/13:45 control of the shuttle/station complex was handed over to the Orbiter in preparation for undocking. Approximately 5 minutes before undocking, the complex went into free drift, $YPR = \sim(0, 24, 0)$. In the MAMS OSS data plot in Figure 9.2.4-1, the undocking event is seen as a $5\text{--}10 \mu g$ spike in the Z_A -axis at GMT 232/14:52 (1.8 hours in plot). ISS underwent an attitude maneuver to return to its nominal TEA attitude of $YPR = (350, 352, 0)$, the effects of which can be seen in the Z_A -axis in the plot. The other spike on the Z_A -axis at GMT 232/16:20 is a thruster firing occurring during momentum management initialization sequence.

9.2.5 10.2 psi Cabin Depressurization

In preparation for an EVA during STS-104 joint operations, the Orbiter cabin was depressurized from 14.7 psi to 10.2 psi at GMT 226/10:05. The venting is directed in the +/- orbiter Z-axis, which during docked configuration is aligned with X_A . This event is evident in Figure 9.2.5-1 as a step in all three axes, the largest offset being in the $+X_A$ direction, approximately $4 \mu g$. A ramping back towards the original baseline due to the pressure (and thus the force) decreasing can also be seen in all three axes. Figure 9.2.5-2 shows that primarily the impact is in the directionality of the quasi-steady vector; the magnitude remains close to the normal for docked configuration.

9.2.6 Station Reboost

The Station's low altitude and large cross sectional area causes its orbit to decay due to atmospheric drag. To compensate, the Shuttle thrusters were used to do incremental reboosts of the Station. MAMS OSS, which is designed for low-level, quasi-steady acceleration measurements, is not able to accurately measure the environment during these station reboosts. Figure 9.2.6-1 shows raw OSS data during one such event during STS-105, Reboost #3 at GMT 229/12:12. The "clipping" seen in the X_A and Y_A axes is a result of the accelerometer saturating while in lower range before switching to a higher range. For these type of events, neither raw or TMF OSS data should be used. Instead refer to SAMS and MAMS HiRAP data. Figure 9.2.6-2 is an interval magnitude of SAMS SE 121f02 data showing the effects of Reboost #3 in the lower frequency range towards the center of the plot.

9.3 Vibratory Microgravity Environment

The vibratory acceleration regime consists of the acceleration spectrum from 0.01 to 300 Hz, with magnitudes expected to vary greatly depending on the nature of the disturbance sources and on the transmissibility from the sources to the location of interest. These higher frequency accelerations are associated with vehicle systems, experiment-related equipment, and crew activity. Table 9.3-1 shows a list of some of the Increment-2 disturbers [9].

TABLE 9.3-1 ISS INCREMENT-2 DISTURBERS

P6 Truss Segment	<ul style="list-style-type: none"> • Stick slip • Beta gimbal
Service Module	<ul style="list-style-type: none"> • Ergometer (unisolated) • High- Gain Antenna • Fans (VS, TCS, Hygiene) • TCS compressor • Treadmill (isolated) • Solar arrays • Pumps (TCS, WSS, Hygiene)
Node 1	<ul style="list-style-type: none"> • Interim Resistive Exercise Device (IRED) • Fans (CCAV, IMV)
US Lab	<ul style="list-style-type: none"> • Ergometer (isolated) • Fans (AAAs, IMV, THC) • Pumps (CDRA, MCA, water separator)
Z1 Segment	<ul style="list-style-type: none"> • Ku-band antenna • CMG
Transient Disturbances	<ul style="list-style-type: none"> • P6 beta gimbal • SM High-Gain Antenna • SM Solar array • Node 1 IRED • Crew push-off / landing

For the vibratory regime, this summary report examines the impact of some of these disturbers, namely, vehicle operation, vehicle subsystems, experiment operations, and crew activity. Section 9.3.1.1 discusses the impact of docking and undocking of Progress Flight 4P, STS-104, and STS-105 on ISS. In section 9.3.2, the SKV-1 air conditioner/dehumidifier is described and characterized. This piece of equipment is part of the vehicle's environmental control system. Section 9.3.3 points out apparent structural modes below 2 Hz, gleaned from acceleration spectra computed over more than 9 days while section 9.3.4 compares snapshots of acceleration measurements to the ISS vehicle vibratory requirements. Note that this comparison does not consider all of the stipulations specified in [21]. Section 9.3.5 focuses on experiment on orbit operation disturbances. Characterization analysis was performed for EXPPCS, ADVASC and MAMS. Section 9.3.8 takes a cursory look at crew activity and crew exercise impact on the ISS environment. Finally, section 10 makes use of PCSA plots to summarize the

overall environment for Increment-2 based on some of the data that has been analyzed to date for the vibratory regime.

9.3.1 Vehicle Operations

There are a number of ISS modes of operation, such as Standard, Reboost, Un/Docking, Microgravity, and so on [2]. Depending on the objectives for a given mode, a different combination of vehicle systems are expected to be operating for at least part of the time. This section examines some of these modes.

9.3.1.1 Dockings and Undockings

9.3.1.1.1 Progress, Flight 4P

A Russian Progress vehicle docked with the ISS at GMT 23-May-2001 00:24. This cargo vehicle docked at the aft docking port of the Service Module. The MAMS HiRAP at GMT 23-May-2001 registered this docking event as a 10 mg impulse at 00:24:20, as seen at about the 7-second mark in Figure 9.3.1.1.1-1. This transient was followed a few seconds later by a slightly larger, 13 mg peak, which occurred at about GMT 23-May-2001 00:24:23. The topmost trace in Figure 9.3.1.1.1-2 affirms that the Progress approached and gave impetus along the ISS +X_A-direction. First contact between the two spacecrafts excited a Y_AZ_A structural mode at about 1 Hz. This can be seen in the Y and Z plots of Figure 9.3.1.1.1-2.

9.3.1.1.2 Space Shuttle Atlantis (STS-104), Flight 7A

The Space Shuttle Atlantis docked with the ISS at GMT 14-July-2001 03:08 to begin Flight 7A joint operations. This was evidenced in the HiRAP spectrogram of Figure 9.3.1.1.2-1, which shows initial contact or softmate as a vertical red streak just before the 30-minute mark. Figure 9.3.1.1.2-2 shows a peak acceleration magnitude of just over 10 mg registered by HiRAP at GMT 14-July-2001 03:08:31, while Figure 9.3.1.1.2-3 shows a peak acceleration magnitude of a little more than 6 mg at GMT 14-July-2001 03:21:04. This was the time of the final, mechanical capture or hardmate and as seen starting at this time in Figure 9.3.1.1.2-1. Once there is a hard coupling of the two vehicles, a structural path for transmission of the Shuttle's Ku-band antenna's 17 Hz dither is established.

The Ku-band antenna is dithered to avoid mechanical stiction while tracking communications satellites, and is mounted on the Shuttle's forward, starboard cargo bay sill. The measurements used to compute the aforementioned spectrogram were collected at the MAMS HiRAP location in EXPRESS Rack 1 of the US Lab. As a means of quantifying transmission of this 17 Hz disturbance from the Shuttle to the ISS, Parseval's theorem was employed to compute cumulative RMS acceleration versus frequency curves. For reference, SAMS on Shuttle during past microgravity missions routinely

registered the dither disturbance between just below 100 μg_{RMS} and up to around 300 μg_{RMS} [22]. For the Atlantis 7A docking, the HiRAP sensor registered this tightly-controlled disturbance as shown in Table 9.3.1.1.2-1.

TABLE 9.3.1.1.2-1 STS-104, FLIGHT 7A KU-BAND ANTENNA DITHER TRANSMISSION

Event	GMT	Sensor	RMS Acceleration (16.93 < f < 17.13 Hz)
Before Hardmate	14-July-2001 03:17:34 - 03:19:34	MAMS HiRAP	0.6 μg_{RMS}
After Hardmate	14-July-2001 03:22:34 - 03:24:34		22.9 μg_{RMS}

After more than 8 days of Flight 7A joint operations, Figure 9.3.1.1.2-4 shows that the Space Shuttle Atlantis undocked from the ISS at GMT 22-July-2001 04:54. This is evidenced by the sudden disappearance of the Shuttle's Ku-band antenna's 17 Hz dither signature at just after the 30-minute mark of the spectrogram. Vehicle separation was initiated by means of four spring-loaded pushers [23]. This undock mechanism pushed the vehicles apart along the X_A -direction as the X_H -axis trace of Figure 9.3.1.1.2-5 shows. At GMT 22-Jul-2001 04:54:26, a large transient occurred, and presumably this was initial vehicle separation. A 5-second zoom in on the time axis of Figure 9.3.1.1.2-5 produced Figure 9.3.1.1.2-6, where a short-lived, but pronounced 6.7 Hz recoil ensued primarily aligned with the X_A -axis.

9.3.1.1.3 Space Shuttle Discovery (STS-105), Flight 7A.1

The Space Shuttle Discovery docked with the ISS at GMT 12-August-2001 18:42 to begin Flight 7A.1 joint operations. The HiRAP spectrogram of Figure 9.3.1.1.3-1 shows softmate as a vertical red streak soon after the 10-minute mark. Figure 9.3.1.1.3-2 shows a peak acceleration magnitude of about 29 mg measured by HiRAP at GMT 12-August-2001 18:42:25, while Figure 9.3.1.1.3-3 shows a hardmate peak acceleration magnitude of about 13.8 mg at GMT 12-August-2001 19:02:35. Note that the time between softmate and hardmate took approximately 20 minutes for the STS-105 docking, while the span was less than 13 minutes for the earlier STS-104 docking. The longer span for STS-105 was due, at least in part, to binding of a spring-type shock absorber on the mating mechanism. This spring is one of many, all of which serve to dampen relative motion between the 2 vehicles before final mating. As discussed in Section 9.3.1.1, once finally mated, onset of the Ku-band dither signature can be seen in Figure 9.3.1.1.3-1.

Again, as a means of quantifying transmission of the Shuttle's 17 Hz antenna dither disturbance to the ISS, Parseval's theorem was employed to compute cumulative RMS acceleration versus frequency curves. For the Discovery 7A.1 docking, the HiRAP sensor registered this disturbance as shown in Table 9.3.1.1.3-1.

TABLE 9.3.1.1.3-1 STS-105, FLIGHT 7A.1 KU-BAND ANTENNA DITHER TRANSMISSION

Event	GMT	Sensor	RMS Acceleration (16.93 < f < 17.13 Hz)
Before Hardmate	12-August-2001 19:00:05 - 19:02:05	MAMS	0.9 μg_{RMS}
After Hardmate	12-August-2001 19:03:05 - 19:05:05	HiRAP	42.0 μg_{RMS}

After nearly 8 days of Flight 7A.1 joint operations, the Space Shuttle Discovery undocked from the ISS at GMT 20-August-2001 14:52. This is evidenced by the red vertical streak at just after the 30-minute mark in Figure 9.3.1.1.3-4. Unlike the STS-104, 7A undocking, there was not the telltale sign of Shuttle departure from the sudden disappearance of the Ku-band antenna 17 Hz dither signature. Figure 9.3.1.1.3-5 shows that the Shuttle's Ku-band antenna stopped dithering at about GMT 20-August -2001 14:15. Again, vehicle separation was initiated by means of four spring-loaded pushers, acting along the X_A -direction as the X_H -axis trace of Figure 9.3.1.1.3-6 shows. At GMT 20-August-2001 14:52:21, a large transient occurred, and presumably this was initial vehicle separation. A 5-second zoom in on the time axis of Figure 9.3.1.1.3-6 produced Figure 9.3.1.1.3-7, where a brief, but prominent 6.7 Hz oscillation arose and was primarily aligned with the X_A -axis.

9.3.2 Vehicle Subsystems

9.3.2.1 SKV-1 FGB Air Conditioner/Dehumidifier

The SKV-1 air conditioner/dehumidifier is located in the FGB module of the ISS and is part of the Environmental Control and Life Support System (ECLSS). As first witnessed on a PIMS real-time display at the GRC TSC, Figure 9.3.2.1-1, the SKV-1 turned off in preparation for an EVA at around GMT 08-June-2001, 09:42:00 as evidenced by the abrupt termination of the horizontal yellow streak. The PSDs shown in Figure 9.3.2.1-2 were computed from HiRAP data not long before that turn-off time. Close examination of the PSDs show that the SKV-1 operates at a fundamental frequency near 23.5 Hz. The spectral peak at this frequency seen on all three orthogonal sensor axes vanished when the SKV-1 was turned off as shown in Figure 9.3.2.1-3.

For further examination of the SKV-1 disturbance source, a time frame spanning more than 2 days starting on GMT 07-August-2001 was analyzed. The SKV-1 spectral signature can be seen just after the large (dark blue) data gap in the SAMS 121f02 spectrogram of Figure 9.3.2.1-4. On this spectrogram, the signature appears as a distinct red horizontal streak at 23.3 Hz. It is not definite when the SKV-1 turned on, but Figure 9.3.2.1-5 shows that it turned off at GMT 07-August-2001, 16:30. A few minutes later, it cycled back on, but at a higher frequency (23.9 Hz) before settling down to 23.4 Hz and then turning back off again at GMT 07-August-2001, 19:40:30. It remained off for about

13.7 hours before turning back on again at GMT 08-August-2001, 09:22:00 as seen in Figure 9.3.2.1-6. Again, the operating frequency starts relatively high and settles down to 23.6 Hz after about 4.5 hours. It then abruptly stepped down in frequency to 23.5 Hz at GMT 08-August-2001 14:15:00. While it is unclear at this time what factors affect its operating characteristics, it is clear that the SKV-1 plays a key role in the vibratory regime, albeit in a narrow range of the acceleration spectrum.

In order to quantify the impact of this disturbance on the vibratory environment, Parseval's theorem was used to parse out the RMS acceleration from the frequency range 23 to 24 Hz. Two 8-hour periods and two SAMS sensor heads (121f02 and 121f04) were used for this purpose. The first period started at GMT 08-August-2001 00:00:00, and was devoid of SKV-1 operation. The SKV-1 operated incessantly, however, during the second period starting at GMT 08-August-2001 16:00:00. The first period (SKV-1 OFF) results for SAMS SE 121f02 and SE 121f04 are shown in Figure 9.3.2.1-7 and Figure 9.3.2.1-8, respectively. The second period (SKV-1 ON) results for SAMS SE 121f02 and SE 121f04 are shown in Figure 9.3.2.1-9 and Figure 9.3.2.1-10, respectively. Table 9.3.2.1-1 summarizes the findings from this analysis.

TABLE 9.3.2.1-1 SKV-1 RMS ACCELERATION (23 < f < 24 Hz)

Event	GMT Start of 8-Hour Span	Sensor	RMS Acceleration (μg_{RMS})	
			Median	Mean
SKV-1 OFF	08-August-2001 00:00:00	SAMS 121f02	6.3	7.8
SKV-1 OFF	08-August-2001 00:00:00	SAMS 121f04	9.4	13.1
SKV-1 ON	08-August-2001 16:00:00	SAMS 121f02	40.7	41.5
SKV-1 ON	08-August-2001 16:00:00	SAMS 121f04	40.0	38.0

From this analysis, the SKV-1 contributes about 30 μg_{RMS} between 23 and 24 Hz in or around the EXPRESS rack 1 location as measured by the SAMS SE 121f02 and 121f04. Note that there exists a short train of disturbances near the frequency range under analysis. These registered with greater magnitude at the Z-panel mounted 121f04 sensor. This accounts, at least in part, for the difference seen for the "SKV-1 OFF" rows in Table 9.3.2.1-1.

9.3.3 Structural Modes

As opportunities arise, directional and precise frequency correlation between measurements and mathematical models will be undertaken. However, this Increment-2 report briefly analyzes some apparent structural modes gleaned from MAMS HiRAP data recorded on GMT June 8, 2001. The major structural components during the Increment-2 build-up are: the Soyuz, Service Module, FGB, Progress M, Z1 Truss, Node 1, PMA-1,

PMA-2, PMA-3, P6 segment (Long Spacer and IEA), US PV arrays, TCS radiators, USLab, MPLM, SpaceLab Pallet, and SSRMS. Most of these components are shown mated in Figures 3.1-1 and 3.2-1.

As cited in [24], key structural mode shapes of the ISS “backbone” are characterized by individual pressurized modules acting as rigid bodies connected at flexible interfaces. The “backbone” of the ISS is formed by the line of modules connected along the X_A -axis, which points in the general flight velocity vector direction for the Assembly Complete configuration. Also, from [24], some target modes selected for analysis are shown in Table 9.3.3-1.

TABLE 9.3.3-1 TARGET MODES FOR ISS ASSEMBLY COMPLETE CONFIGURATION

Target Mode #	Frequency (Hz)
297	0.44141
427	0.90176
454	1.01158

Limited computational resources prohibit computation of acceleration spectra with the resolution shown in the table above. To achieve the frequency resolution shown would require operating on over a day's worth of contiguous vibratory data. Direct comparison to predicted data is provisional since the acceleration data currently available were collected for Increment-2, and not in the Assembly Complete configuration. However, for the purpose of this report, these target modes were used in lieu of mathematical model structural frequencies for this Increment-2 report. The color spectrogram of Figure 9.3.3-1 spans 8 hours starting at GMT 08-June-2001, 08:00:00.

It shows the acceleration spectra below 2 Hz in an effort to capture low frequency structural modes. The horizontal yellow or red streaks that span the duration of the spectrogram point to what appear to be vehicle structural modes. The exact nature of these is beyond the scope of this document, but the spectral peaks at about 0.4 and 1 Hz are close to the first two target mode values of Table 9.3.3-1. Spectral averaging of the constituent PSDs that comprise this spectrogram yields the blue trace of Figure 9.3.3-2. The black trace in the figure represents a non-averaged, snapshot PSD for comparison. Note from this figure that the averaged PSD shows spectral peaks at about 0.40, 0.56, and 0.93 Hz. Also, the averaged PSD shows that near 1.3 Hz there are at least 2 closely spaced spectral peaks and possibly another pair at about 1.8 Hz. Further analyses and correlations will be undertaken to study, characterize, and quantify these low frequency dynamics in a later report, particularly as the ISS is assembled.

9.3.4 Vehicle Vibratory Requirements

The current configuration of the ISS and sensor mounting locations do not meet the specifications called out in [21]:

The vibratory acceleration limits apply at the structural mounting interfaces to the internal user payload locations. In the case of the ISPR, this points to the structural interfaces between the rack and the payload, on the payload side of the interfaces. If an intermediate structure were incorporated into the design between the user payload and the ISPR, e.g. an active rack isolation system, the specification shall apply at the user payload side of its interface with such a system.

... but that notwithstanding, measurements collected by SAMS 121f06 and MAMS HiRAP were processed for comparison to the ISS system combined vibratory acceleration limits and the results are shown in Figures 9.3.4-1 to 9.3.4-3. These three figures show crew impact below 10 Hz, ADVASC and EXPPCS impacts (discussed in next section) on HiRAP location. EXPPCS impact on HiRAP is shown at about 12 Hz (fundamental frequency of sample mix motor) along with 2nd through 16th harmonics. Whereas SAMS 121f06 shows that EXPPCS impacts the entire measured spectrum. It must be pointed out that the ISS requirement curve is only valid for assembly complete, ISS microgravity mode operations, on an ARIS rack, and with the ARIS Rack control system functioning. The data that are being compared here with the ISS requirement were not collected under the conditions mentioned above and are shown here only to illustrate how close the ISS microgravity environment is to the assembly complete requirement. The reader should be careful in drawing any final conclusion when looking at these curves (Increment-2 vs. ISS assembly complete requirement).

9.3.5 Experiment Operations

Microgravity experiment procedures typically employ mechanical equipment to prepare, conduct, analyze, diagnose, or preserve some aspect of the investigation. The forces produced by the moving parts of such equipment are transmitted in varying degrees to the spacecraft structure depending on the operating characteristics and on any mechanisms for vibration isolation.

9.3.5.1 EXPPCS Sample Mix

The EXPPCS was located in EXPRESS Rack (ER) 2. It has a number of moving parts, but the sample mixer is of particular interest from an acceleration environment perspective. In order to eliminate sedimentation and to produce uniform distribution, the initial EXPPCS procedures call for mixing each colloidal sample for a period of approximately one hour. The color spectrogram shown in Figure 9.3.5.1-1 shows an example of the sample mixer in operation starting at about GMT 04-June-2001, 22:20:40 and lasting for over an hour with a 50% duty cycle.

This spectrogram was computed from SAMS 121f06 measurements and shows the acceleration spectrum as a function of time. The sensor head was located about 1½ feet from the mixer on the front-panel of the EXPPCS test section. As expected, extreme acceleration levels were registered. The period shown starts at GMT 04-June-2001,

22:10:00 and covers an 80-minute span. The red vertical streaks mark portions of the duty cycle when the mixer was active.

For improved temporal resolution and a more precise accounting of the measured accelerations, the interval minimum/maximum time history of Figure 9.3.5.1-2 was examined. That figure clearly shows the large accelerations that occur while the mixer is preparing a sample cell for an operational run. The acceleration vector magnitudes detected by this sensor were nominally about 150 mg with peak values routinely in excess of 200 mg. As indicated by the time axis tick marks, this mixer has a 50% duty cycle with each half-cycle being 30-seconds in duration.

For improved frequency resolution and a more precise accounting of the spectral content during sample mix operations, the PSDs of Figure 9.3.5.1-3 were computed. From close inspection of this figure, we conjecture that the fundamental frequency of this disturbance was 12 Hz and with significant 2nd through 16th harmonics within the passband of this sensor. The 9th harmonic at 108 Hz was the most pronounced component and was aligned primarily with the sensor's YZ-plane. In strong contrast to this, the acceleration spectra during a 25-second span when the sample mix operation was off are seen in the PSDs of Figure 9.3.5.1-4.

Closer examination by means of the cumulative RMS acceleration versus frequency plot of Figure 9.3.5.1-5, serves to quantify this disturbance as a function of frequency.

During this 25-second period while the mixer was on, the overall RMS acceleration was slightly more than 80 mg_{RMS} for the frequency range from 0.06 to 200 Hz. For this same range, but during a 25-second span while the mixer was off, the cumulative RMS acceleration versus frequency plot of Figure 9.3.5.1-6 yields an overall RMS acceleration value more than an order of magnitude smaller at about 1.7 mg_{RMS}.

Further analysis of the sample mix operation was performed using other SAMS SEs. The color spectrograms of Figure 9.3.5.1-7 and Figure 9.3.5.1-8 show 5 cycles of a mix operation starting at about GMT 05-July-2001 23:45:20 for SAMS SE 121f03 and 121f04, respectively. The impact of these were examined at 2 SAMS sensor locations: (1) 121f03 on the Z-panel of ER2, and (2) 121f04 on the Z-panel of ER1. The 5 cycles are quite clear in the interval min/max plot of Figure 9.3.5.1-9 for 121f03. This sensor was nearer to the mix equipment than 121f04 as seen in Figure 9.3.5.1-10. Peak acceleration during the 5 mix cycles was about 10 mg for 121f04, and over 22 mg for 121f03. These accelerations, however, are about an order of magnitude less than those shown for the sample mix operations highlighted in Figure 9.3.5.1-2. Note that Figure 9.3.5.1-9 and Figure 9.3.5.1-10 were plotted in SSA coordinates and that the primary difference was registered on the X_A-axis.

9.3.5.2 EXPPCS Rheology

Rheology is performed at several different frequencies for each cell. The frequency range of operation is between 0 to 20 Hz. The same motor used to perform the Mix/Melt is used

PIMS ISS Increment-2 Microgravity Environment Summary Report: May to August 2001

for rheology. Rheology is performed on each sample when the sample has reached its final state.

According to the EXPPCS operations timeline shown in Table 9.3.5.2-1, a rheology was performed starting at GMT 25-June-2001 10:58:40. The color spectrogram shown in Figure 9.3.5.2-1 shows the end of an extended sample mix operation (not the usual 30-second duty cycle), which lasted from about GMT 25-June-2001 10:48:24 to 10:58:30 (temporal resolution of 16.384 seconds). The spectrogram below 20 Hz by itself does not yield conclusive indication of the exact impact of the rheology. It was noticed that occasional, brief spectral peaks do appear at about 7.8 Hz. For example, one of these peaks started at about GMT 25-June-2001 11:23:50 and lasted a little longer than 50 seconds. These must not be attributable solely to rheology operations because they appear before the aforementioned extended sample mix even begins.

TABLE 9.3.5.2-1 EXPPCS OPERATIONS TIMELINE

Operation	GMT	
	Start	End
mix/melt	02-June-2001 22:23:56	02-June-2001 22:53:56
mix/melt	02-June-2001 23:26:55	02-June-2001 23:56:55
mix/melt	03-June-2001 00:29:54	03-June-2001 00:59:54
mix/melt	03-June-2001 19:00:53	03-June-2001 19:30:53
mix/melt	03-June-2001 20:03:52	03-June-2001 20:33:52
mix/melt	04-June-2001 22:50:40	04-June-2001 23:20:40
mix/melt	09-June-2001 01:03:46	09-June-2001 01:33:46
mix/melt	09-June-2001 04:53:11	09-June-2001 05:23:11
mix/melt	09-June-2001 23:42:22	10-June-2001 00:12:22
mix/melt	10-June-2001 05:32:51	10-June-2001 06:02:51
mix/melt	11-June-2001 21:09:54	11-June-2001 21:39:54
mix/melt	14-June-2001 08:38:16	14-June-2001 09:08:16
mix/melt	14-June-2001 12:30:14	14-June-2001 13:00:14
mix/melt	14-June-2001 14:41:49	14-June-2001 15:11:49
mix/melt	23-June-2001 04:15:00	23-June-2001 04:45:00
mix/melt	23-June-2001 04:18:34	23-June-2001 04:48:34
mix/melt	24-June-2001 18:27:56	24-June-2001 18:57:56
mix/melt	24-June-2001 21:37:40	24-June-2001 22:07:40
mix/melt	25-June-2001 10:28:40	25-June-2001 10:58:40
rheology	25-June-2001 10:58:40	25-June-2001 11:28:40
mix/melt	29-June-2001 11:05:12	29-June-2001 11:35:12
mix/melt	05-July-2001 22:00:21	05-July-2001 22:30:21
mix/melt	05-July-2001 23:20:22	05-July-2001 23:50:22
mix/melt	06-July-2001 00:47:06	06-July-2001 01:17:06
mix/melt	17-July-2001 13:53:13	17-July-2001 14:23:13
mix/melt	23-July-2001 06:54:54	23-July-2001 07:24:54
mix/melt	26-July-2001 23:32:31	27-July-2001 00:02:31
mix/melt	27-July-2001 00:30:40	27-July-2001 01:00:40
mix/melt	27-July-2001 04:25:14	27-July-2001 04:55:14
mix/melt	05-Sept-2001 01:54:12	05-Sept-2001 02:24:12
mix/melt	06-Sept-2001 15:53:43	06-Sept-2001 16:23:43
mix/melt	06-Sept-2001 16:14:46	06-Sept-2001 16:44:46
mix/melt	20-Sept-2001 03:20:39	20-Sept-2001 03:50:39
mix/melt	20-Sept-2001 04:12:34	20-Sept-2001 04:42:34

PIMS ISS Increment-2 Microgravity Environment Summary Report: May to August 2001

9.3.6 ADVASC

The ADVASC experiment has a number of fans, blowers, and at least 2 pumps among its payload equipment. Vibratory disturbances attributable to the payload fans can be qualified from the spectrograms of Figures 9.3.6-1 and 9.3.6-2 considered in conjunction with the experiment operations timeline shown in Table 9.3.6-1.

TABLE 9.3.6-1 ADVASC EXPERIMENT OPERATIONS TIMELINE

Event Causing Disturbance	GMT		Note
	Start of Disturbance	End of Disturbance	
Payload fans running	10-May-2001 10:13:42	25-May-2001 16:56:02	
Root tray loop 1 pump activation	10-May-2001 10:20:43	10-May-2001 10:21:43	
Root tray loop 2 pump activation	10-May-2001 10:28:29	10-May-2001 10:29:29	
Nub set 1 pump activation	10-May-2001 10:45:16	10-May-2001 10:46:16	
Nub set 2 pump activation	10-May-2001 11:02:17	10-May-2001 11:03:17	
Nub set 1 pump activation	11-May-2001 07:12:11	11-May-2001 07:13:11	
Root tray loop 1 pump activation	11-May-2001 10:29:59	11-May-2001 10:30:59	
Nub set 2 pump activation	11-May-2001 14:33:22	11-May-2001 14:34:22	
Payload fans running	25-May-2001 17:39:02	27-May-2001 11:10:53	
Nub set 1 pump activation	25-May-2001 17:57:32	25-May-2001 17:58:32	
Nub set 2 pump activation	25-May-2001 18:14:33	25-May-2001 18:15:33	
Root tray loop 1 pump activation	25-May-2001 19:52:33	25-May-2001 19:53:33	
Root tray loop 1 pump activation	25-May-2001 21:30:19	25-May-2001 21:31:19	
Root tray loop 1 pump activation	25-May-2001 23:08:05	25-May-2001 23:09:05	
Root tray loop 1 pump activation	26-May-2001 03:57:20	26-May-2001 03:58:20	
Root tray loop 1 pump activation	26-May-2001 05:35:08	26-May-2001 05:36:08	
Payload fans running	27-May-2001 17:33:53	28-May-2001 12:07:53	
Payload fans running	28-May-2001 12:34:08	02-June-2001 16:41:46	see Figure 9.3.6-1
Payload fans running	02-June-2001 16:57:46	02-June-2001 18:03:03	
Payload fans running	02-June-2001 18:05:03	22-June-2001 07:15:17	
Payload fans running	22-June-2001 07:18:17	24-June-2001 16:05:30	
Payload fans running	24-June-2001 16:07:30	03-July-2001 02:37:14	
Payload fans running	03-July-2001 02:39:14	03-July-2001 06:49:17	
Payload fans running	03-July-2001 06:51:17	17-July-2001 17:44:10	
Payload fans running	17-July-2001 17:46:10	19-July-2001 02:26:58*	see Figure 9.3.6-2

* ADVASC logbook reported this time as ~ GMT 19-July-2001 03:30:00, but HiRAP acceleration measurements indicate time shown here in table.

PIMS ISS Increment-2 Microgravity Environment Summary Report: May to August 2001

Notice in the spectrogram of Figures 9.3.6-1 that 5 persistent horizontal streaks (4 red, 1 yellow) cease precisely at the times shown in the shaded “End of Disturbance” column of the ADVASC timeline of Table 9.3.6-1 and resume at the times in the shaded “Start of Disturbance” column. Also, the spectrogram of Figures 9.3.6-2 shows deactivation of the ADVASC payload just after the 53-minute mark (GMT 19-July-2001 02:26:58). Again, notice the cessation of 5 strong, spectral peaks at that time. This provided strong evidence correlating these 5 vibratory signatures with ADVASC payload equipment. Positive identification for all 5 of these disturbances were made possible by information received regarding operating characteristics provided by the ADVASC team. These operating characteristics are shown in Table 9.3.6-2.

As a means of quantifying the contribution of these ADVASC disturbances to the overall RMS acceleration measured by the HiRAP, a span when they were on was compared to a span when they were off. The PSDs of Figure 9.3.6-3 show this comparison. The red trace is a one-minute snapshot of the acceleration spectrum during which the ADVASC payload fans were running (“ADVASC ON” starting at GMT 02-June-2001 16:00:00), while the green trace shows when those fans were off (“ADVASC OFF” starting at GMT 02-June-2001 16:44:30). In and of themselves, these PSDs do not adequately quantify the contribution of ADVASC disturbances to the vibratory environment. For this, the PSDs were used to extract the frequency information shown in the first 2 columns of Table 9.3.6-2 and then applied Parseval's theorem to the PSDs for ADVASC ON (red trace) and ADVASC OFF (green trace) to yield the results shown in the “RMS Acceleration” columns. Two other disturbances were considered in this analysis besides the 5 attributed to ADVASC. These 2 were the narrowband spectral peaks at 67.9 and 70.1 Hz that straddled the ADVASC broadband disturbance centered at 69.5 Hz. Close examination of Figures 9.3.6-1 during the period when ADVASC was off (from about 16:41 to 16:57) shows these “straddlers” near 70 Hz, no longer obscured by the lower, broadband ADVASC disturbance.

TABLE 9.3.6-2 SNAPSHOT OF ADVASC RMS ACCELERATION CONTRIBUTIONS

Frequency (Hz)			ADVASC Disturbance	RMS Acceleration (μg _{RMS})		Note
HiRAP Measured		Expected*		ADVASC ON	ADVASC OFF	
Center	Range					
49.4	49.1 - 49.7	48.3	2900 RPM fan	41.6	19.0	narrowband
57.6	57.3 - 57.9	52 - 55	air pump	568.9	31.4	narrowband
67.9	67.6 - 68.1		no ⁺	120.7	115.7	narrowband
69.5	68.1 - 70.9	71.7	4300 RPM blower	512.9	97.4	broadband
70.1	69.7 - 70.3		No+	202.3	71.4	narrowband
76.5	73.0 - 79.7	78.3	4700 RPM blower*	940.9	86.9	broadband
88.0	87.6 - 88.4	88.3	5300 RPM CPU fan*	284.3	32.8	narrowband

* from Don Isham's e-mail on 9/17/2001 [from measurements made on ground and other sources]

+ narrowband straddler of ADVASC broadband (68.1 to 70.9 Hz) disturbance

* at other times in Increment-2, this disturbance shifts slightly in frequency

For an alternative spectral perspective, the PSDs of Figure 9.3.6-3 were integrated, and then square-rooted in cumulative fashion. The results plotted in Figure 9.3.6-4 along with those of Table 9.3.6-2, show that 3 of the ADVASC disturbances (the air pump, 4300 RPM blower, and 4700 RPM blower) account for most of the ADVASC contribution to the vibratory environment below 100 Hz as measured by the HiRAP. To gain more of a global view of this contribution, each of the constituent PSDs that comprise the spectrogram of Figure 9.3.6-1 were integrated over the frequency ranges shown in the 2nd column of Table 9.3.6-2, then square-rooted to produce RMS acceleration values every 8.192 seconds. For example, Figure 9.3.6-5 shows the 0-100 Hz RMS acceleration values for same time frame as the spectrogram of Figure 9.3.6-1. This 8-hour span shows that while the ADVASC equipment was operating, the RMS acceleration level was around 1 mg_{RMS}. In contrast, when the ADVASC equipment was turned off, the RMS acceleration level was lower by a factor of about 3, down to around 0.3 mg_{RMS}. Considering the measured spectrum (below 100 Hz) for the “ADVASC ON” span of Table 9.3.6-2, the RMS acceleration value was just over 1293 µg_{RMS}, while for the “ADVASC OFF” span the value was about 436 µg_{RMS}. Note that the last 2 hours of Figure 9.3.6-5 shows heightened RMS acceleration levels. These are due to EXPPCS sample mix operations.

In order to track ADVASC equipment operating characteristics and stability over time, Figure 9.3.6-6 was generated. That Figure shows ADVASC Equipment On, starting at GMT 02-June-2001, 16:00:00 (blue trace) compared to its operation at the later time starting at GMT 06-June-2001, 00:00:00 (red trace). The 4700-RPM blower (upper broadband) and 5300-RPM CPU fan (upper narrowband) disturbances shifted down in frequency. The narrowband spectral peak went from 88 to about 87.6 Hz. This may have been due to varying loads on the power supply. The PSDs suggest the RMS values shown in Table 9.3.6-2, however, should be approximately the same, with the exception of having to slightly shift the frequency integration range down to 71.7-78.5 Hz for the 4700-RPM blower disturbance and down to 87.2-87.8 Hz for disturbance 5300-RPM CPU fan.

9.3.7 MAMS Thermal Cooling Fan Characterization

MAMS typically dissipates 78.4 Watts of power and utilizes the EXPRESS Rack AAA air system as the primary means of cooling. Two inlet vents on the rear cover are protected with 282 µmesh filters. A 35-cfm fan, also with protective grille and mesh filter, is mounted at the single rear exhaust vent [20]. The MAMS internal cooling fan may be turned off (from ground command) for brief periods in order to reduce, or to prevent microgravity disturbances. However, the cooling fan must be re-enabled to prevent heat build-up within MAMS. In order to characterize the MAMS cooling fan disturbance, PIMS commanded the fan off for a period of about 5 minutes while monitoring the HiRAP and SAMS sensors to capture any off/on signature associated with the fan off mode.

The vertical, dashed white lines in the spectrogram of Figure 9.3.7-1 mark the brief period when the MAMS fan was off. The fan was turned off just before GMT 30-August-2001 15:45, then turned back on again just after GMT 30-August-2001 15:50. The health of the instrument depends on the cooling provided by this fan, however, a brief interruption was deemed justifiable in the interest of characterizing it as a vibratory disturbance source in the vicinity of the MAMS. The MAMS team coordinated with the cadre at the MSFC to issue the appropriate commands in order to make this snapshot characterization possible. Qualitatively, we see that a strong (red) horizontal streak that stops and starts at the dashed, vertical lines was accompanied by a weaker (yellow) horizontal streak that was slightly lower in frequency. To quantify these, Figure 9.3.7-2 shows 2 PSDs: a red trace computed from SAMS 121f02 data while the MAMS fan was on (starting at GMT 30-August-2001 15:42:30), and a green trace computed from SAMS 121f02 data while the MAMS fan was off (starting at GMT 30-August-2001, 15:45:18). Close examination of these 2 traces above 180 Hz shows the two spectral peaks we attribute to the MAMS fan. The lower peak at 182.6 Hz is weaker than the upper peak centered at 183.2 Hz. Having computed these PSDs, we again utilized Parseval's theorem to produce the results in Table 9.3.7-1.

TABLE 9.3.7-1 SNAPSHOT OF MAMS FAN RMS ACCELERATION CONTRIBUTION

Frequency (Hz)		MAMS Disturbance	RMS Acceleration (μg _{RMS})		Note
121f02 Measured			Fan ON	Fan OFF	
Center	Range				
182.6	182.3 - 182.9	fan	35.4	20.8	lower peak
183.2	182.9 - 183.7	fan	88.8	23.4	upper peak
182.9	182.3 - 183.7	fan	95.6	31.5	

When we consider the RMS acceleration for the measured spectrum below 200 Hz, the MAMS fan is not a principal spectral contributor because the RMS level was about 3,357 μg_{RMS} while the fan was running, and about 3,362 μg_{RMS} for the brief period that it was off (differences elsewhere in the acceleration spectrum overtake the MAMS fan contribution). However, if one were concerned with a relatively narrow range of the acceleration spectrum, specifically from 182.3 Hz to 183.7 Hz in the vicinity of the MAMS instrument, then this snapshot shows that the RMS acceleration level decreases by more than 60 μg_{RMS} when the MAMS fan turns off. For instrument health considerations though, this fan cannot be turned off for an extended period of time. When investigators require MAMS support on the ISS, this fan will run.

9.3.8 Crew Activity

Experimental setups, equipment transfer or stowage, exercise, and simple locomotion all contribute to the disturbance category called crew activity. These actions give rise to reactive forces, which are manifested as acceleration disturbances transferred through the

vehicle's structure. In-depth analyses will seek to correlate acceleration effects with periods of crew inactivity, like sleep and Public Affairs Office (PAO) events. These PAO events are typically question-and-answer or demonstration periods with all or some of the crew gathered in one area. This has a quieting effect on the microgravity environment because crew activity is reduced from nominal conditions, that is, the crew is less likely to impart push-off and impact transients on the vehicle's structure. In addition, crew conferences and briefings may be examined and should result in a similar quieting. Exactly how much of a quieting effect these periods have remains to be analyzed. For this summary report, crew waking period, and crew exercising using the Treadmill Vibration Isolation System (TVIS) as well as the Ergometer are examined.

9.3.8.1 Crew Wake

Figure 9.3.8.1-1 shows a period not long before the crew wakes and a period that starts soon after. This plot was derived from HiRAP measurements and shows a spectral comparison of two 4-minute periods. The black trace is the PSD for a time slice starting at GMT 03-June-2001, 08:40:00, which was near the end of a sleep period. The red trace is the PSD for a time slice starting at GMT 03-June-2001, 08:48:00, which was not long after the crew woke. This brief wake period does not encompass the full gamut of crew activity, but does serve to show how the crew impacts the low-frequency portion of the vibratory acceleration spectrum, particularly below about 6 Hz. Using Parseval's theorem, we can quantify the difference in this frequency range in terms of the RMS acceleration for the frequency band from 0.06 to 6 Hz. The RMS acceleration level in this range rose from about 9 μg_{RMS} during the sleep period to about 40 μg_{RMS} just after the crew woke up.

9.3.8.2 Exercise

9.3.8.2.1 Ergometer

While timeline information for crew exercise has proved elusive to date, a sweep of the roadmap spectrograms that accompany this report show the telltale twin peaks signature of ergometer exercise for various durations and starting at approximately the GMTs shown in the list below.

Approximate GMT Start of Ergometer Exercise Signature:

06-June-2001 11:55	19-July-2001 01:45
12-June-2001 10:45	10-August-2001 13:55
14-June-2001 11:55	18-August-2001 11:45
19-June-2001 14:10	18-August-2001 12:30
25-June-2001 12:00	18-August-2001 16:15

For example, the spectrogram of Figure 9.3.8.2.2-1 shows the signature below 5 Hz of ergometer exercise starting just before 12:00 and lasting about 36 minutes. Similar signatures were seen in the roadmap spectrogram sets for one or more of the HiRAP and SAMS sensors at about the times listed above. In the following report, more resources will be allocated to track precise crew exercise timelines so that a more detailed analysis of crew exercise can be performed for both TVIS and the Ergometer.

10 PCSA

The large database of PSDs used to generate the roadmap spectrograms found on the supplemental CD that accompanies this report, also served as input for PCSA. This is a frequency domain analysis technique whereby a two-dimensional histogram is calculated from a large number of PSDs [25]. Historically, a peak detection algorithm had been used to pass only significant spectral peaks from the constituent PSDs to the histogram routine. From here forward, however, all PSD values are input to that histogram routine. This does not alter the objective for this type of display, which still remains the examination of the acceleration spectral characteristics for a long period of data. Dominant or persistent spectral contributors are still readily apparent, but processing time is shorter because peak detection is averted. Loosely speaking, every PSD value is treated here as a significant peak. This lends an alternative interpretation to the nomenclature used for this analysis technique. In the present case, the word principal does not apply to the input of the two-dimensional algorithm, but rather to information conveyed by the resultant. In addition to highlighting strong principal spectral components, this resultant serves to summarize magnitude and frequency variations of persistent spectral contributors regardless of magnitude. As a tradeoff from the temporal resolution afforded by spectrograms, this type of display offers better frequency and PSD magnitude resolution. The large database of PSDs that was used for this analysis is detailed in the tables that follow.

TABLE 10-1 MAMS HIRAP (100 HZ) PCSA PARAMETERS

Roadmap Set #	Resolution		GMT	
	Frequency	Temporal		
	(Hz)	(seconds)	From	To
0001	0.1221	8.192	30-May-2001 16:00	07-June-2001 00:00
0018	0.1221	8.192	12-July-2001 16:00	17-July-2001 16:00
0024	0.1221	8.192	22-July-2001 00:00	23-July-2001 00:00
0035	0.1221	8.192	25-July-2001 08:00	01-August-2001 00:00
0047	0.1221	8.192	12-August-2001 00:00	14-August-2001 00:00
0048	0.1221	8.192	17-August-2001 00:00	21-August-2001 00:00
<i>Total Number of PSDs: 262,209</i>			<i>Total Number of Hours: 596.7</i>	

TABLE 10-2 SAMS 121F06 (200 HZ) PCSA PARAMETERS

Roadmap Set #	Resolution		GMT	
	Frequency	Temporal		
	(Hz)	(seconds)	From	To
0010	0.1221	8.192	28-June-2001 08:00	29-June-2001 16:00
0019	0.1221	8.192	15-July-2001 08:00	16-July-2001 00:00
0021	0.1221	8.192	19-July-2001 16:00	22-July-2001 00:00
0052	0.1221	8.192	17-August-2001 00:00	21-August-2001 00:00
<i>Total Number of PSDs: 66,890</i>			<i>Total Number of Hours: 152.2</i>	

TABLE 10-3 SAMS 121F03 (200 HZ) PCSA PARAMETERS

Roadmap Set #	Resolution		GMT	
	Frequency	Temporal		
	(Hz)	(seconds)	From	To
0033	0.1221	8.192	28-Jul-2001 00:00	31-July-2001 00:00
0045	0.1221	8.192	07-Aug-2001 08:00	11-August-2001 00:00
0051	0.1221	8.192	18-Aug-2001 00:00	19-August-2001 00:00
<i>Total Number of PSDs: 70,334</i>			<i>Total Number of Hours: 160.0</i>	

Note from these tables that the total number of hours in the last row is derived from temporal resolution and the number of PSDs used. This number is smaller than the sum of the GMT spans shown for each subset because there were gaps in those spans. Figure 10-1 shows the resultant PCSA plot corresponding to Table 10-1, Figure 10-2 corresponds to Table 10-2, and Figure 10-3 corresponds to Table 10-3.

Careful examination of Figures 10-1 through 10-3 yielded these observations:

- Shuttle's Ku-band antenna dither signature at 17 Hz from operations with the Shuttle docked was much weaker in the 121f06 PCSA than in the HiRAP PCSA.
- SKV-1 disturbance at 23.5 Hz was much weaker in the 121f06 PCSA than in the HiRAP PCSA.
- ADVASC disturbances discussed in section 9.3.6 dominate the acceleration spectra near HiRAP.
- Disturbances at and above about 180 Hz dominate the 121f06 spectra, while those near about 160 Hz dominate the 121f03 spectra during the time frames analyzed.

11 Summary of Findings

Tables 11.1-1 and 11.2-1 summarize some of the many disturbances recorded by MAMS and SAMS for the quasi-steady and the vibratory regimes during the Increment-2 period (May to August, 2001) that PIMS project analyzed thus far. Note that, MAMS and SAMS were not continuously active during the time span mentioned above. It is PIMS hope that this Increment report will shed some light on the complexity of characterizing the reduced gravity environment of the ISS and also will show how complex and dynamic such an environment is.

11.1 Quasi-steady Acceleration Regime Summary

This section highlights the significant findings of the quasi-steady acceleration analysis.

TABLE 11.1-1 SUMMARY OF FINDINGS FOR INCREMENT-2: QUASI-STEADY

Event	GMT	Observation
Soyuz TM-31 Undocking	06-May-2001 00:19:58	Peak magnitude in X_A -axis: 12 μg
Progress (4P) Docking	23-May-2001 00:24:23	Peak magnitude in X_A , Y_A -axes: 10 μg
STS-104 (7A) Docking	14-July-2001 03:21:04	Peak vector magnitude: 6 μg
STS-105 (7A.1) Docking	12-Aug-2001 19:02:35	Peak vector magnitude: 5 μg
STS-105 (7A.1) Undocking	20-Aug-2001 14:52:00	Peak vector magnitude: 6 μg
10.2 Cabin Depressurization	14-July-2001 10:05:00	Peak difference in X_A -axis: 4.0 μg
XPOP Attitude	Various	Mean magnitude: 2.0 μg
TEA Attitude	Various	Mean magnitude: 1.3 μg
STS-105 Joint Ops	12-Aug-2001 19:00:00	Mean magnitude: 2.9 μg

11.2 Vibratory Acceleration Regime Summary

This section highlights the significant findings for the vibratory acceleration analysis.

PIMS ISS Increment-2 Microgravity Environment Summary Report: May to August 2001

TABLE 11.2-1 SUMMARY OF FINDINGS FOR INCREMENT-2: VIBRATORY ANALYSIS

Event	GMT	Sensor	Observation
Progress (4P) Docking	23-May-2001 00:24:23	MAMS HiRAP (100 Hz)	Peak vector magnitude: 13 mg
Shuttle (7A) Docking Softmate	14-July-2001 03:08:31	MAMS HiRAP (100 Hz)	Peak vector magnitude: 10 mg
Shuttle (7A) Docking Hardmate	14-July-2001 03:21:04	MAMS HiRAP (100 Hz)	Peak vector magnitude: 6 mg
Shuttle (7A.1) Docking Softmate	12-Aug-2001 18:42:25	MAMS HiRAP (100 Hz)	Peak vector magnitude: 29 mg
Shuttle (7A.1) Docking Hardmate	12-Aug-2001 19:02:35	MAMS HiRAP (100 Hz)	Peak vector magnitude: 14 mg
SKV-1 OFF	08-Aug-2001 00:00-08:00	SAMS 121f02 (25 Hz)	23 < f < 24 Hz: less than 8 μ g _{RMS}
SKV-1 ON	08-Aug-2001 16:00-23:59	SAMS 121f02 (25 Hz)	23 < f < 24 Hz: more than 37 μ g _{RMS}
ADVASC OFF	02-June-2001	MAMS HiRAP (100 Hz)	0 < f < 100 Hz: 0.3 mg _{RMS}
ADVASC ON	02-June-2001	MAMS HiRAP (100 Hz)	0 < f < 100 Hz: 1.0 mg _{RMS}
EXPPCS Sample Mix	04-June-2001	SAMS 121f06 ER2 test section (200 Hz)	Peak vector magnitude: 150 mg
EXPPCS Sample Mix	05-July-2001	SAMS 121f03 ER2 Z- panel (100 Hz)	Peak vector magnitude: 22 mg
EXPPCS Sample Mix	05-July-2001	SAMS 121f04 ER1 Z- panel (100 Hz)	Peak vector magnitude: 10 mg
MAMS Fan OFF	30-Aug-2001 15:42:30-15:44:42	SAMS 121f02 (200 Hz)	182.3 < f < 183.7 Hz: 31.5 μ g _{RMS}
MAMS Fan ON	30-Aug-2001 15:45:18-15:47:30	SAMS 121f02 (200 Hz)	182.3 < f < 183.7 Hz: 95.6 μ g _{RMS}
Before TVIS	28-June-2001 09:45 - 09:46	SAMS 121f04 (100 Hz)	6 < f < 22 Hz: 65.7 μ g _{RMS}
During TVIS	28-June-2001 10:35 -10:36	SAMS 121f04 (100 Hz)	6 < f < 22 Hz: 502.8 μ g _{RMS}
Crew Asleep	03-June-2001 08:40:00-08:44:00	MAMS HiRAP (100 Hz)	0.06 < f < 6 Hz: 9 μ g _{RMS}
Crew Awake	03-June-2001 08:48:00-08:52:00	MAMS HiRAP (100 Hz)	0.06 < f < 6 Hz: 40 μ g _{RMS}

12 References

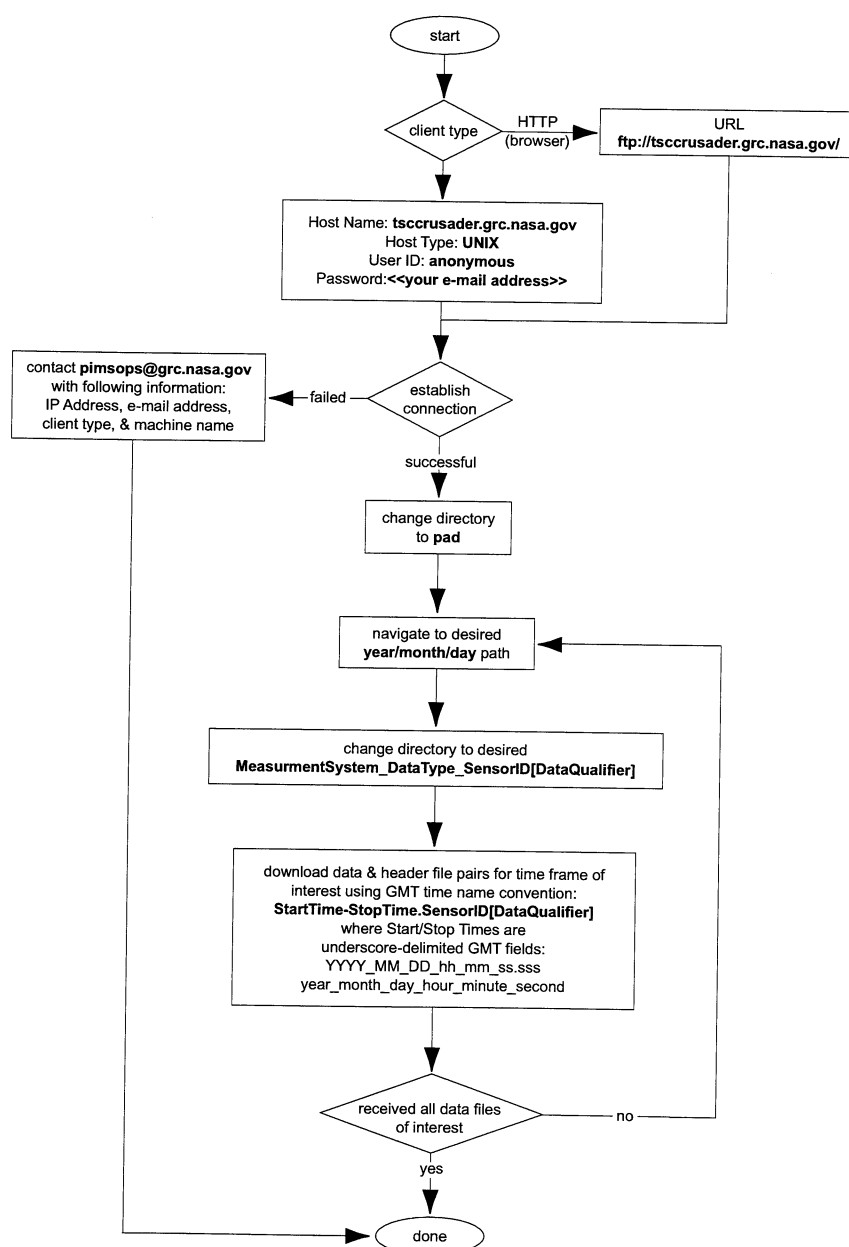
1. Hamacher, H., Fluid Sciences and Materials Science in Space, Springer-Verlag, 1987.
2. International Space Station User's Guide Release 2.0, NASA.
3. Expedition Two (Press Kit): Open for Business-Shuttle Press kit March 6, 2001.0219
4. The International Space Station Fact Book, NASA, October 2000.
5. International Space Station Coordinate Systems, SSP-30219, Revision E.
6. International Space Station Flight Attitudes, D-684-10198-06 DCN-002, December 1, 1999.
7. International Space Station Research Plan—Office of Biological and Physical Research, NASA, August 2000.
8. Steelman, April., "Flight 6A Microgravity Analysis," Microgravity AIT, August 1999.
9. On-Orbit Vehicle Configuration Data Book for Mission 6A, Shuttle-ISS NSTS-37324-6A, Rev. 001, NASA, March 01.
10. Expedition Two Overview Fact Sheet, NASA, March 2001.
11. Microgravity Environment Interpretation Tutorial (MEIT), NASA Glenn Research Center, March 2001.
12. EXPRESS RACKS 1 and 2 Fact Sheet, NASA, February 2001.
13. EXPRESS Rack, Flight 6A On-Orbit Configuration, Teledyne Brown Engineering DL 5221003, Nov. 99.
14. Expedition Two Fact Sheets: Expedition Two Payload Overview, NASA, March 2001.
15. Software Requirements for Processing Microgravity Acceleration Data from the International Space Station, PIMS-ISS-001, May 2000.
16. Canopus Systems, Inc., OARE Technical Report 149, STS-78 (LMS-1) Final Report, CSI-9604, September 1996.

PIMS ISS Increment-2 Microgravity Environment Summary Report: May to August 2001

17. Canopus Systems, Inc., OARE Technical Report 151, STS-94 (MSL-1) Final Report, CSI-9704, August 1997.
18. Hogg, Robert V., "Adaptive Robust Procedures: A Partial Review and Some Suggestions for Future Applications and Theory," Journal of the American Statistical Association, Vol. 69, December 1974.
19. Canopus System, Inc., Microgravity Environment Interpretation Tutorial 2001 Presentation, Section 5, James Fox, March 2001.
20. Canopus System, Inc., Microgravity Acceleration Measurement System For the International Space Station, Maintenance and Operation Manual, CSI 0101/MAMS TR-008, March 2001.
21. Microgravity Analysis Integration Team, "Microgravity Control Plan (Revision B)," Report No: SSP-50036 B, the Boeing Company, Houston, TX, NASA Contract No. NAS15-1000 (DRIVE-16), February 1999.
22. Rogers, M.J.B., Hrovat, K., McPherson, K., DeLombard, R., and Reckart, T. (1999) Summary Report of Mission Acceleration Measurements for STS-87. NASA/TM—1999-208647, pp. 34–35.
23. ICD-A-21438-OOR, Prepared by The Boeing Company, Human Space Flight and Exploration under Subcontract 1970483303, PDRD P1226, May 7, 2001, DRD-1.2.2.6 Contract NAS9-20000- P.S4A-41.
24. Bartkowicz, T., "Integrated Loads and Dynamics Verification Plan (Revision A)," Report No: D684-10288-01, The Boeing Company, Houston, TX, NASA Contract No., NAS15-10000, August 1998.
25. DeLombard, R., McPherson, K., Hrovat, K., and Moskowitz, M. (1997) Comparison Tools for Assessing the Microgravity Environment of Missions, Carriers and Conditions, NASA TM–107446.

Appendix A. On-line Access to PIMS Acceleration Data Archive

Acceleration data measured by the MAMS and the SAMS on the ISS are available over the Internet via FTP from a NASA GRC file server. The flow chart shown in Appendix A. Figure 1 diagrams a procedure that can be used to download data files of interest:



Appendix A. Figure 1. On-Line Data Access Flow Chart

PIMS ISS Increment-2 Microgravity Environment Summary Report: May to August 2001

A fictitious file listing is shown in Appendix A. Figure 2 depicting the PIMS Acceleration Data (PAD) file system hierarchy.

Name	Size
2000_02_03_10_32_45.549-2000_02_03_10_42_45.558.121f01	586KB
2000_02_03_10_32_45.549-2000_02_03_10_42_45.558.121f01.header	1KB
2000_02_03_10_42_45.562+2000_02_03_10_52_45.570.121f01	586KB
2000_02_03_10_42_45.562+2000_02_03_10_52_45.570.121f01.header	1KB
2000_02_03_10_52_45.574+2000_02_03_10_55_43.057.121f01	174KB
2000_02_03_10_52_45.574+2000_02_03_10_55_43.057.121f01.header	1KB
2000_02_03_11_05_34.589-2000_02_03_11_15_34.581.121f01	586KB
2000_02_03_11_05_34.589-2000_02_03_11_15_34.581.121f01.header	1KB
2000_02_03_11_15_34.601+2000_02_03_11_24_17.091.121f01	511KB
2000_02_03_11_15_34.601+2000_02_03_11_24_17.091.121f01.header	1KB
2000_02_03_11_24_17.112-2000_02_03_11_34_17.104.121f01	586KB
2000_02_03_11_24_17.112-2000_02_03_11_34_17.104.121f01.header	1KB

Appendix A. Figure 2. Screenshot of Sample PAD File Listing

For the directory highlighted on the left of this sample listing, the measurement system is “sams2” and the sensor identifier is “121f01”. On the right, there is a partial listing of the acceleration header and data files available for this sensor collected on the day indicated (day 3). These files are named according to the PIMS-ISS-001 document [15].

If you encounter difficulty in accessing the data using this procedure, then send an electronic mail message to pimsops@grc.nasa.gov. Please describe the nature of the difficulty, and give a description of the hardware and software you are using to access the file server, including the domain name and/or IP address from which you are connecting.

Appendix B. Some Useful Acceleration Data and Microgravity Related URLs

Below is a list of some URLs that the microgravity scientific community might find very useful. They are all microgravity related. NASA does not endorse or cannot be held liable for the information contained on any site, which is not NASA's. The PIMS Project provides this listing only as a service to the microgravity community.

1. For more information on the EXPPCS experiment go to:
<http://microgravity.grc.nasa.gov/6712/PCS.htm>
2. For more information on EXPRESS RACK go to:
<http://liftoff.msfc.nasa.gov/Shuttle/msl/science/express.html>
3. For more information on ARIS-ICE go to: <http://www.scipoc.msfc.nasa.gov>
4. For more information on Expedition Two go to:
<http://www1.msfc.nasa.gov/NEWSROOM/background/facts/exp2fact.html>
5. For more information on Microgravity Acceleration Measurement go to:
http://microgravity.grc.nasa.gov/MSD/MSD_htmls/mmap.html
6. For more information on MAMS OSS, MAMS HiRAP and SAMS go to:
<http://tsccrusader.grc.nasa.gov/pims>
7. For information on MAMS, SAMS data request go to:
<http://tsccrusader.grc.nasa.gov/pims/html/RequestDataPlots.html>
8. For information on upcoming Microgravity Environment Interpretation Tutorial (MEIT) go to:
<http://www.grc.nasa.gov/WWW/MMAP/PIMS/MEIT/meitmain.html>
9. For information on upcoming Microgravity Meeting Group (MGMG) go to:
http://www.grc.nasa.gov/WWW/MMAP/PIMS/MGMG/MGMG_main.html
10. For information on SAMS go to:
http://microgravity.grc.nasa.gov/MSD/MSD_htmls/sams.html
11. For information on MAMS/HiRAP go to:
http://microgravity.grc.nasa.gov/MSD/MSD_htmls/mams.html
12. For information on ADVASC go to:
<http://www1.msfc.nasa.gov/NEWSROOM/background/facts/advasc.html>

Appendix C. Acronym List and Definition

Acronyms used in this Summary Report are listed below. A more extensive list of NASA ISS-related acronyms can be found through the Internet at:

<http://spaceflight.nasa.gov/station/reference/index.html>

ACRONYM	DEFINITION
AAA	Avionics Air Assembly
ADVASC	Advanced Astroculture
AOS	Acquisition of Signal
ARIS	Active Rack Isolation System
ARIS-ICE	ARIS ISS Characterization Experiment
BCTA	Bias Calibration Table Assembly
CAM	Centrifuge Accommodation Module
CBM	Common Berthing Mechanism
CDRA	Carbon Dioxide Removal Assembly
CMG	Control Moment Gyro
CPCG-H	Commercial Protein Crystal Growth-High Density
DC	Direct Current (electrical acronym generalized for mean value)
ECLSS	Environmental Control and Life Support System
EE	Electronics Enclosure
ER 1/2	EXPRESS Rack 1 or 2
ESA	European Space Agency
EVA	Extravehicular Activity
EXPPCS	Experiment of Physics of Colloids in Space
EXPRESS	Expedite the Processing of Experiments to the Space Station
FGB	Functional Cargo Block (Russian translation: Funktsionalui Germatischeskii Block)
g	acceleration due to free-fall (9.81 m/s^2)
GMT	Greenwich Mean Time
GRC	NASA Glenn Research Center
GSE	Ground Support Equipment
HiRAP	High Resolution Accelerometer Package
HOSC	Huntsville Operation Support Center
Hz	Hertz
ICU	Interim Control Unit
IMV	Intermediate Ventilation System
ISS	International Space Station
JSC	NASA Johnson Space Center
kbps	kilobits per second
KSC	NASA Kennedy Space Center
LAB	U.S. Laboratory Module
LOS	Loss of Signal
LVLH	Local Vertical Local Horizontal
MAMS	Microgravity Acceleration Measurement System
MCA	Major Constituent Analyzer

PIMS ISS Increment-2 Microgravity Environment Summary Report: May to August 2001

MCOR	Medium-rate Communication Outage Recorder
MCPS	MAMS Control Processor Subsystem
MMAP	Microgravity Measurement and Analysis Project
MPLM	Mini Pressurized Logistics Module or Multipurpose Logistics Module
MSFC	NASA Marshall Space Flight Center
NASA	National Aeronautics and Space Administration
NASDA	National Space Development Agency of Japan
OARE	Orbital Acceleration Research Experiment
OSS	OARE Sensor Subsystem
OTO	One-Third Octave
PAD	PIMS Acceleration Data
PAO	Public Affairs Office
PCSA	Principal Component Spectral Analysis
PDSS	Payload Data Services System
PI	Principal Investigator
PIMS	Principal Investigator Microgravity Services
PMA	Pressurized Mating Adapter
PSD	Power Spectral Density
PV	Photovoltaic
QTH	Quasi-steady Three-dimensional Histogram
RMS	Root-Mean-Square
RSS	Root-Sum-Square
SAMS	Space Acceleration Measurement System
SE	Sensor Enclosure
SO	Starboard Truss Segment 0
SSA	Space Station Analysis
SSRMS	Space Station Remote Manipulator System
STS	Space Transportation System
TCS	Temperature Control System
TEA	Torque Equilibrium Attitude
THC	Temperature/Humidity Control System
TMF	Trimmed Mean Filtered
TSC	Telescience Support Center
TVIS	Treadmill Vibration Isolation System
VS	Vacuum System
XPOP	X Principal Axis Perpendicular to the Orbit Plane
XVV	X body axis toward the Velocity Vector
μg	micro-g, $1 \times 10^{-6}\text{g}$
WSS	Water Separator System
WWW	World Wide Web

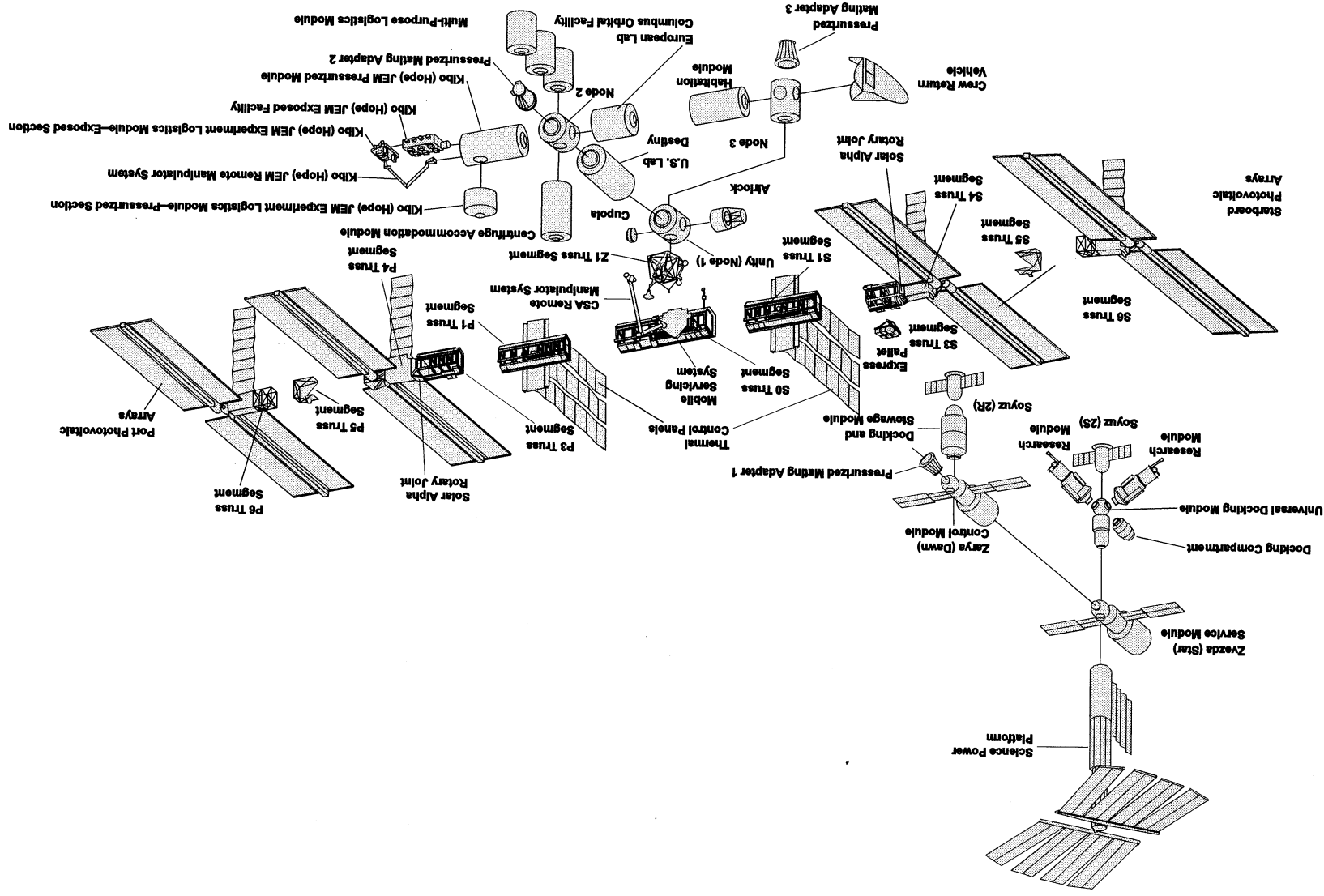


Figure 2.1-1 International Space Station at Assembly Complete

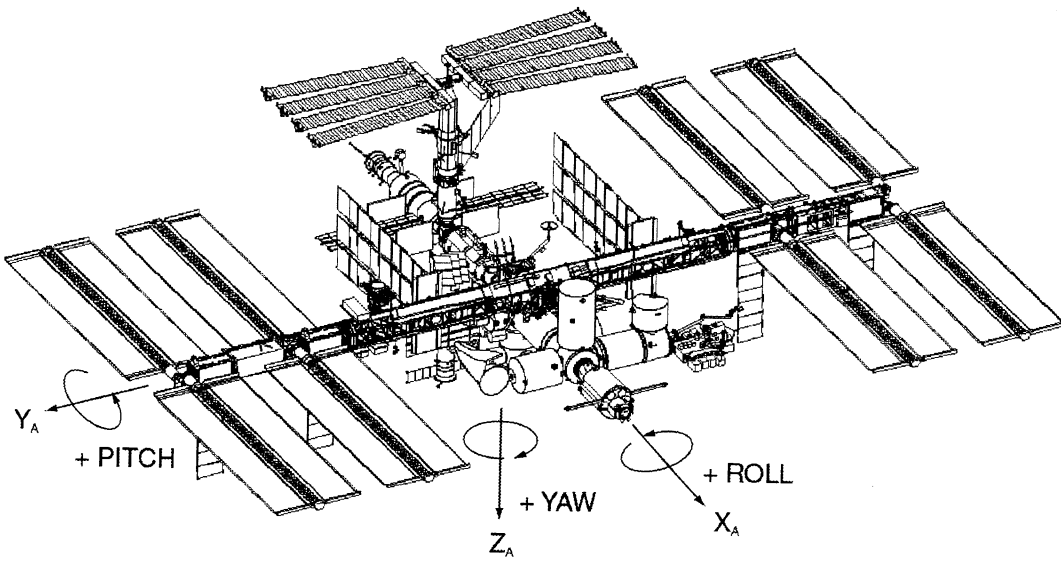


Figure 2.2-1 Space Station Analysis Coordinate System

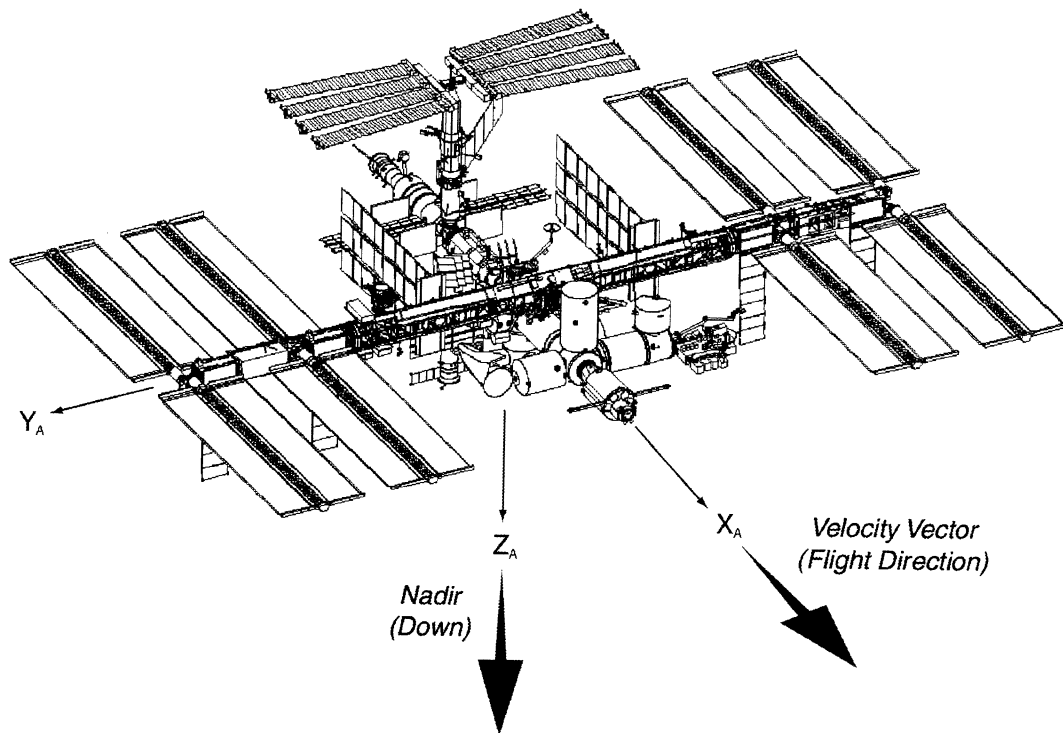


Figure 2.3-1 ISS XVV Flight Attitude

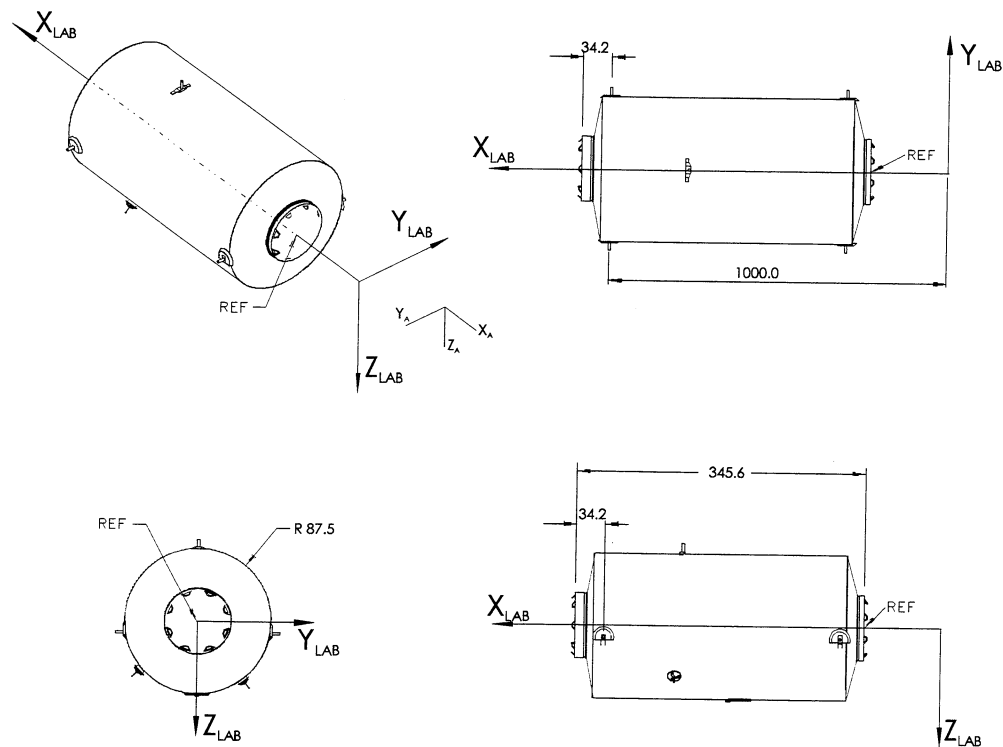


Figure 2.4-1 United States Laboratory Module (Destiny) Coordinate System

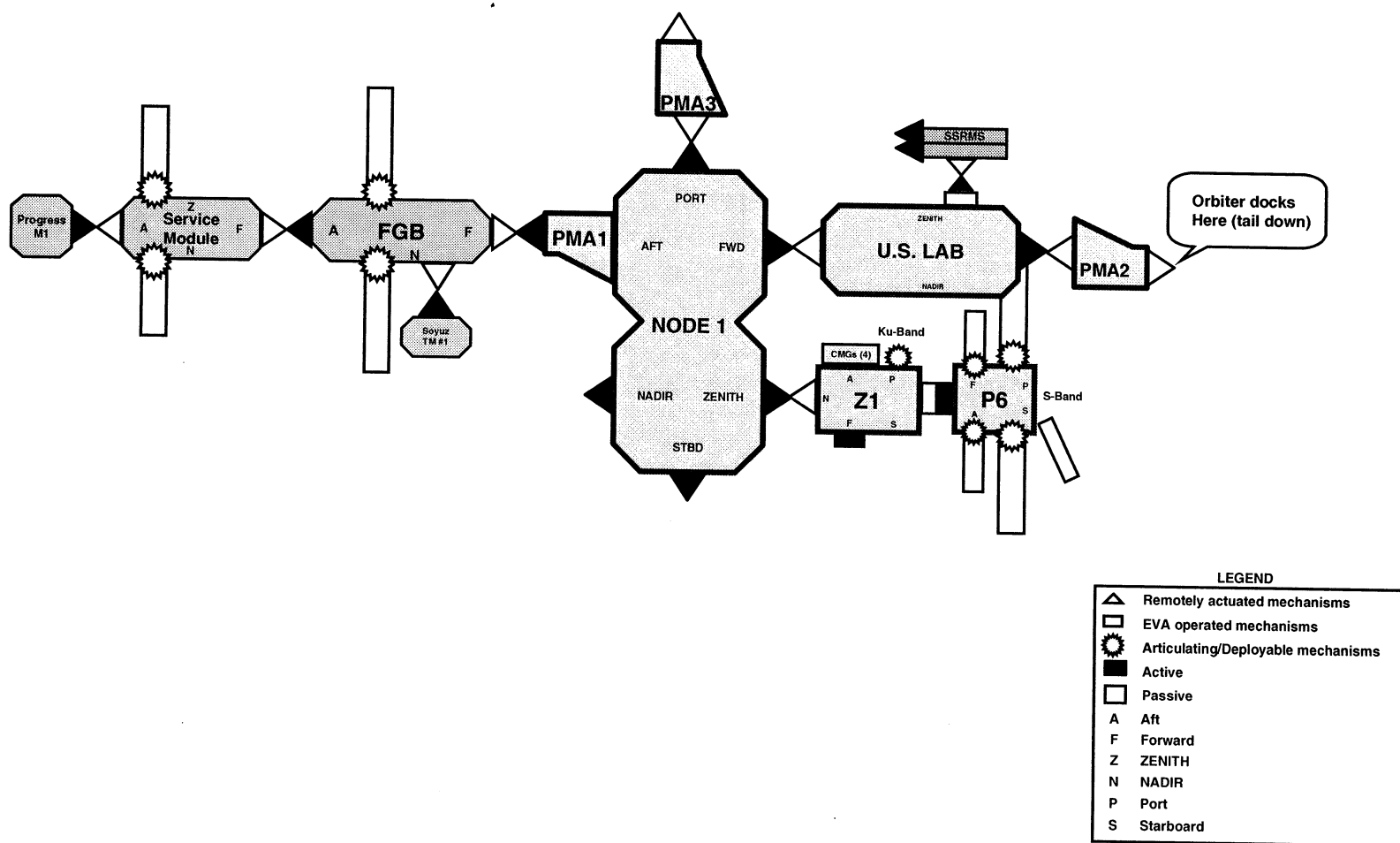


Figure 3.1-1 ISS Increment-2 Configuration

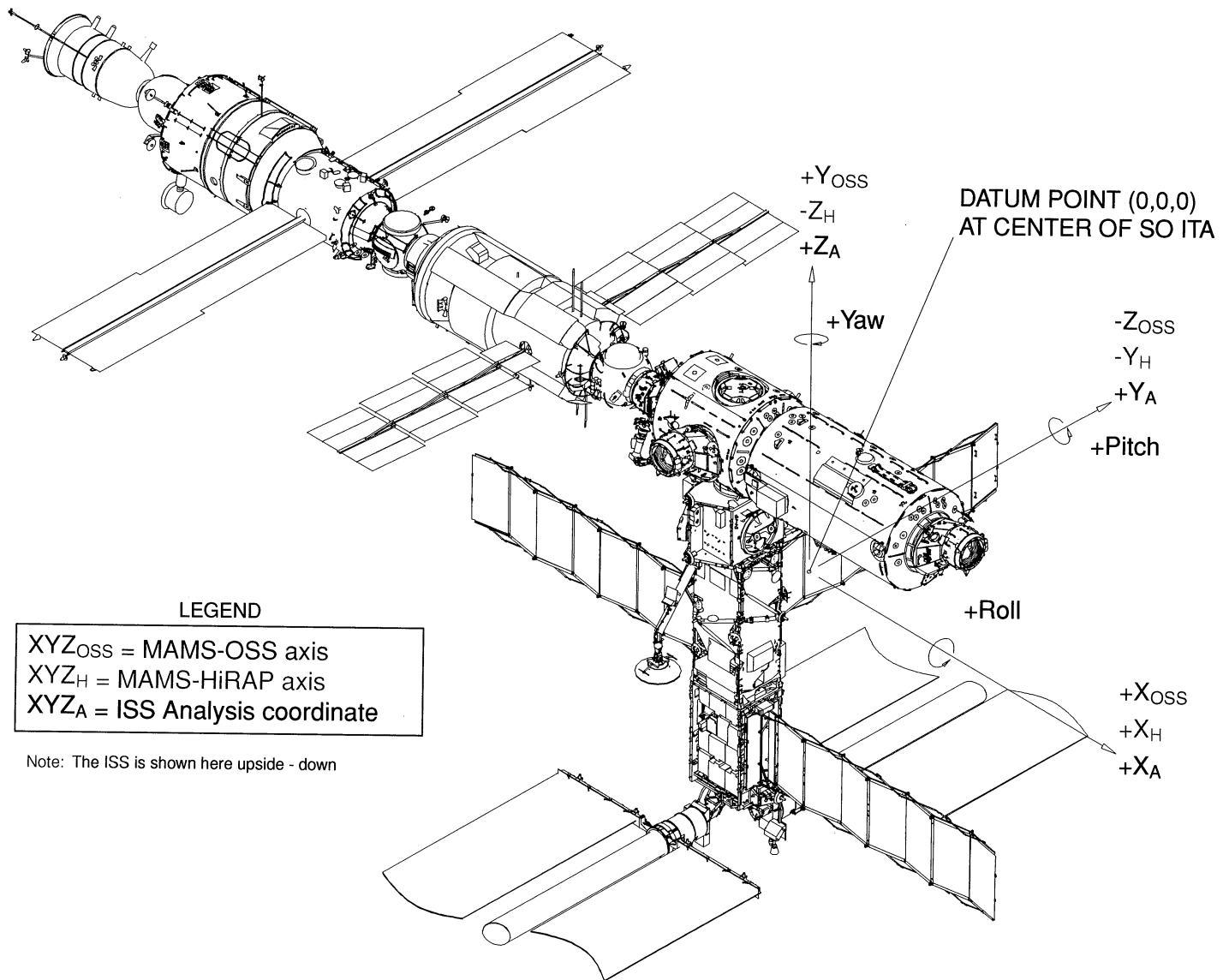


Figure 3.2-1 Increment-2 Coordinate Systems

Inertial Attitude With The X Principal Axis Perpendicular to Orbit Plane, Z Nadir At Noon

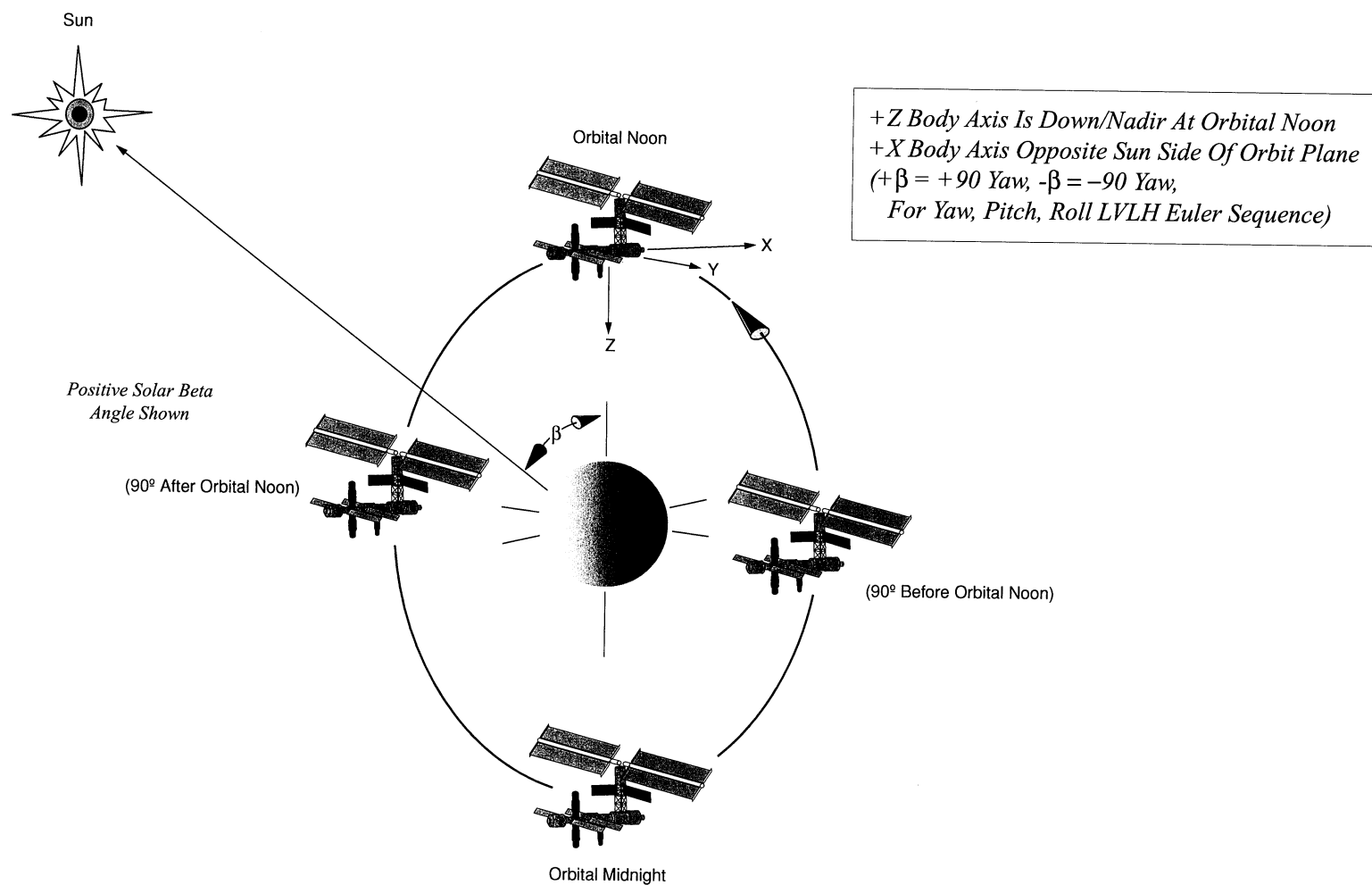


Figure 3.3-1 ISS in the XPOP Inertial Flight Attitude

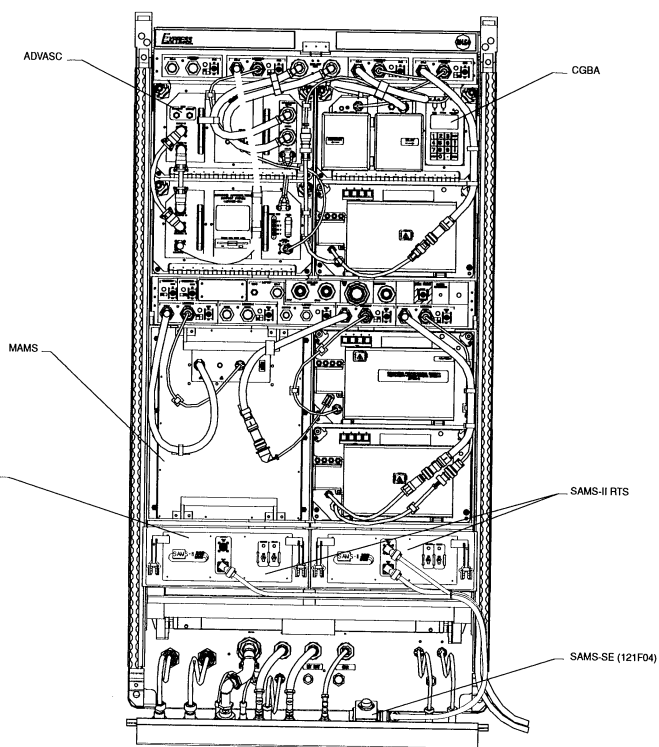


Figure 5-1 EXPRESS Rack 1
6A On-Orbit Configuration

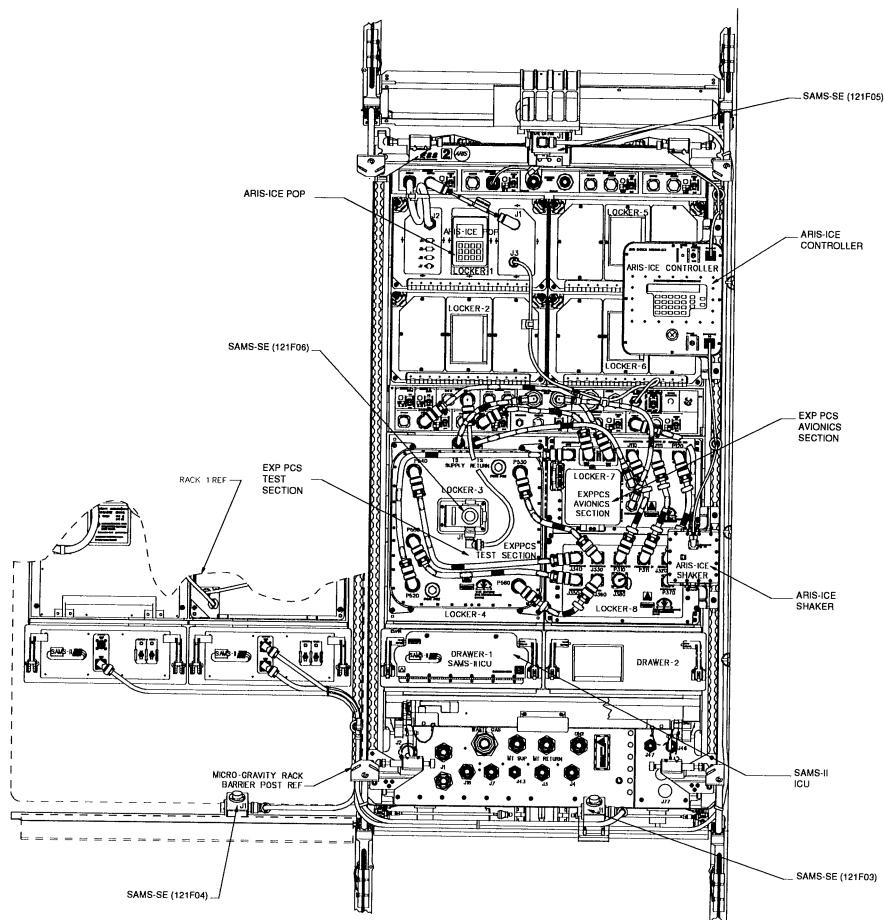


Figure 5-2 EXPRESS Rack 2
6A/7A On-Orbit Configuration

TMF Process

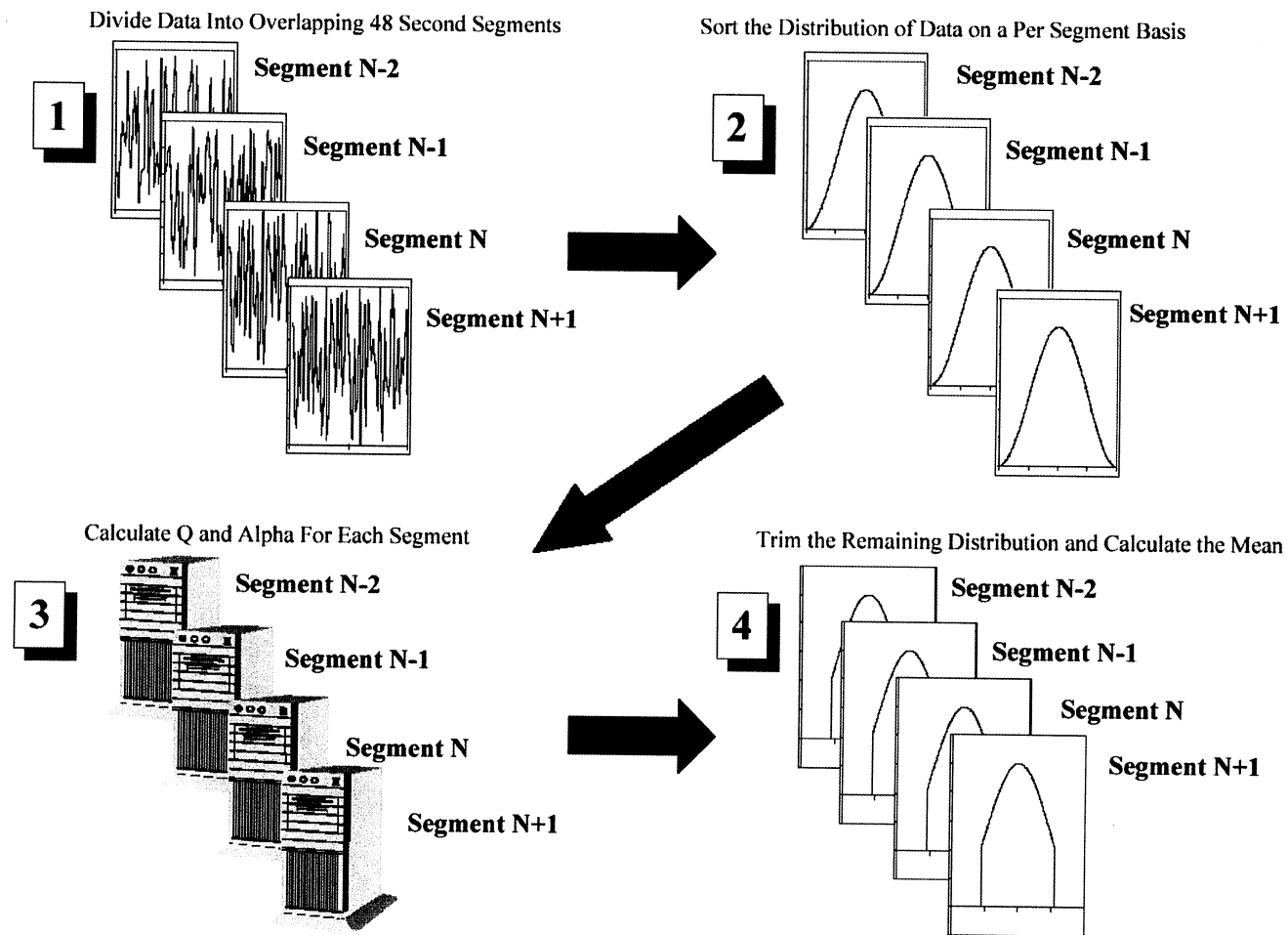


Figure 8.1.1-1 Trimmed Mean Filter Process

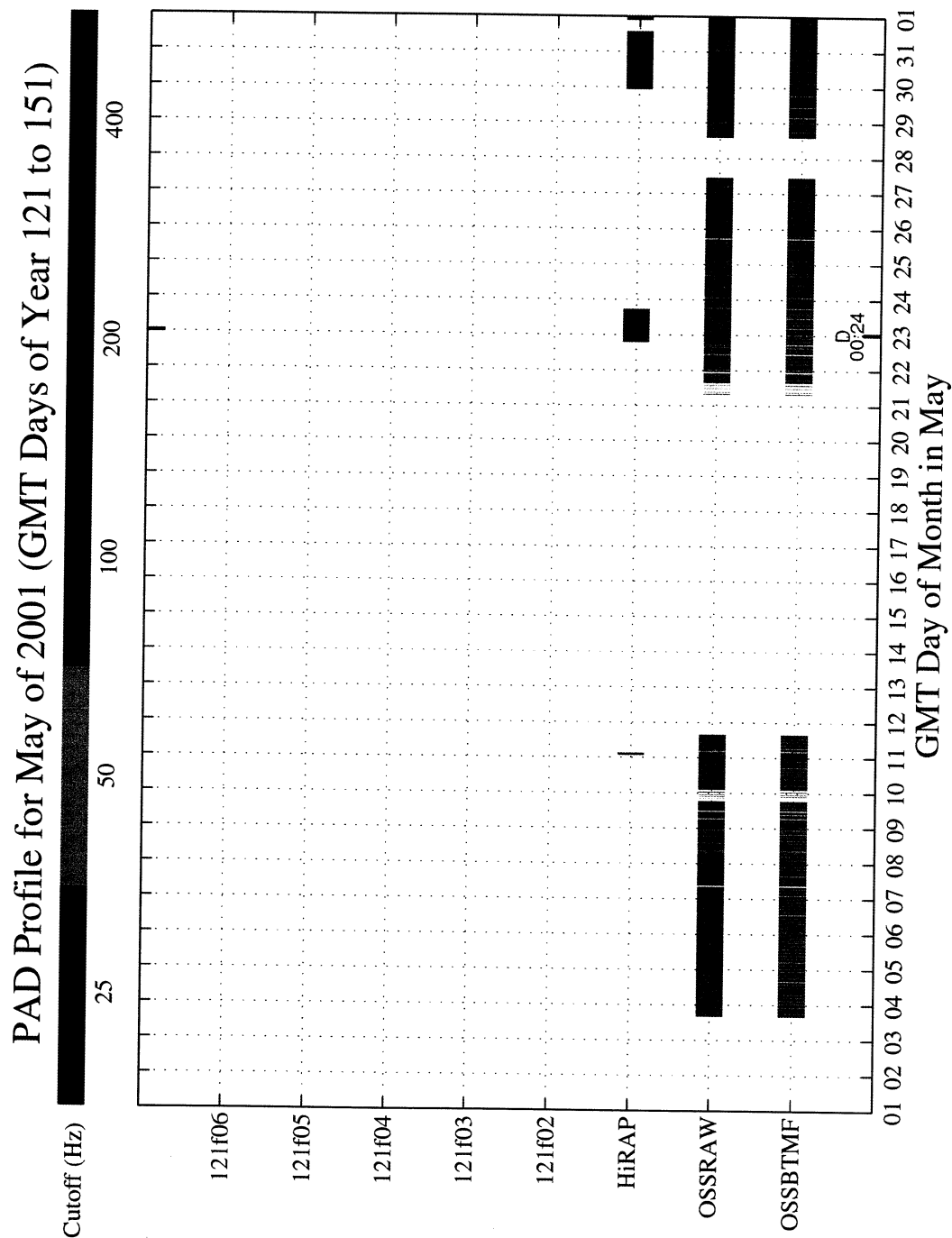


Figure 8.2-1 PAD Profile for May of 2001

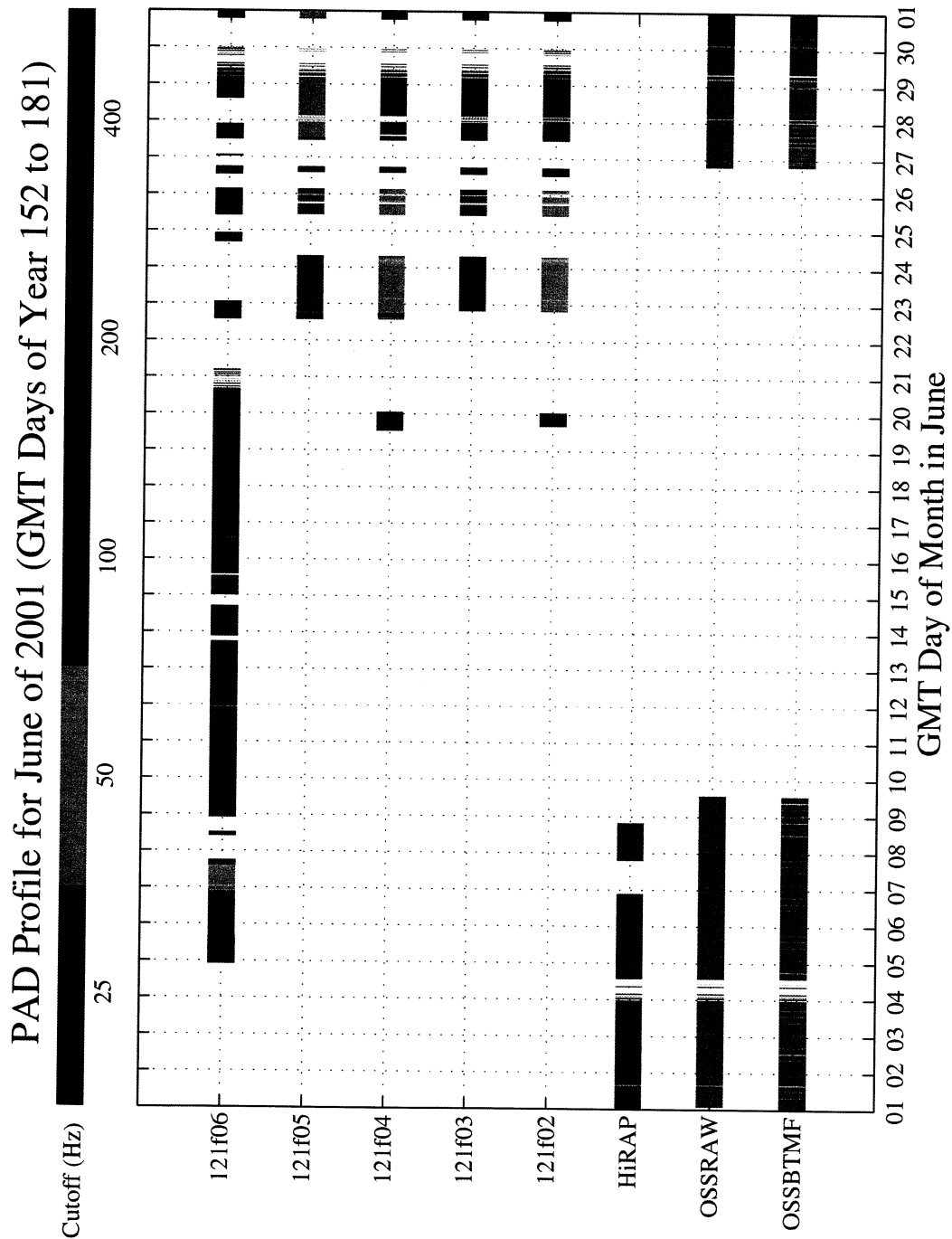


Figure 8.2-2 PAD Profile for June of 2001

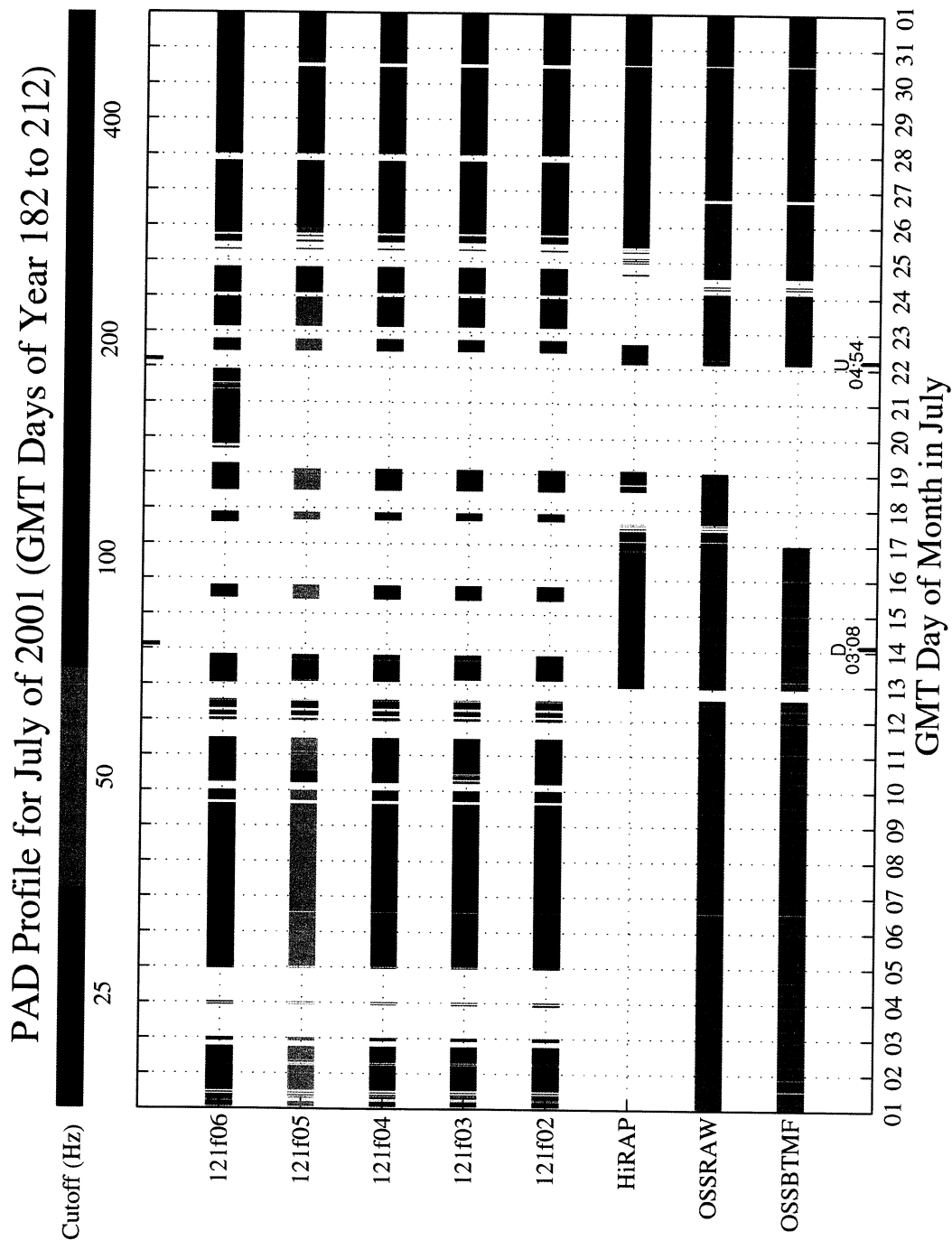


Figure 8.2-3 PAD Profile for July of 2001

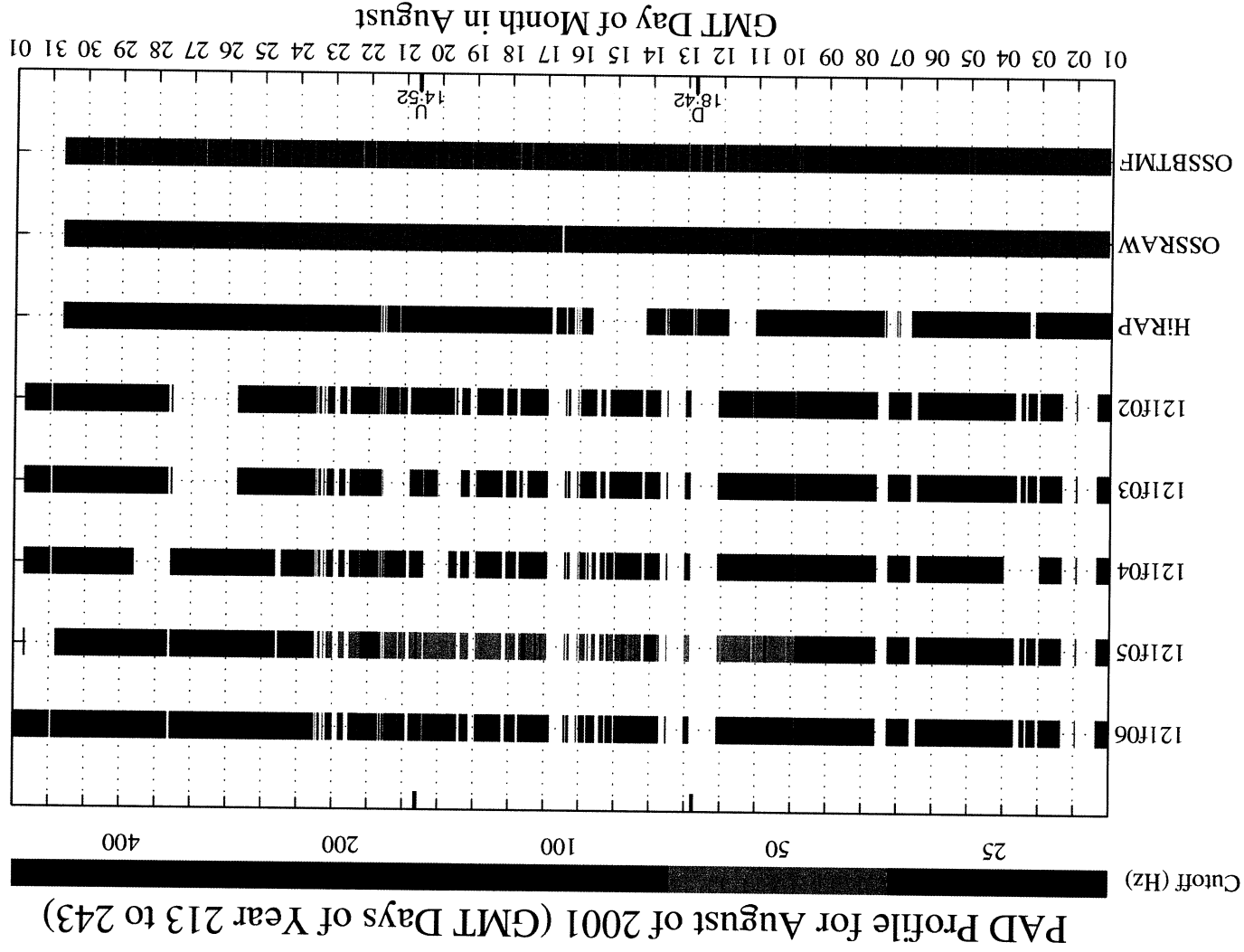


Figure 8.2-4 PAD Profile for August of 2001

PIMS ISS Increment-2 Microgravity Environment Summary Report: May to August 2001

mams, ossbtmf at LAB102, ERI, Lockers 3.4:[135.28 -10.68 132.12]
0.0625 sa/sec (1.0 Hz)

+ZLV +XVV Torque Equilibrium Attitude

Increment: 2, Flight: 6A
SSAnalysis[0.0 0.0 0.0]

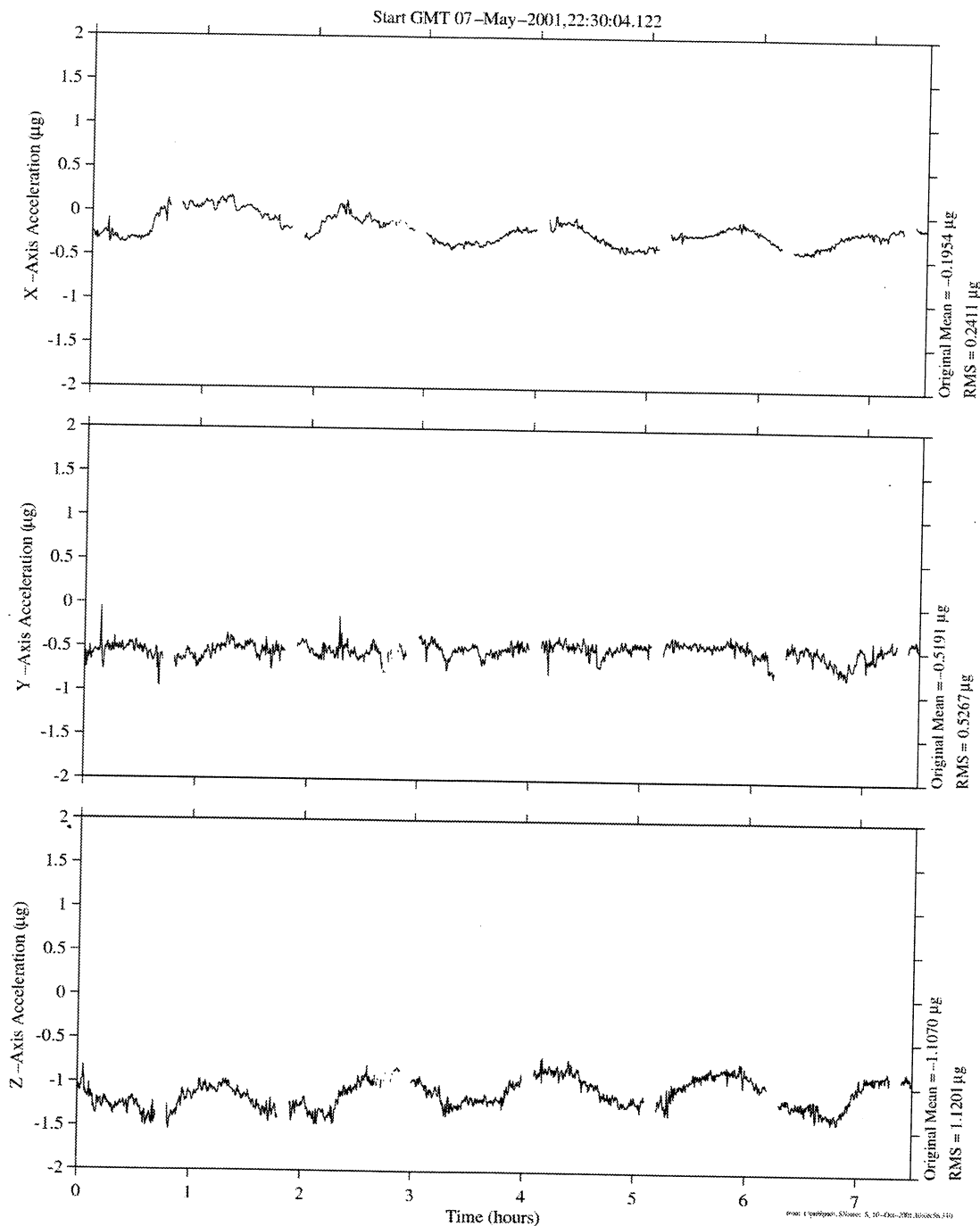


Figure 9.1.1-1 Time Series of Crew Sleep Period During Torque Equilibrium Attitude (OSS)

PIMS ISS Increment-2 Microgravity Environment Summary Report: May to August 2001

mams, osshint at LAB102, ER1, Lockers 3,4:[135.28 -10.68 132.12]
0.0625 sa/sec (1.0 Hz)

Increment: 2, Flight: 6A
SSAnalysis[0.0 0.0 0.0]

+ZLV +XVV Torque Equilibrium Attitude

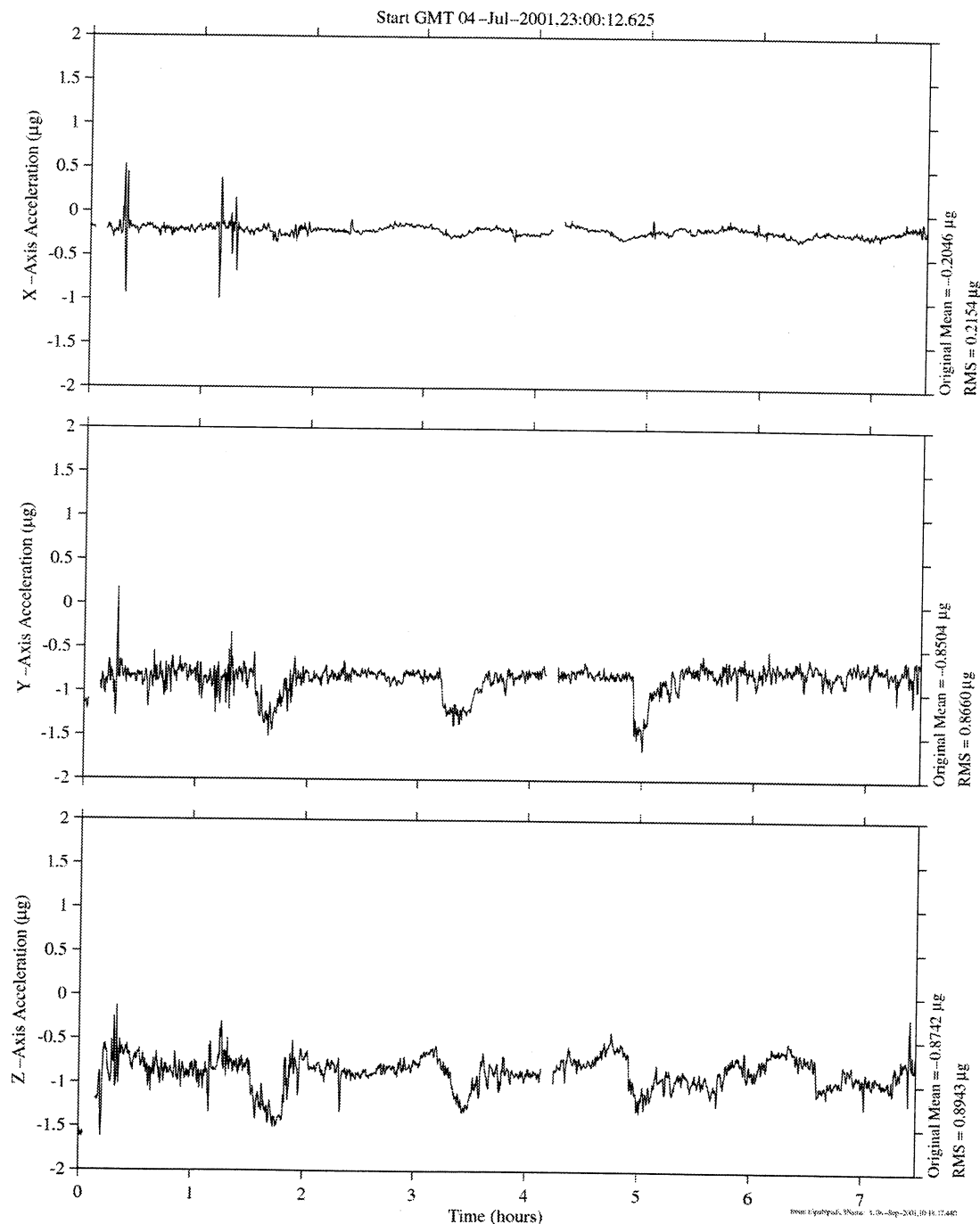
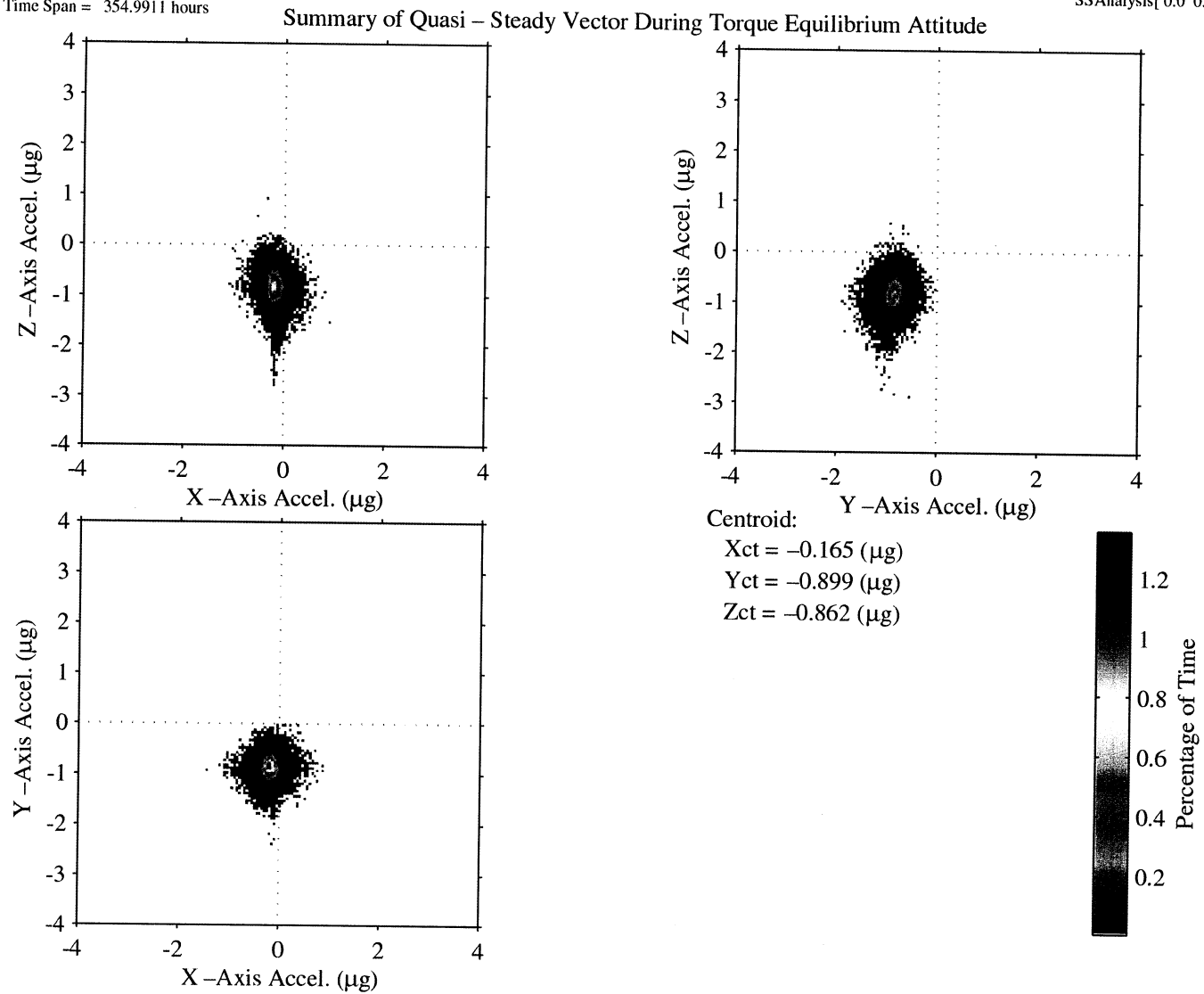


Figure 9.1.1-2 Time Series of Crew Sleep During Torque Equilibrium Attitude (OSS)

mams, ossbtmf at LAB102, ER1, Lockers 3,4:[135.28 -10.68 132.12]
 0.0625 sa/sec (1.0 Hz)
 Time Span = 354.9911 hours

Increment: 2, Flight: 6A
 SSAnalysis[0.0 0.0 0.0]

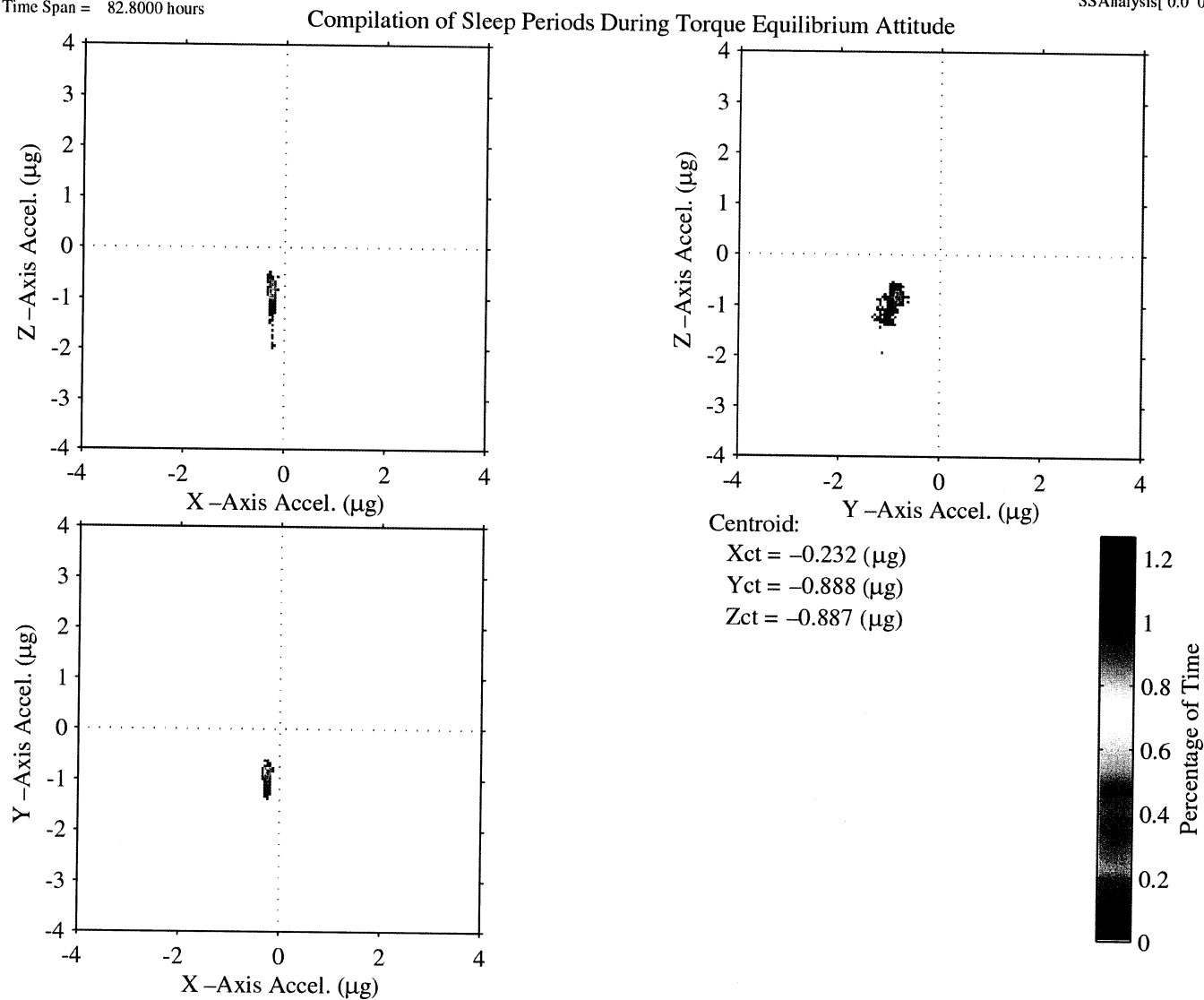


from: I:\publpad\, SName: 5_06-Sep-2001.11:56:23.860

Figure 9.1.1-3 QTH of Torque Equilibrium Attitude Compilation of GMT 123/21:00:10 for 187 hours and GMT 184/08:00:09 for 168 hours (OSS)

mams, ossbtmf at LAB1O2, ER1, Lockers 3,4:[135.28 -10.68 132.12]
 0.0625 sa/sec (1.0 Hz)
 Time Span = 82.8000 hours

Increment: 2, Flight: 6A
 SSAnalysis[0.0 0.0 0.0]



from: t:\pub\pad\, SName: S_06-Sep-2001,11:56:23,860

Figure 9.1.1-4 QTH of Crew Sleep Periods Compilation During TEA of GMT 123/21:00:10 and GMT 184/08:00:09 for 82 hours (OSS)

PIMS ISS Increment-2 Microgravity Environment Summary Report: May to August 2001

mams, ossbmf at LAB102, ER1, Lockers 3,4:[135.28 -10.68 132.12]
0.0625 sa/sec (1.0 Hz)

Increment: 2, Flight: 6A
SSAnalysis[0.0 0.0 0.0]

Crew Sleep Period During XPOP Attitude

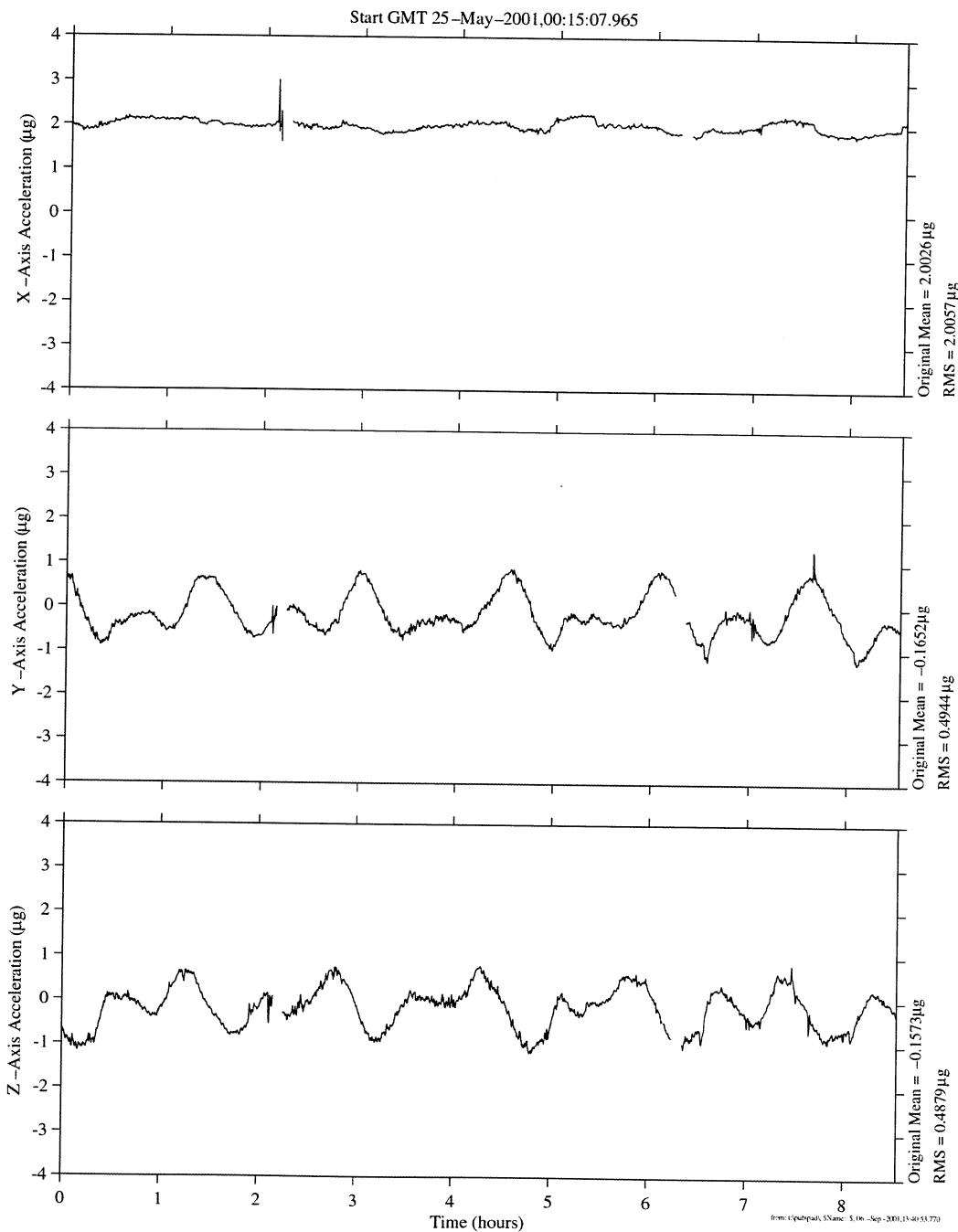
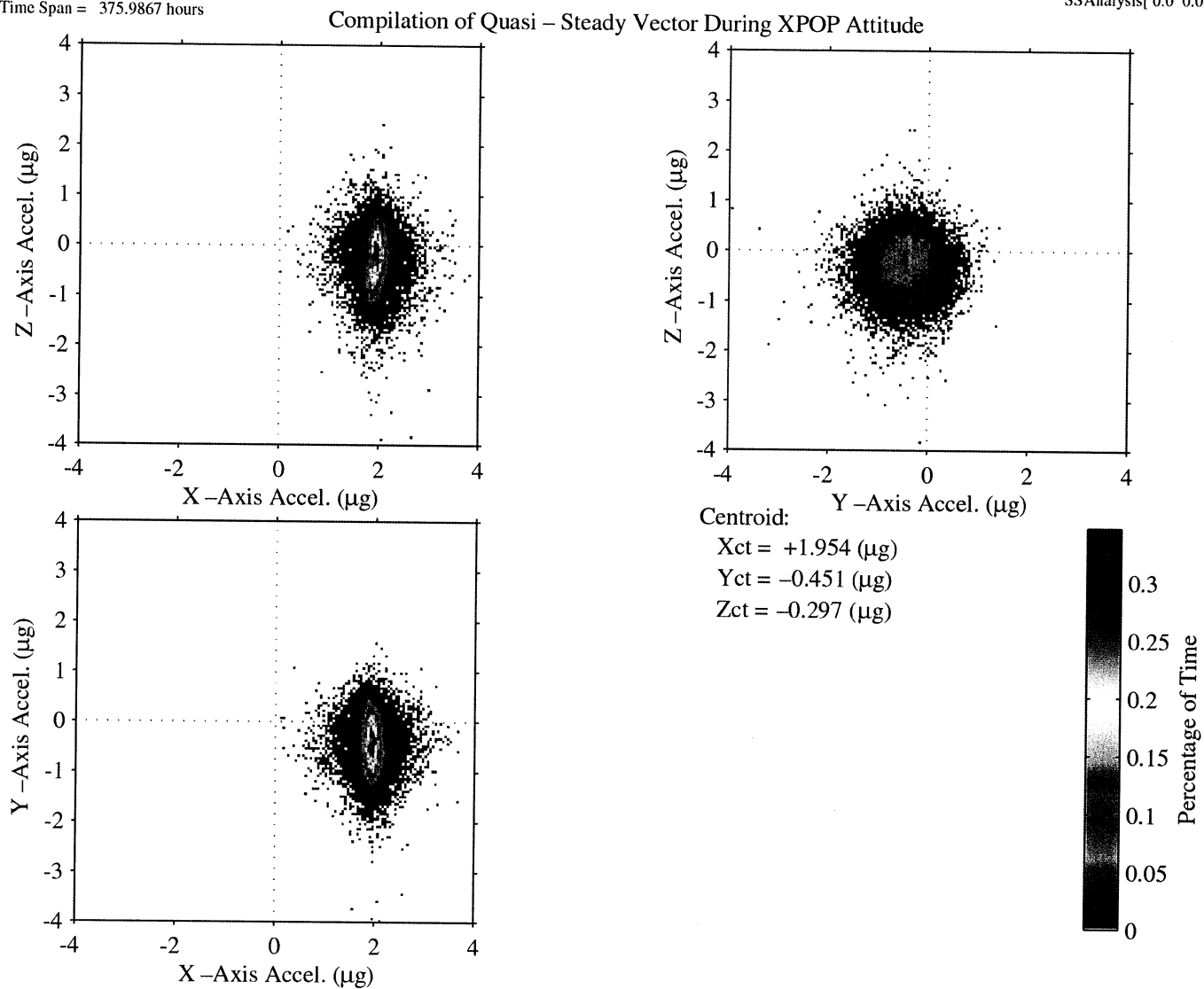


Figure 9.1.2-1 Time Series of Crew Sleep Period During XPOP Attitude

mams, ossbtmf at LAB1O2, ER1, Lockers 3,4:[135.28 -10.68 132.12]
 0.0625 sa/sec (1.0 Hz)
 Time Span = 375.9867 hours

Increment: 2, Flight: 6A
 SSAnalysis[0.0 0.0 0.0]

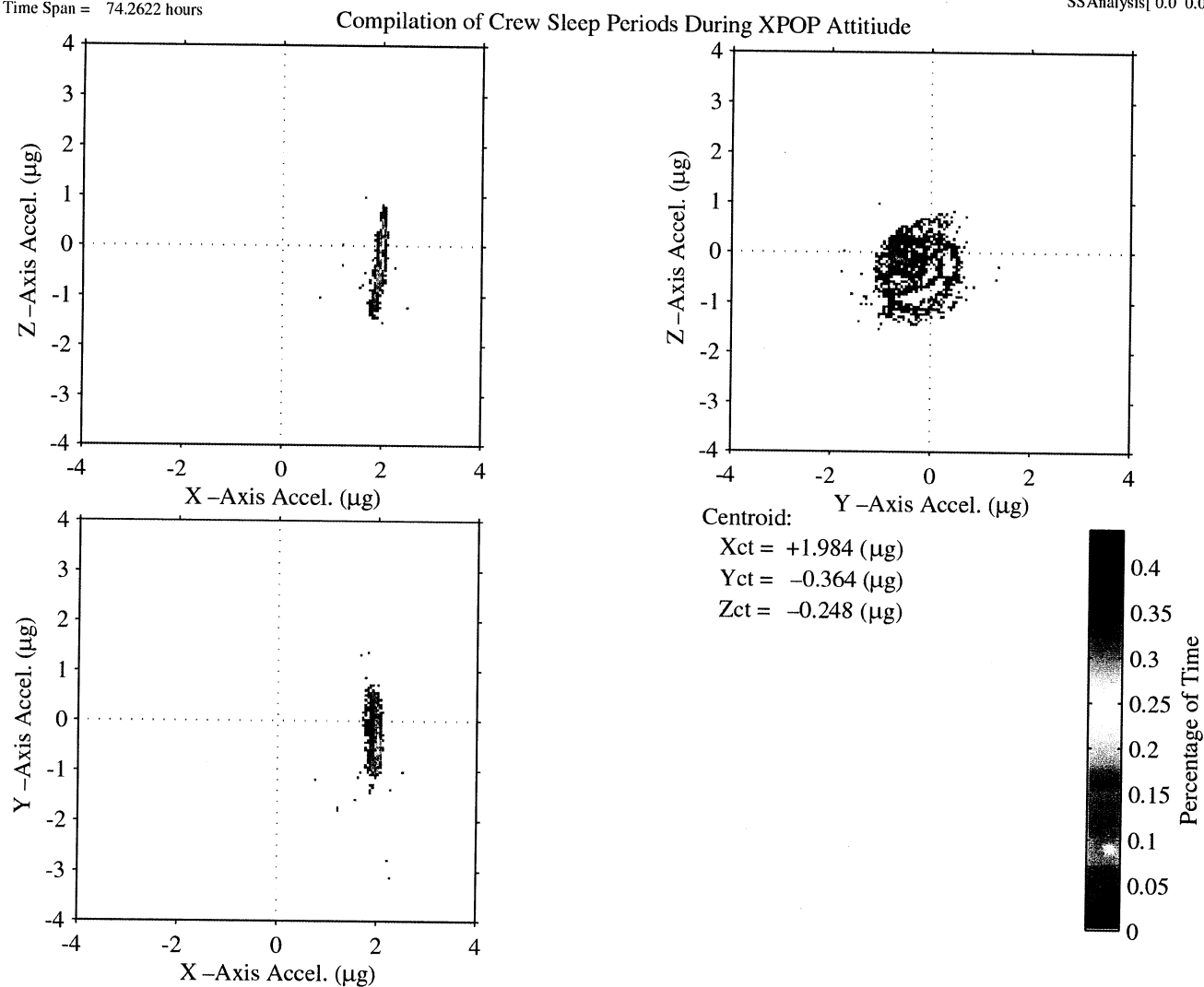


from: t:\pub\pd\5Name: 5_06-Sep-2001,11:56:23.860

Figure 9.1.2-2 QTH Summary of XPOP Attitude 101 hours beginning GMT 143/06:00:07, 167 hours beginning GMT 150/16:00:13 and 108 hours beginning GMT 157/18:00:09 (OSS)

mams, ossbtmf at LAB1O2, ER1, Lockers 3,4:[135.28 -10.68 132.12]
 0.0625 sa/sec (1.0 Hz)
 Time Span = 74.2622 hours

Increment: 2, Flight: 6A
 SSAnalysis[0.0 0.0 0.0]



from: t:\pub\pad\5Name: 5_06-Sep-2001.11:56:23.860

Figure 9.1.2-3 QTH Summary of Crew Sleep Periods During XPOP Attitude 101 hours beginning GMT 143/06:00:07, 167 hours beginning GMT 150/16:00:13 and 108 hours beginning GMT 157/18:00:09

PIMS ISS Increment-2 Microgravity Environment Summary Report: May to August 2001

mams, ossbmf at LAB102, ER1, Lockers 3,4:[135.28 -10.68 132.12]
0.0625 sa/sec (1.0 Hz)

Soyuz TM -31 Undocking

Increment: 2, Flight: 6A
SSAnalysis[0.0 0.0 0.0]

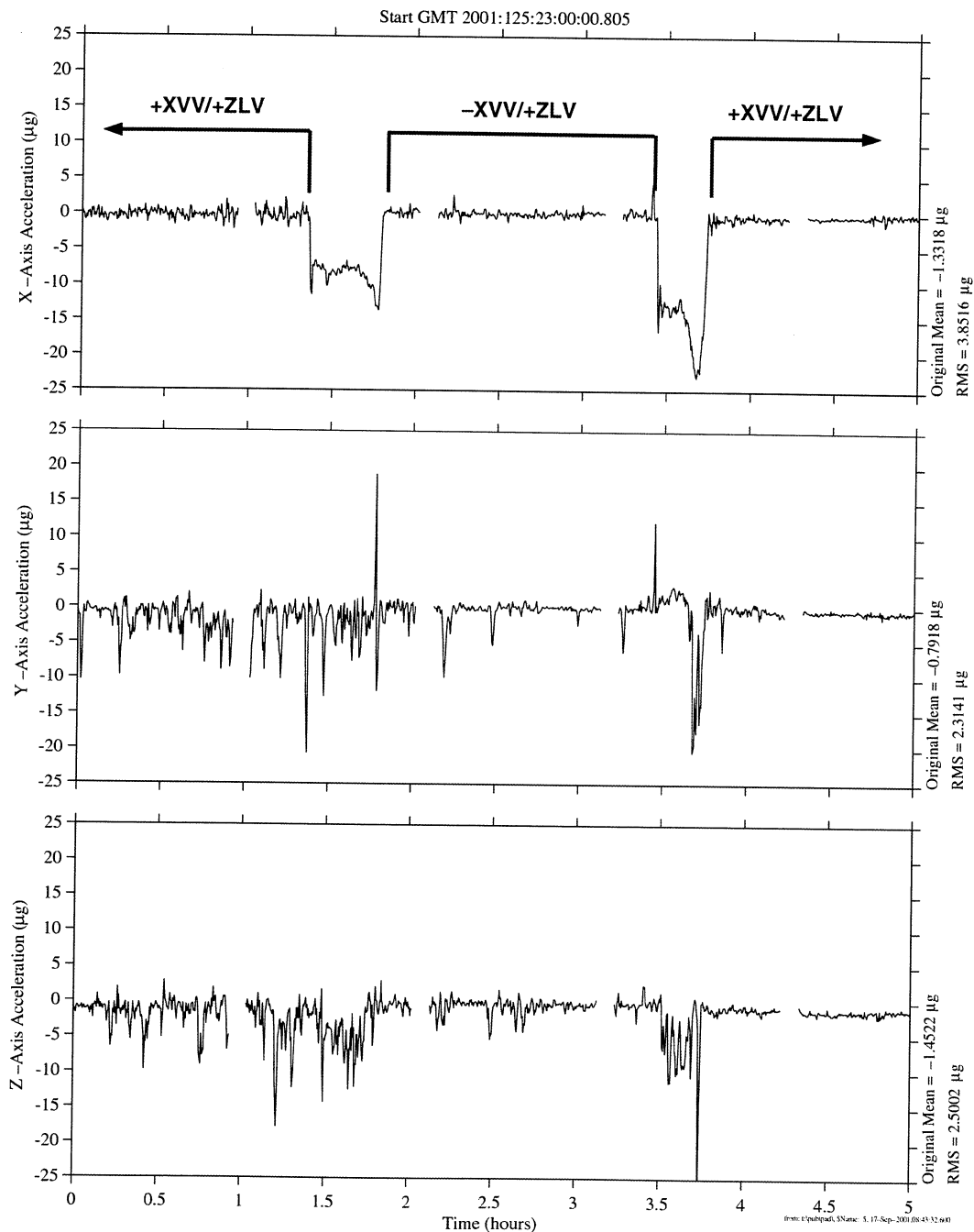


Figure 9.2.1-1 Time Series of Attitude Change for Undocking of Soyuz TM-31 (OSS)

PIMS ISS Increment-2 Microgravity Environment Summary Report: May to August 2001

mams. ossbtfm/ at LAB102, ER1, Lockers 3,4:[135.28 -10.68 132.12]
0.0625 sa/sec (1.0 Hz)

4P Progress Docking

Increment: 2, Flight: 6A
SSAnalysis[0.0 0.0 0.0]

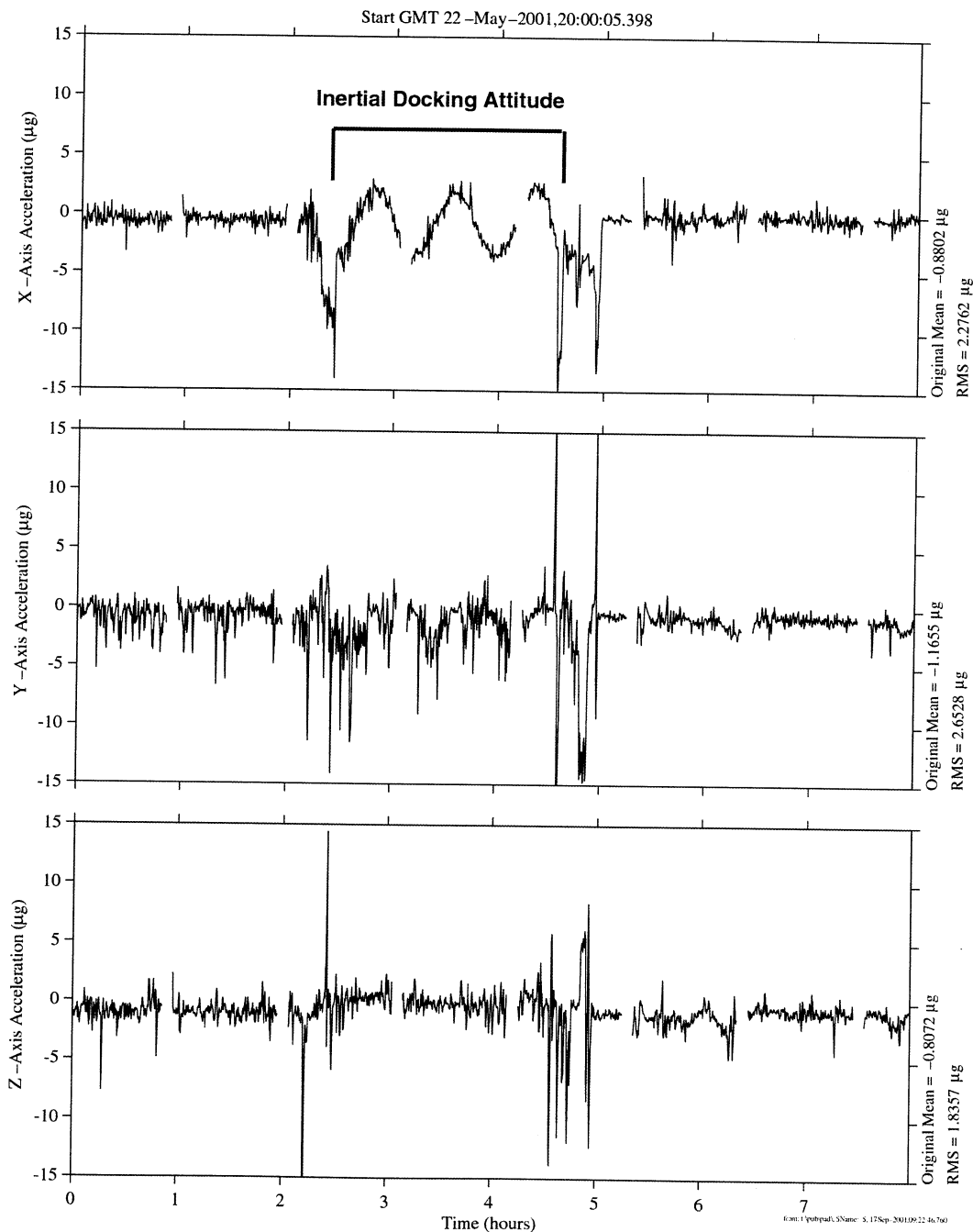


Figure 9.2.2-1 Time Series of Docking Attitude for Progress (4P) Docking (OSS)

PIMS ISS Increment-2 Microgravity Environment Summary Report: May to August 2001

naans, ossbmf at LAB102, ER1, Lockers 3.4:[35.28 -0.68 132.12]
0.0625 sa/sec (1.0 Hz)

Increment: 2, Flight: 6A
SSAnalysis[0.0 0.0 0.0]

STS - 104 Docking Events

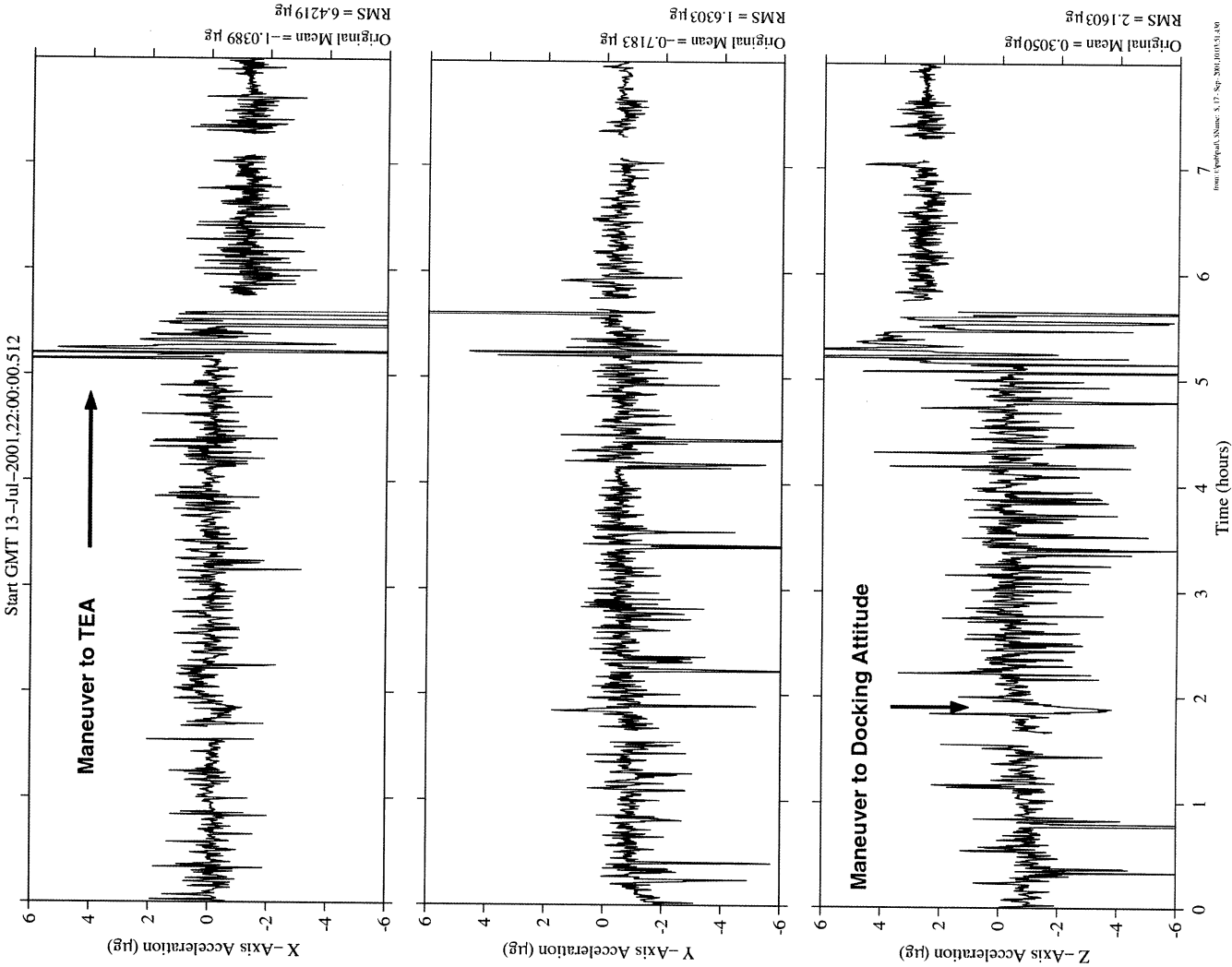


Figure 9.2.3-1 Time Series of Atlantis Docking During STS-104 (OSS)

PIMS ISS Increment-2 Microgravity Environment Summary Report: May to August 2001

namis_ossbim1 at LAB102. ERI. Lockers 3.4:[135.28 -10.68 132.12]
0.0025 s/sacc (1.0 Hz)

Increment: 2, Flight: 7A
SSAnalysis[0.0 0.0 0.0]

STS-105 Docking

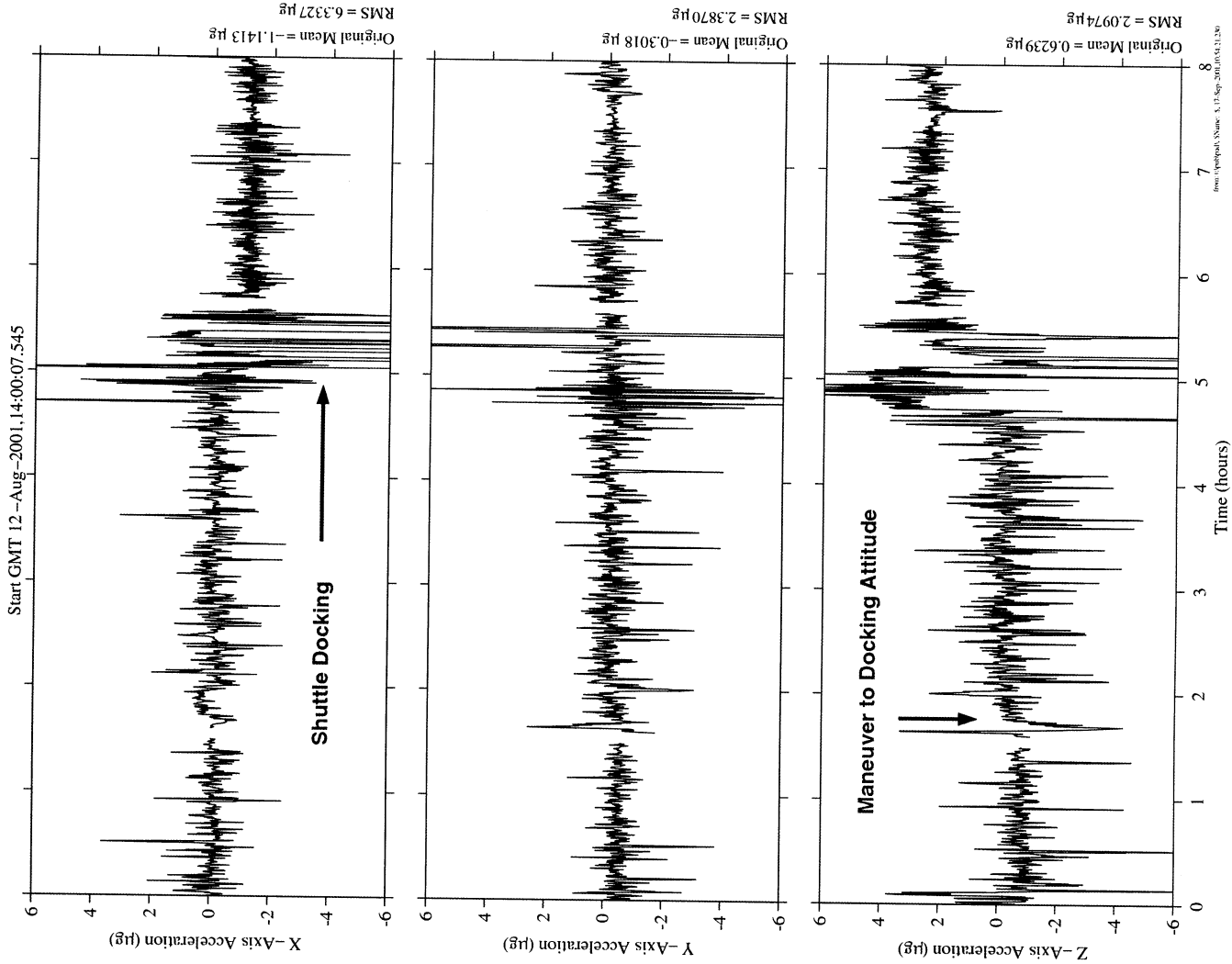


Figure 9.2.3.2 Time Series of Discovery Docking During STS-105 (OSS)

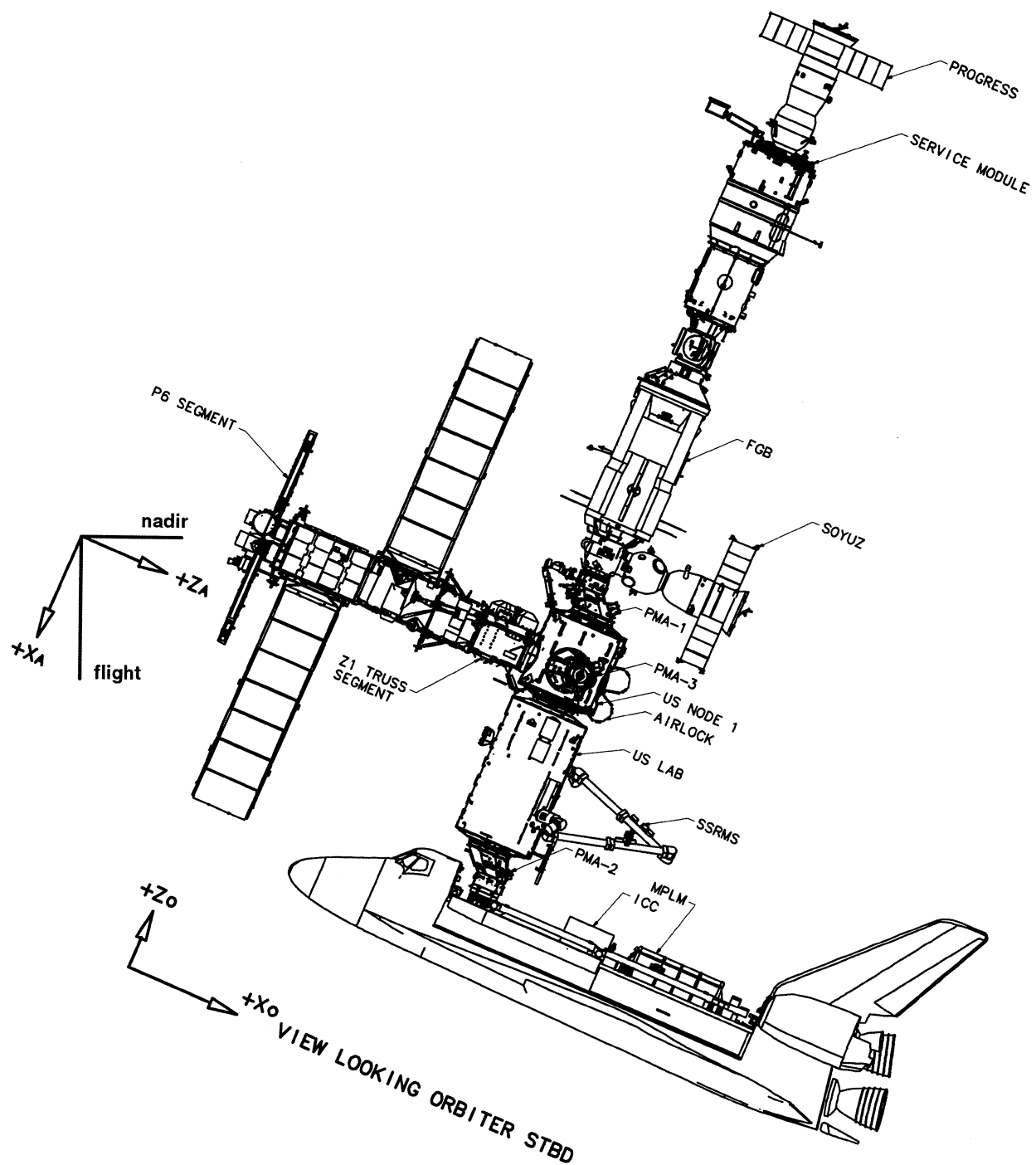
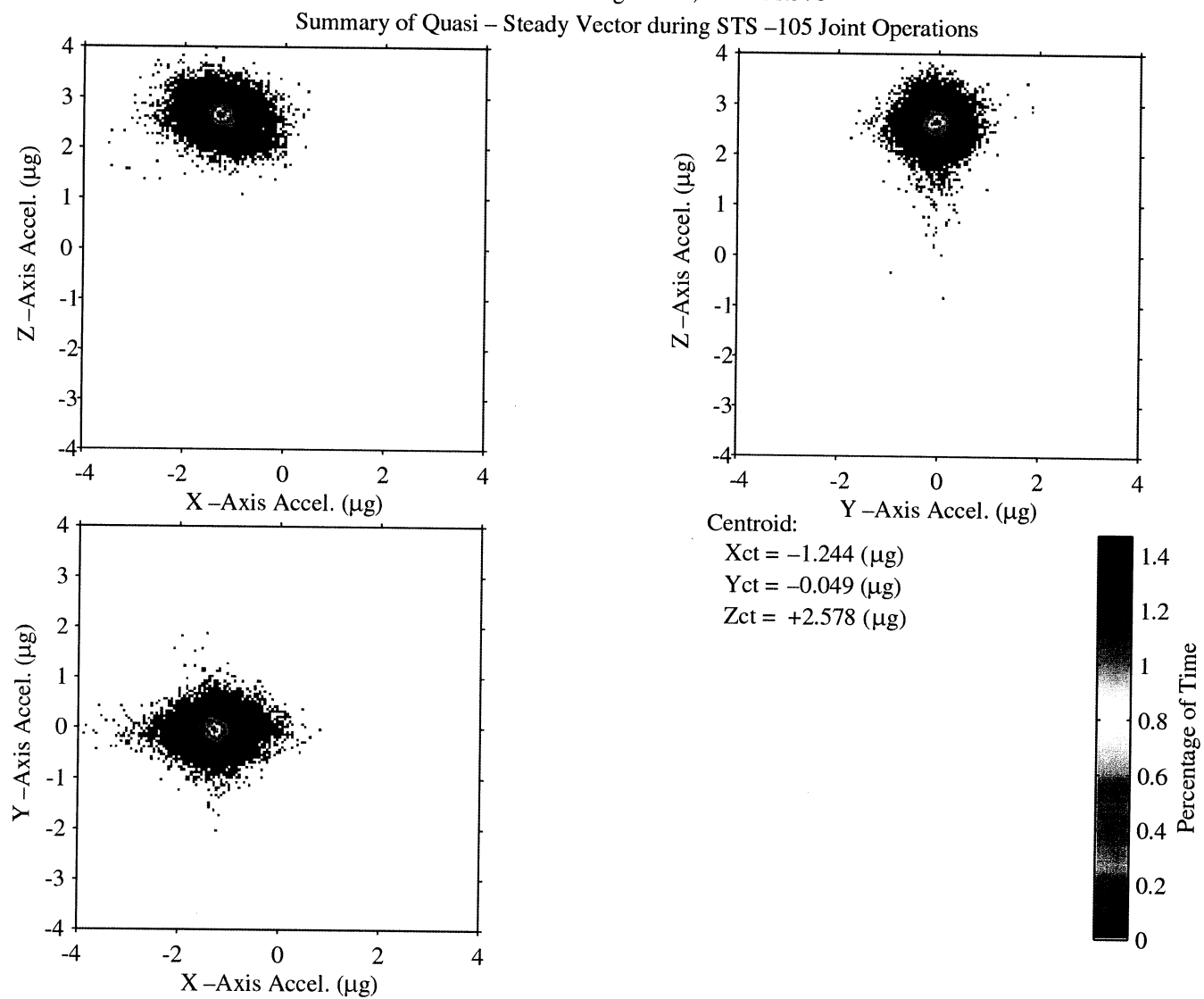


Figure 9.2.3-3 +ZLV +XVV Bias Attitude for STS-105

mams, ossbtmf at LAB102, ER1, Lockers 3,4:[135.28 -10.68 132.12]
 0.0625 sa/sec (1.0 Hz)
 Time Span = 187.5022 hours

Start GMT 12 -Aug -2001,19:00:01.578

Increment: 2, Flight: 7A
 SSAnalysis[0.0 0.0 0.0]



from: t:\pub\pdf\test\5Name: 5_10-Sep-2001,10:20:00.700

Figure 9.2.3-4 QTH of STS-105 Joint Operations (OSS)

PIMS ISS Increment-2 Microgravity Environment Summary Report: May to August 2001

mams, ossbtmf at LAB102, ER1, Lockers 3,4:[135.28 -10.68 132.12]
0.0625 sa/sec (1.0 Hz)

STS-105 Undocking

Increment: 3, Flight: 7A.1
SSAnalysis[0.0 0.0 0.0]

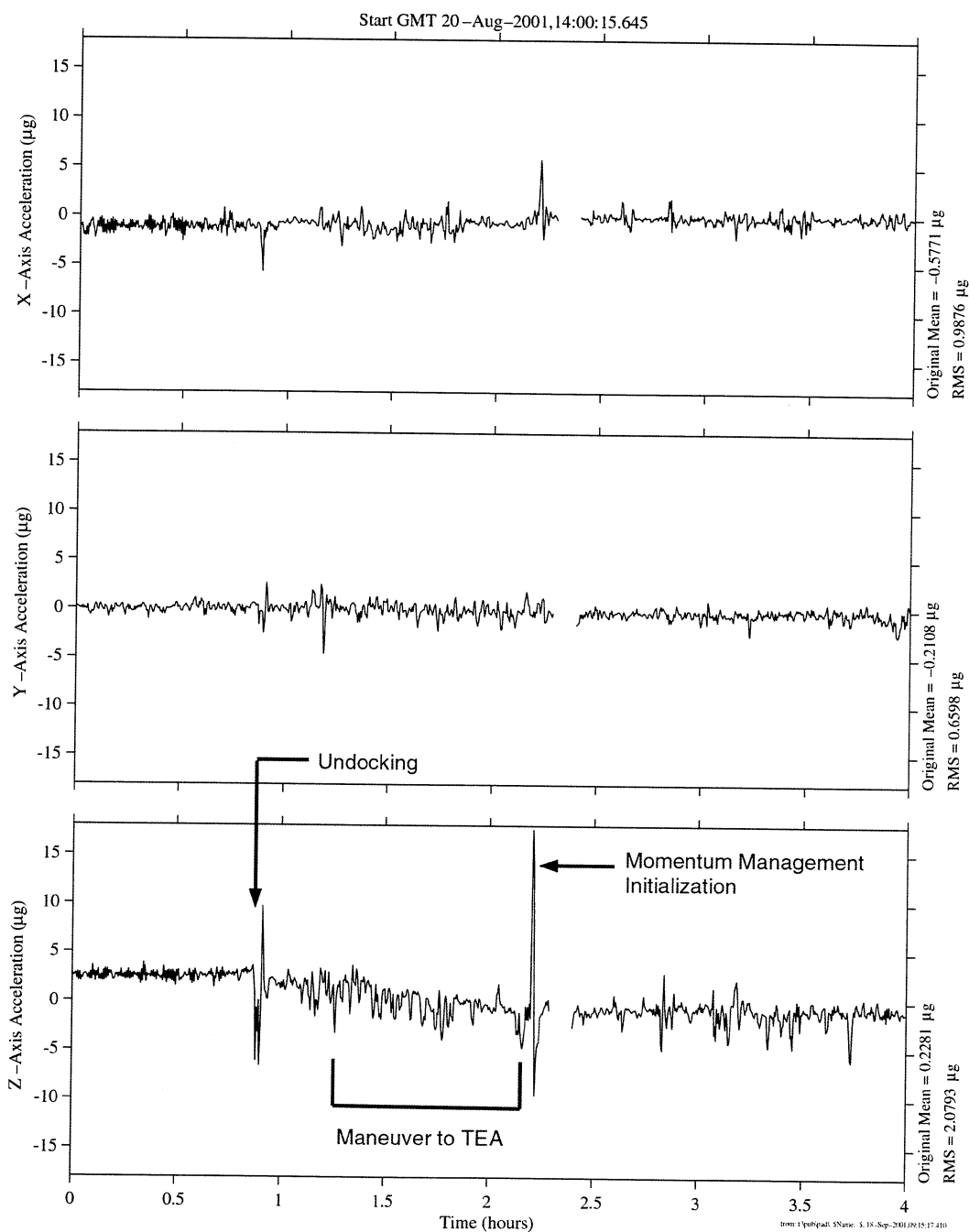


Figure 9.2.4-1 Time Series of STS-105 Undocking Events (OSS)

PIMS ISS Increment-2 Microgravity Environment Summary Report: May to August 2001

main: ossbmf at LAB102.ER1, Lockers 3.4:[35.28 -10.68 [32.12]
0.0025 su/sec (1.0 Hz)

Increment: 2, Flight: 6A
SS Analysis(0.0 0.0 0.0)

10.2 Orbiter Cabin Depressurization During STS -104

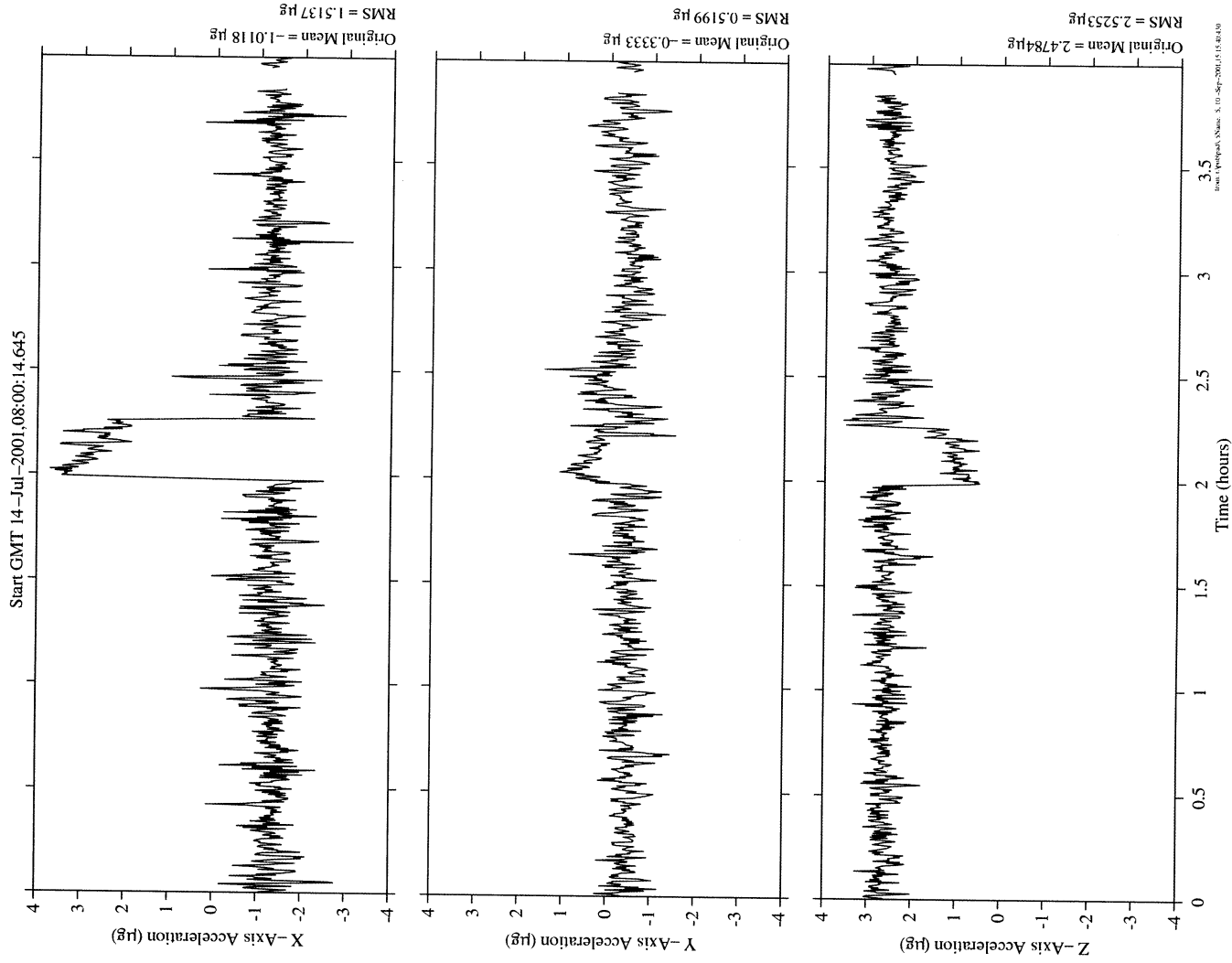


Figure 9.2.5-1 Time Series of Cabin Depressurization in Preparation for EVA (OSS)

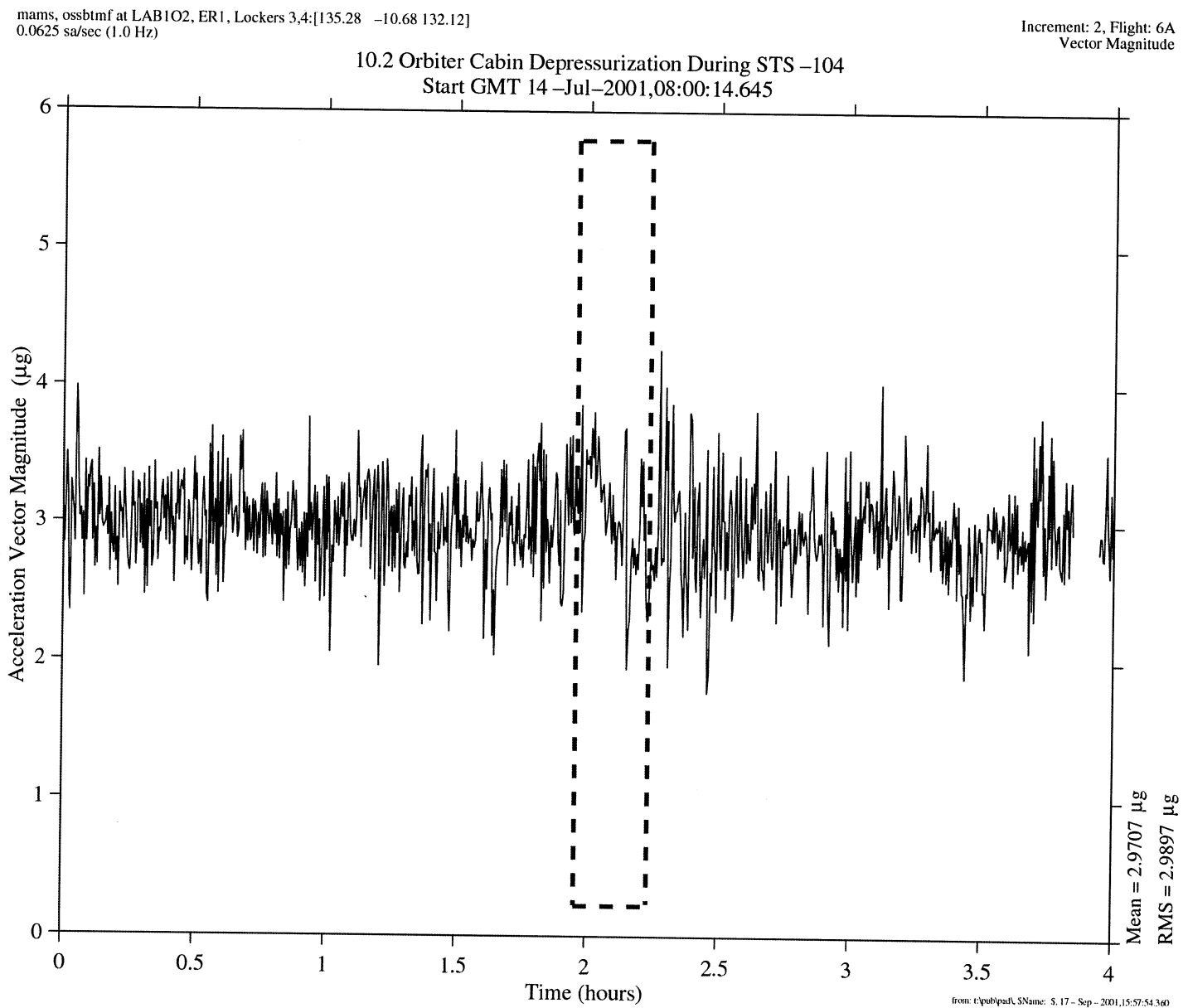


Figure 9.2.5-2 QTH of Orbiter Depressurization (OSS)

PIMS ISS Increment-2 Microgravity Environment Summary Report: May to August 2001

mams, ossraw at LAB102, ER1, Lockers 3,4:[135.28 -10.68 132.12]
10.0 sa/sec (1.00 Hz)

Reboost #3 During STS -105 Joint Operations

Increment: 2, Flight: 7A
SSAnalysis[0.0 0.0 0.0]

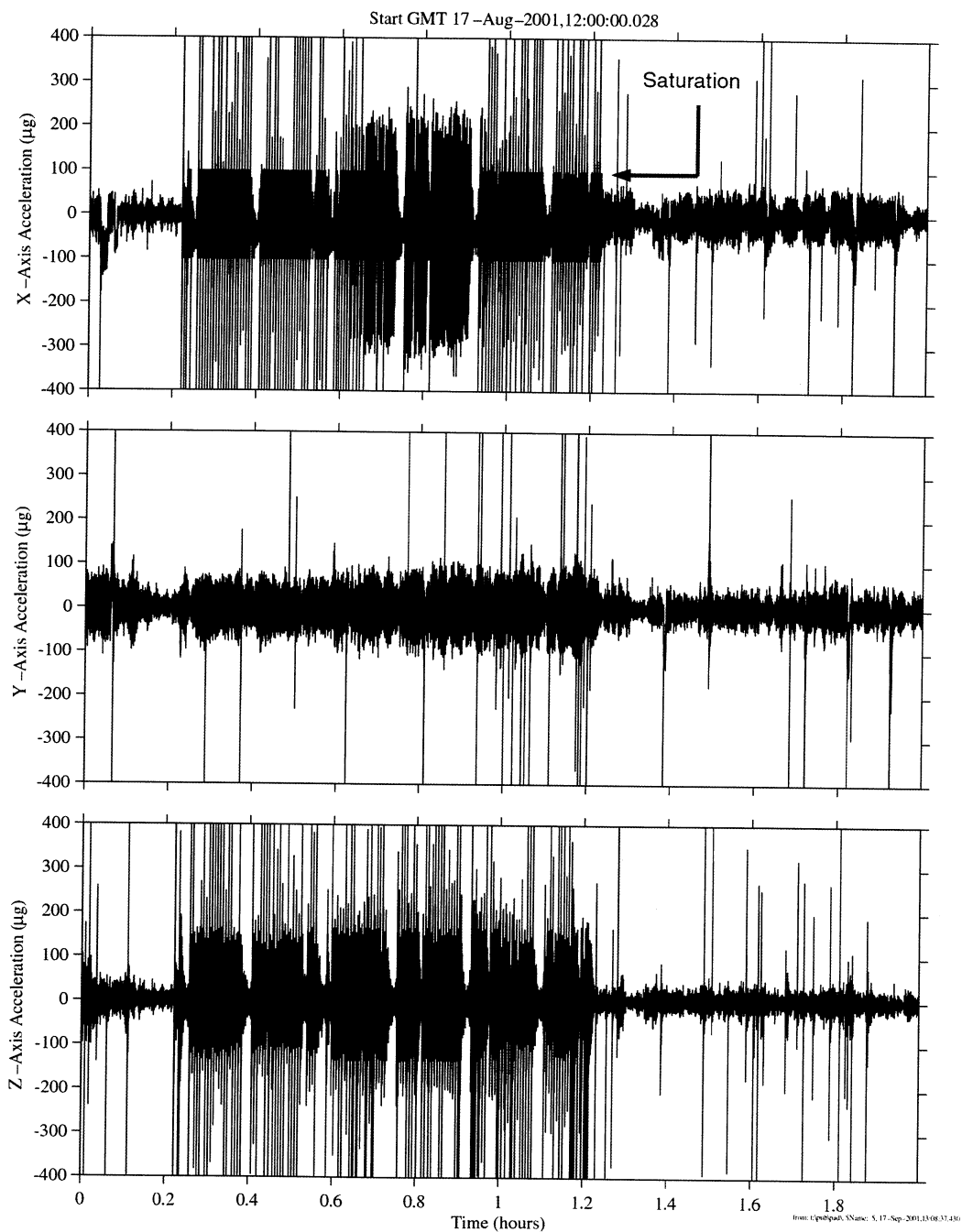


Figure 9.2.6-1 Time Series of MAMS OSS Sensor Saturation During Station Reboost (OSS)

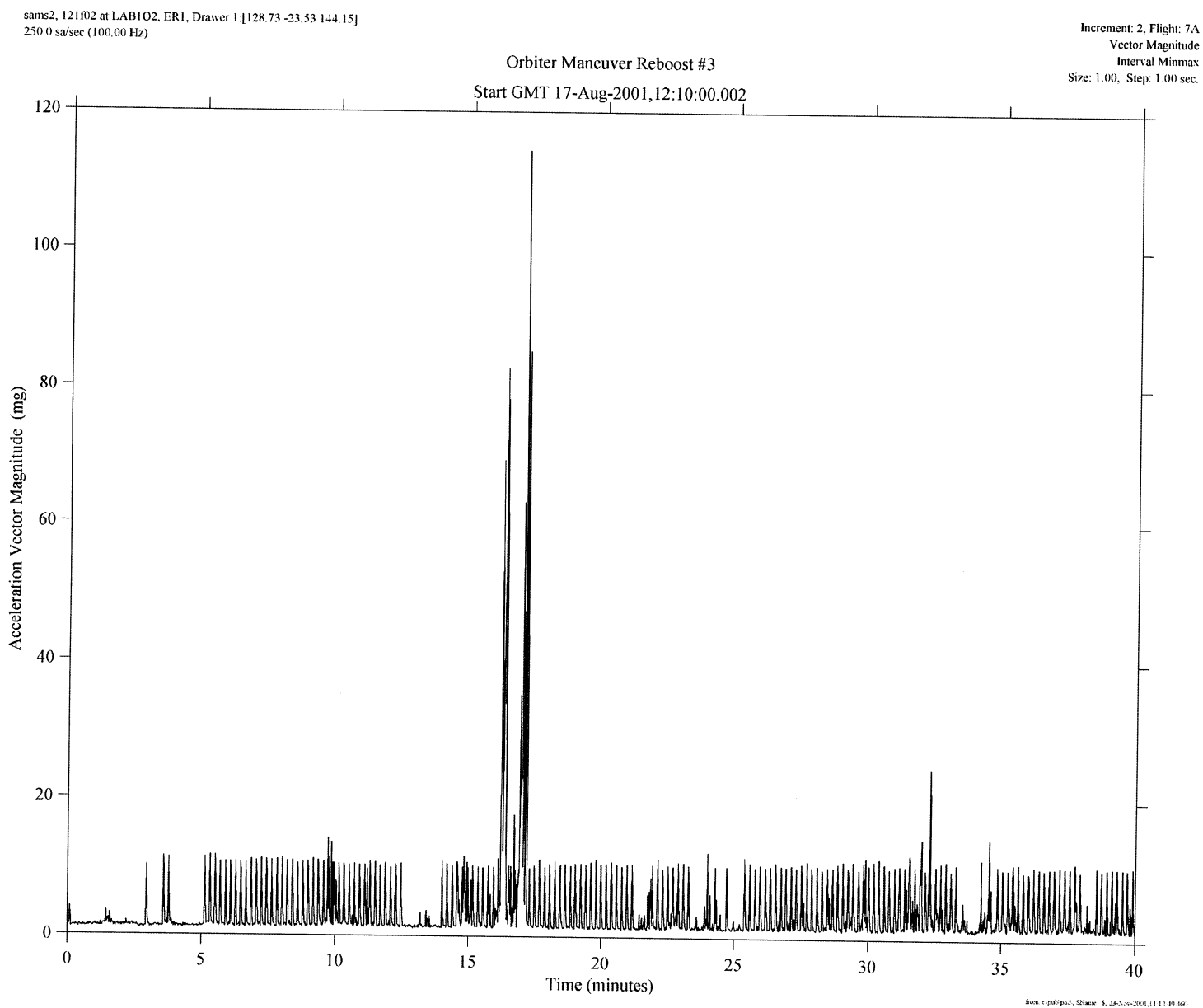


Figure 9.2.6-2 Interval Magnitude of STS-105 Reboost #3 (121f02)

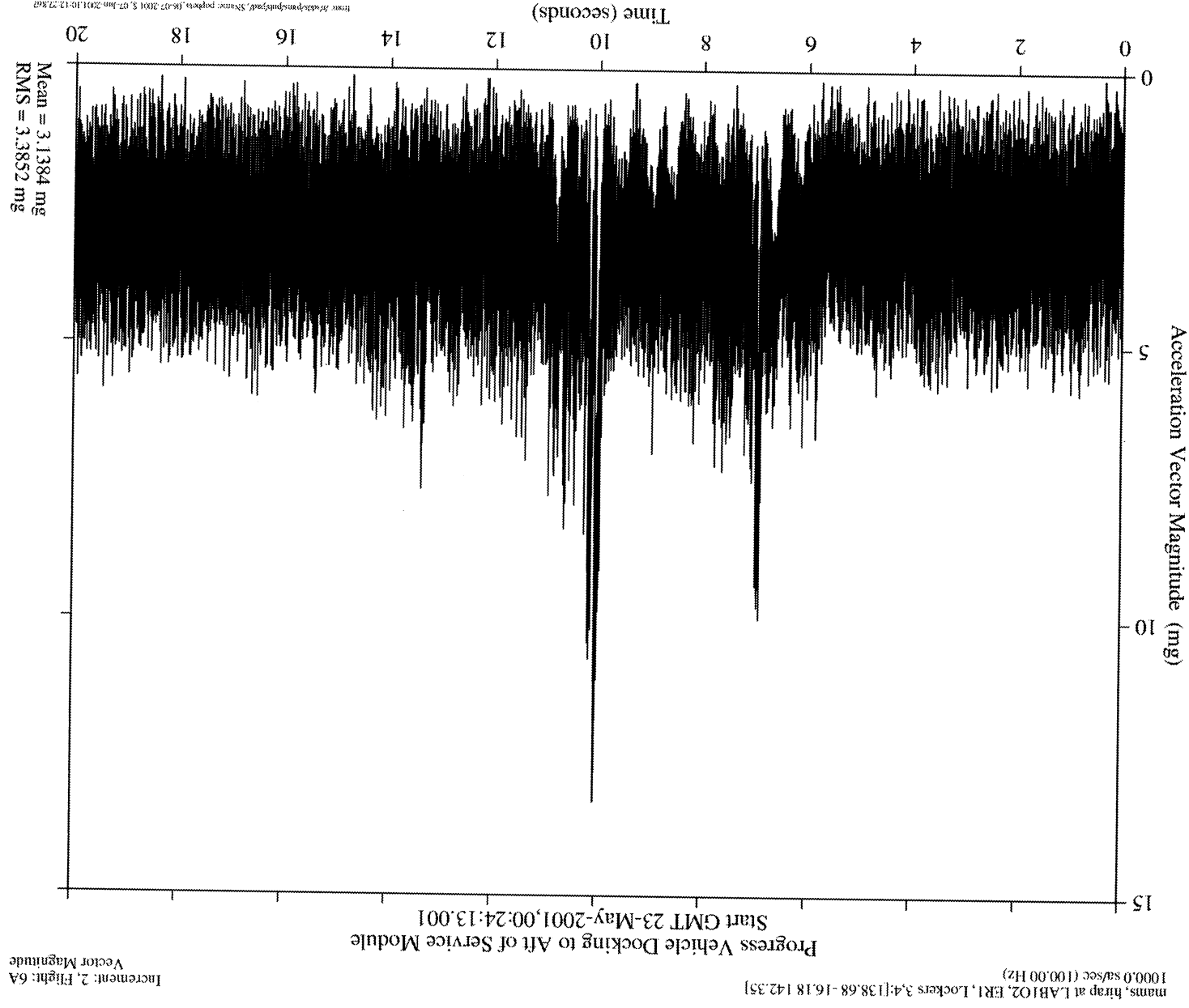


Figure 9.3.1.1.1-1 Acceleration Magnitude of Progress (4P) Docking (HIRAP)

PIMS ISS Increment-2 Microgravity Environment Summary Report: May to August 2001

mams, hirap at LAB102, ER1, Lockers 3,4:[138.68 -16.18 142.35]
1000.0 sa/sec (100.00 Hz)

Progress Vehicle Docking to Aft of Service Module

Increment: 2, Flight: 6A
hirap[180.0 0.0 0.0]

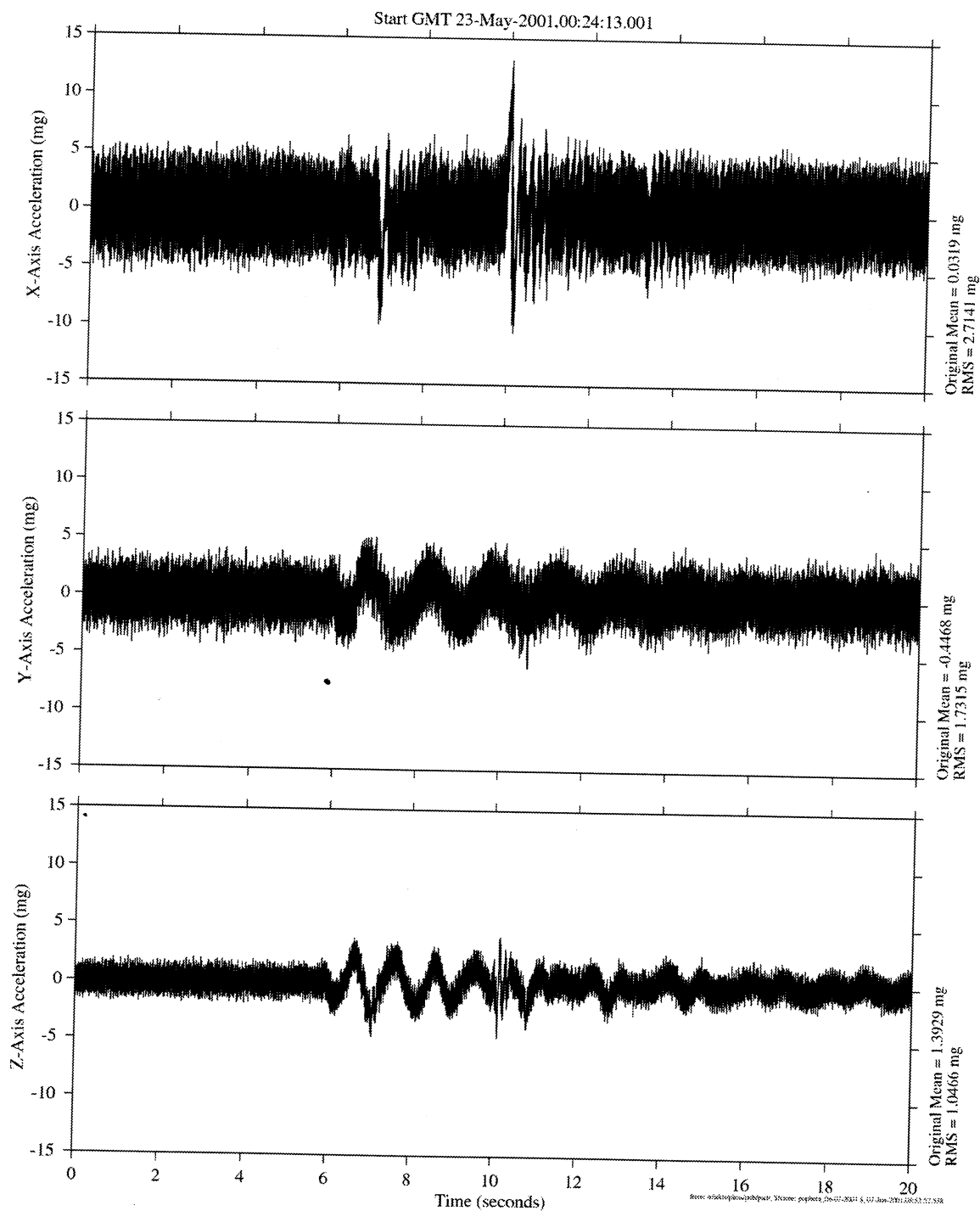


Figure 9.3.1.1.1-2 Time Series of Progress (4P) Docking (HiRAP)

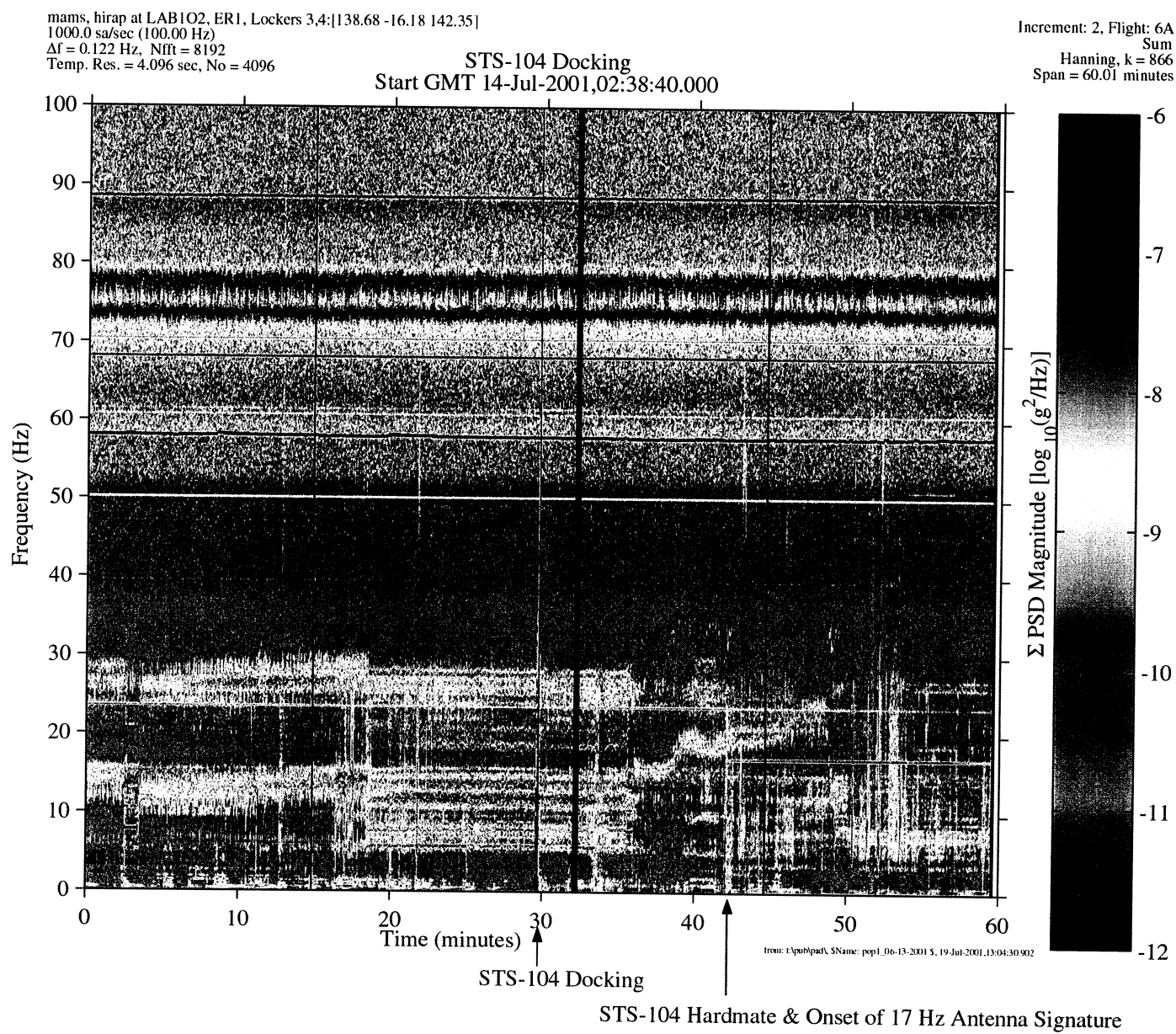


Figure 9.3.1.1.2-1 Spectrogram of Shuttle (7A) Docking (HiRAP)

Increment: 2, Flight: 6A
Vector Magnitude
Interval Minimax
Size: 0.10, Step: 0.10 sec.

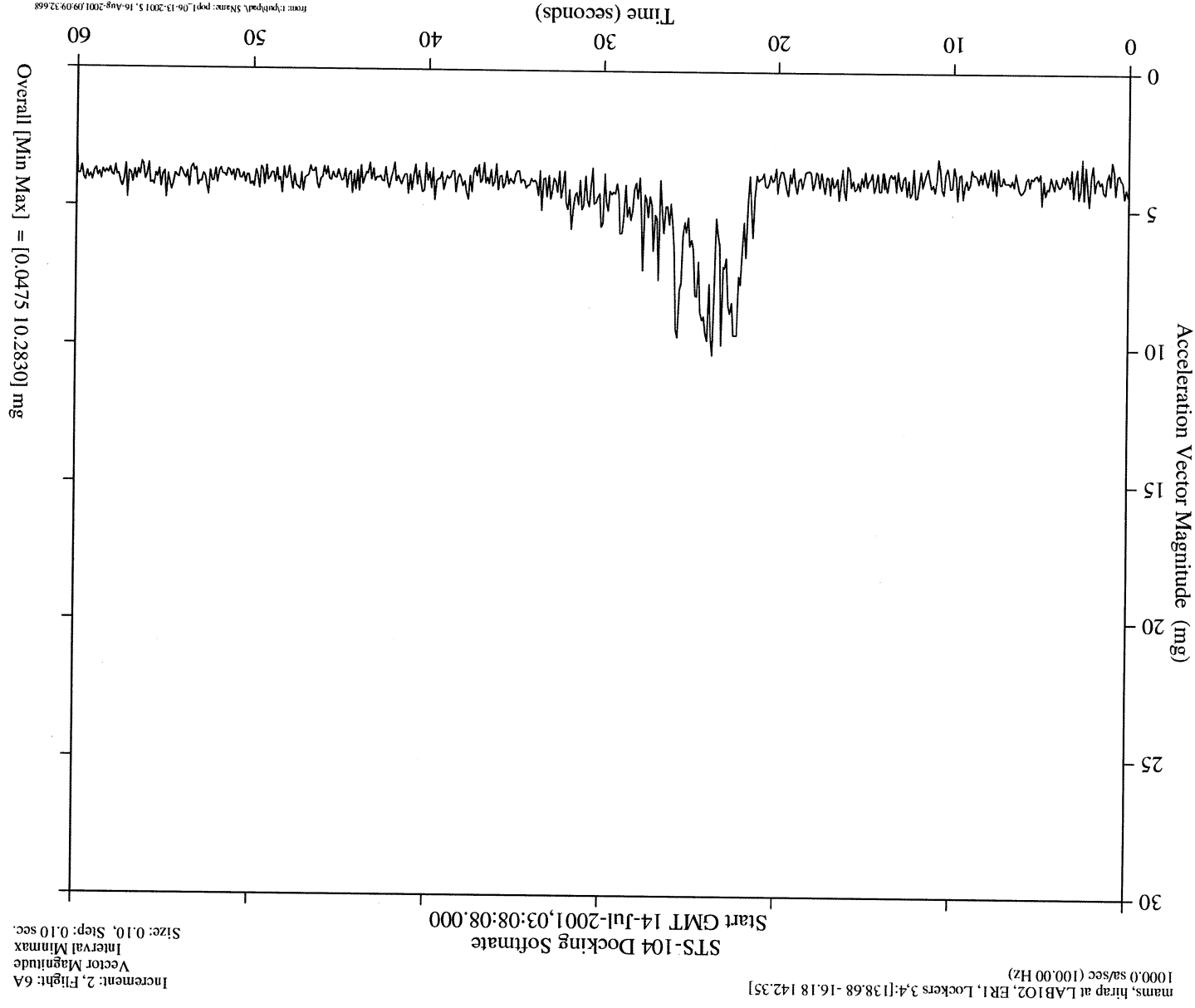


Figure 9.3.1.1.2-2 Acceleration Magnitude of Shuttle (7A) Docking Softmate (HiRAP)

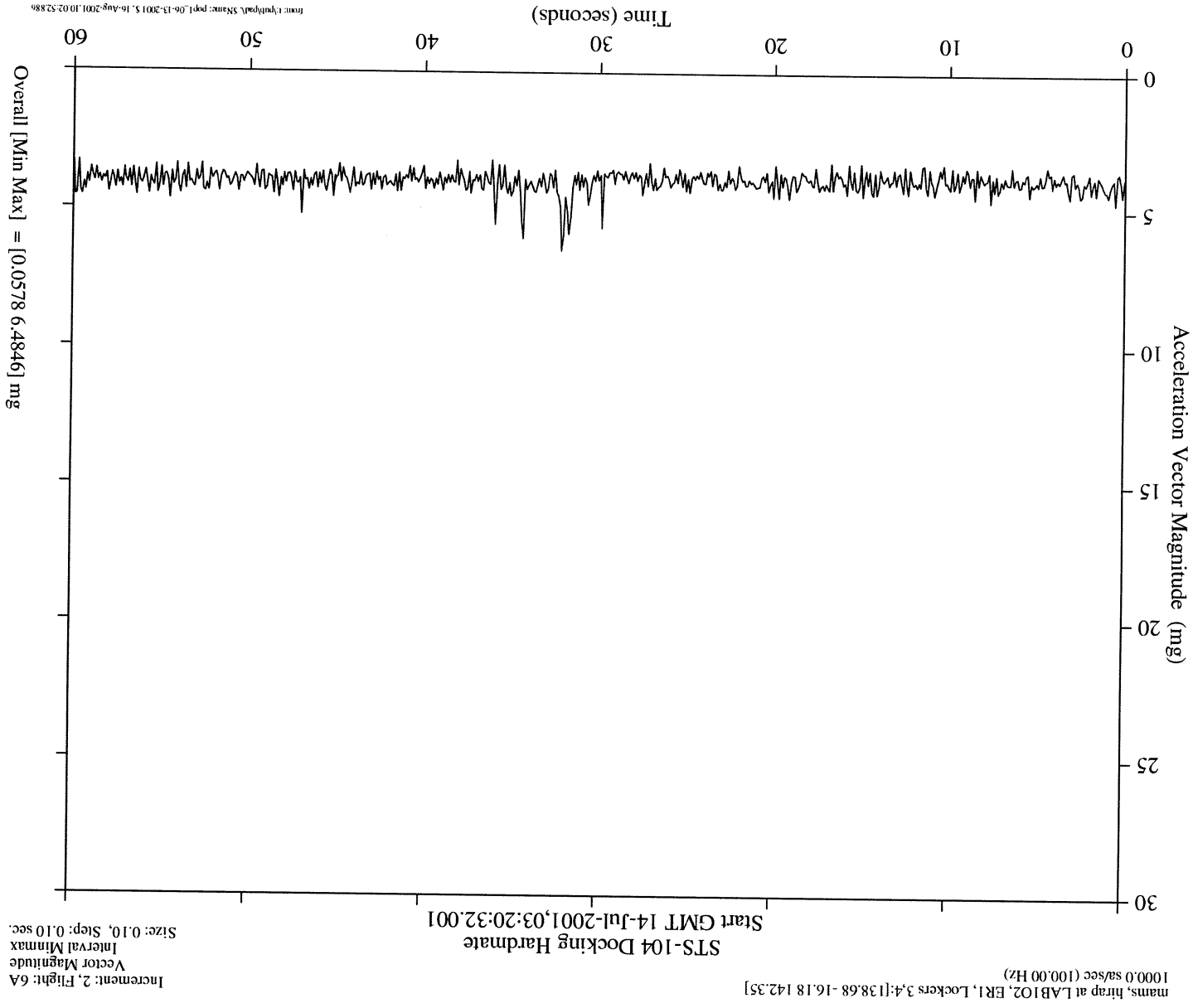


Figure 9.3.1.1.2-3 Acceleration Magnitude of Shuttle (7A) Docking Hardmate (HIRAP)

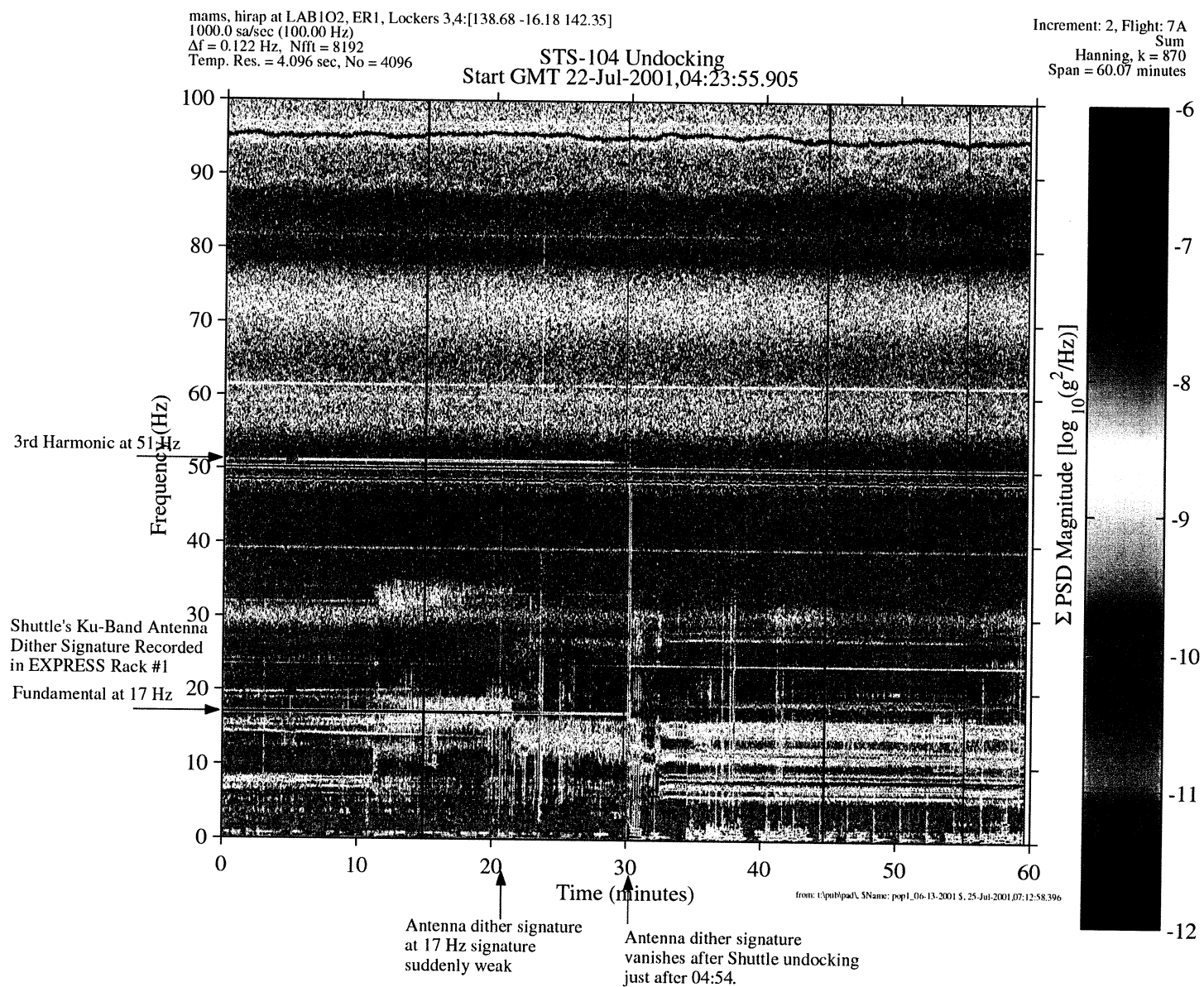


Figure 9.3.1.1.2-4 Spectrogram of Shuttle (7A) Undocking (HiRAP)

PIMS ISS Increment-2 Microgravity Environment Summary Report: May to August 2001

mams, hirap at LABIO2, ER1, Lockers 3.4:[138.68 -16.18 142.35]
1000.0 sa/sec (100.00 Hz)

STS-104 Undocking

Increment: 2, Flight: 7A
hirap[180.0 0.0 0.0]

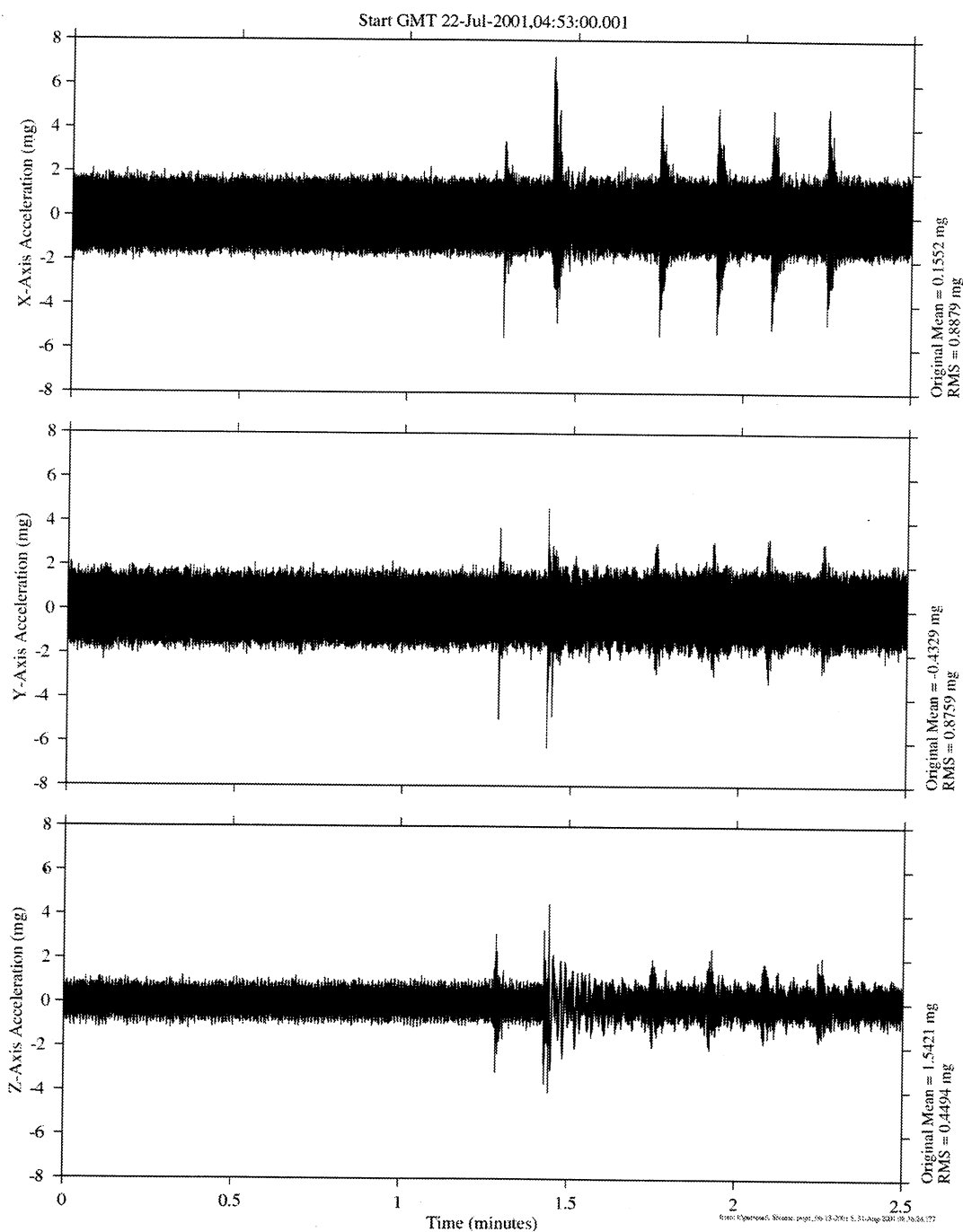


Figure 9.3.1.1.2-5 Time Series of Shuttle (7A) Undocking (HiRAP)

PIMS ISS Increment-2 Microgravity Environment Summary Report: May to August 2001

mams, hirap at LAB102, ER1, Lockers 3,4:[138.68 -16.18 142.35]
1000.0 sa/sec (100.00 Hz)

STS-104 Undocking

Increment: 2, Flight: 7A
hirap[180.0 0.0 0.0]

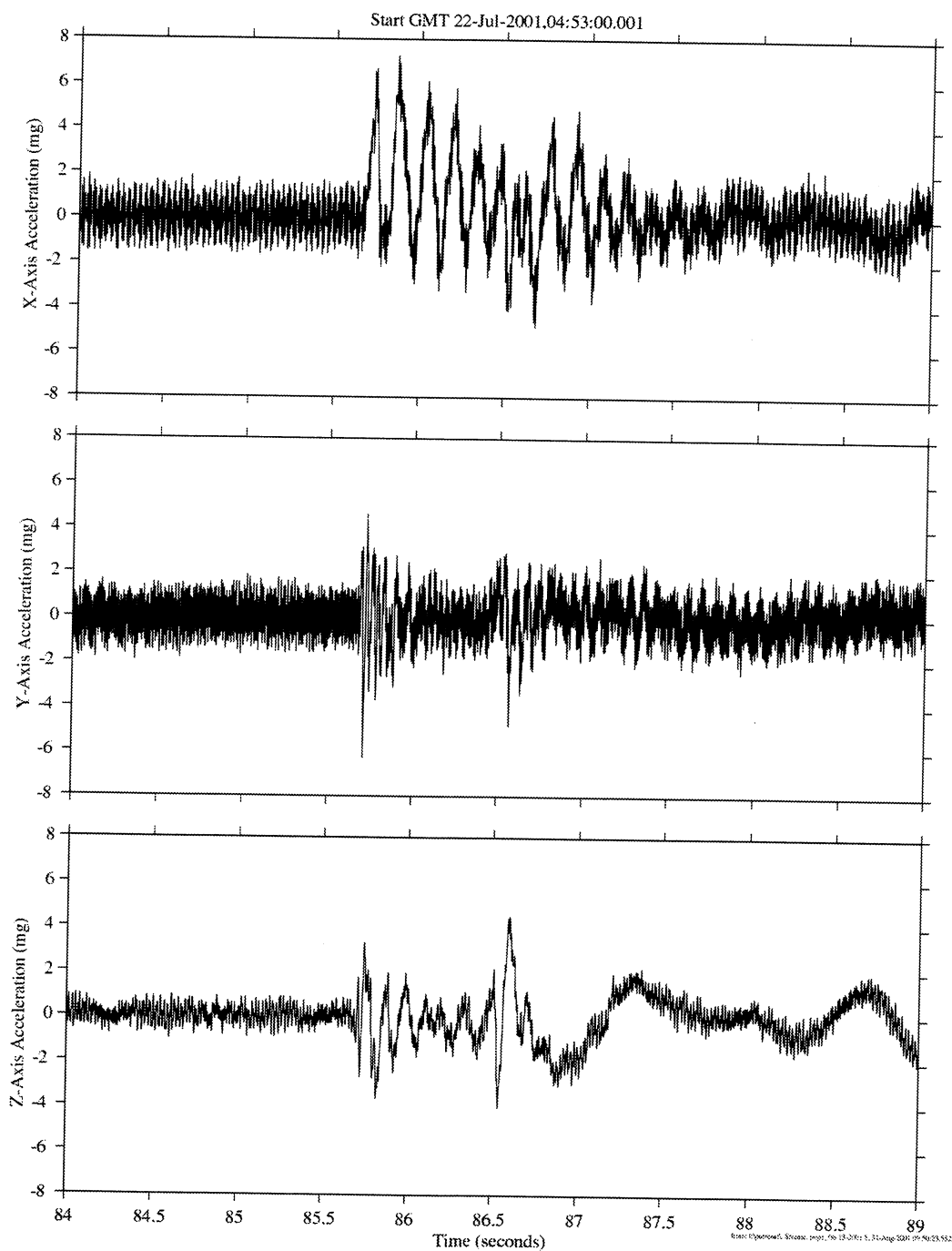


Figure 9.3.1.1.2-6 Time Series of Shuttle (7A) Undocking (HiRAP)

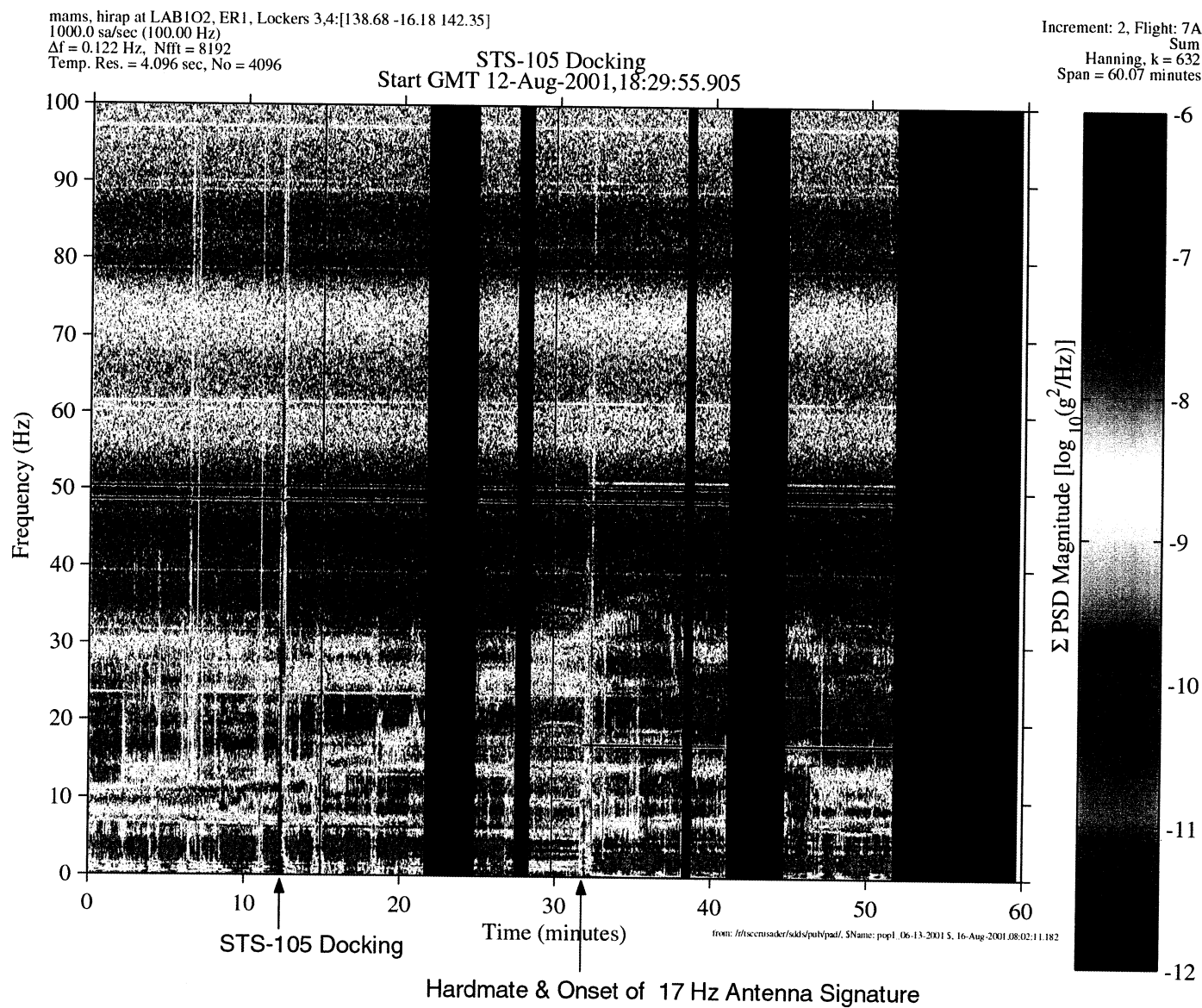


Figure 9.3.1.1.3-1 Spectrogram of Shuttle (7A.1) Docking (HiRAP)

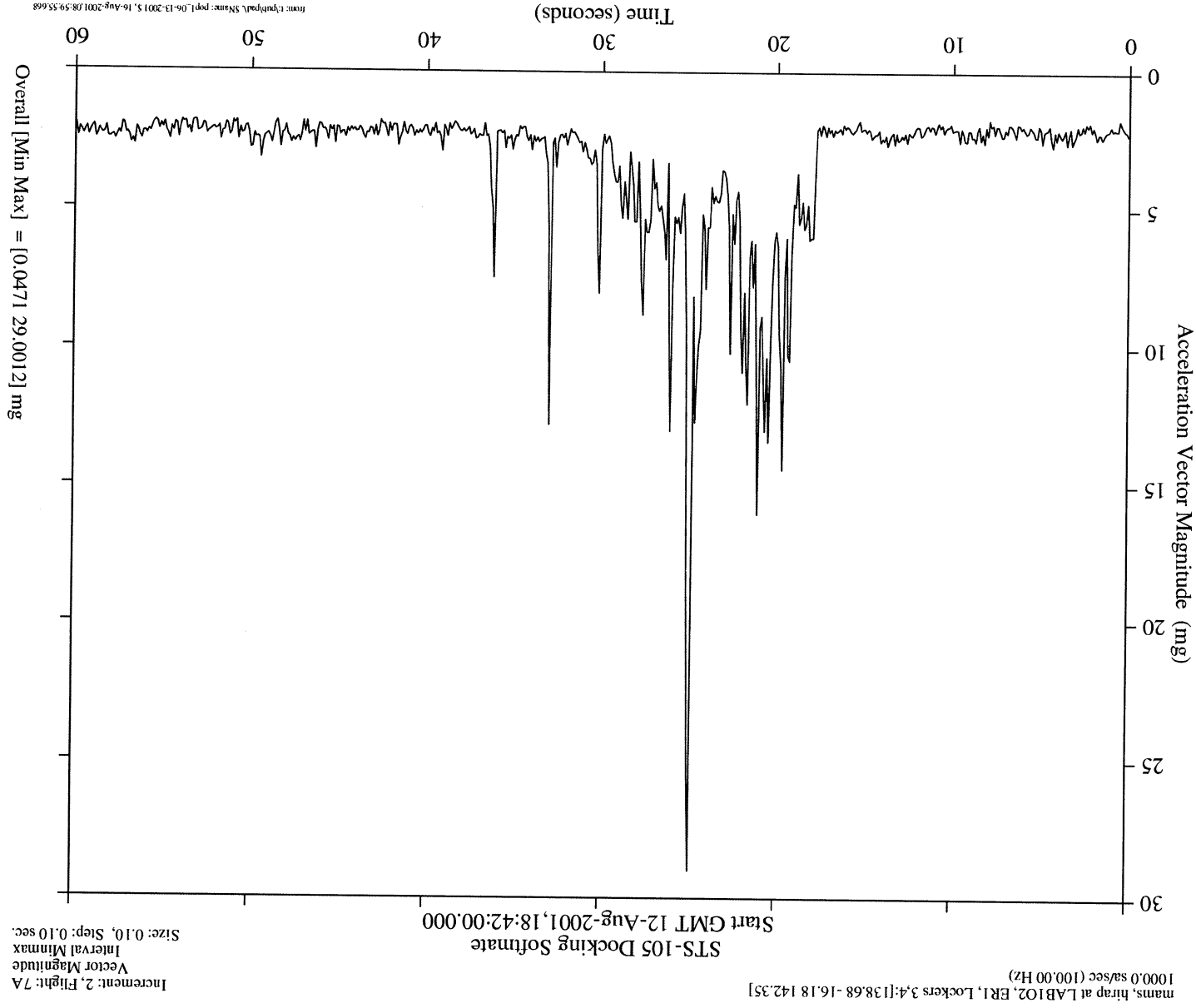


Figure 9.3.1.1.3-2 Acceleration Magnitude of Shuttle (7A.1) Docking Softmate (HIRAP)

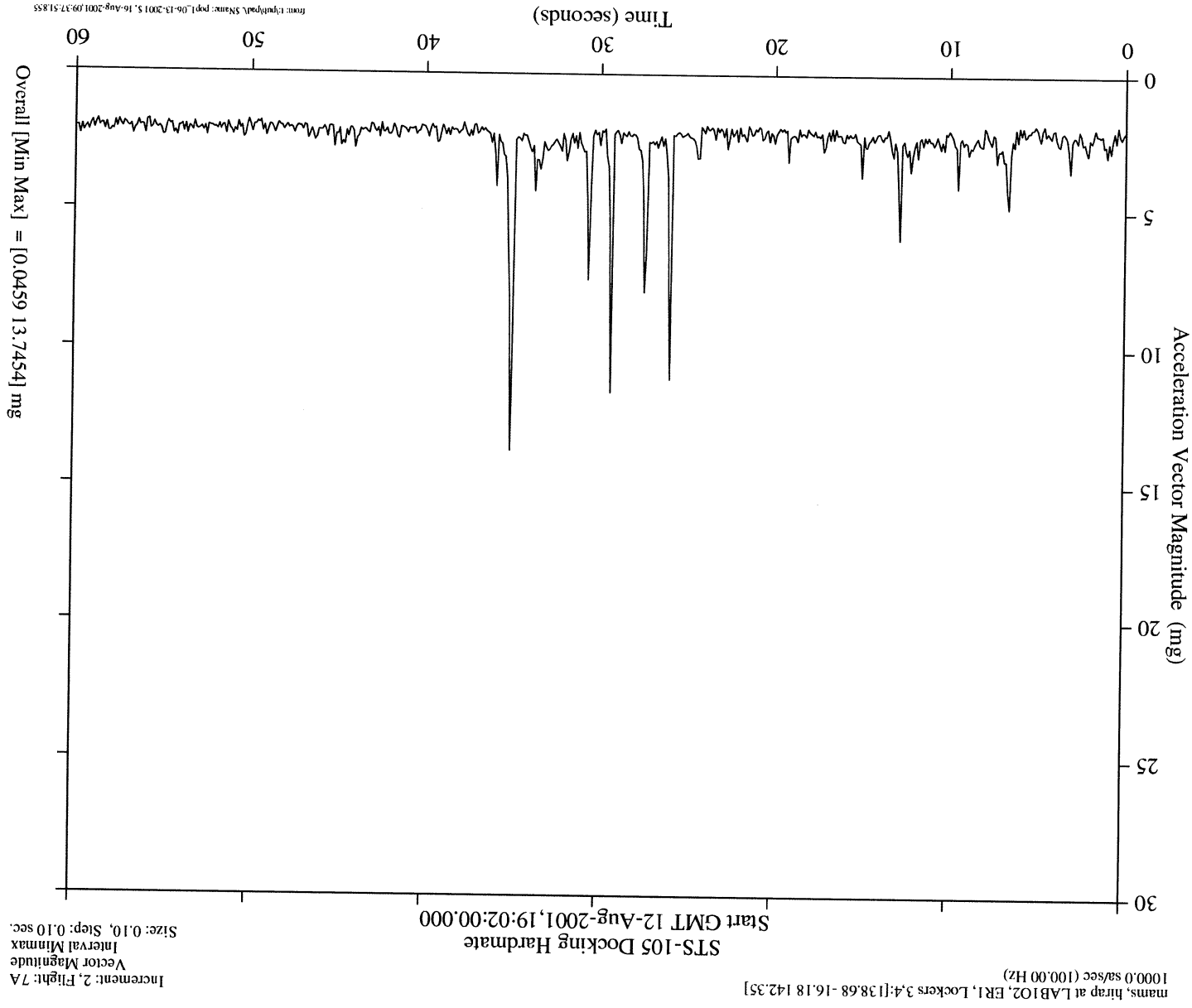


Figure 9.3.1.1.3-3 Acceleration Magnitude of Shuttle (7A.1) Docking Hardmate (HiRAP)

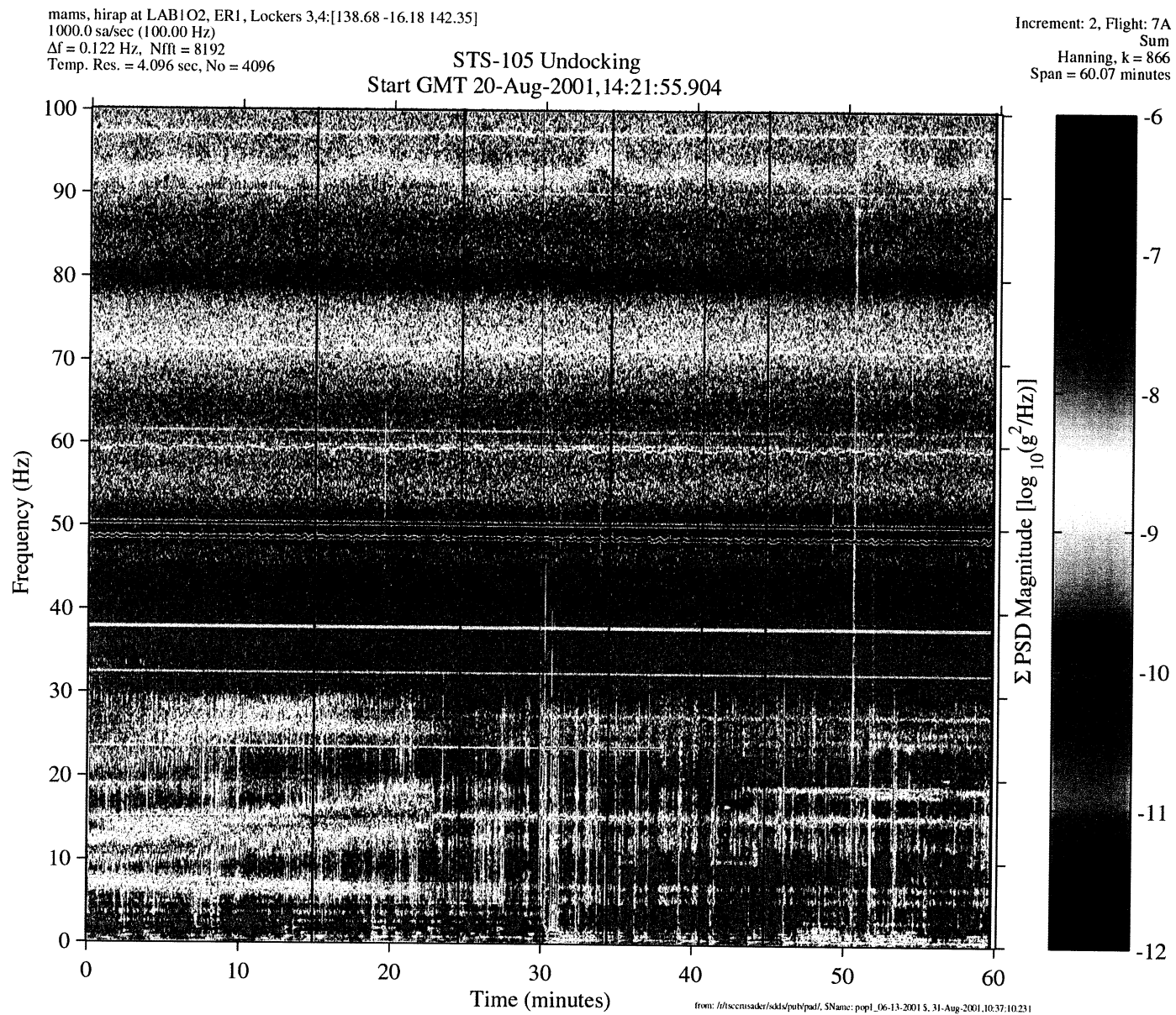


Figure 9.3.1.1.3-4 Spectrogram of Shuttle (7A.1) Undocking (HiRAP)

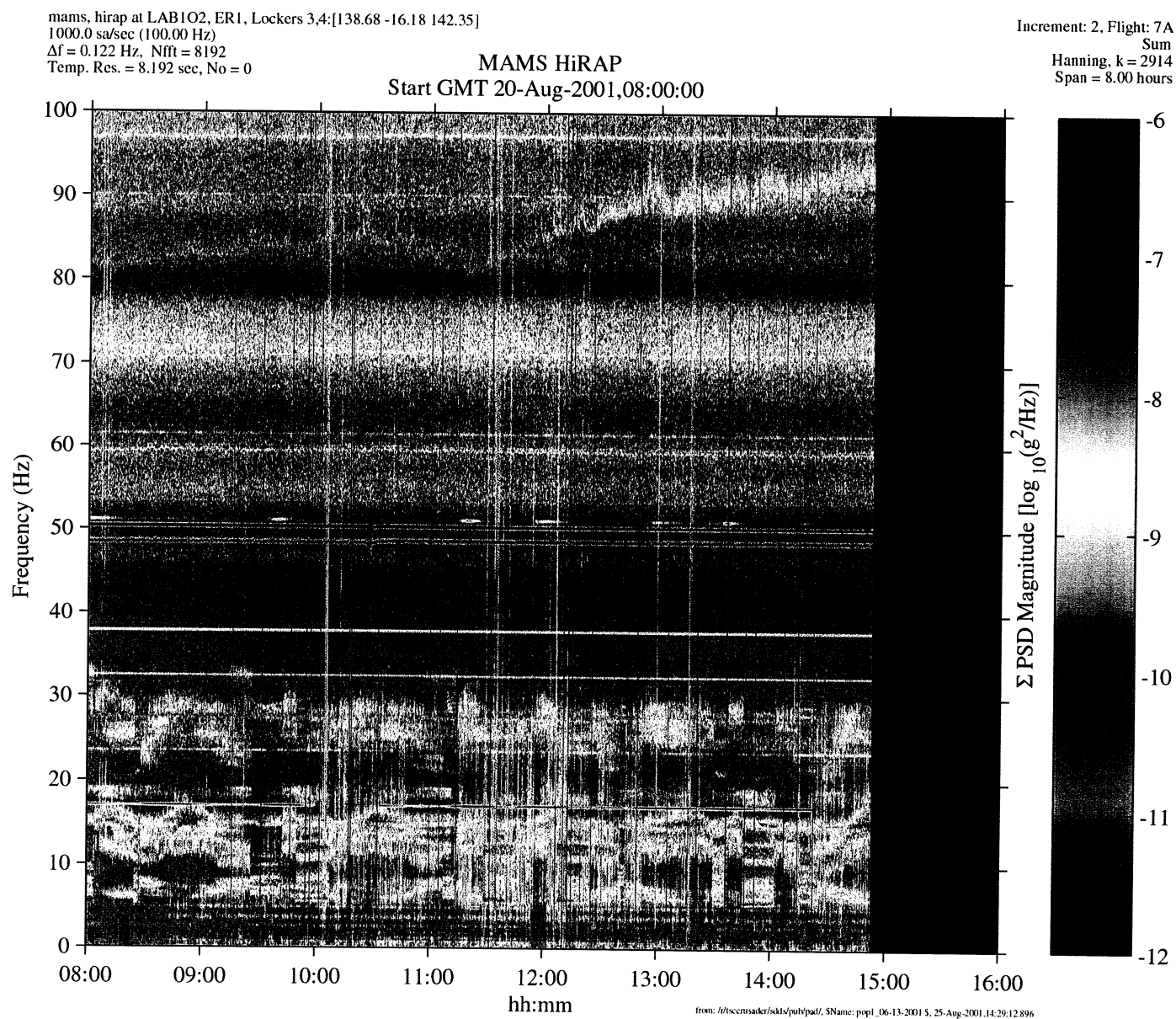


Figure 9.3.1.1.3-5 Spectrogram of Shuttle's Ku-band Dither Signature Off (HiRAP)

PIMS ISS Increment-2 Microgravity Environment Summary Report: May to August 2001

mams, hirap at LAB102, ER1, Lockers 3,4:[138.68 -16.18 142.35]
1000.0 sa/sec (100.00 Hz)

STS-105 Undocking

Increment: 3, Flight: 7A.1
hirap[180.0 0.0 0.0]

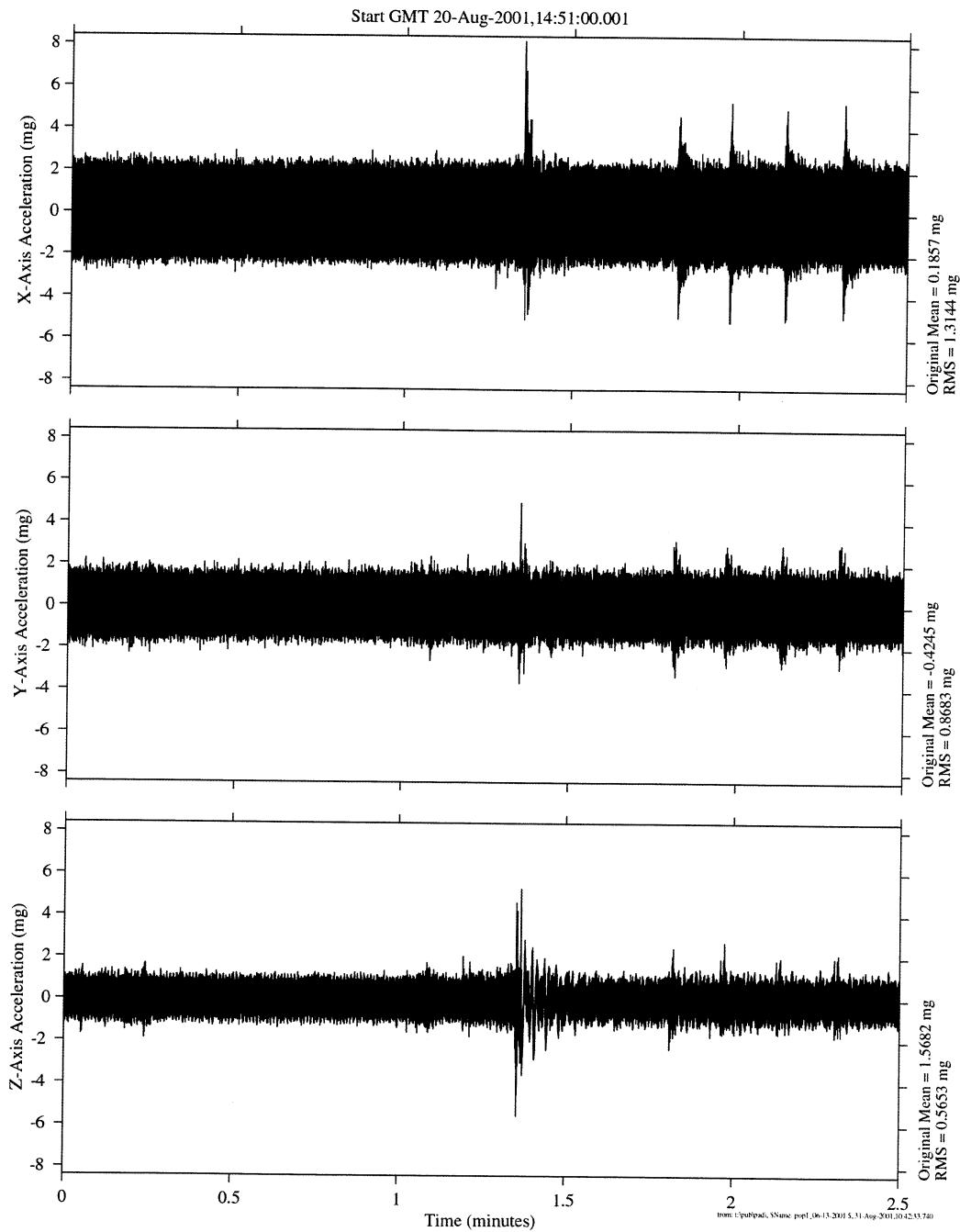


Figure 9.3.1.1.3-6 Time Series of Shuttle (7A.1) Undocking (HiRAP)

PIMS ISS Increment-2 Microgravity Environment Summary Report: May to August 2001

mams, hirap at LAB102, ER1, Lockers 3,4:[138.68 -16.18 142.35]
1000.0 sa/sec (100.00 Hz)

STS-105 Undocking

Increment: 3, Flight: 7A.1
hirap[180.0 0.0 0.0]

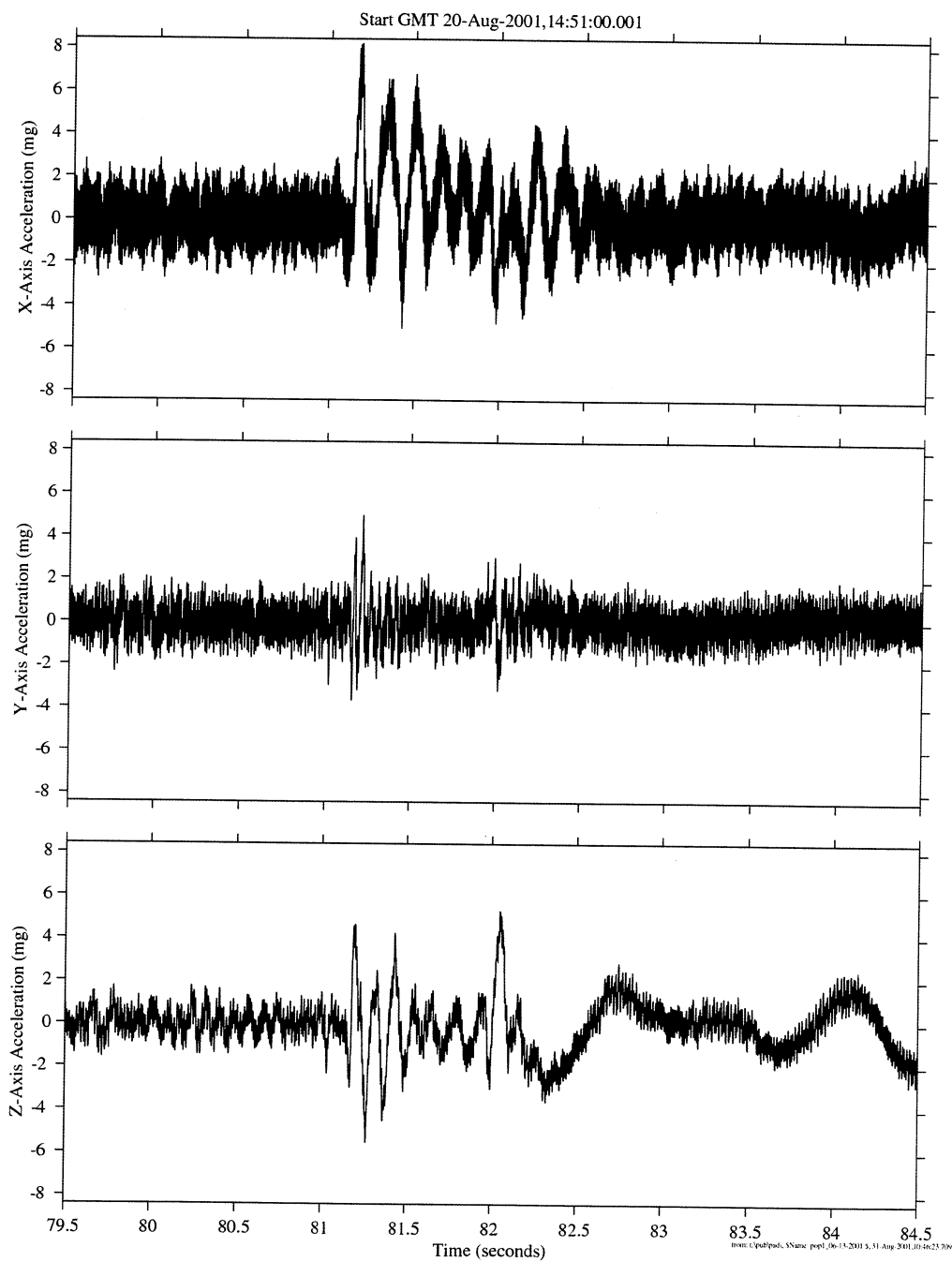


Figure 9.3.1.1.3-7 Time Series of Shuttle (7A.1) Undocking (HiRAP)

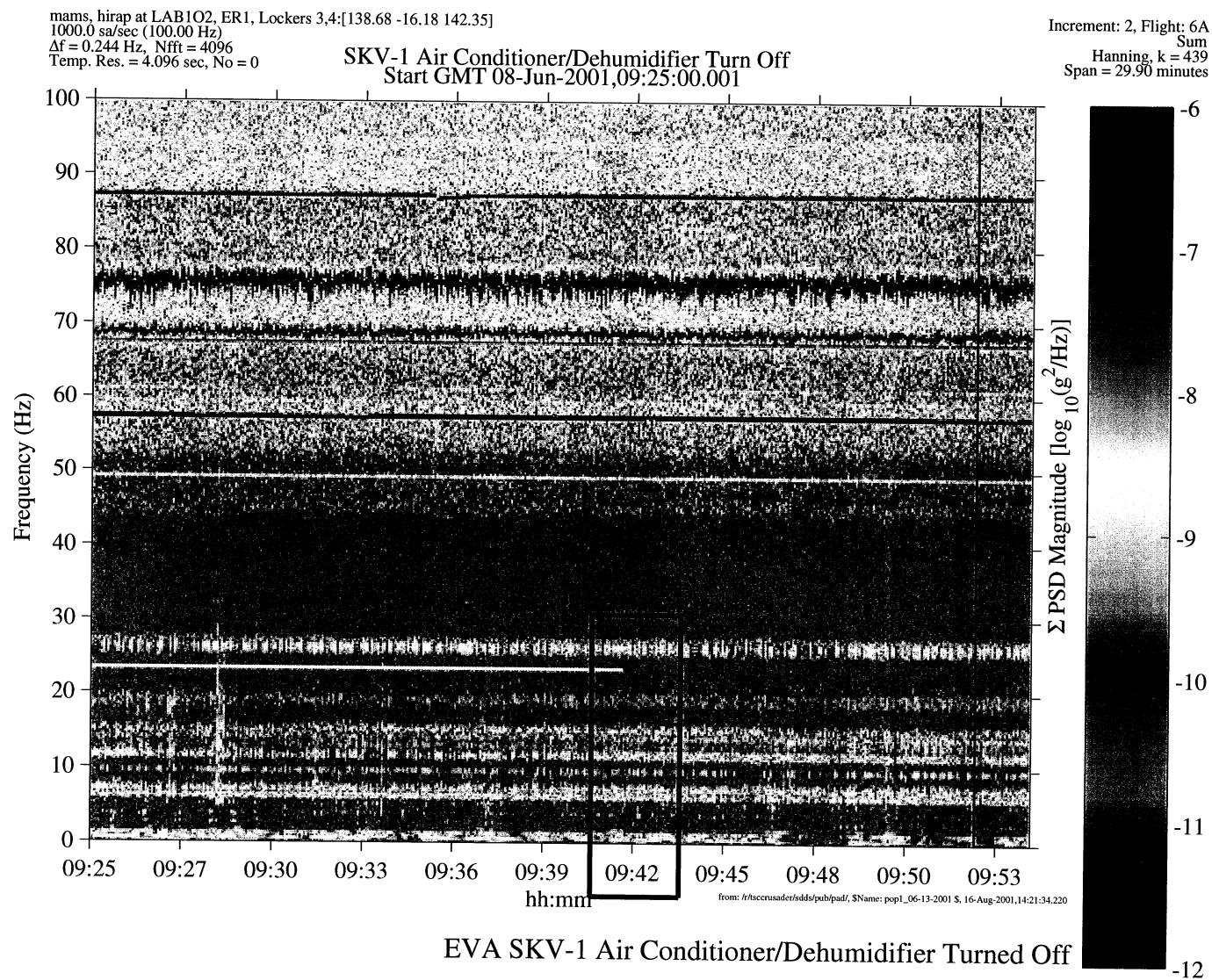


Figure 9.3.2.1-1 Spectrogram of SKV-1 Air Conditioner/Dehumidifier Turn Off (HiRAP)

PIMS ISS Increment-2 Microgravity Environment Summary Report: May to August 2001

mams, hirap at LAB1O2, ER1, Lockers 3.4:[138.68 -16.18 142.35]
1000.0 sa/sec (100.00 Hz)
 $\Delta f = 0.031$ Hz, Nfft = 32768
P = 43.8%, No = 14364

SKV-1 Air Conditioner/Dehumidifier ON

Increment: 2, Flight: 6A
hirap[180.0 0.0 0.0]
Hanning, k = 9
Span = 180.00 sec.

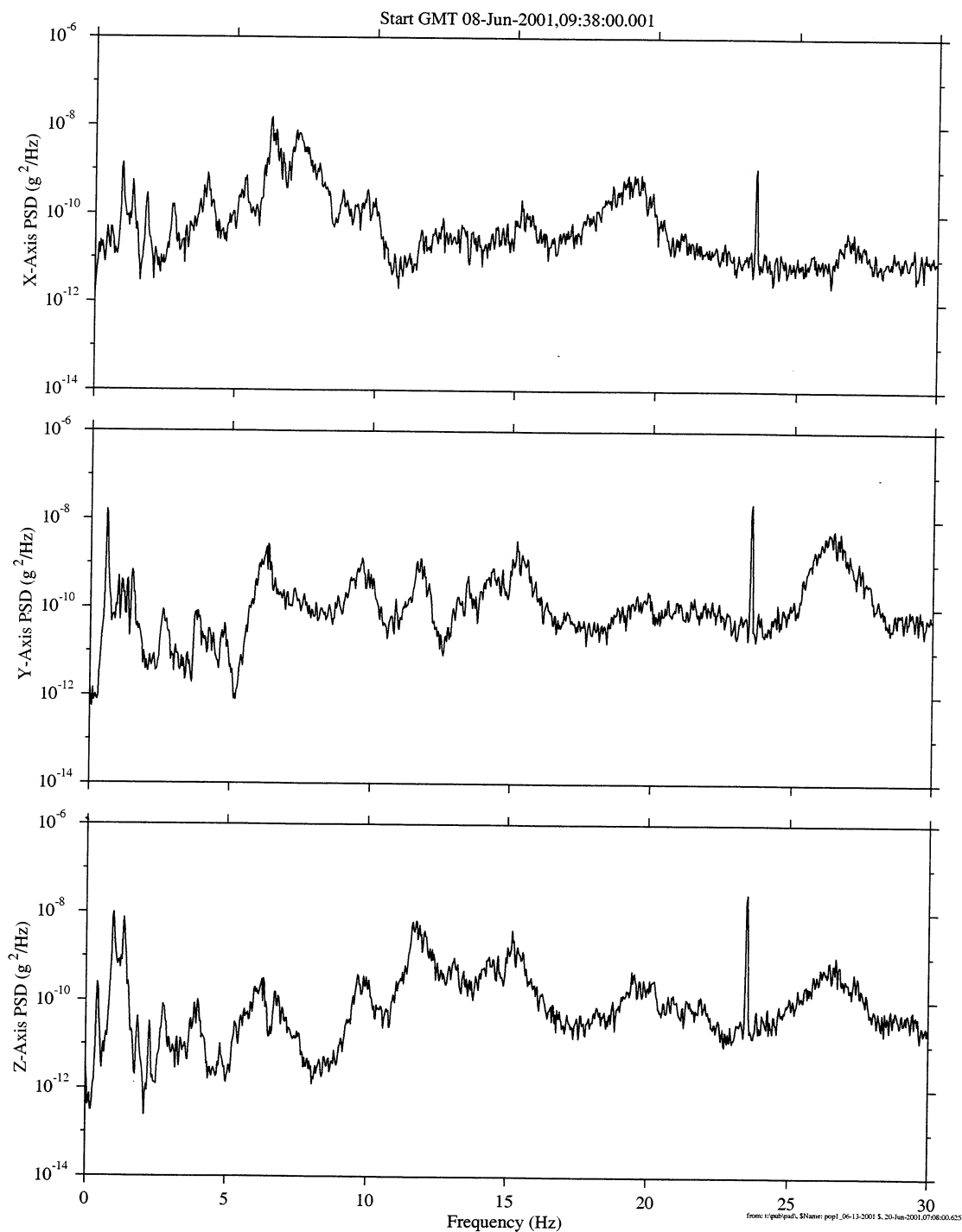


Figure 9.3.2.1-2 PSD of SKV-1 Air Conditioner/Dehumidifier On (HiRAP)

PIMS ISS Increment-2 Microgravity Environment Summary Report: May to August 2001

mams, hirap at LAB102, ER1, Lockers 3,4:[138.68 -16.18 142.35]
 1000.0 sa/sec (100.00 Hz)
 $\Delta f = 0.031$ Hz, Nfft = 32768
 P = 43.8%, No = 14364

SKV-1 Air Conditioner/Dehumidifier OFF

Increment: 2, Flight: 6A
 hirap[180.0 0.0 0.0]
 Hanning, k = 9
 Span = 180.00 sec.

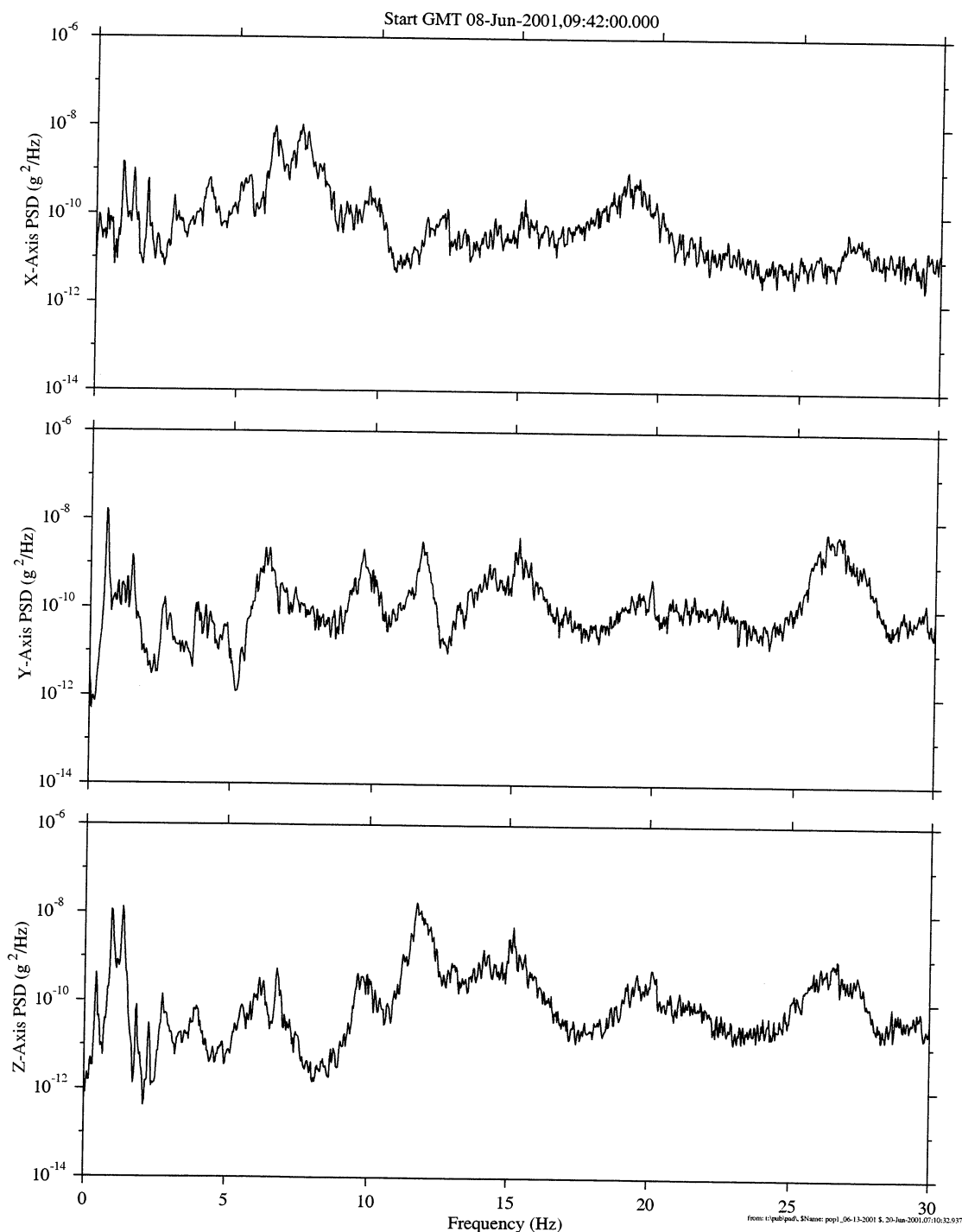


Figure 9.3.2.1-3 PSD of SKV-1 Air Conditioner/Dehumidifier Off (HiRAP)

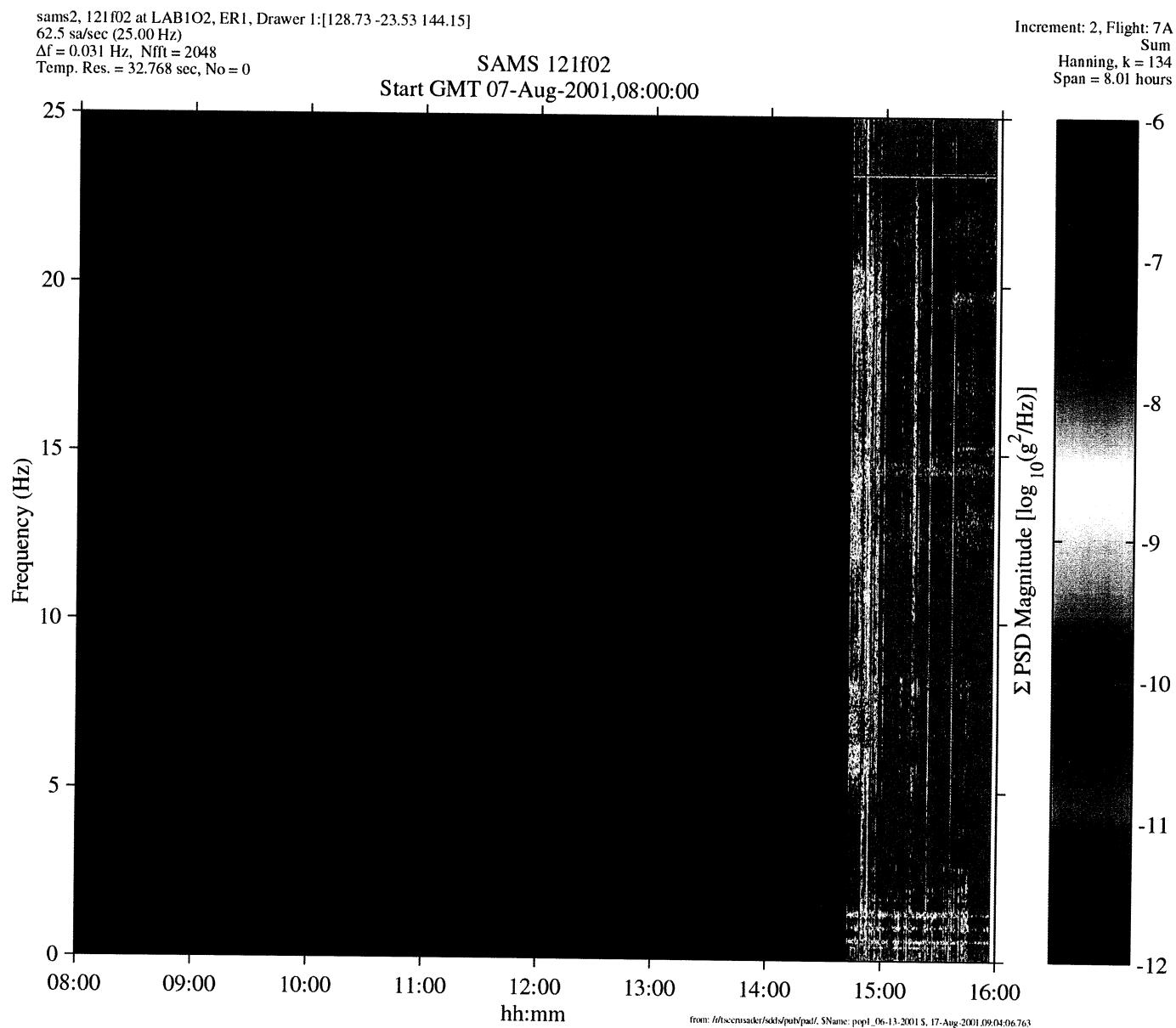


Figure 9.3.2.1-4 Spectrogram of SKV-1 Spectral Signature On (121f02)

sams2, 121f02 at LAB102, ER1, Drawer 1:[128.73 -23.53 144.15]
 62.5 sa/sec (25.00 Hz)
 $\Delta f = 0.031$ Hz, Nfft = 2048
 Temp. Res. = 32.768 sec, No = 0

SAMS 121f02
 Start GMT 07-Aug-2001, 16:00:00

Increment: 2, Flight: 7A
 Sum
 Hanning, k = 864
 Span = 8.01 hours

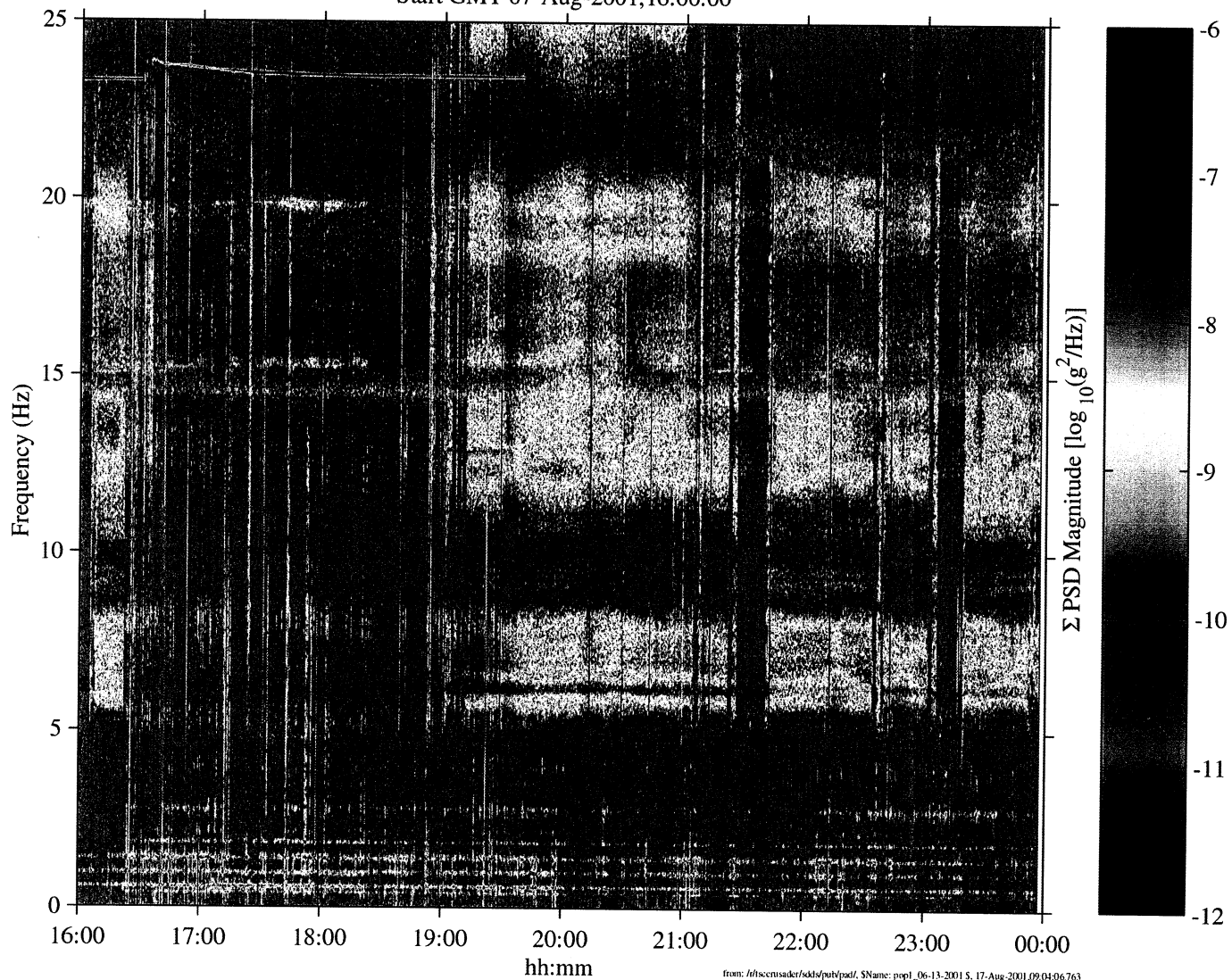


Figure 9.3.2.1-5 Spectrogram of SKV-1 Spectral Signature Off (121f02)

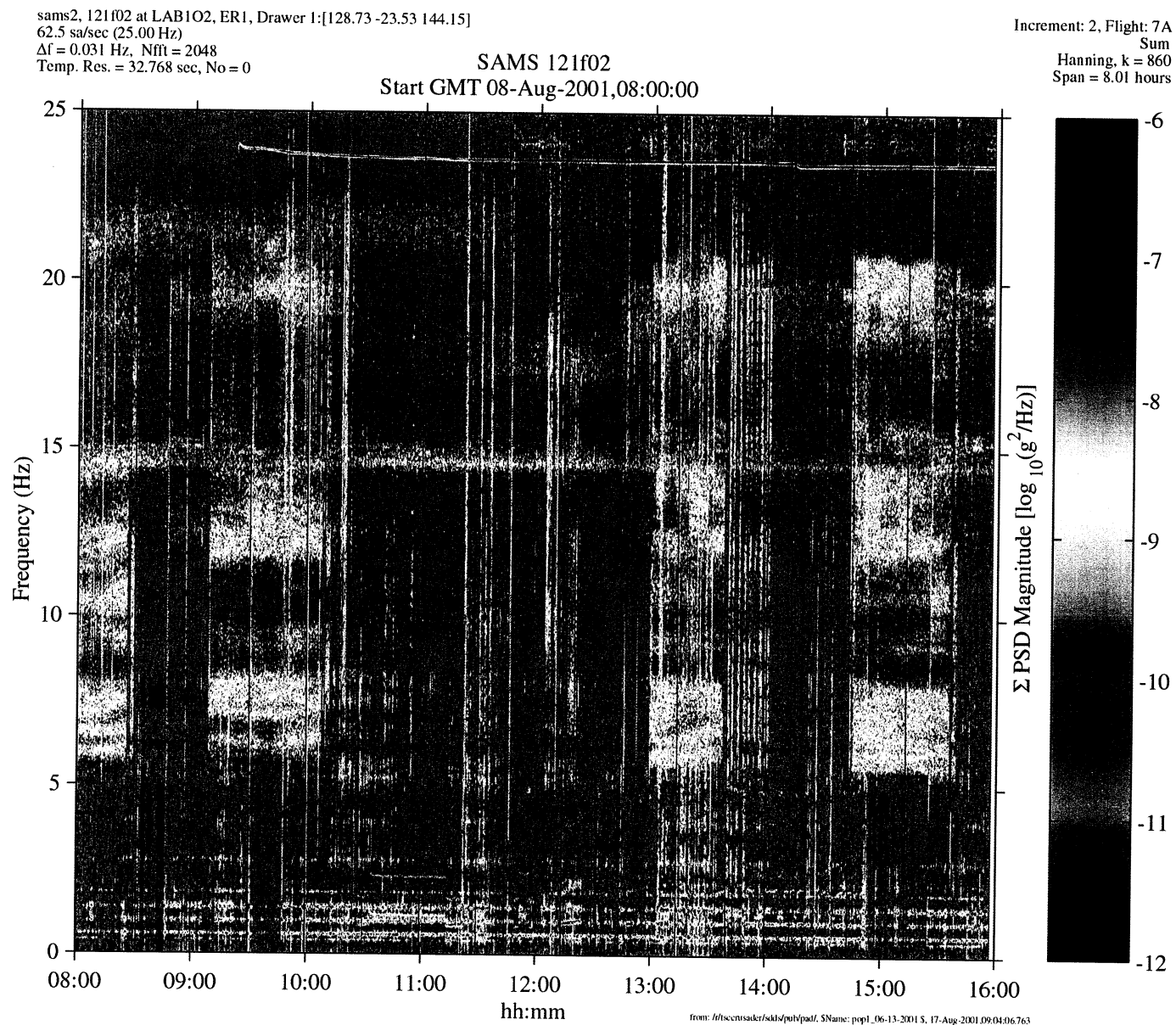


Figure 9.3.2.1-6 Spectrogram of SKV-1 Spectral Signature On (121f02)

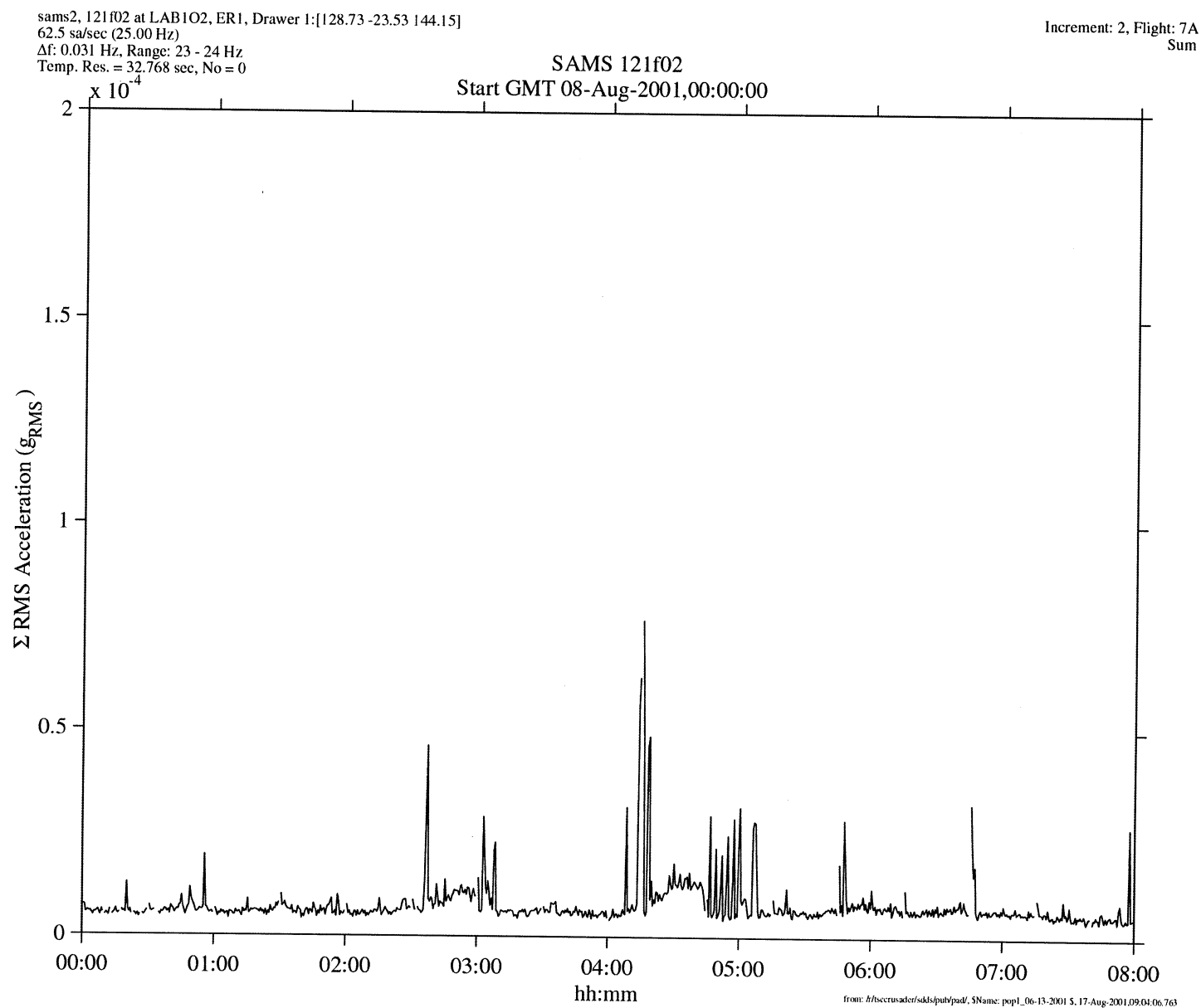


Figure 9.3.2.1-7 Interval RMS of SKV-1 Off (121f02)

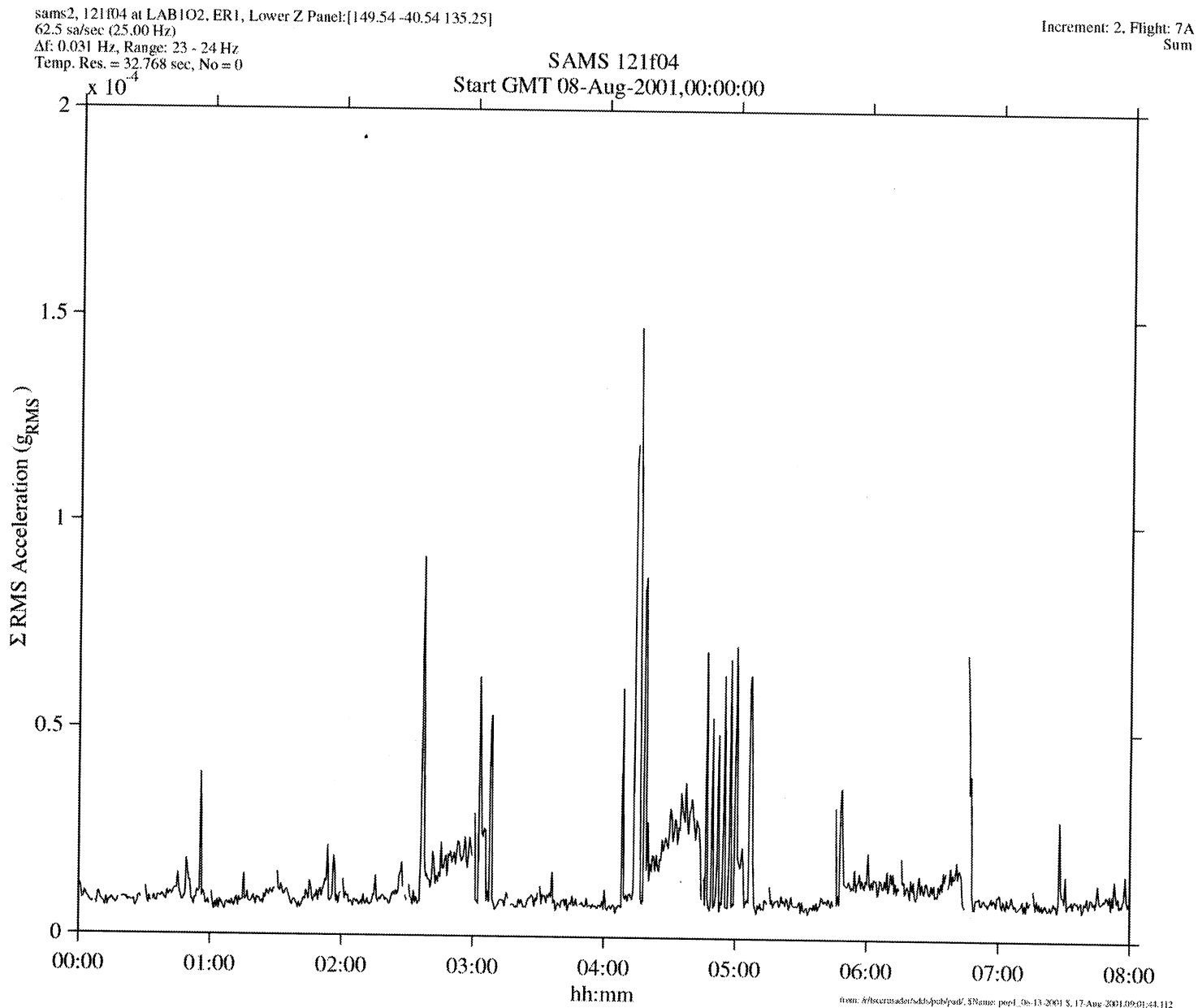


Figure 9.3.2.1-8 Interval RMS of SKV-1 Off (121f04)

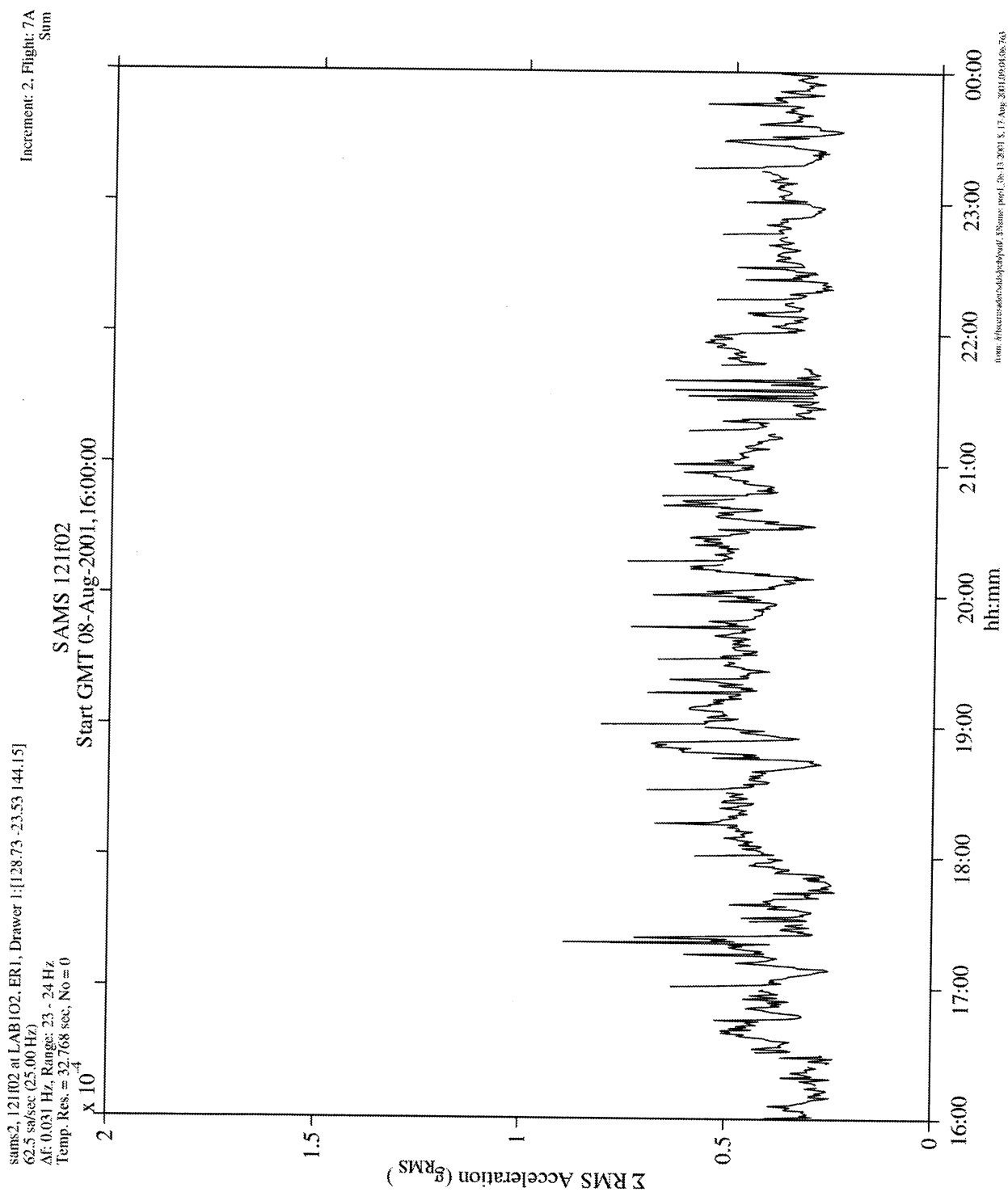


Figure 9.3.2.1-9 Interval RMS of SKV-1 On (121f02)

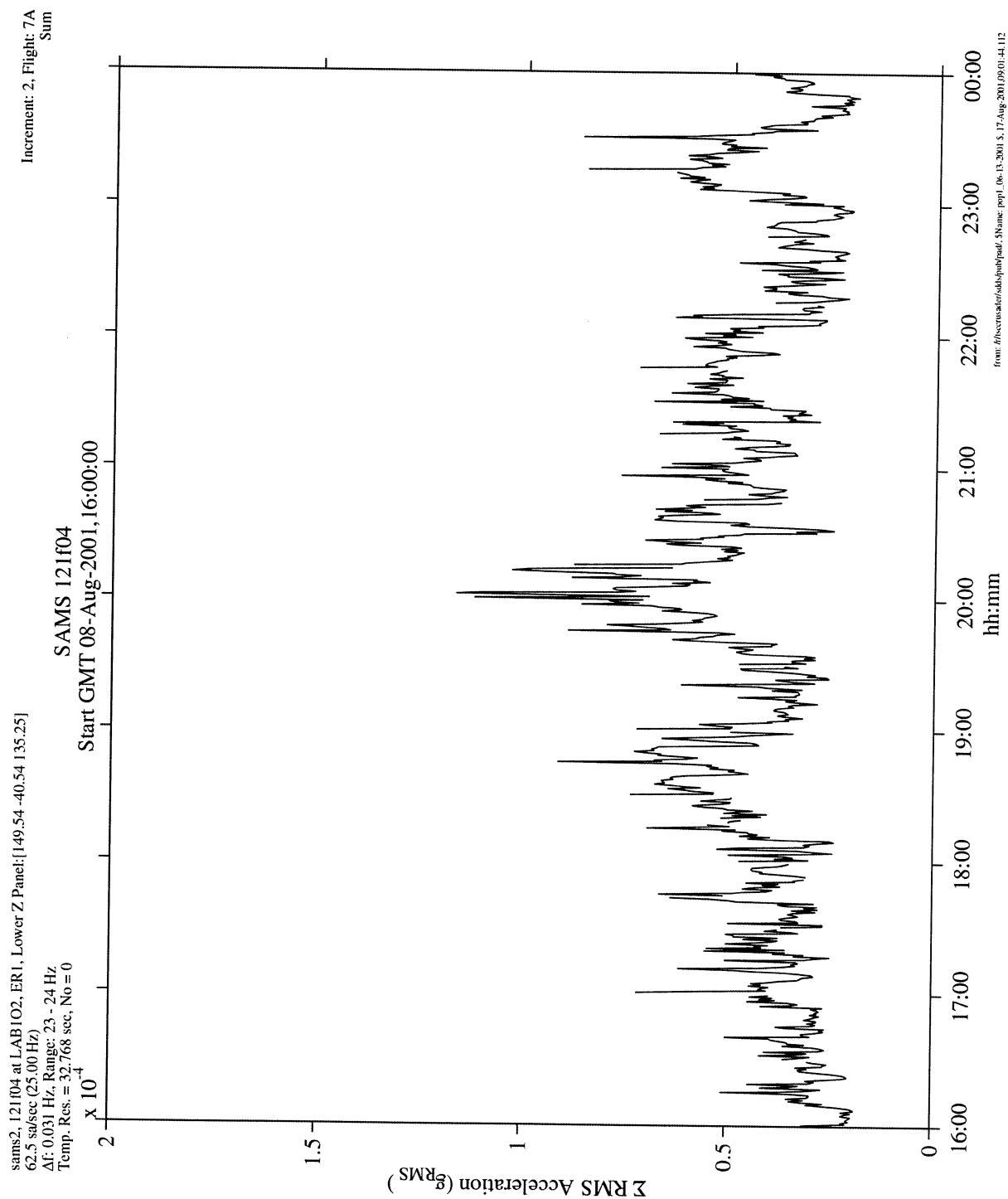


Figure 9.3.2.1-10 Interval RMS of SKV-1 On (121f04)

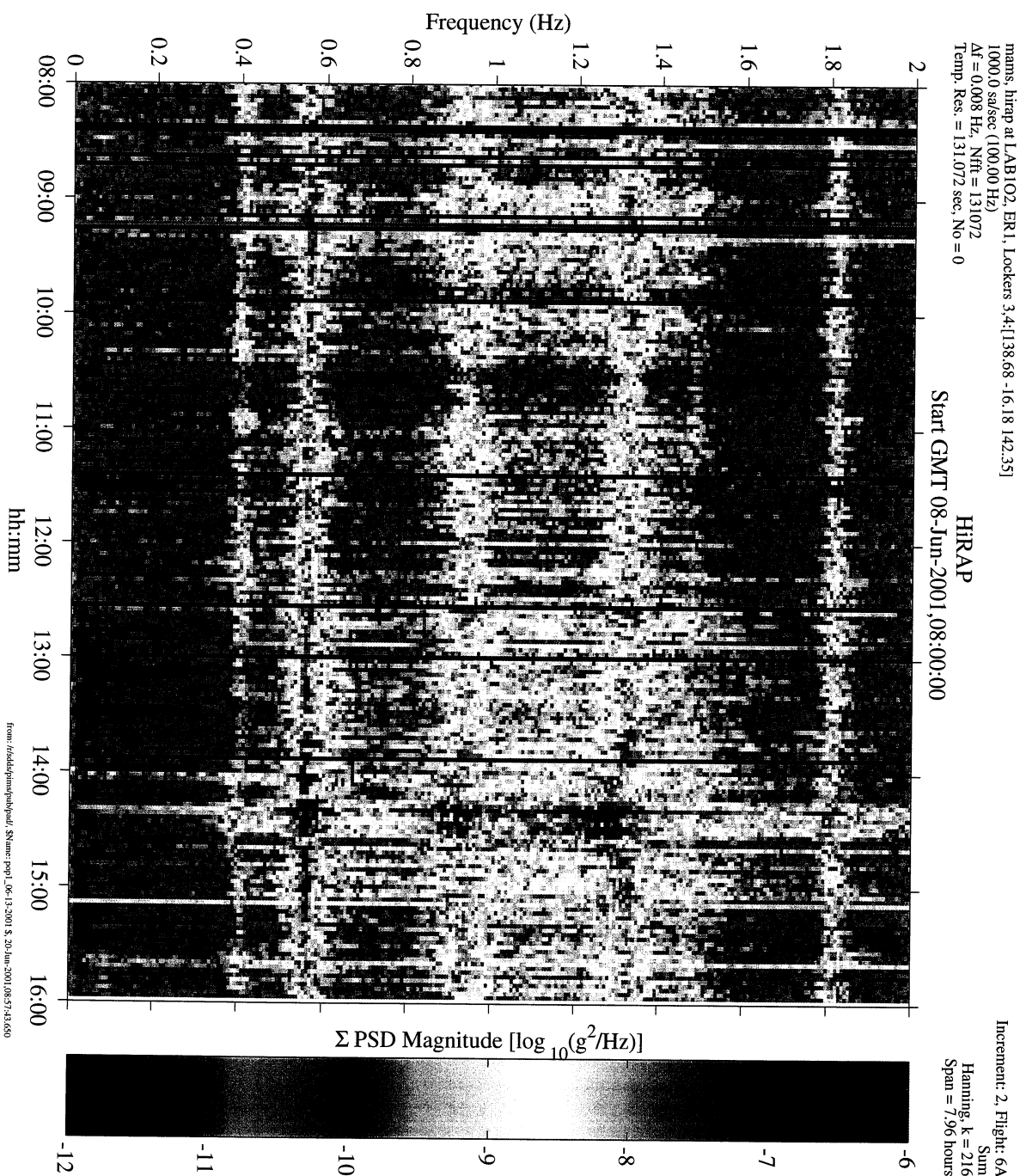


Figure 9.3.3-1 Spectrogram of Below 2 Hz (HiRAP)



Figure 9.3.3-2 PSD of Spectral Averaged 8-Hour Period Below 2 Hz (HiRAP)

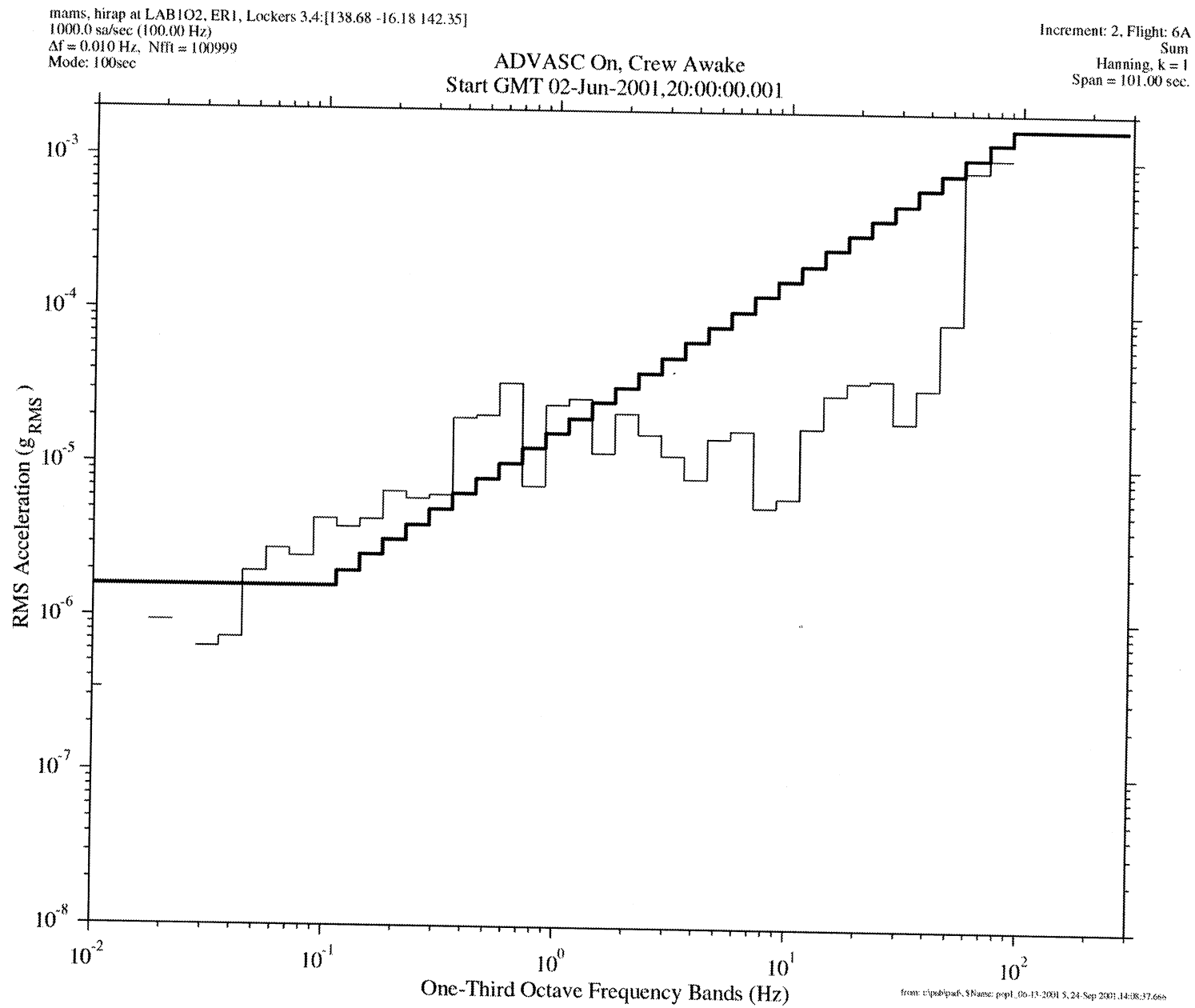


Figure 9.3.4-1 OTO of ADVASC On and Crew Awake (HiRAP)

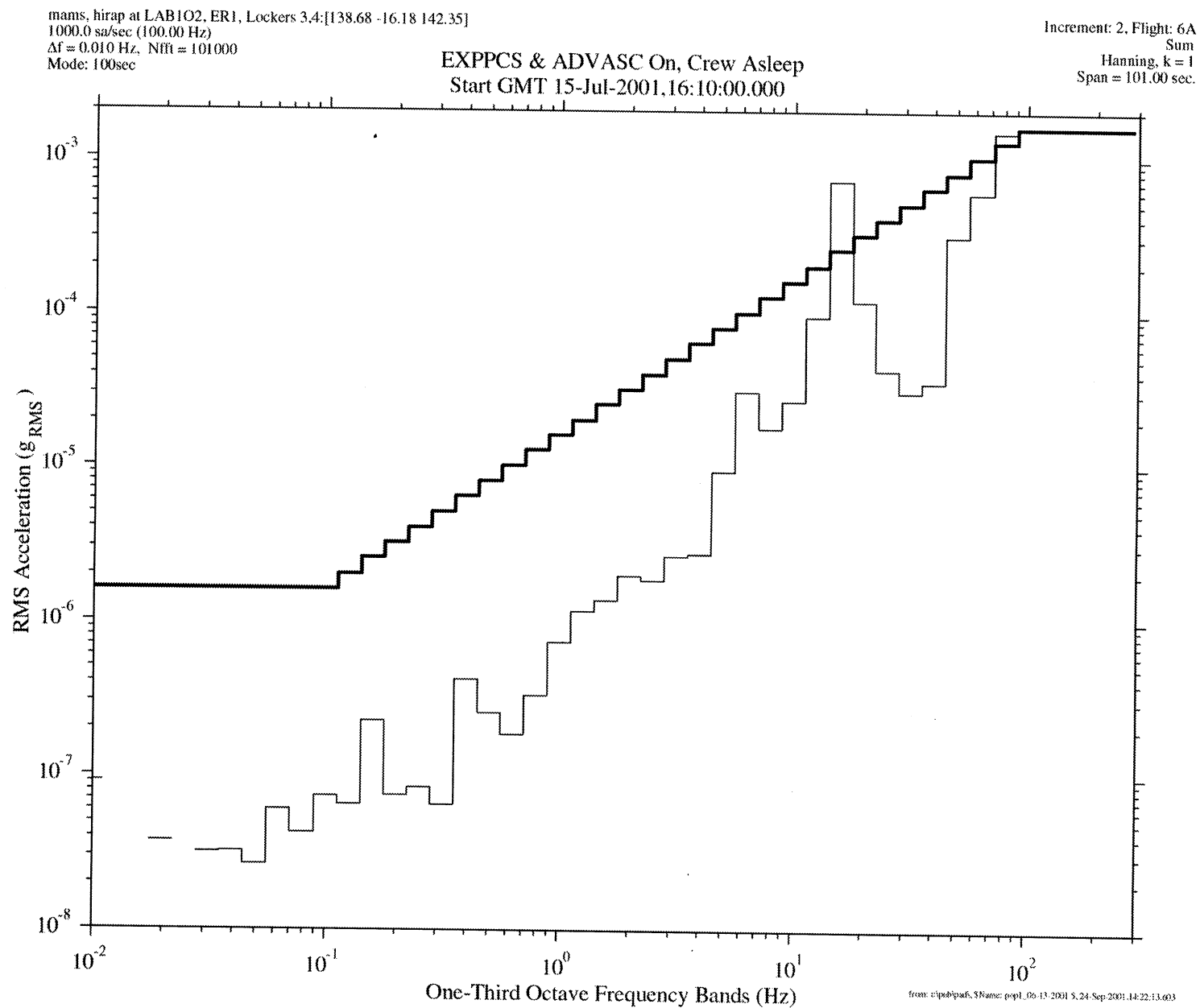


Figure 9.3.4-2 OTO of EXPPCS and ADVASC On and Crew Asleep (HiRAP)

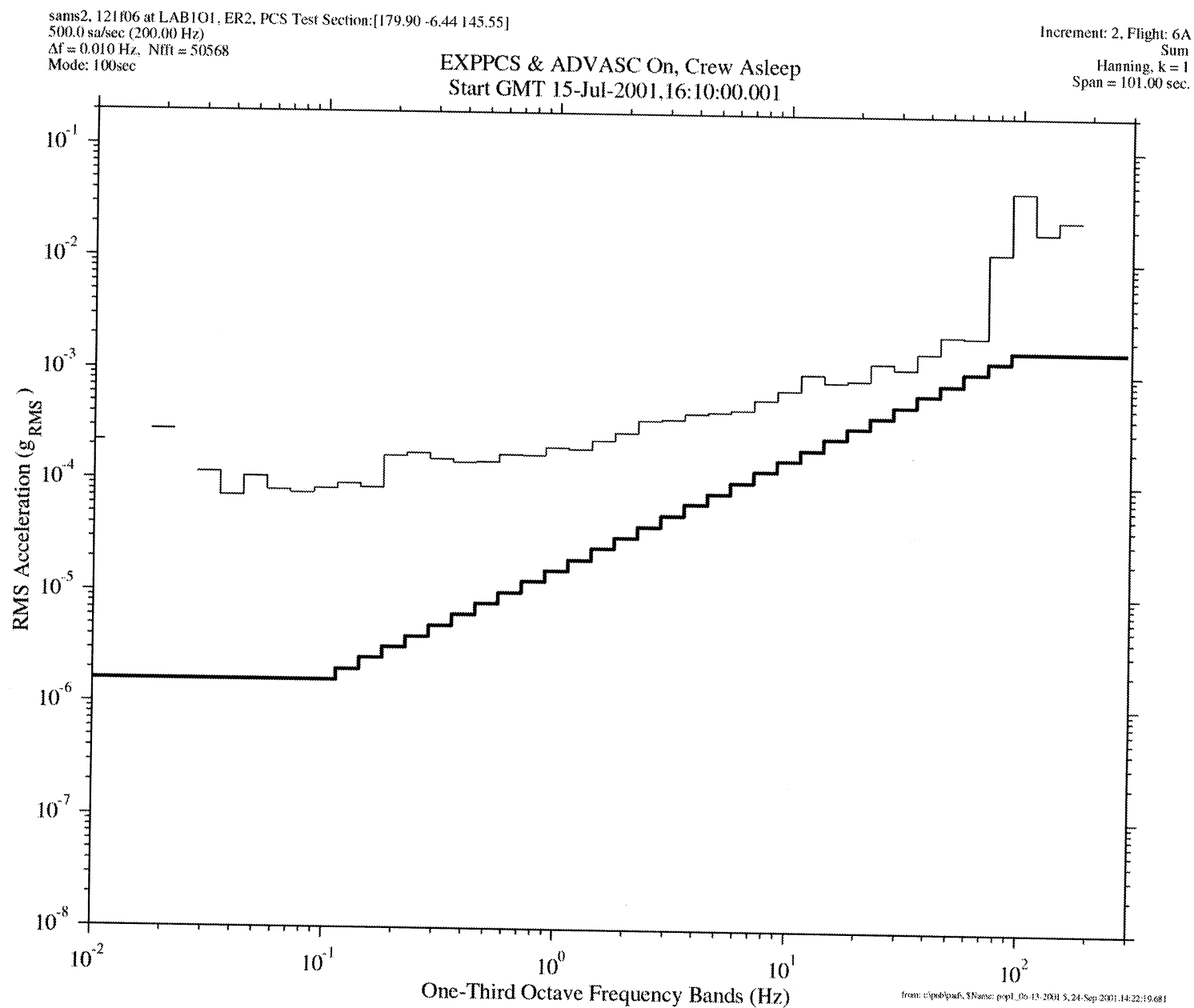


Figure 9.3.4-3 OTO of EXPPCS and ADVASC On and Crew Asleep (121f06)

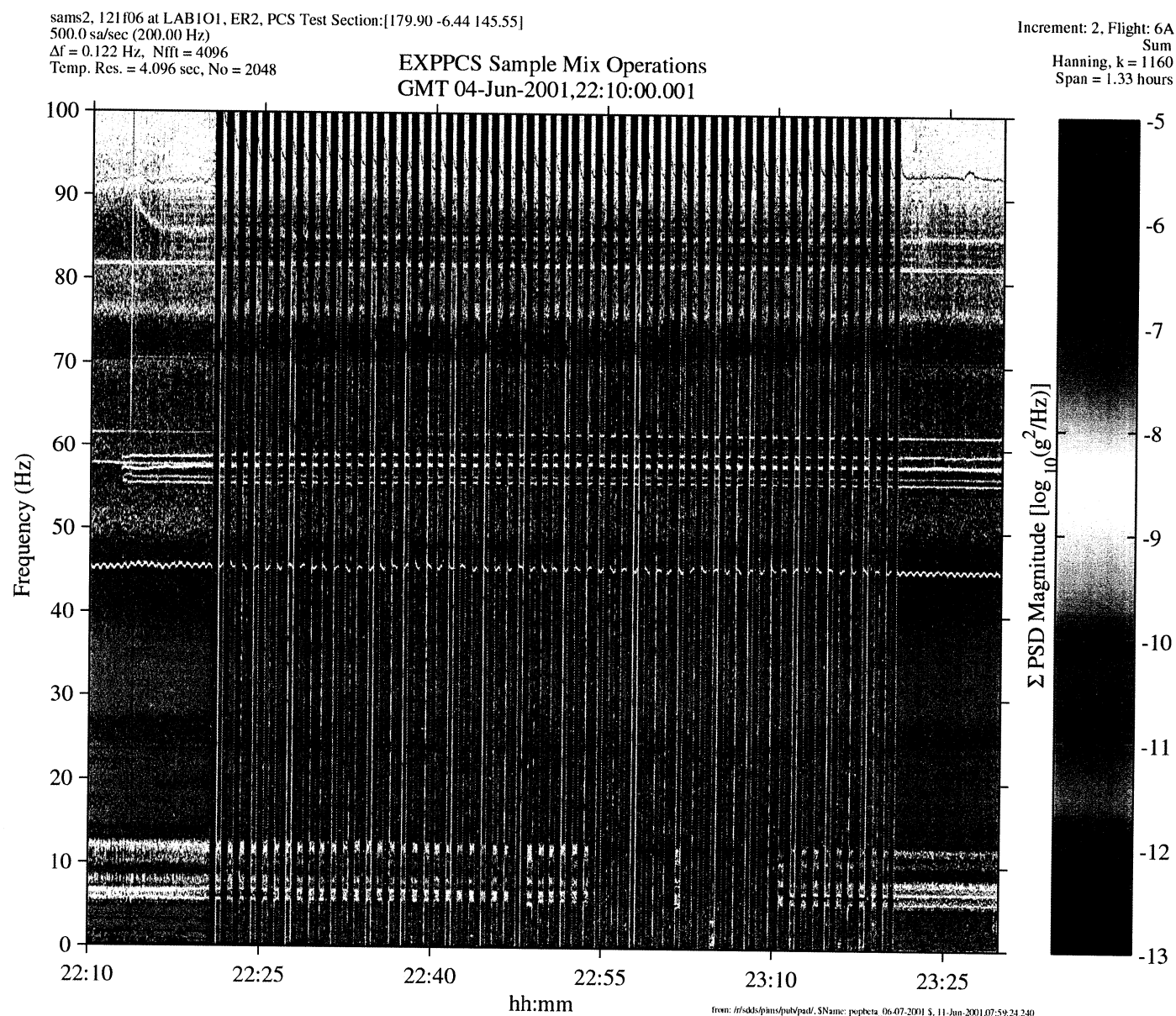


Figure 9.3.5.1-1 Spectrogram of EXPPCS Sample Mix Operation (121f06)

PIMS ISS Increment-2 Microgravity Environment Summary Report: May to August 2001

sams2, 121f06 at LAB101, ER2, PCS Test Section:[179.90 -6.44 145.55]
500.0 sa/sec (200.00 Hz)

30-Second Duty Cycle of EXPPCS Sample Mix Operations

Increment: 2, Flight: 6A
121f06[180.0 90.0 0.0]
Interval Minmax
Size: 0.25, Step: 0.25 sec.

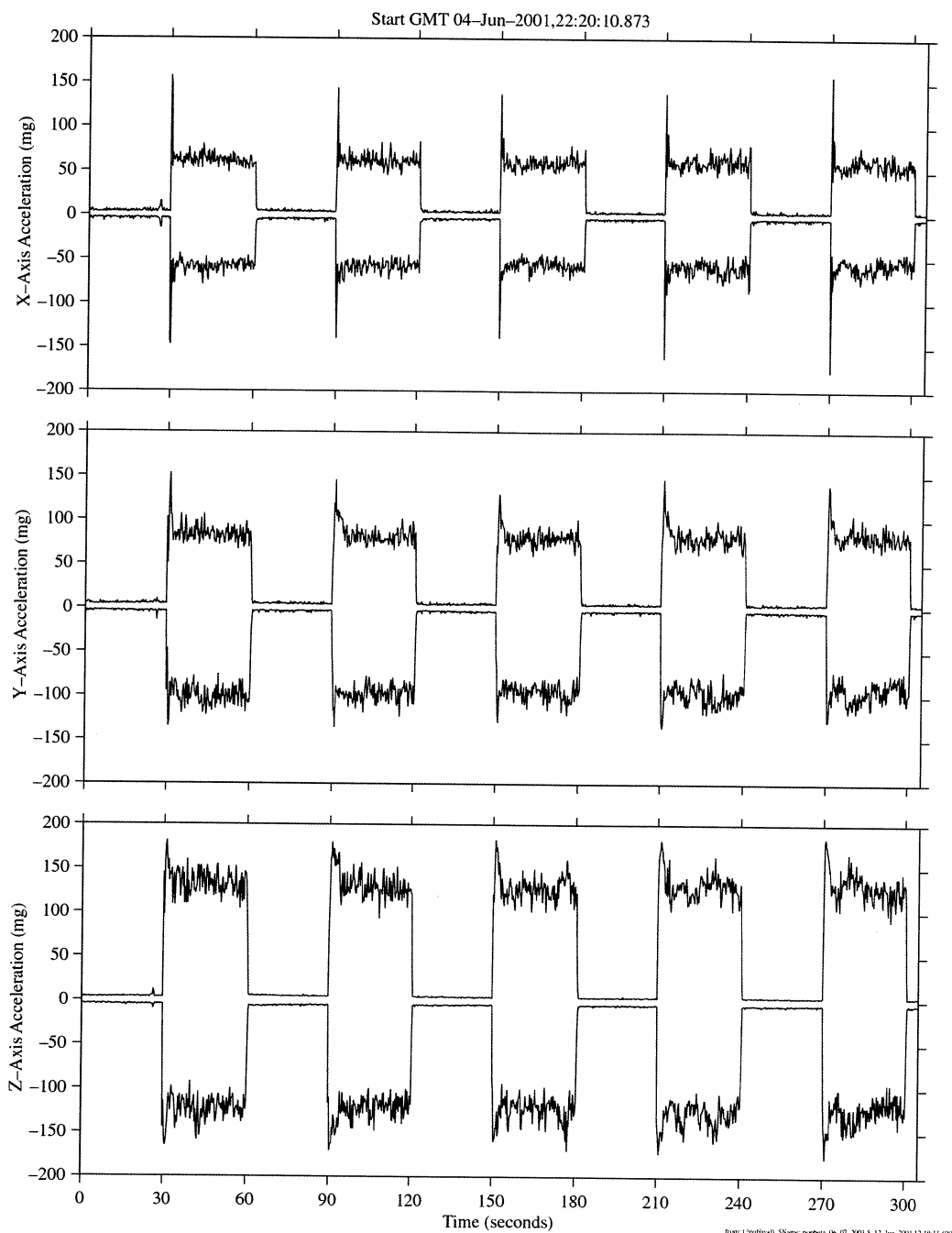


Figure 9.3.5.1-2 Interval Min/Max of EXPPCS Sample Mix Operation On (121f06)

PIMS ISS Increment-2 Microgravity Environment Summary Report: May to August 2001

sams2, 121f06 at LAB101, ER2, PCS Test Section:[179.90 -6.44 145.55]
500.0 su/sec (200.00 Hz)
 $\Delta f = 0.061$ Hz, Nfft = 8192
P = 47.4%, No = 3884

EXPPCS Sample Mix On

Increment: 2, Flight: 6A
121f06[180.0 90.0 0.0]
Hanning, k = 2
Span = 25.00 sec.

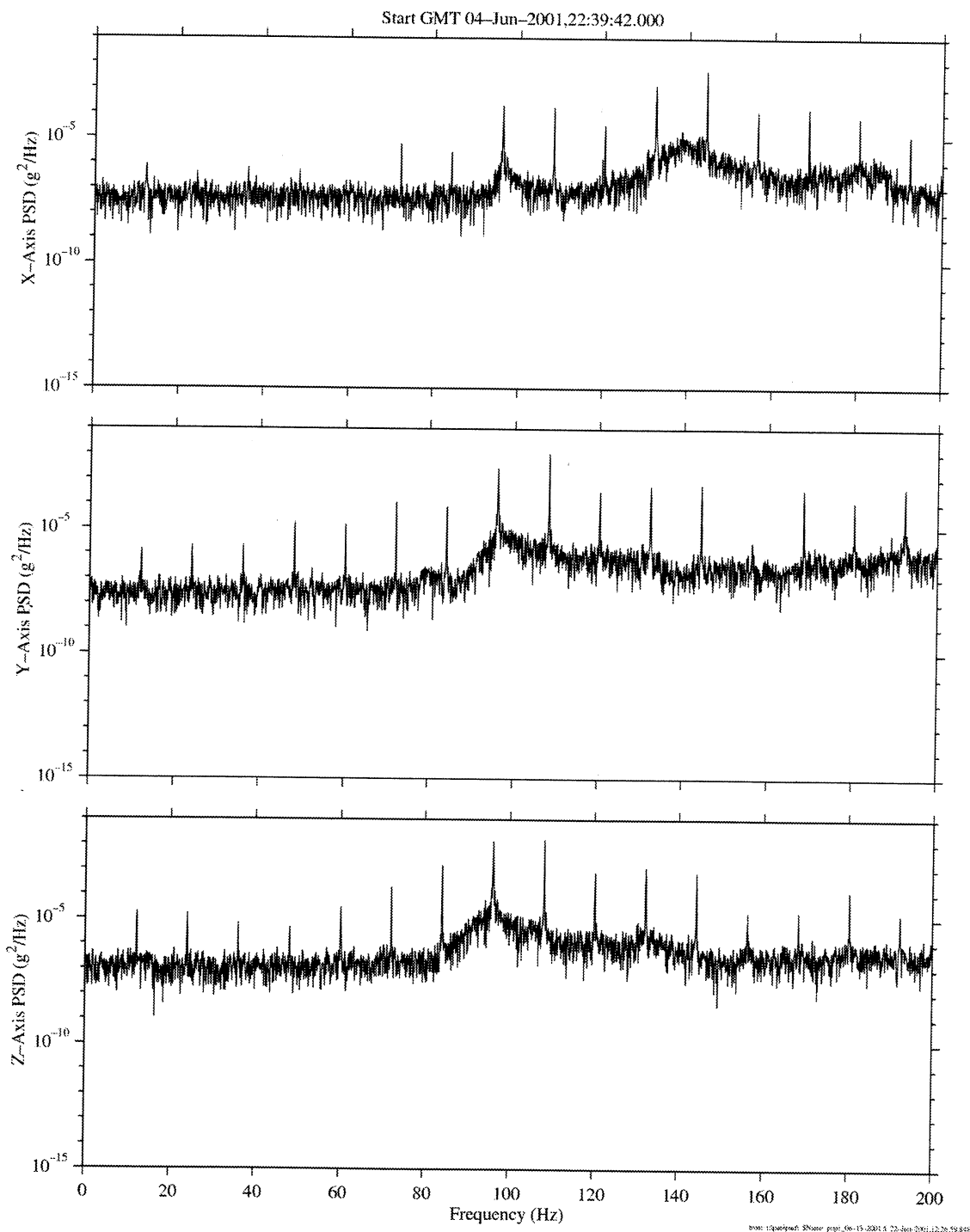


Figure 9.3.5.1-3 PSD of EXPPCS Sample Mix Operation On (121f06)

PIMS ISS Increment-2 Microgravity Environment Summary Report: May to August 2001

sams2, 121f06 at LAB101, ER2, PCS Test Section:[179.90 -6.44 145.55]
500.0 sq/sec (200.00 Hz)
 $\Delta f = 0.061$ Hz, $N(f) = 8192$
 $P = 47.4\%$, $N_0 = 3884$

EXPPCS Sample Mix Off

Increment: 2, Flight: 6A
121f06[180.0 90.0 0.0]
Hanning, $k = 2$
Span = 25.00 sec.

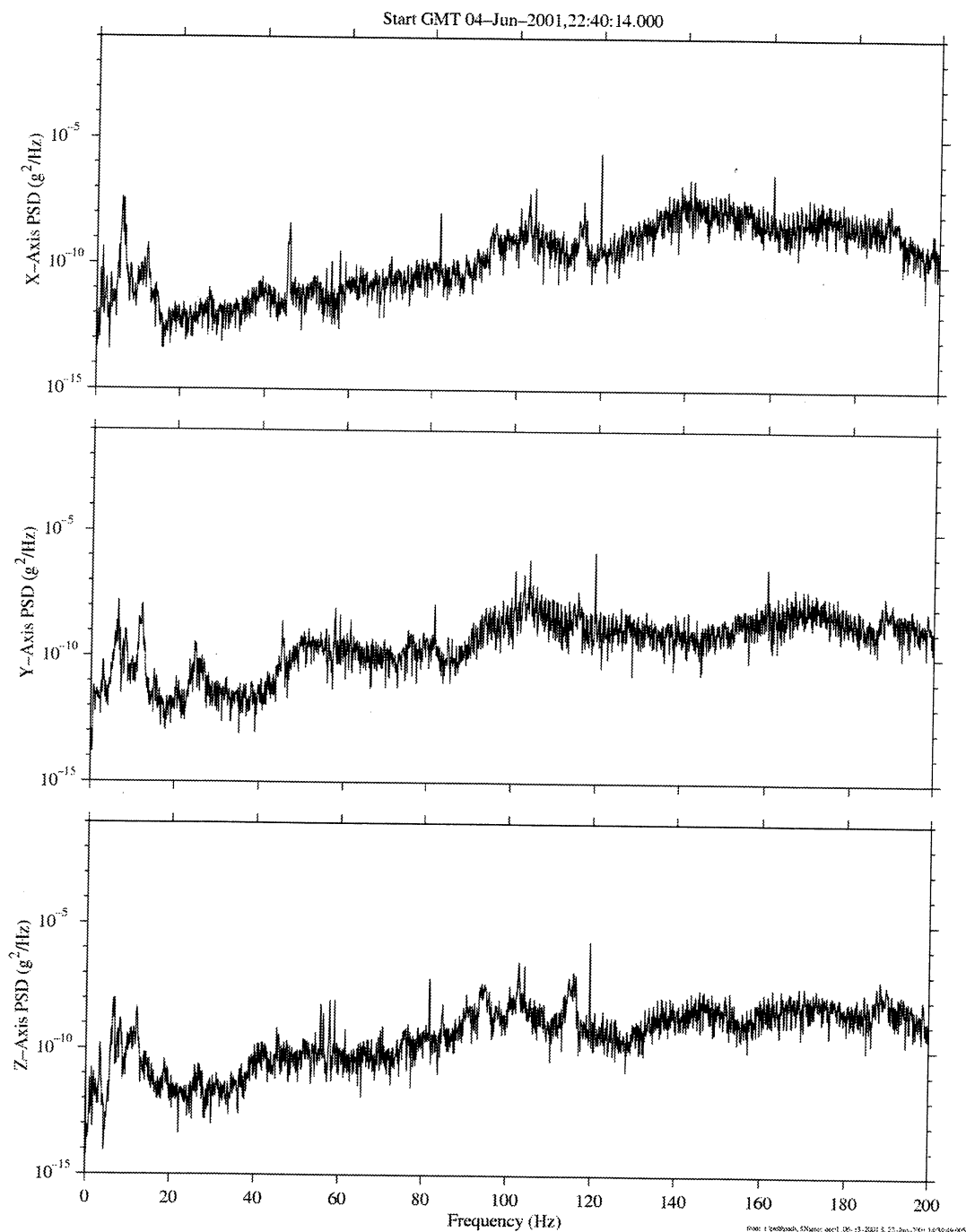


Figure 9.3.5.1-4 PSD of EXPPCS Sample Mix Operation Off (121f06)

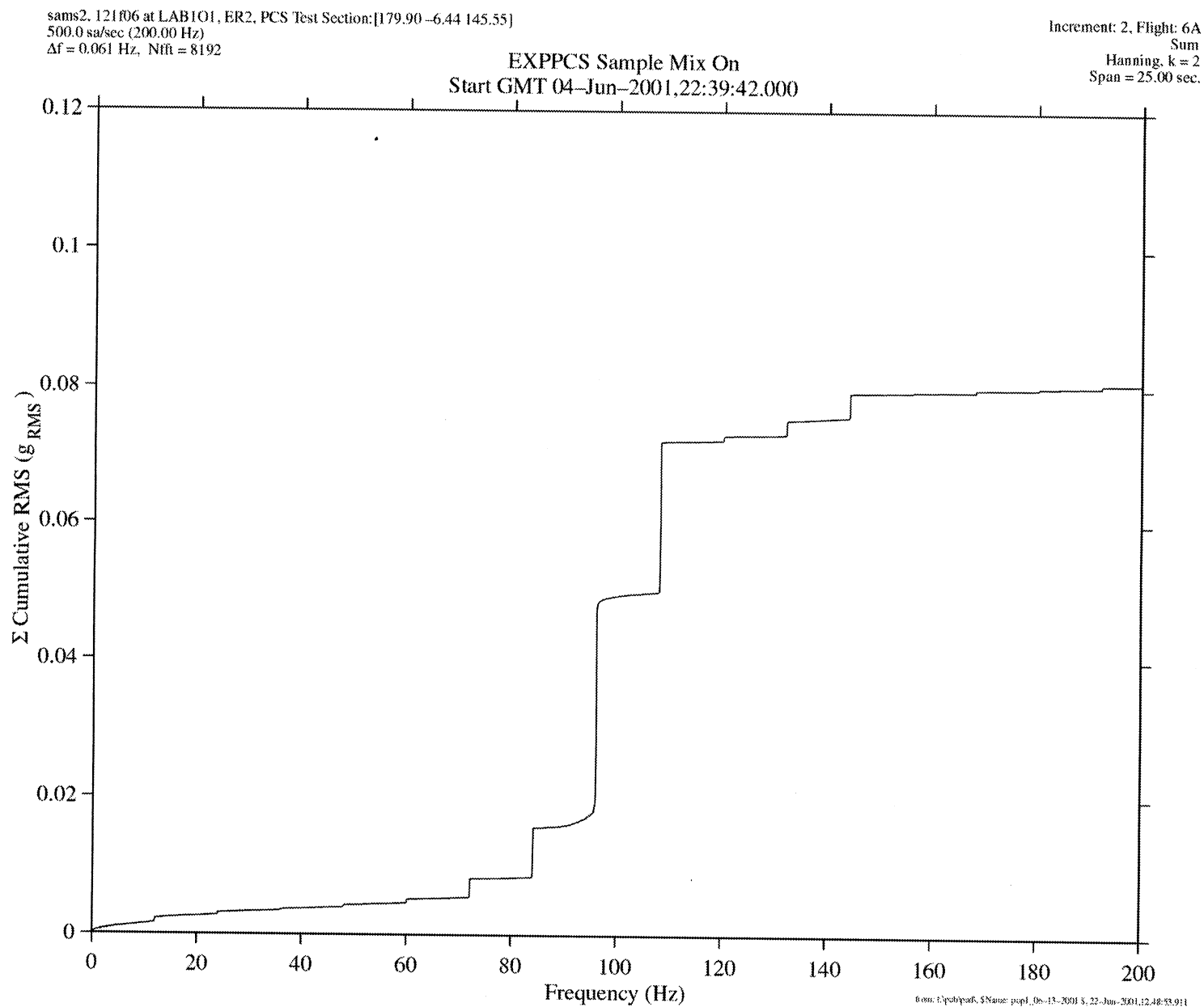
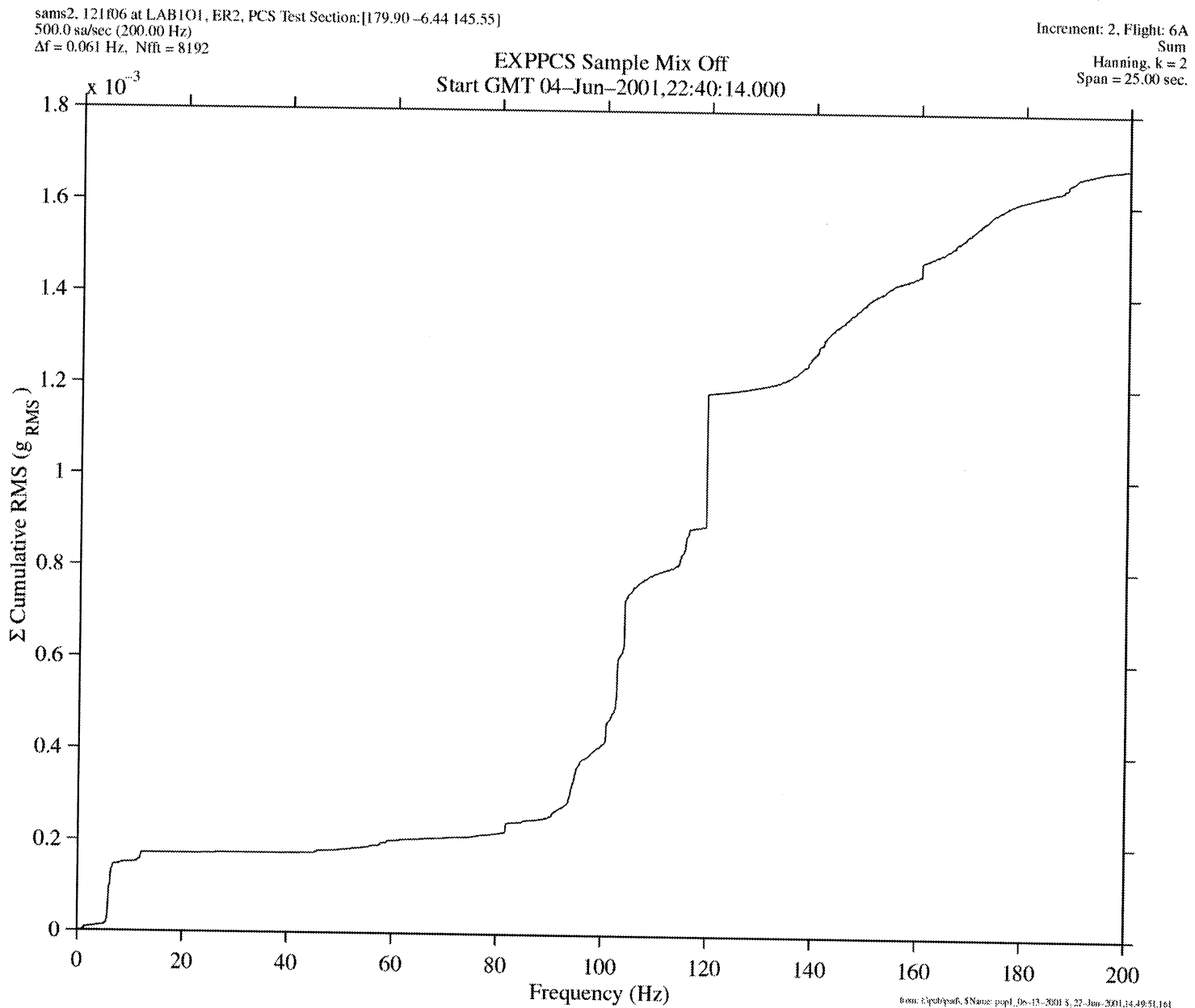


Figure 9.3.5.1-5 Cumulative RMS of EXPPCS Sample Mix Operation On (121f06)



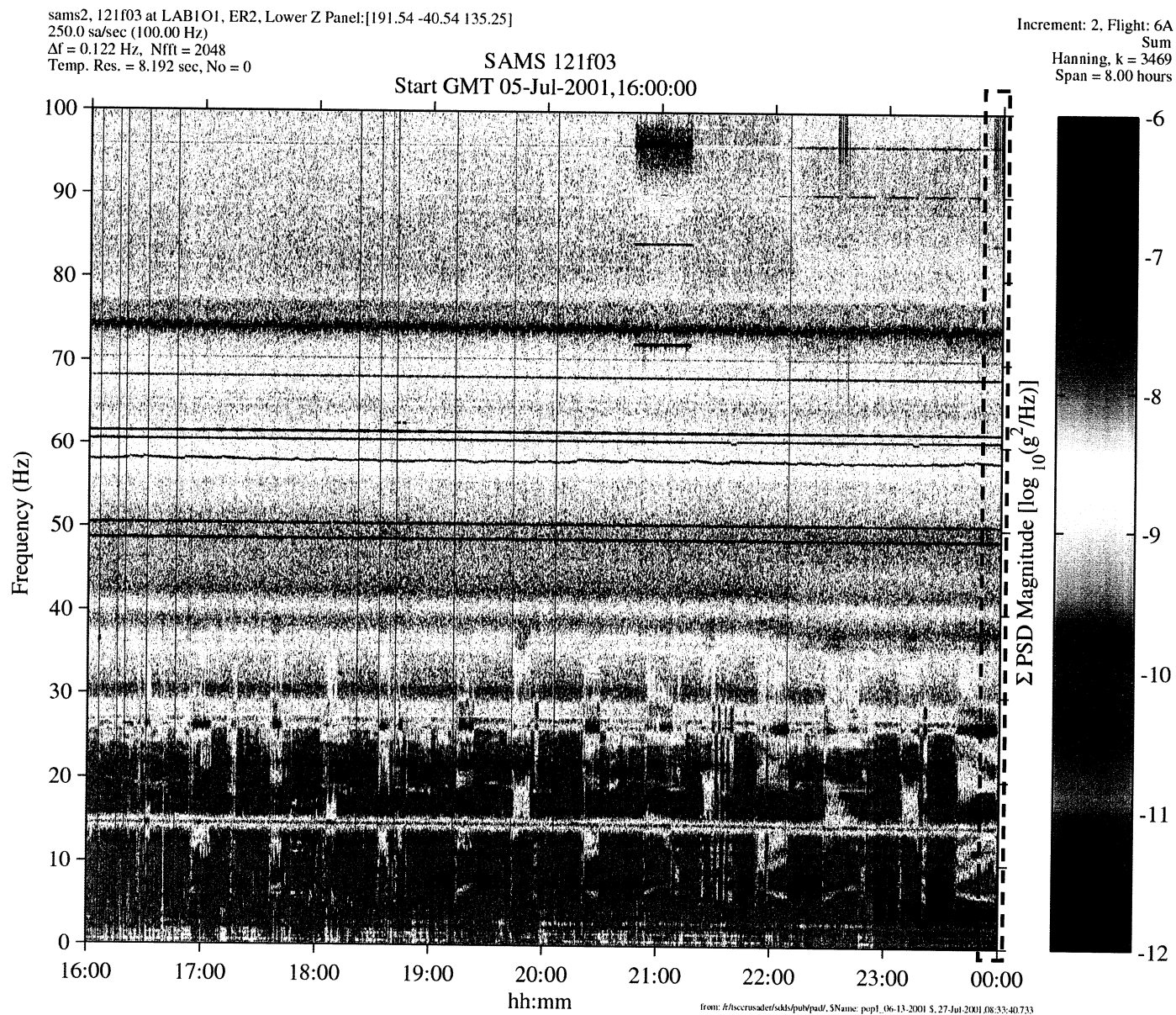


Figure 9.3.5.1-7 Spectrogram of EXPPCS Sample Mix Operation On (121f03)

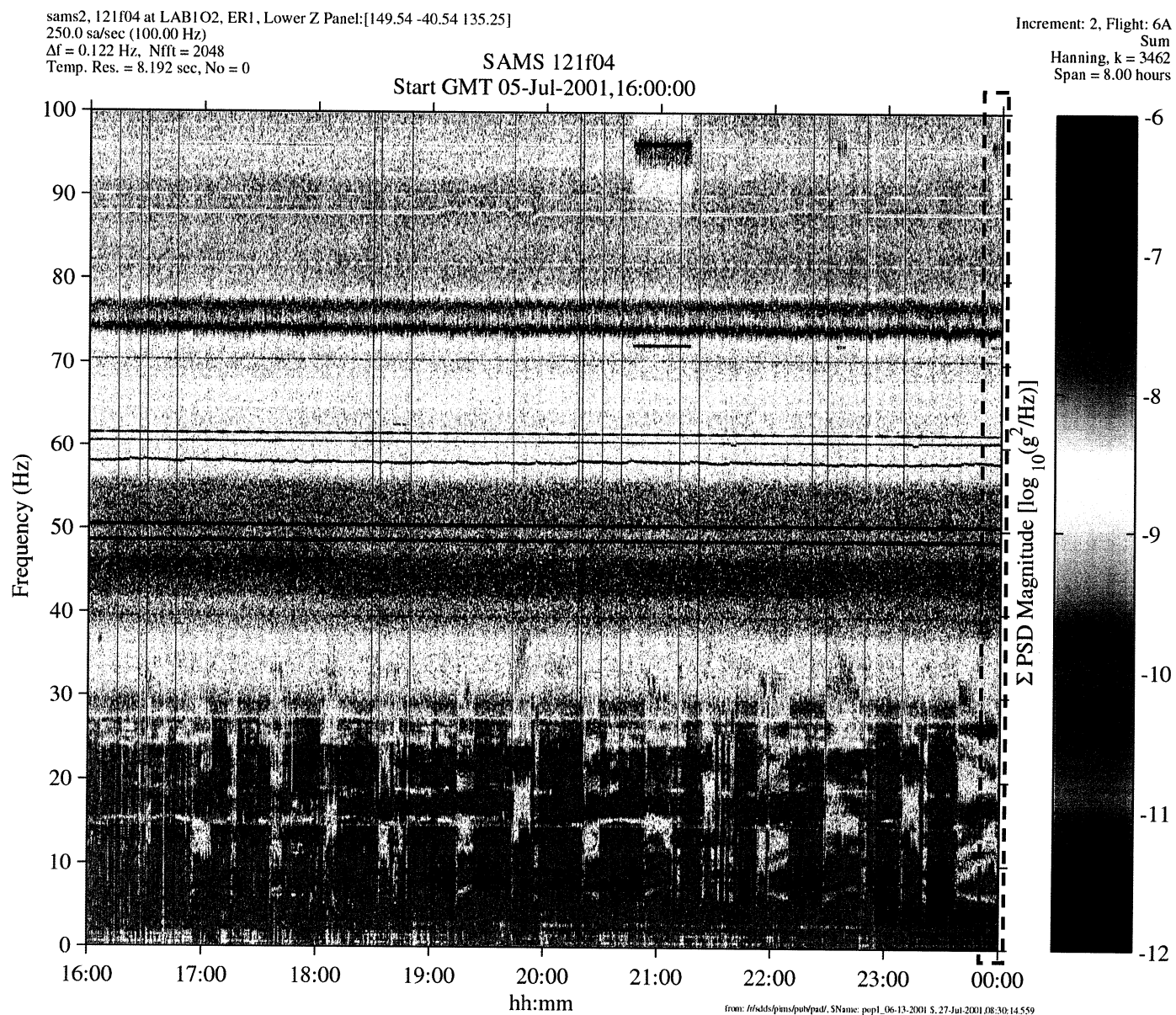


Figure 9.3.5.1-8 Spectrogram of EXPPCS Sample Mix Operation On (121f04)

PIMS ISS Increment-2 Microgravity Environment Summary Report: May to August 2001

sams2, 121f03 at LAB101, ER2, Lower Z Panel:[191.54 -40.54 135.25]
250.0 sa/sec (100.00 Hz)

EXPPCS Sample Mix

Increment: 2, Flight: 6A
SSAnalysis[0.0 0.0 0.0]
Interval Minmax
Size: 0.25, Step: 0.25 sec.

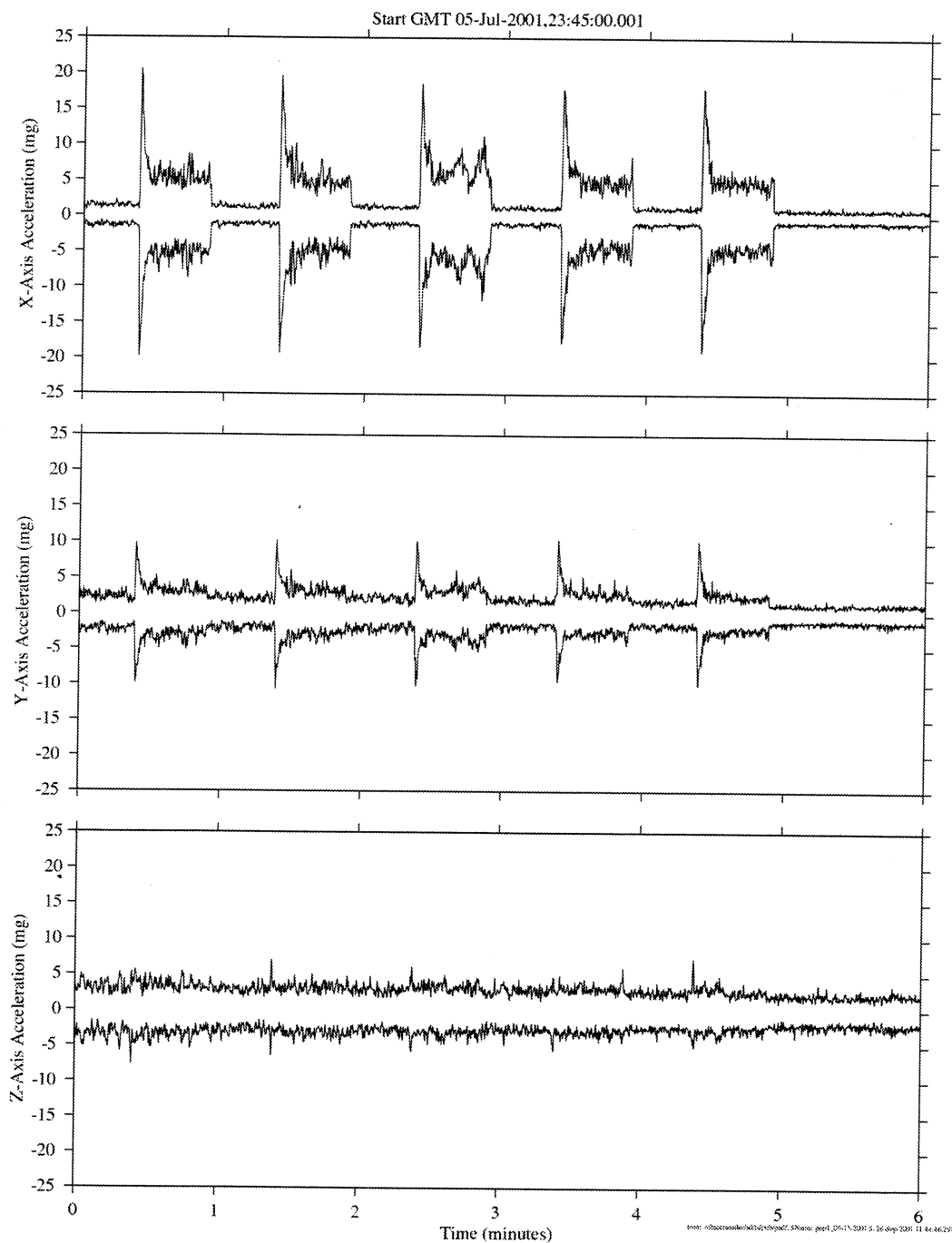


Figure 9.3.5.1-9 Interval Min/Max of EXPPCS Sample Mix Operation On (121f03)

PIMS ISS Increment-2 Microgravity Environment Summary Report: May to August 2001

sams2, 121004 at LAB102, ERI, Lower Z Panel:[149.54 -40.54 135.25]
250.0 sa/sec (100.00 Hz)

EXPPCS Sample Mix

```
Increment: 2, Flight: 6A
SSAnalysis[ 0.0 0.0 0.0]
Interval Minmax
Size: 0.25, Step: 0.25 sec.
```

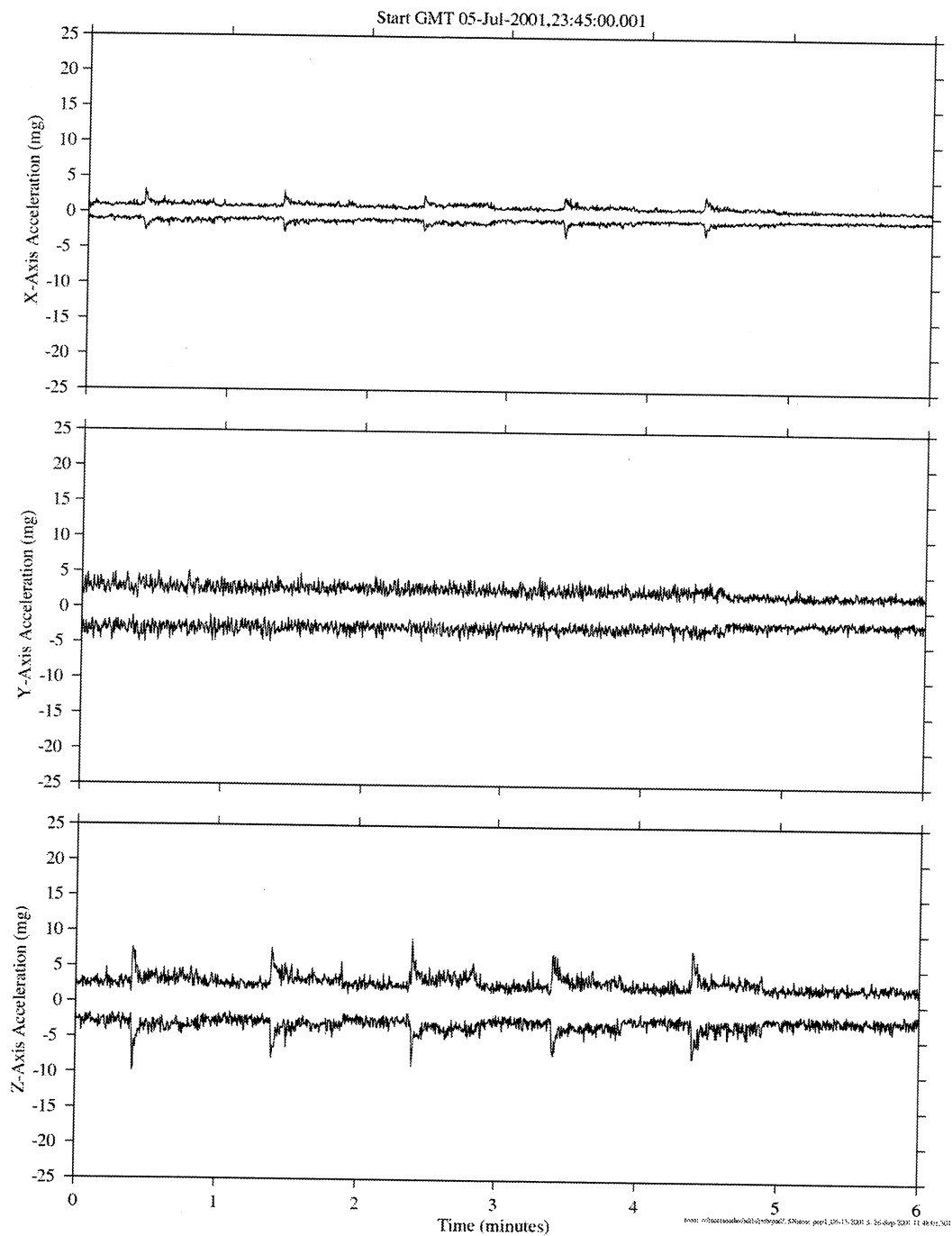


Figure 9.3.5.1-10 Interval Min/Max of EXPPCS Sample Mix Operation On (121f04)

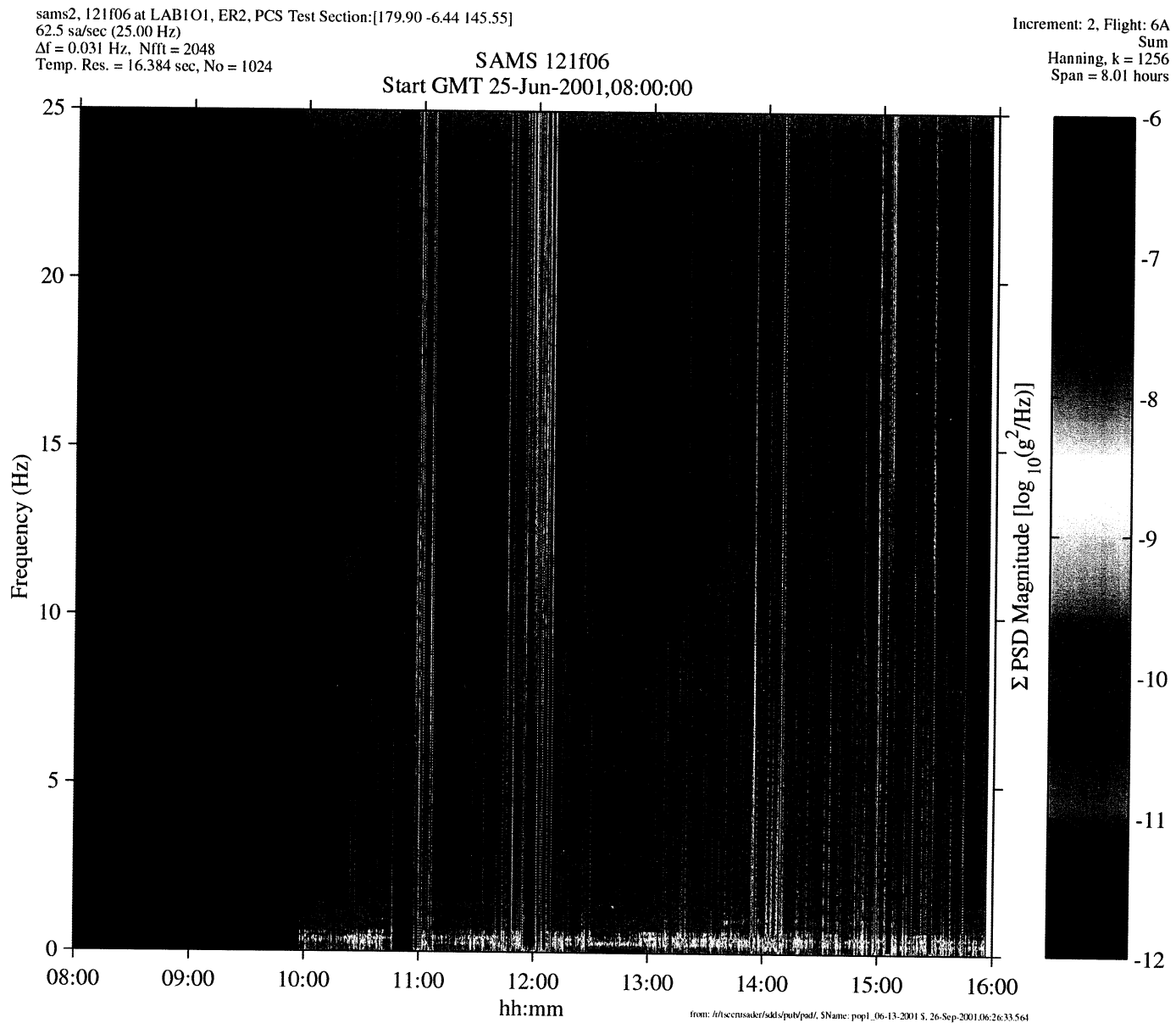


Figure 9.3.5.2-1 Spectrogram of EXPPCS Rheology On (121f06)

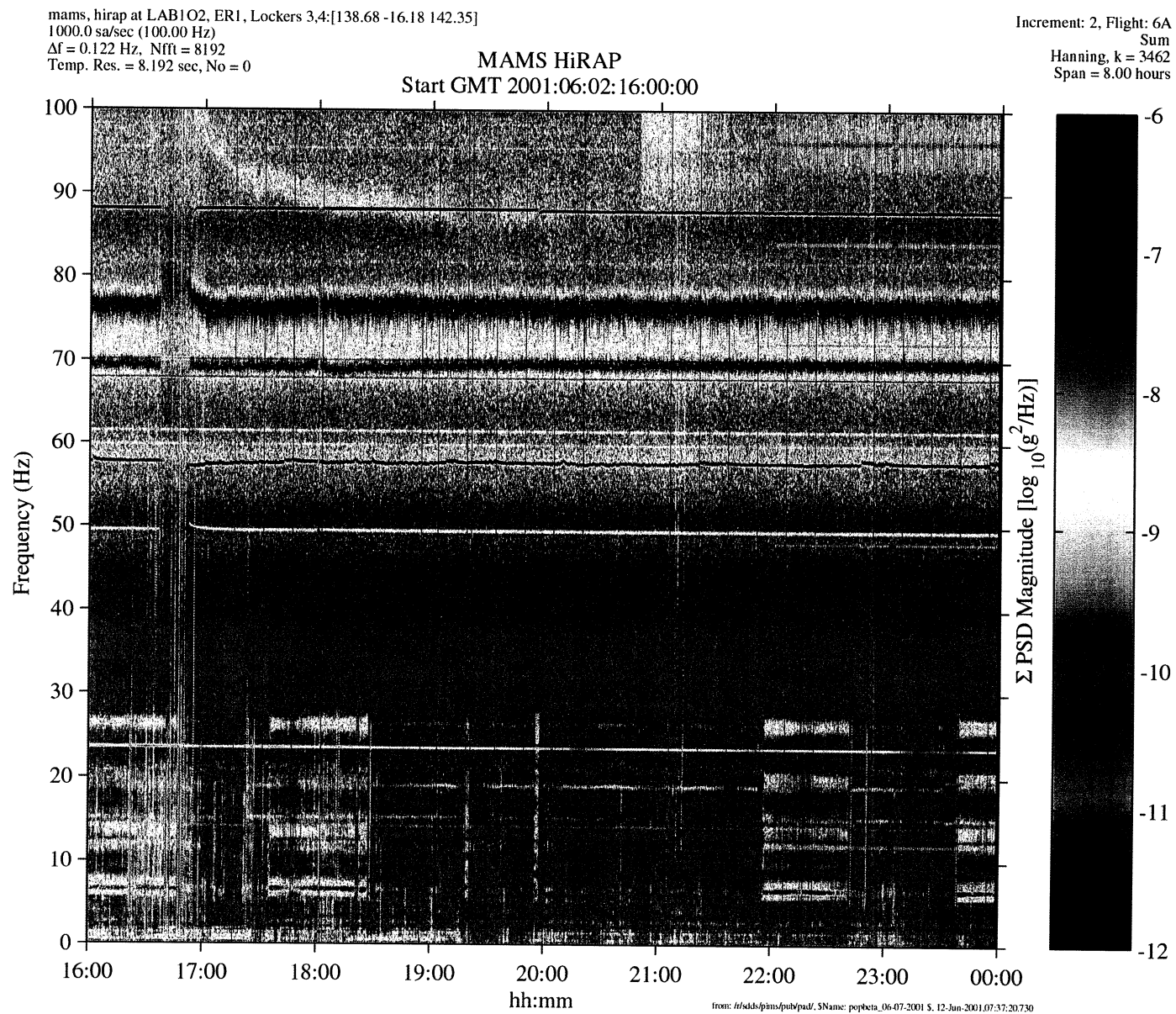


Figure 9.3.6-1 Spectrogram of ADVASC Equipment On and Off (HiRAP)

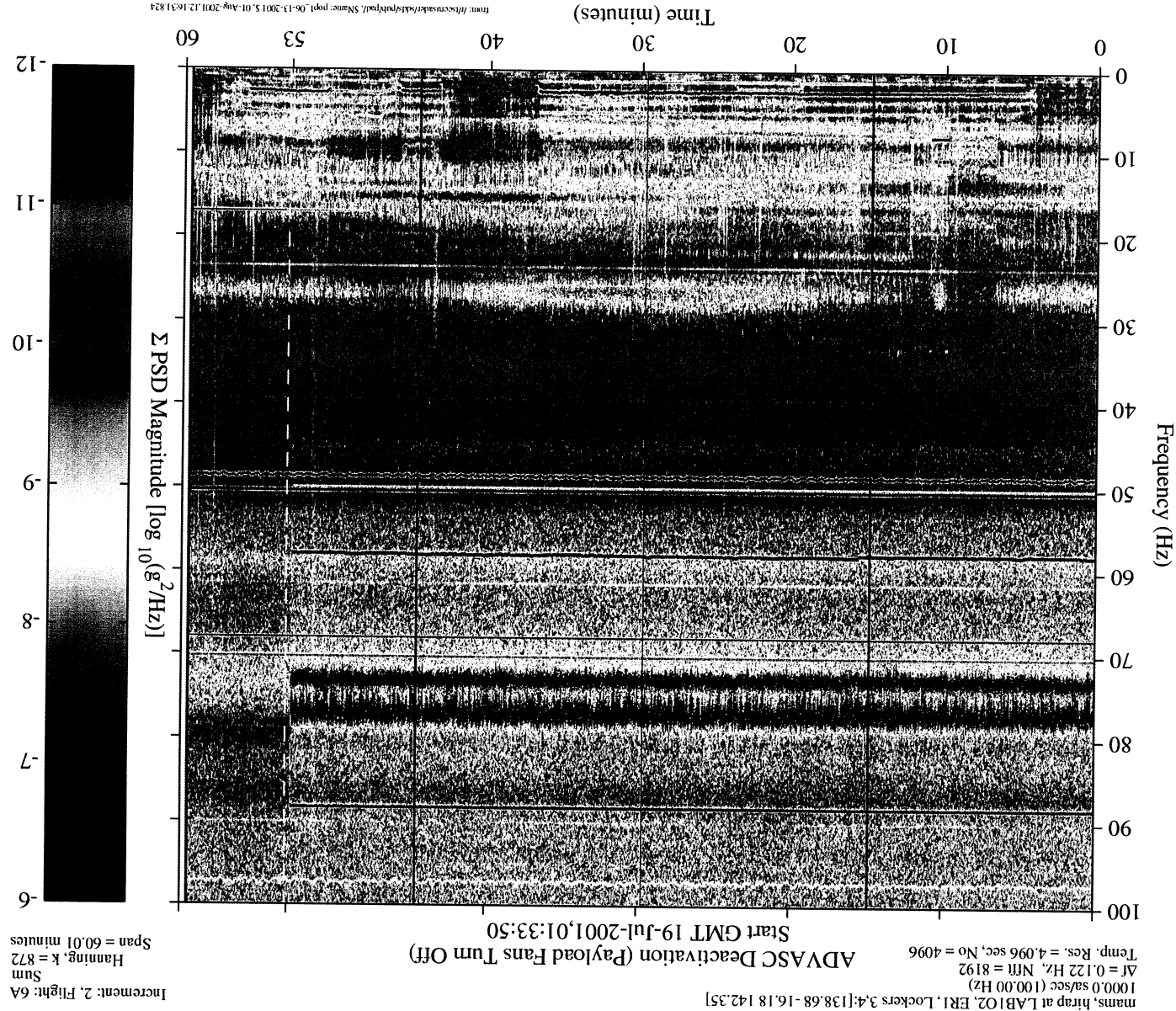


Figure 9.3.6-2 Spectrogram of ADVASC Deactivation (HiRAP)

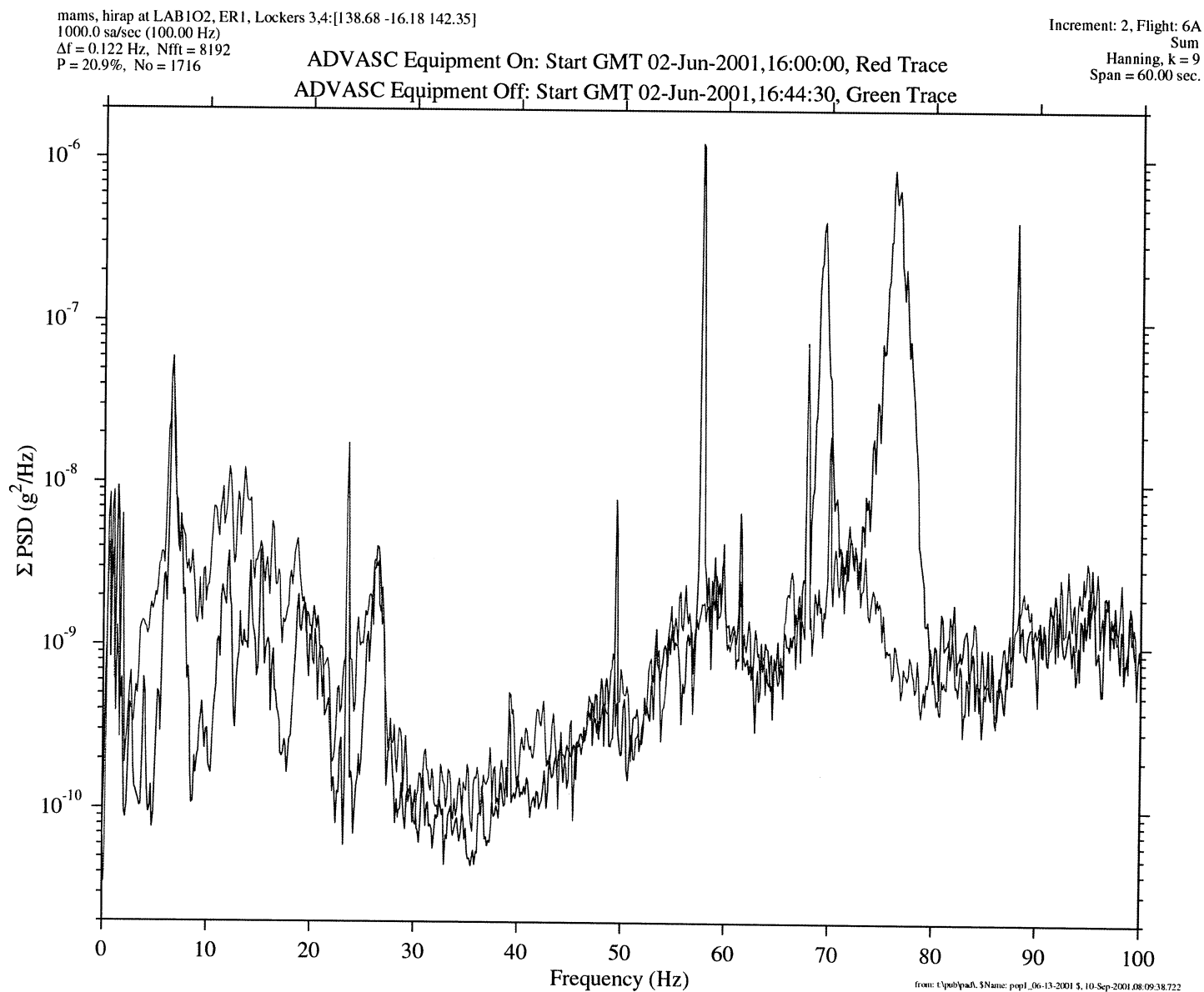


Figure 9.3.6-3 PSD of ADVASC Equipment On and Off (HiRAP)

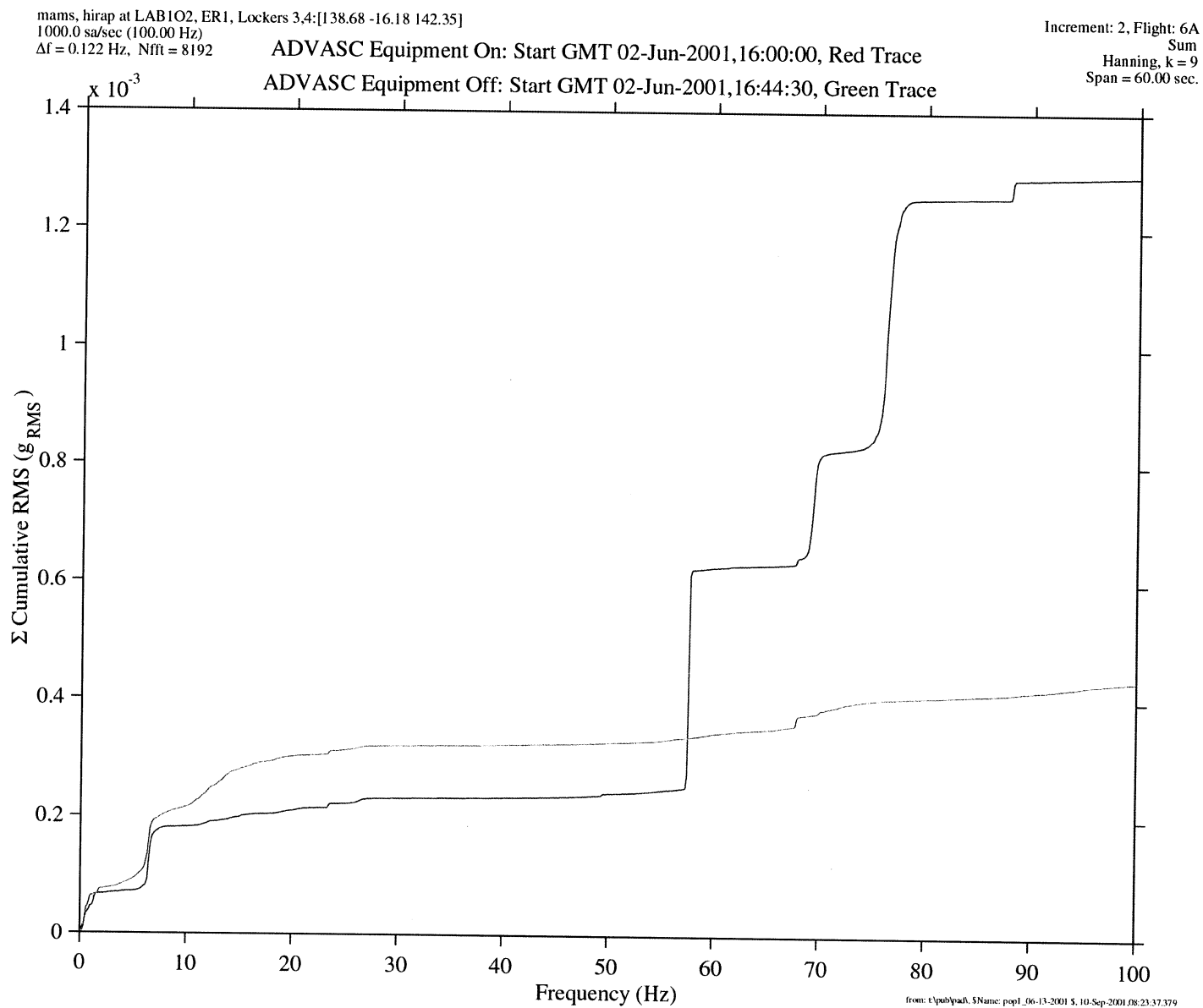


Figure 9.3.6-4 Cumulative RMS of ADVASC Equipment On and Off (HiRAP)

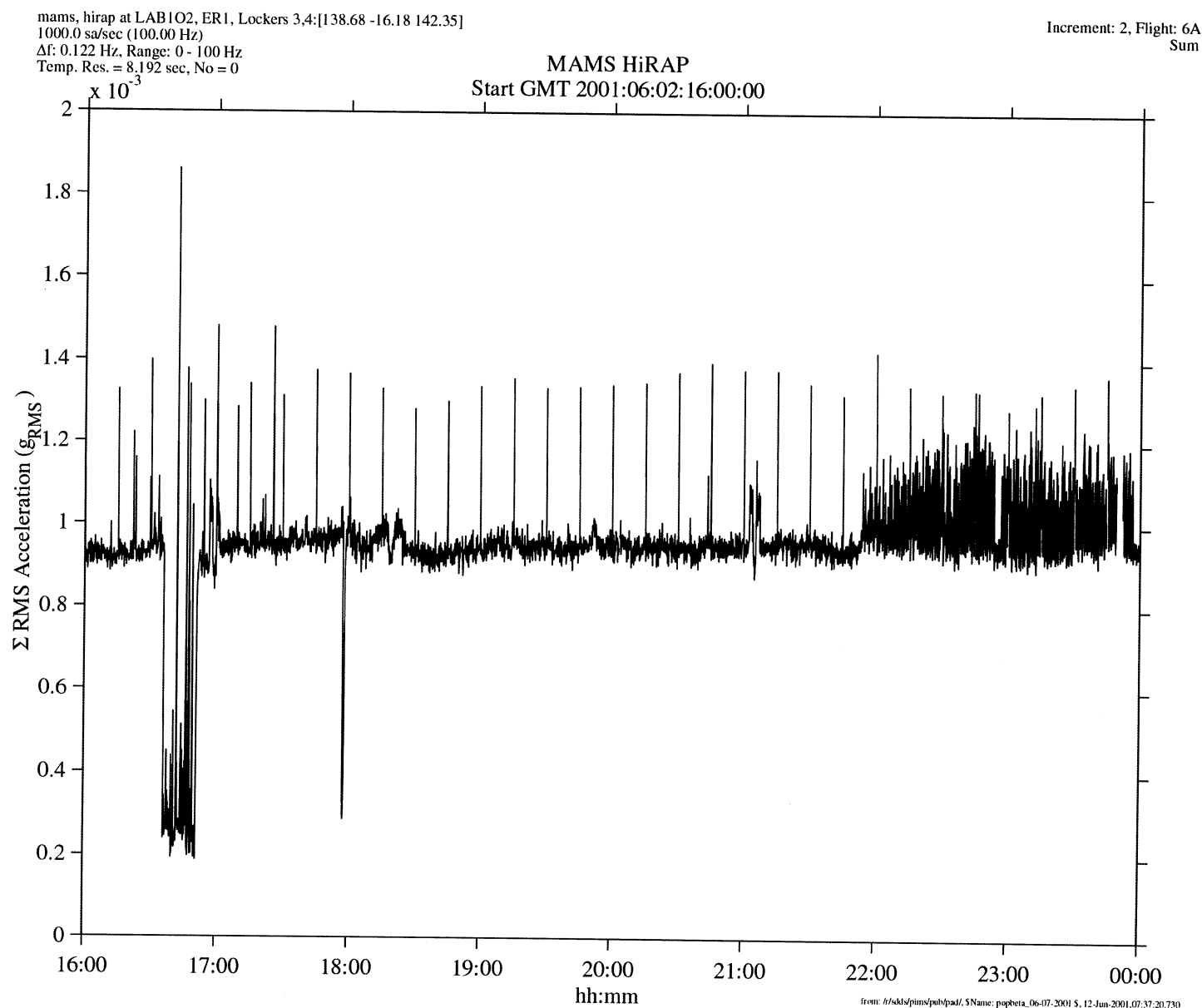
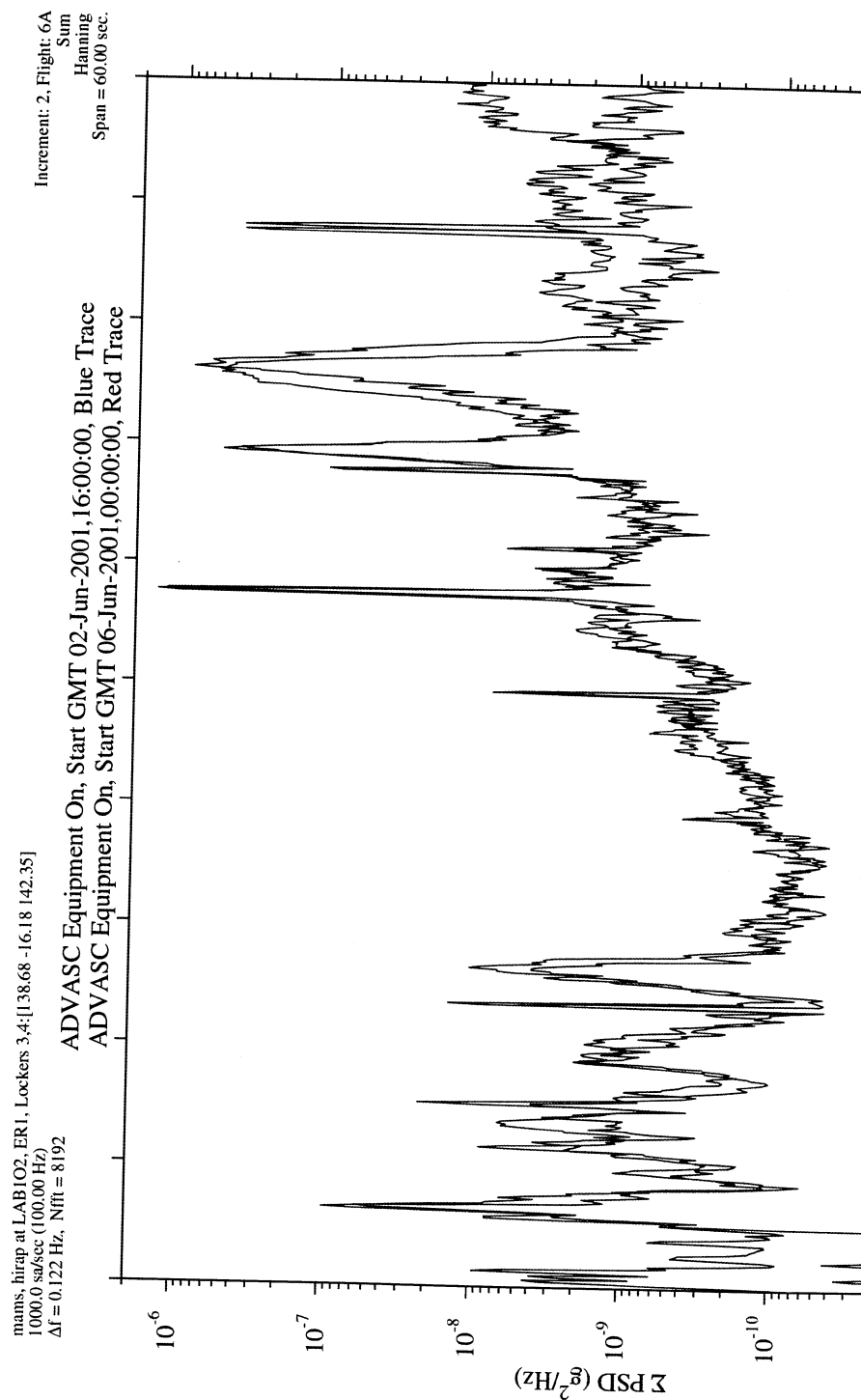
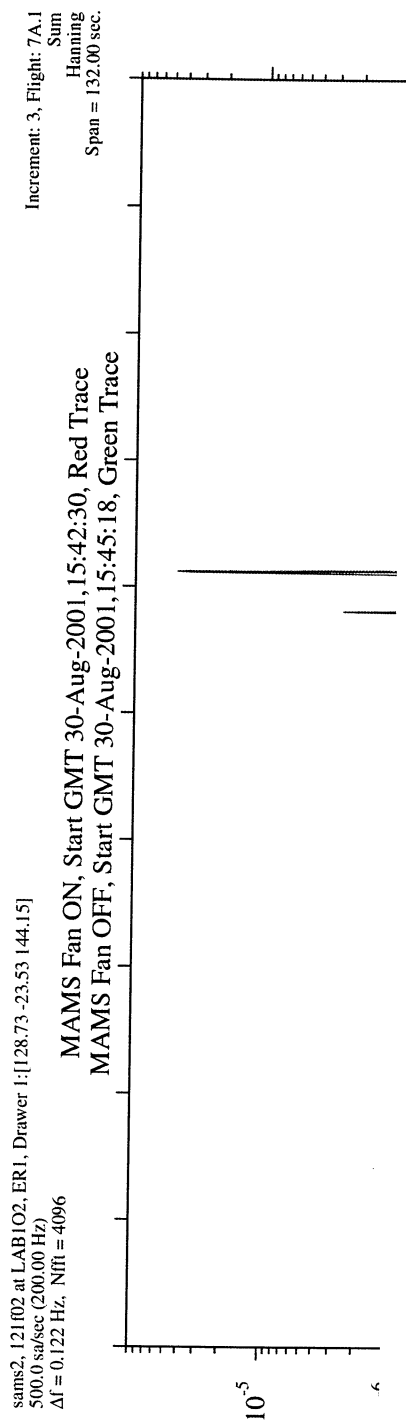


Figure 9.3.6-5 Interval RMS of ADVASC Equipment On and Off (HiRAP)



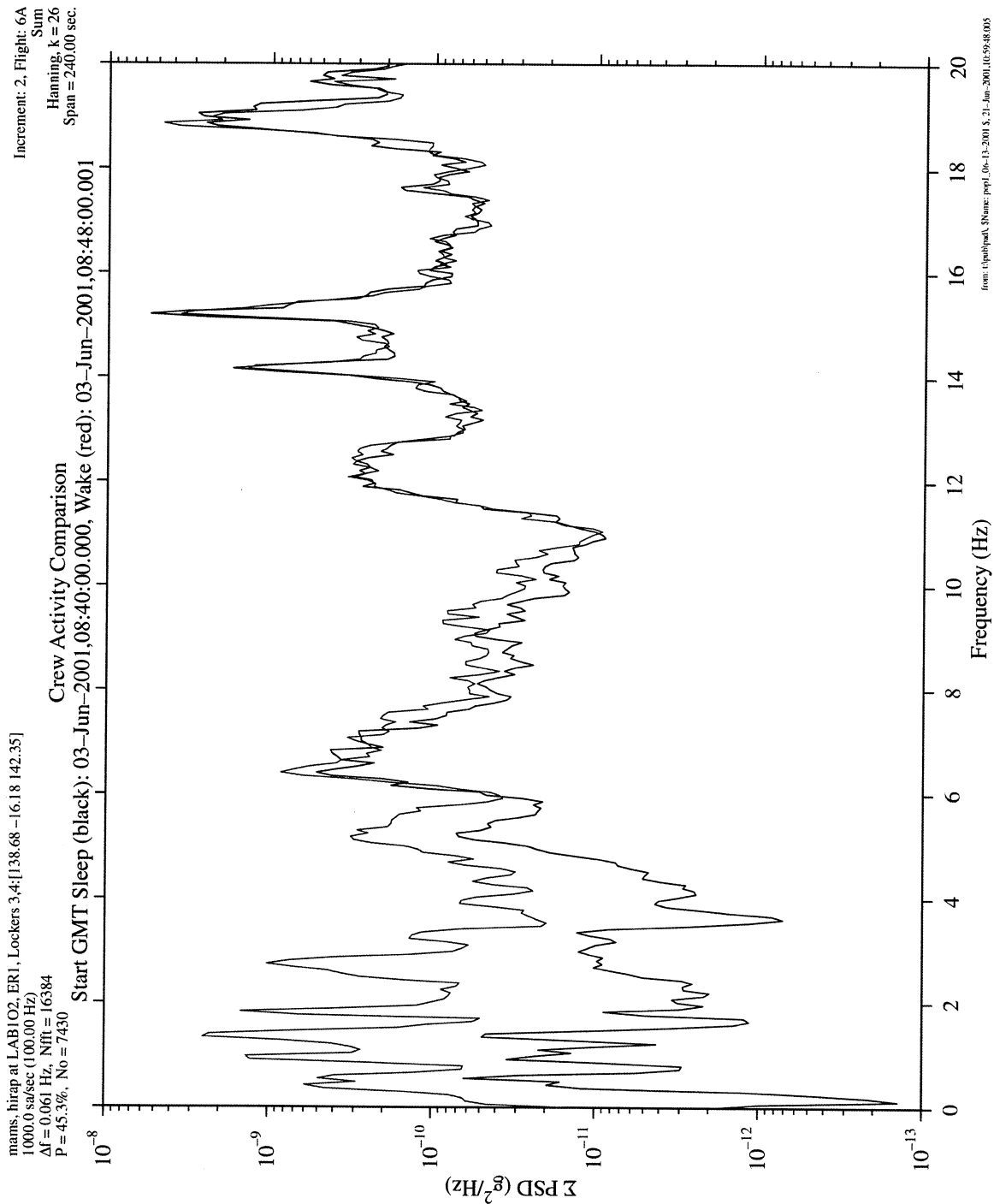


Figure 9.3.8.1-1 PSD of Crew Sleep and Wake (HiRAP)

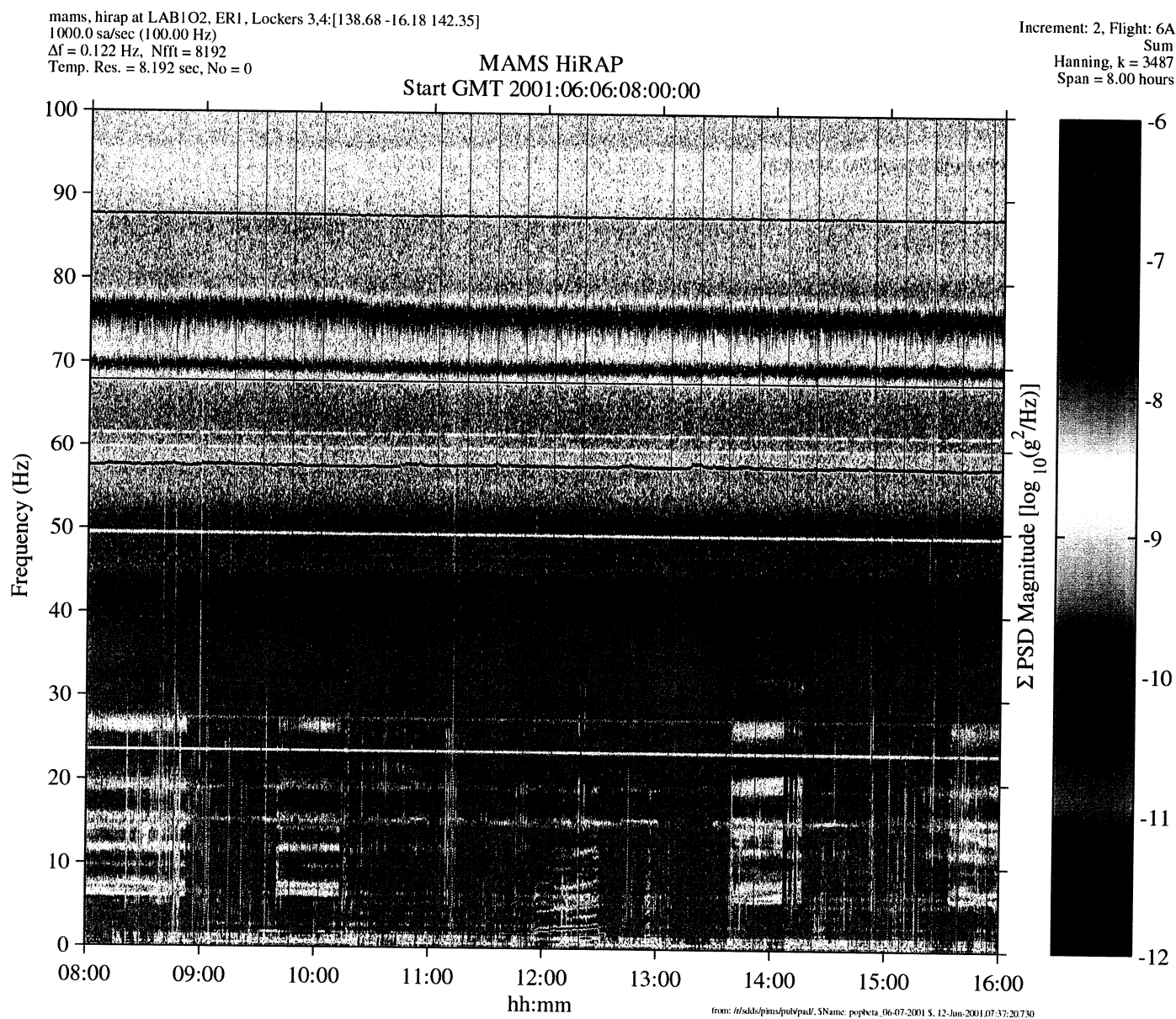


Figure 9.3.8.2.2-1 Spectrogram of Ergometer Signature (HiRAP)

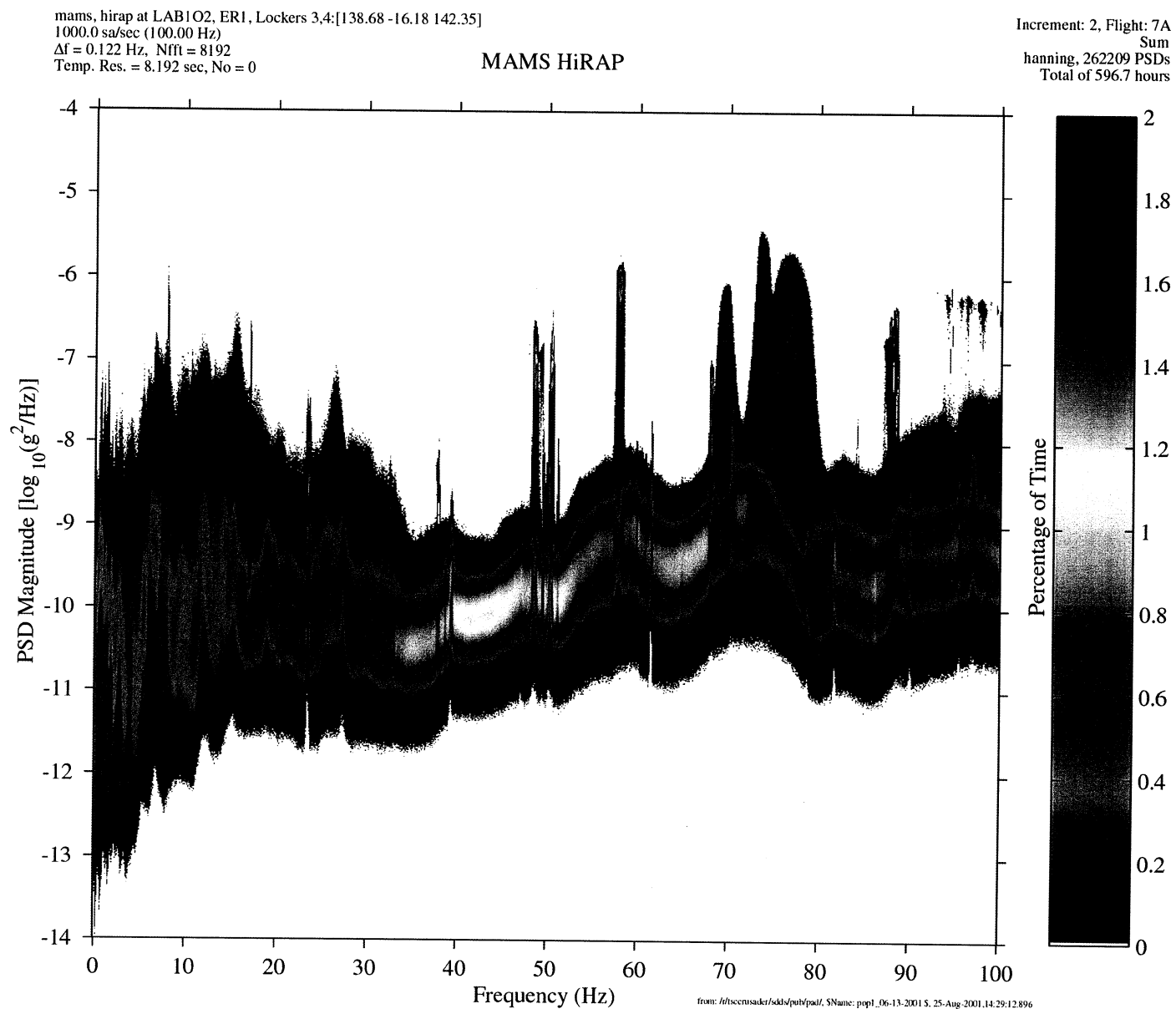


Figure 10-1 PCSA of Below 100 Hz (HiRAP)

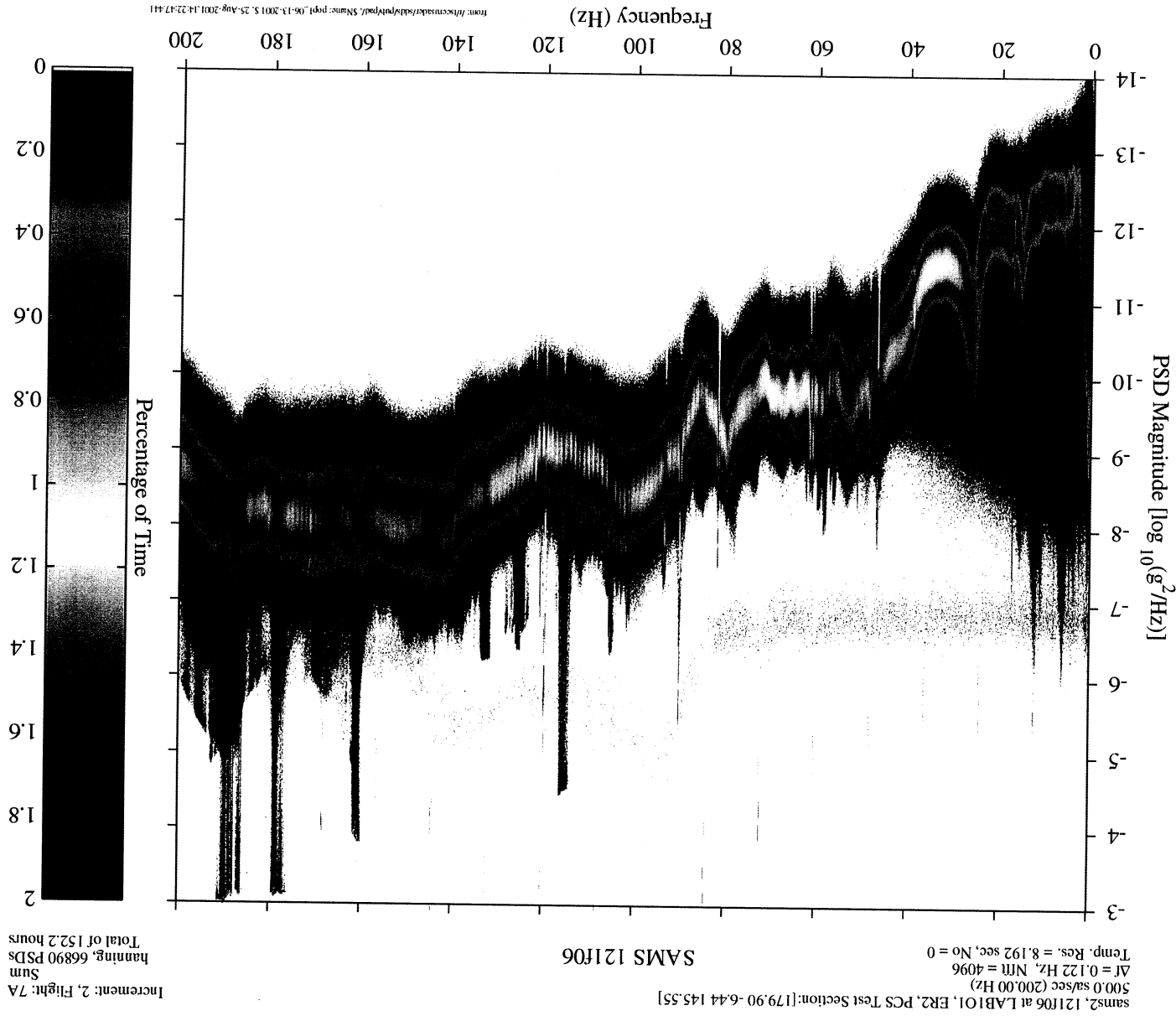


Figure 10-2 PCSA of Below 200 Hz (121f06)

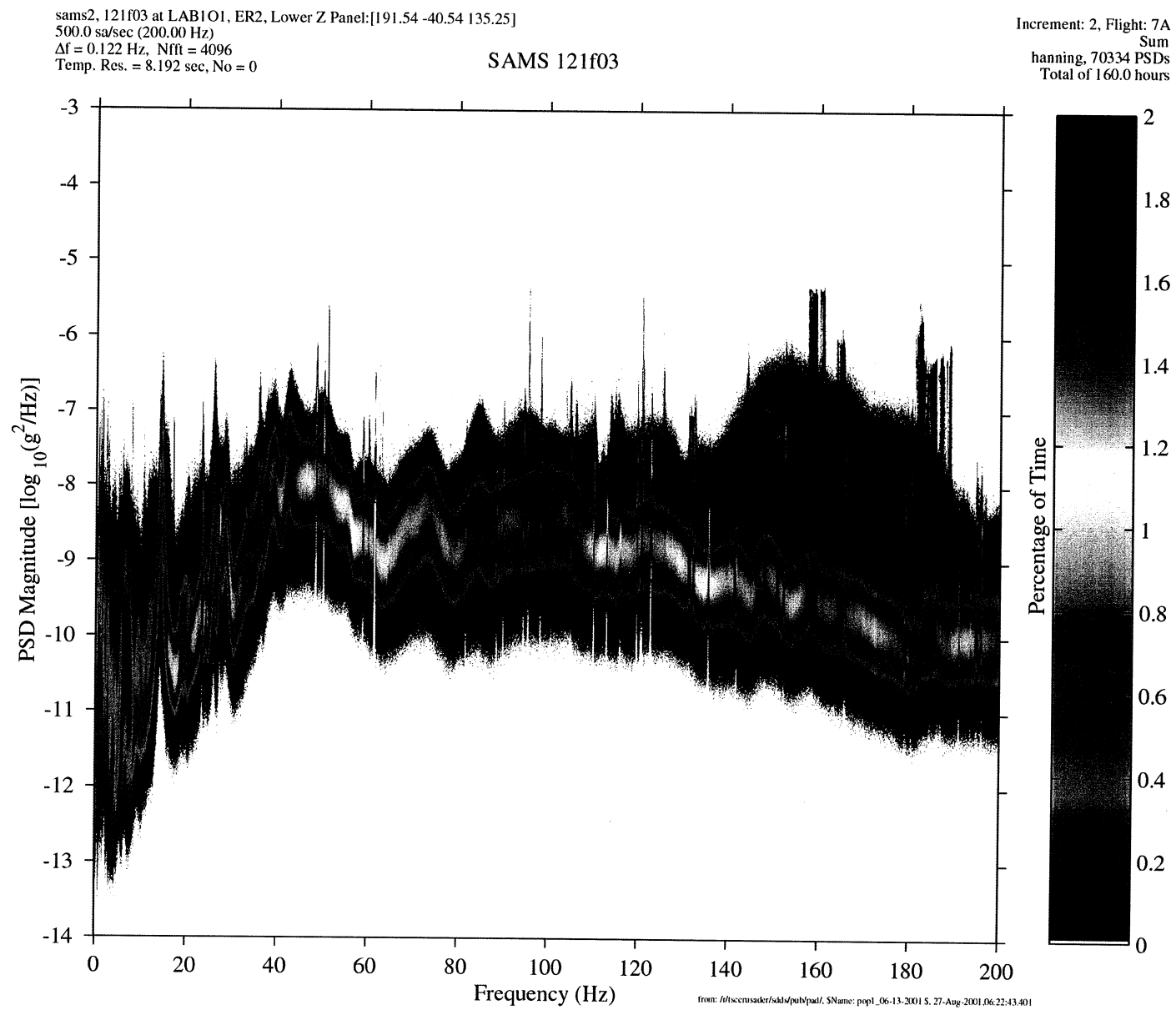


Figure 10-3 PCSA of Below 200 Hz (121f03)

REPORT DOCUMENTATION PAGE			Form Approved OMB No. 0704-0188	
Public reporting burden for this collection of information is estimated to average 1 hour per response, including the time for reviewing instructions, searching existing data sources, gathering and maintaining the data needed, and completing and reviewing the collection of information. Send comments regarding this burden estimate or any other aspect of this collection of information, including suggestions for reducing this burden, to Washington Headquarters Services, Directorate for Information Operations and Reports, 1215 Jefferson Davis Highway, Suite 1204, Arlington, VA 22202-4302, and to the Office of Management and Budget, Paperwork Reduction Project (0704-0188), Washington, DC 20503.				
1. AGENCY USE ONLY (Leave blank)	2. REPORT DATE January 2002	3. REPORT TYPE AND DATES COVERED Technical Memorandum		
4. TITLE AND SUBTITLE International Space Station Increment-2 Microgravity Environment Summary Report		5. FUNDING NUMBERS WU-398-95-0G-00		
6. AUTHOR(S) Kenol Jules, Kenneth Hrovat, Eric Kelly, Kevin McPherson, and Timothy Reckart				
7. PERFORMING ORGANIZATION NAME(S) AND ADDRESS(ES) National Aeronautics and Space Administration John H. Glenn Research Center at Lewis Field Cleveland, Ohio 44135-3191		8. PERFORMING ORGANIZATION REPORT NUMBER E-13146		
9. SPONSORING/MONITORING AGENCY NAME(S) AND ADDRESS(ES) National Aeronautics and Space Administration Washington, DC 20546-0001		10. SPONSORING/MONITORING AGENCY REPORT NUMBER NASA TM-2002-211335		
11. SUPPLEMENTARY NOTES Kenol Jules and Kevin McPherson, NASA Glenn Research Center; Kenneth Hrovat, Eric Kelly, and Timothy Reckart, Zin Technologies, Inc., 3000 Aerospace Parkway, Brook Park, Ohio 44142. Responsible person, Kenol Jules, organization code 6727, 216-977-7016.				
12a. DISTRIBUTION/AVAILABILITY STATEMENT Unclassified - Unlimited Subject Categories: 19 and 35 Available electronically at http://gltrs.grc.nasa.gov/GLTRS This publication is available from the NASA Center for AeroSpace Information, 301-621-0390.		12b. DISTRIBUTION CODE		
13. ABSTRACT (Maximum 200 words) This summary report presents the results of some of the processed acceleration data, collected aboard the International Space Station during the period of May to August 2001, the Increment-2 phase of the station. Two accelerometer systems were used to measure the acceleration levels during activities that took place during the Increment-2 segment. However, not all of the activities were analyzed for this report due to time constraints, lack of precise information regarding some payload operations and other station activities. The National Aeronautics and Space Administration sponsors the Microgravity Acceleration Measurement System and the Space Acceleration Microgravity System to support microgravity science experiments, which require microgravity acceleration measurements. On April 19, 2001, both the Microgravity Acceleration Measurement System and the Space Acceleration Measurement System units were launched on STS-100 from the Kennedy Space Center for installation on the International Space Station. The Microgravity Acceleration Measurement System unit was flown to the station in support of science experiments requiring quasi-steady acceleration measurements, while the Space Acceleration Measurement System unit was flown to support experiments requiring vibratory acceleration measurement. Both acceleration systems are also used in support of vehicle microgravity requirements verification. The International Space Station Increment-2 reduced gravity environment analysis presented in this report uses acceleration data collected by both sets of accelerometer systems: 1) The Microgravity Acceleration Measurement System, which consists of two sensors: the Orbital Acceleration Research Experiment Sensor Subsystem, a low frequency range sensor (up to 1 Hz), is used to characterize the quasi-steady environment for payloads and the vehicle, and the High Resolution Accelerometer Package, which is used to characterize the vibratory environment up to 100 Hz. 2) The Space Acceleration Measurement System, which is a high frequency sensor, measures vibratory acceleration data in the range of 0.01 to 300 Hz. This summary report presents analysis of some selected quasi-steady and vibratory activities measured by these accelerometers during Increment-2 from May to August 20, 2001.				
14. SUBJECT TERMS SAMS; MAMS; Microgravity; Quasi-steady; Vibratory; Transient; International Space Station			15. NUMBER OF PAGES 141	
			16. PRICE CODE	
17. SECURITY CLASSIFICATION OF REPORT Unclassified	18. SECURITY CLASSIFICATION OF THIS PAGE Unclassified	19. SECURITY CLASSIFICATION OF ABSTRACT Unclassified	20. LIMITATION OF ABSTRACT	